Universidad Politécnica de Valencia

Departamento de Ingeniería Gráfica

PhD Thesis

Contributions to the Development of Objective Techniques for Presence Measurement in Virtual Environments by means of Brain Activity Analysis

Beatriz Rey Solaz

PhD Advisor:

Dr. Mariano Alcañiz Raya

Valencia, July 2010

Para Jose

Acknowledgments

Me gustaría expresar mi agradecimiento a todas las personas que me han apoyado para que este trabajo saliera adelante.

En primer lugar, quiero agradecerle a mi director de tesis, Mariano Alcañiz, por haber confiado siempre en mí, por toda su ayuda y por haber creído en este proyecto.

También me gustaría dar las gracias a todos mis compañeros de LabHuman durante estos años. Ha sido mucho tiempo el que hemos pasado juntos y su presencia siempre ha hecho más llevadero y agradable el trabajo.

También ha sido fundamental el apoyo del equipo de LabPsitec, con tantos proyectos juntos, tantos congresos y tantos buenos consejos. Muchas gracias.

Por otra parte, quiero transmitir un agradecimiento especial a todas las personas que han participado de una u otra manera en el desarrollo de este trabajo.

Sobre todo, quiero agradecer a Pepe Tembl y Vera Parkhutik, doctores del Hospital Universitari la Fe, por las tardes pasadas en el Politécnico para poder llevar a cabo todas las sesiones experimentales y por toda su ayuda.

También quiero dar las gracias a Valery Naranjo y Xavier Bornàs, por su apoyo y consejos en los análisis de las señales.

Otra persona que cabe destacar y sin la cual no se hubiera podido llevar a cabo este proyecto ha sido José Lores, de la empresa Almevan, S.L. Le agradezco todas sus facilidades para poder disponer del equipo de Doppler Transcraneal utilizado en las pruebas.

Y, por último, pero no menos importante, quiero transmitir mi más sincero agradecimiento a todas las personas que voluntariamente han pasado por los experimentos que se han llevado a cabo en la presente tesis.

También me gustaría dar las gracias a todas las personas de mi entorno personal, amigos y familia, que han estado a mi lado durante este tiempo.

Quiero dar las gracias a José María, María José, César y David, por escucharme, por sus consejos y por su apoyo durante toda esta etapa.

También me gustaría acordarme en estos agradecimientos de mis abuelos Antonio y Remedios y de mi tía Gloria, a los que tengo tan presentes, por todo su amor y por su capacidad de emocionarse con mis estudios aunque no los comprendieran.

Me gustaría dar las gracias especialmente a mis padres Juan y Clotilde, porque han estado siempre a mi lado y todo lo que me han transmitido desde niña ha sido la base que ha hecho posible que esta tesis se llevara a cabo. También quiero darle las gracias a Pablo y Mari Carmen, que comprenden muy bien el camino que he tenido que recorrer para llegar aquí.

Finalmente, doy las gracias a Jose, por darme la fuerza para poder llevar a cabo mis proyectos, por estar a mi lado siempre, por comprenderme, por apoyarme... Sencillamente, gracias por estar ahí.

Resumen

El concepto de presencia, entendida como la sensación de "estar ahí", en un entorno virtual, aunque se esté físicamente en un lugar diferente (por ejemplo, en el laboratorio), ha sido ampliamente estudiado en el ámbito de la realidad virtual para comprender mejor los mecanismos psicológicos que acompañan a las experiencias virtuales.

En la literatura, se han propuesto distintas técnicas para medir presencia. Las técnicas subjetivas se basan fundamentalmente en la aplicación de cuestionarios que permiten obtener información acerca de la forma en que el usuario ha percibido la exposición al mundo virtual. Por otra parte, las técnicas objetivas se basan en el análisis de comportamientos del usuario durante la exposición al entorno virtual y en la monitorización de señales fisiológicas (tales como el electrocardiograma y la conductividad de la piel) para estudiar los posibles cambios en parámetros de las mismas durante dicha exposición.

Uno de los ámbitos que está despertando más interés en los últimos años es el análisis de la actividad cerebral como técnica para obtener información acerca del grado de presencia. En esta tesis, se propone el uso de la técnica de Doppler transcraneal (DTC) para monitorizar la actividad cerebral durante la exposición a entornos virtuales.

DTC es una técnica basada en ultrasonidos, no invasiva y con una alta resolución temporal, que no había sido utilizada hasta ahora en combinación con entornos virtuales. Permite medir la velocidad de flujo sanguíneo en las arterias principales del cerebro. Se ha utilizado ampliamente para monitorizar la hemodinámica cerebral durante la realización de tareas

cognitivas en investigación psicofisiológica. Estos estudios previos han mostrado que la velocidad de flujo sanguíneo medida por DTC se incrementa cuando los usuarios realizan una actividad cognitiva en comparación con periodos de reposo.

El objetivo global de la presente tesis es analizar si la técnica de DTC puede ser una herramienta complementaria para analizar la activación cerebral durante la exposición a entornos virtuales y si, por tanto, se puede utilizar como una herramienta para estudiar presencia desde un punto de vista neurocientífico.

Las hipótesis de partida son las siguientes:

1. DTC se podrá utilizar fácilmente en combinación con sistemas de realidad virtual, ya que se trata de una técnica no invasiva y que ya ha sido utilizada en estudios previos de investigación psicofisiológica.

2. Los datos de velocidad de flujo sanguíneo medidos por DTC se podrán utilizar para analizar cambios de actividad cerebral durante la exposición a entornos virtuales, permitiendo el uso de la técnica para el estudio de presencia desde una perspectiva neurocientífica.

3. Habrá diferencias en las variaciones observadas en la velocidad de flujo sanguíneo durante la exposición a sistemas de realidad virtual con distintos niveles de inmersión y distintos métodos de navegación, que irán asociados a distintos niveles de presencia en los participantes.

4. Habrá correlaciones entre el grado de presencia en entornos virtuales medido por cuestionarios y ciertos parámetros de la velocidad de flujo sanguíneo obtenidos durante la exposición a dichos entornos.

5. Cada uno de los distintos factores individuales que componen una experiencia virtual (tales como percepción visual o tareas motoras para navegar) tendrán una influencia en las variaciones observadas en la velocidad de flujo sanguíneo.

Para estudiar las hipótesis planteadas, se realizaron cuatro experimentos distintos, en los que se analizó la velocidad de flujo sanguíneo en distintas condiciones:

1. **Análisis de velocidad de flujo sanguíneo en distintas condiciones de navegación**. En este estudio, se monitorizó la velocidad de flujo sanguíneo por medio de DTC durante la exposición a un entorno virtual altamente inmersivo en diferentes condiciones de navegación.

2. **Análisis de la velocidad de flujo sanguíneo cerebral en distintas condiciones de inmersión**. En este estudio, la velocidad de flujo sanguíneo se monitorizó utilizando DTC durante la exposición a una configuración de realidad virtual menos inmersiva, para así comparar los resultados con los obtenidos en el primer estudio con la configuración altamente inmersiva.

3. **Análisis de la velocidad de flujo sanguíneo cerebral durante una tarea de percepción visual**. En este estudio, se analizó la influencia de un aspecto separado de la experiencia virtual (estimulación visual simple) sobre la velocidad de flujo sanguíneo. En este caso, la señal se monitorizó mientras el usuario se exponía a condiciones cambiantes de iluminación.

4. **Análisis de la velocidad de flujo sanguíneo cerebral durante la realización de tareas motoras**. En este caso, la señal se monitorizó mientras el participante realizaba tareas motoras simples para controlar un joystick. De esta forma, se podía analizar la influencia de este factor en las variaciones de velocidad de flujo sanguíneo observadas durante las experiencias de realidad virtual.

Durante los dos primeros estudios, se observó que había un incremento en la velocidad de flujo sanguíneo cuando los participantes se exponían a un entorno virtual. Este incremento podía deberse a la interacción compleja de distintos factores como tareas de interacción visuoespacial, tareas de atención, la creación y ejecución de un plan motor, cambios emocionales y variaciones de presencia. De hecho, las variaciones en la velocidad de flujo sanguíneo observadas eran distintas dependiendo del tipo de navegación y del grado de inmersión. Se encontraron correlaciones significativas entre la velocidad media de flujo sanguíneo en las arterias cerebrales medias

durante la exposición a las distintas configuraciones de realidad virtual y determinadas respuestas a los cuestionarios de presencia utilizados.

El resto de estudios realizados en esta tesis se centraron en el análisis de factores individuales (visuales y motores) que contribuyen a la experiencia virtual. Se aplicaron técnicas de procesado de señal que no habían sido utilizadas previamente para el estudio de la velocidad de flujo sanguíneo en experimentos psicofisiológicos, basadas en análisis espectral y en la obtención de parámetros no lineales de la señal en distintas condiciones experimentales. Los resultados mostraron diferencias entre los periodos de reposo y los periodos de realización de las tareas. Estos resultados pueden contribuir de forma importante al análisis de la influencia de factores individuales como la percepción visual y las tareas motoras en las variaciones de velocidad de flujo sanguíneo observadas durante la exposición a entornos virtuales.

Globalmente, los resultados de los distintos estudios han mostrado que la técnica de DTC se puede combinar fácilmente con entornos virtuales, incluso altamente inmersivos, ya que la calidad de las señales capturadas no se ve afectada por el hecho de estar navegando en un entorno virtual y, además, la monitorización de la señal de DTC no afecta a la capacidad de los participantes de centrar su atención en el entorno virtual. Sobre la base de los estudios realizados en la presente tesis, futuros trabajos con DTC podrán profundizar en el estudio de la presencia generada por distintos tipos de entornos y configuraciones de realidad virtual desde un punto de vista neurocientífico.

Abstract

The concept of presence, understood as the sensation of "being there", in a virtual environment, although being physically in a different place (for example, the experimental room), has been widely studied in the field of virtual reality to better understand the psychological mechanisms underlying virtual experiences.

In the literature, different techniques to measure presence have been proposed. Subjective techniques are mainly based on the use of questionnaires that allow the extraction of information about how the user has perceived the exposure to the virtual world. On the other hand, objective techniques are based on the analysis of user behavior during the exposure to the virtual environment and on the monitoring of physiological signals (such as electrocardiogram and skin conductance) to study possible changes in their parameters during the exposure.

One of the fields that is generating a growing interest in recent years is the analysis of brain activity to obtain information about the degree of presence. In this PhD Thesis, the use of Transcranial Doppler (TCD) is proposed to monitor brain activity during the exposure to virtual environments.

TCD is an ultrasound-based technique, which is non-invasive and has a high temporal resolution. It has not been used before in combination with virtual environments. It allows the measurement of blood flow velocity (BFV) in the main arteries of the brain. It has been widely used to monitor cerebral hemodynamics during cognitive tasks in psychophysiological research. These previous studies have shown that BFV measured

by TCD increases when users are doing a cognitive task when compared with repose periods.

The global objective of this PhD Thesis is to analyze if the TCD technique can be a complementary tool to analyze brain activity during the exposure to virtual environments and if, consequently, it can be used as a tool to study presence from a neuroscientific point of view.

The initial hypotheses are the following:

1. TCD will be easily used in combination with virtual reality systems, because it is a non-invasive technique that has been previously used in psychophysiological research.

2. It will be possible to use the BFV data obtained using TCD to analyze changes of brain activity during the exposure to virtual environments, allowing the use of the technique to study presence from a neuroscientific perspective.

3. There will be differences in the observed BFV variations during the exposure to virtual reality systems with different levels of immersion and different navigation methods, which will be associated to different levels of presence in participants.

4. There will be correlations between the degree of presence in virtual environments measured by questionnaires and certain parameters of the BFV obtained during the exposure to the environments.

5. Each of the different individual factors that constitute a virtual experience (such as visual perception or motor tasks to navigate) will have an influence on the observed BFV variations.

To study the proposed hypotheses, four different experiments were conducted, during which the BFV was analyzed in different conditions:

1. **Analysis of BFV in different navigation conditions**. In this study, BFV was monitored using TCD during the exposure to a highly immersive virtual environment in different navigation conditions.

2. **Analysis of BFV in different immersive conditions**. In this study, BFV was monitored using TCD during the exposure to a less immersive virtual reality configuration, in order to compare the results with those obtained in the first study with the highly immersive configuration.

3. **Analysis of BFV during a visual perception task**. In this study, the influence on BFV of a single aspect of the virtual experience (simple visual stimulation) was analyzed. In this case, the signal was monitored while the user was exposed to changing illumination conditions.

4. **Analysis of BFV during motor tasks**. In this case, the signal was monitored while the participant performed simple motor tasks to control a joystick. That way, the influence of this factor on the observed BFV variations during the virtual reality experience could be analyzed.

During the first two studies, it was observed that there was an increase in BFV when the participants were exposed to a virtual environment. This increase could be generated by the complex interaction of different factors, such as visuospatial interaction tasks, attention tasks, the creation and execution of a motor plan, emotional changes and presence variations. In fact, observed BFV variations were different depending on the kind of navigation and the degree of immersion. Significant correlations between mean BFV in middle cerebral arteries during the exposure to the different virtual reality configurations and specific responses of the presence questionnaires were found.

The other studies that were included in this PhD Thesis were focused on the analysis of individual factors (visual and motor factors) that contribute to the virtual experience. Signal processing techniques that had not been applied previously for the study of BFV in psychophysiological experiments were applied, based on spectral analysis and on the calculus of non-lineal parameters of the BFV signal in the different experimental conditions. Results showed differences between the repose periods and the periods during which the tasks were performed. These results can have

an important contribution for the analysis of the influence of individual factors such as visual perception and motor tasks on the observed BFV variations during the exposure to virtual environments.

Globally, the results from the different studies have shown that the TCD technique can be combined easily with virtual environments, even in the highly immersive ones, because the quality of the captured signals is not affected by the fact of being navigating in a virtual environment. Furthermore, the TCD signal monitoring does not affect to the capability of participants of focusing their attention on the virtual environment. On the basis of the studies conducted in the present PhD Thesis, future works with TCD could deepen in the study of presence generated by different kinds of virtual reality environments and configurations from a neuroscientific point of view.

Resum

El concepte de presència, entesa com la sensació de "ser-hi" en un entorn virtual, encara que trobant-se físicament a un lloc diferent (per exemple, al laboratori), ha estat àmpliament estudiat en l'àmbit de la realitat virtual, per tal de comprendre millor els mecanismes psicològics que acompanyen les experiències virtuals.

En la literatura, s'han proposat diferents tècniques per mesurar presència. Les tècniques subjectives es basen fonamentalment en l'aplicació de qüestionaris que permeten obtenir informació sobre la forma amb què l'usuari ha percebut l'exposició al mon virtual. Per altra part, les tècniques objectives es basen en l'anàlisi de comportaments de l'usuari durant l'exposició a l'entorn virtual i en la monitorització de senyals fisiològics (tals com l'electrocardiograma i la conductivitat de la pell) per tal d'estudiar els possibles canvis en paràmetres dels mateixos durant l'exposició.

Un dels àmbits que està generant més interés en els darrers anys és l'anàlisi de l'activitat cerebral com a tècnica per obtenir informació al voltant del grau de presència. En aquesta tesi, es proposa l'ús de la tècnica de Doppler Transcranial (DTC) per tal de monitoritzar l'activitat cerebral durant l'exposició a entorns virtuals.

DTC és una tècnica basada en ultrasons, no invasiva i amb una elevada resolució temporal, que no havia estat utilitzada fins ara en combinació amb entorns virtuals. Permet obtenir la velocitat de flux sanguini en les artèries principals del cervell. S'ha utilitzat àmpliament per monitoritzar l'hemodinàmica cerebral durant la realització de tasques cognitives en recerca psicofisiològica. Aquests estudis previs han mostrat que la velocitat

de flux sanguini que proporciona el DTC s'incrementa quan els usuaris realitzen una tasca cognitiva en comparació amb períodes de repòs.

L'objectiu global de la present tesi és analitzar si la tècnica de DTC pot ser una eina complementària per analitzar l'activació cerebral durant l'exposició a entorns virtuals i si, per tant, es pot utilitzar com a eina per estudiar presència des d'un punt de vista neurocientífic.

Les hipòtesi de sortida són les següents:

1. DTC es podrà utilitzar fàcilment en combinació amb sistemes de realitat virtual, ja que es tracta d'una tècnica no invasiva i que ja ha estat utilitzada en estudis previs de recerca psicofisiològica.

2. Les dades de velocitat de flux sanguini proporcionades per DTC es podran utilitzar per a analitzar canvis d'activitat cerebral durant l'exposició a entorns virtuals, permetent l'ús de la tècnica per a l'estudi de presència des d'una perspectiva neurocientífica.

3. Hi haurà diferències en les variacions observades en la velocitat de flux sanguini durant l'exposició a sistemes de realitat virtual amb diferents nivells d'immersió i diferents mètodes de navegació que aniran associats a diferents nivells de presència en els participants.

4. Hi haurà correlacions entre el grau de presència en entorns virtuals indicat pels qüestionaris i determinats paràmetres de la velocitat de flux sanguini obtinguts durant l'exposició als entorns.

5. Cadascun dels diferents factors individuals que composen una experiència virtual (tals com percepció visual o tasques motores per a navegar) tindran una influència en les variacions observades en la velocitat de flux sanguini.

Per tal d'estudiar les hipòtesi plantejades, es realitzaren quatre experiments diferents, durant els quals es va analitzar la velocitat de flux sanguini en diferents condicions:

1. **Anàlisi de la velocitat de flux sanguini en diferents condicions de navegació**. En aquest estudi, es va monitoritzar la velocitat de flux sanguini utilitzant DTC durant l'exposició a un entorn virtual altament immersiu en diferents condicions de navegació.

2. **Anàlisi de la velocitat de flux sanguini cerebral en diferents condicions d'immersió**. En aquest estudi, la velocitat de flux sanguini es va monitoritzar utilitzant DTC durant l'exposició a una configuració de realitat virtual menys immersiva, per tal de comparar els resultats amb els obtinguts en el primer estudi amb la configuració altament immersiva.

3. **Anàlisi de la velocitat de flux sanguini cerebral durant una tasca de percepció visual**. En aquest estudi, es va analitzar la influència d'un aspecte separat de l'experiència virtual (estimulació visual simple) sobre la velocitat de flux sanguini. En aquest cas, el senyal es va monitoritzar mentre l'usuari s'exposava a condicions canviants d'il·luminació.

4. **Anàlisi de la velocitat de flux sanguini cerebral durant la realització de tasques motores**. En aquest cas, el senyal es va monitoritzar mentre el participant realitzava tasques motores simples per a controlar un joystick. D'aquesta manera, es podia analitzar la influència d'aquest factor en les variacions de velocitat de flux sanguini observades durant les experiències de realitat virtual.

Durant els dos primers estudis, es va observar que hi havia un increment en la velocitat de flux sanguini quan els participants s'exposaven a un entorn virtual. Aquest increment podia estar degut a la interacció complexa de diferents factors com tasques d'interacció visuoespacial, tasques d'atenció, la creació i execució d'un pla motor, canvis emocionals i variacions de presència. De fet, les variacions en la velocitat de flux sanguini observades eren diferents depenent del tipus de navegació i del grau d'immersió. Es van trobar correlacions significatives entre la velocitat mitjana de flux sanguini en les artèries cerebrals mitges durant l'exposició a les diferents configuracions de realitat virtual i determinades respostes als qüestionaris de presència utilitzats.

La resta d'estudis realitzats en aquesta tesi es van centrar en l'anàlisi de factors individuals (visuals i motors) que contribueixen a l'experiència virtual. S'aplicaren tècniques de processat de senyal que no havien estat utilitzades prèviament per a l'estudi de la velocitat de flux sanguini en

experiments psicofisiològics, basades en anàlisi espectral i en l'obtenció de paràmetres no lineals del senyal en diferents condicions experimentals. Els resultats mostraren diferències entre els períodes de repòs i els períodes de realització de les tasques. Aquests resultats poden contribuir de forma important a l'anàlisi de la influència de factors individuals com la percepció visual i les tasques motores en les variacions de velocitat de flux sanguini observades durant l'exposició a entorns virtuals.

Globalment, els resultats dels diferents estudis han mostrat que la tècnica de DTC es pot combinar fàcilment amb entorns virtuals, fins i tot altament immersius, ja que la qualitat dels senyals capturats no es veu afectada pel fet d'estar navegant en un entorn virtual i, a més a més, la monitorització del senyal de DTC no afecta a la capacitat dels participants de focalitzar la seua atenció en el mon virtual. Basant-se en els estudis realitzats en la present tesi, futurs treballs amb DTC podran aprofundir en l'estudi de la presència generada per diferents tipus d'entorns i configuracions de realitat virtual des d'un punt de vista neurocientífic.

Contents

Chapter 1

Introduction

Immersive virtual environments (VEs) allow users to have unique experiences that were never before possible. Although participants of virtual reality (VR) experiences know from a cognitive point of view that the VE is not a real place, they act and think as if the VE were real. VEs take advantage of people's imaginative ability to psychologically transport them to another place. That is the essence of the concept of presence. Presence is the sense of "being there" (in a VE) although being physically in a different place (for example, the experimental room). The concept of presence has been widely analyzed to improve our understanding of the psychological mechanisms underlying VR experiences [1, 2, 3, 4].

One of the key aspects of the analysis is presence measurement. How can presence be measured? Different techniques and their combinations have been proposed and used to measure presence in VE [5, 6]. One attempt to measure presence has focused on the use of psychological measurement instruments like rating scales and subjective reports [7, 8, 9], commonly known as subjective measures of presence. Another group of presence measures (objective measures) has been based on the measurement of the physiological and behavioral responses to stimuli in an immersive VE [10, 11, 12, 13, 14]. However, no measure of presence has been universally accepted.

Recently, the application of brain activity monitoring techniques to contribute to presence measurement has been proposed. Presence has been

presented as an object of study for neuroscientists [15]. Some studies using techniques such as electroencephalogram (EEG) and functional magnetic resonance imaging (fMRI) to analyze brain activity during presence experiences have been published during the development of the present PhD Thesis [16, 17, 18].

In this work, transcranial Doppler sonography (TCD) is proposed as an alternative brain activity measurement technique that has never been used before in conjunction with VE. TCD is a non-invasive and secure technique based on ultrasounds that was first used in 1982 [19]. This tool has been widely applied to monitor cerebral hemodynamics during the performance of cognitive tasks in psychophysiological research. These previous studies have shown that mean blood flow velocity (BFV) obtained using TCD increases if users are doing a cognitive activity when compared to baseline periods [20, 21].

The present work has been developed as a collaboration between the *Instituto Interuniversitario de Investigación en Bioingeniería y Tecnología Orientada al Ser Humano* (*LabHuman group*) with a team of neurologists of the *Servicio de Neurología* from the *Hospital Universitari La Fe* (José Tembl and Vera Parkhutik). LabHuman had previous experience on the presence research field. In fact, my interest on the presence research field started during the EMMA Project (Engaging Media for Mental Health Applications), an European Community funded research project (IST-2001-39192), coordinated by LabHuman, which was focused on the analysis of the relationship between presence and emotions.

The starting point of the present work is the hypothesis that TCD may be a complementary tool to study brain activation and to analyze changes in regional cerebral blood flow (CBF) when a subject is being exposed to a VE, and thus it could be a tool to study presence in VEs from a neuroscientific point of view. The studies that have been proposed and developed to study this hypothesis will be described in the following sections.

1.1 Hypothesis and objectives

The general objectives of the present PhD Thesis are the following:

- To analyze if the TCD technique can be easily applied to subjects that are being exposed to VE. This implies that: (1) the use of TCD does not interfere with the user's capability to navigate and focus the attention on the VE; (2) measuring TCD while the subject is immersed in a VE does not modify the quality of the registries.

- To study BFV measured by TCD in VR settings associated with different levels of presence.

- To look for correlations of these BFV values with traditional presence measurements such as questionnaires.

- To analyze the contribution of individual factors of the VR experience to the changes in BFV.

The hypotheses associated to these objectives are the following:

- TCD will be easily applied in combination with VR settings. This hypothesis is supported by the non-invasiveness of the technique and by the fact that it has been successfully applied in previous studies in psychophysiogical research.

- BFV data measured by TCD can be used to analyze changes in brain activity when a subject is being exposed to a VE, and, consequently, the technique can be used to study presence in VEs from a neuroscientific point of view.

- Differences in BFV measured by TCD will be found in VR settings and experimental conditions associated with different levels of presence.

- There will be correlations between presence measured by questionnaires and parameters calculated from the BFV signal in the different experimental conditions.

- Each of the individual factors that constitute a VR experience (such as visual perception and motor tasks to navigate) will have an influence on the observed variations in the BFV signal.

In order to fulfill the previous objectives and to analyze if the previous hypotheses are correct, four different studies have been conducted during the present PhD Thesis:

1. **BFV analysis in different navigation conditions.** In this study, BFV was monitored using TCD during the exposure to a VE in a highly immersive configuration in different navigation conditions.

2. **BFV analysis in different immersive conditions.** In this study, BFV was monitored using TCD during the exposure to a less immersive VR configuration, in order to compare the results with those from the first study with the highly immersive configuration.

3. **BFV Analysis during a Visual Perception Task.** In this study, the influence of a single aspect of the VR experience (simple visual stimulation) on the BFV signal was analyzed. BFV was monitored while the user was exposed to changing conditions of illumination.

4. **BFV Analysis during Motor Tasks.** In this case, BFV was monitored while the participant performed simple motor tasks to control a joystick, in order to analyze the influence of this factor on the BFV variations observed during VR experiences.

In the following subsections, the specific hypotheses and objectives from each of these studies are presented.

1.1.1 BFV analysis in different navigation conditions

The subjects of this experiment were exposed to a VE with two different navigation conditions (free navigation and automatic navigation) in a highly immersive configuration: a CAVE-like system. A CAVE (Cave Automatic Virtual Environment) is an immersive VR environment where projectors are directed to the walls of a room-sized cube. Two breaks in presence (BIPs) were forced in the experience during the free navigation conditions by means of abrupt interruptions in the projection of the VE (with different intensity in each of the BIPs). TCD was used to monitor BFV in middle cerebral arteries (MCAs) and anterior cerebral arteries

(ACAs) during the experience. A presence measurement questionnaire (SUS-questionnaire [22]) was used to validate the variations in presence that the subject experienced in the different situations. The exact experimental design will be described later.

In this study, the main goal is to analyze if there are BFV variations when subjects are exposed to a VE.

One secondary objective is to compare the BFV variations in different moments of the VR experience associated to the two navigation conditions and to check if there is a correlation between accepted measures of presence and the observed BFV variations.

Another secondary objective is to obtain the BFV response during the situations that cause a BIP and during the recoveries to the normal state of the VE after the BIP, thus complementing the results obtained in previous studies about BIPs that have monitored peripheral physiological measures [23]. As two BIPs of different intensity are used, it will be analyzed if the intensity of the BIP has any influence on the temporal and magnitude features of the BFV signal during the analyzed periods.

The hypotheses of this work are the following:

- There will be differences in the presence measurement questionnaire results corresponding to the two navigation conditions. Higher presence scores are expected in the user-controlled navigation.
- It is expected a global increment in BFV values during the exposure to virtual environments when compared with baseline periods. Since middle cerebral arteries (MCAs) supply mainly lateral parts of the brain involved in the creation of a motor plan, which is potentially implied in a presence experience, it is expected a BFV increment in these arteries. Increments in anterior cerebral arteries (ACAs), which supply the prefrontal cortex, are also expected, due to the emotional components and executive control functions potentially related with a presence experience.
- The BFV variation in the free navigation condition will be higher than the variation in the automatic navigation condition, at least in some of the vessels, because more brain areas are involved and active when the user is controlling the navigation.

- There will be a variation in the BFV signal in response to each BIP, which can be studied by means of parameters that evaluate the temporal and magnitude evolution of this signal. In the moment of formulating the hypothesis, it was not clear if an increment or decrement would be observed. A possibility was that the BIP would generate an increase of brain activity, occasioned by the possible surprise and rise in the level of attention due to an unexpected event. Another possibility was that the BIP would generate a decrease in brain activity due to the sudden disappearance of stimuli and navigation from the VE that generated a decrease in presence.

- There will be a variation in the BFV signal when the normal navigation is recovered after each BIP, which will also be studied calculating parameters about the temporal and magnitude evolution of the BFV signal.

1.1.2 BFV analysis in different immersive conditions

This study was performed as a continuation of the previous study, in order to analyze if the BFV variations obtained with a highly immersive configuration (the CAVE-like system) were maintained if a less immersive configuration was used (projection in a single screen). A reduced number of volunteers participated in the experiment.

The main goal of the study is to analyze if the BFV variations that are observed when subjects are exposed to a VE are different in environments with different levels of immersion, understanding this concept as the degree to which a virtual environment submerges the perceptual system of the user [24] (in a stereoscopic CAVE-like environment and in a monoscopic single projection screen), and with different navigation possibilities (self-guided versus automatic navigation). Another objective is to check if BFV variations are related with presence variations when subjects are exposed to different immersive and navigation conditions of the VE.

A high sense of presence measured by questionnaires is expected in the stereoscopic CAVE-like environment because more sensory cues are available (it allows users to perceive objects in three dimensions and move

around these objects with the corresponding perspective correction depending on the instantaneous position of the user's head). Furthermore, previous studies support this hypothesis [25, 26, 27].

A higher level of presence is also expected in the self-controlled navigation condition as supported by previous studies [28].

Finally, it is hypothesized that BFV variations between repose and exposure to the VE will be higher in the configurations that generate a higher level of presence.

1.1.3 BFV analysis during a visual perception task

In this study, the cerebral hemodynamic response to a specific kind of task was analyzed: visual perception. This is an issue that has been previously studied with TCD, using experimental designs that included visual stimuli with different degrees of complexity [29, 30, 31, 32, 33, 34, 35]. In this case, a simple visual perception task was selected, similar to that used in the study from Aaslid [29]. Given the importance of occipital (posterior) brain regions in visual perception, the bilateral posterior cerebral arteries (PCAs) signal was monitored as in previous studies.

The main goal of the study is to analyze BFV responses to a simple visual perception task presented in a hardware configuration similar to the settings used in VR experiences (a large screen where a uniform white illumination was projected). Furthermore, another important goal of this work is to apply signal processing methods to isolate the variations in BFV caused by the visual perception task from the variations caused by other factors. In order to do that, the frequency analysis can be useful to identify spectral components associated with the variations in BFV generated by cognitive stimuli in order to achieve a deeper understanding of the processes that occur in response to these stimuli.

The hypothesis regarding BFV responses to the presented visual stimuli in the large screen is that there will be an increment similar to those observed in the previous studies that have included visual stimuli with approximately the same degree of complexity [29]. Regarding the signal processing methods, the initial hypothesis is that, by analyzing the low-frequency components of the frequency spectrum, it will be possible to

isolate the variations caused by the cognitive stimuli from the variations caused by other factors, therefore yielding a more precise analysis of the magnitude and temporal evolution of the BFV in response to the stimuli.

1.1.4 BFV analysis during motor tasks

In this study, the cerebral hemodynamic response to another specific kind of task that occurs during the exposure to VE was analyzed: motor tasks to control a joystick.

The objectives of this study are basically two:

1. To study the MCAs BFV responses to a simple motor task usually performed in VE (hand movements to control the joystick).

2. To analyze if there are differences between repose and hand-movement periods in the non-linear parameters of the maximum BFV signal in the MCAs (such as entropy, correlation dimension, fractal dimension and maximum Lyapunov exponent, that will be described later). There are previous studies using TCD that have found differences in BFV non-linear parameters corresponding to different experimental conditions [36, 37, 38], although these experimental conditions were not associated to the performance of different cognitive tasks.

The main hypothesis of this study is that an increment in the complexity measures will be observed if the user is performing hand movements to control the joystick when compared with repose periods.

1.2 Structure

The present document is organized in the following chapters:

- **CHAPTER 1: Introduction**. It is the current chapter, which covers introductory aspects about the present PhD Thesis. The following points are described: a description of the motivation of the present PhD thesis, a summary of the different studies that have been conducted (including their objectives and specific hypotheses),

and the current description of the different chapters included in the document.

- **CHAPTER 2: Presence**. In this chapter, the state of the art about presence studies is described. Different points about presence during VR experiences are detailed, including: the concept of presence and its different dimensions, the causes and consequences of presence, and the relationship of presence with other factors related to the VR experience such as performance, emotions, and technological issues. A special section is dedicated to presence measurement techniques due to its importance for the present PhD Thesis. In this section, traditional measures of presence during the exposure to VE are analyzed, including both subjective and objective methods. The recent application of neurological measurement techniques for presence research is summarized, including works that have applied EEG or fMRI. The previous research about breaks in presence and its application for presence measurement is also described.

- **CHAPTER 3: Transcranial Doppler Monitoring**. This chapter describes the technique of Transcranial Doppler Monitoring and the state of the art of this technique in fields of application related to the goals of the present PhD Thesis. The chapter starts with a description of the physical bases of Doppler ultrasound (with an explanation of the Doppler effect and the Doppler ultrasound principles). Then, the particularities of the Transcranial Doppler ultrasound technique are described, including aspects such as the devices used for the measurement, features of the BFV signal measured by TCD and its relationship with cerebral blood flow, cerebral areas supplied by the different cerebral arteries that can be monitored using TCD, and the advantages and disadvantages of TCD when compared with other techniques to monitor brain activity. The chapter continues with a description of previous studies in psychophysiological research that have applied TCD to monitor brain activity during the performance of different cognitive tasks, including visual perception, language tasks, motor tasks, emotions, vigilance and attention tasks and video games playing. Finally, the chapter dedicates a final sec-

tion to summarize the signal processing techniques that have been applied in previous TCD studies to analyze the BFV signal monitored using this technique. Mostly linear techniques have been applied, so the greatest part of this section is dedicated to the description of this kind of techniques. The rest of the chapter describes some studies that have applied non-linear analysis to the study of the BFV signal, although not in the field of psychophysiological studies.

- **CHAPTER 4: Methods**. This chapter describes the methods that have been applied in the different studies that have been conducted in the present PhD Thesis: (1) BFV analysis in different navigation conditions, (2) BFV analysis in different immersive conditions, (3) BFV analysis during a visual perception task, and (4) BFV analysis during motor tasks. For each of the studies, several points are described, including the hardware and software used, the number and characteristics of the participants, the monitored vessels, the experimental procedure, the questionnaires used to analyze different aspects of the experiment and the data analysis techniques that have been applied to analyze the BFV signal. These data analysis techniques vary depending on the study, and range from simple analysis such as the calculus of the mean or more complex procedures based on spectral analysis or on the obtention of non-linear parameters of the BFV signals. The statistical techniques applied to compare between different experimental conditions are also summarized in this chapter.

- **CHAPTER 5: Results**. In this chapter, the results from the different studies are summarized.

  In the case of the study about BFV in different navigation conditions, one of the aspects that is included is a comparison of SUS questionnaire responses and mean BFV between the different navigation conditions, and a correlation analysis between questionnaire responses and mean BFV values at each period. A comparison of percentage BFV variations between repose and navigation in the different experimental conditions is also described. Finally, the temporal variations in BFV during BIPs and during the recoveries from

BIPs are summarized (the analysis includes the calculus of the BFV maximum percentage variation and response time).

In the study about BFV in different immersive conditions, the results from SUS questionnaires and the BFV variations between repose and navigation in the different experimental conditions are described.

In the study about visual perception tasks, the results from the spectral analysis of the BFV signal are described, and the temporal parameters from the low-frequency estimation of this BFV signal are detailed (maximum percentage variation and response time, obtained taking into account the information of the spectral analysis).

Finally, in the study about motor tasks, the non-linear parameters calculated in the different experimental conditions are indicated and the differences between conditions are summarized.

- **CHAPTER 6: Discussion**. In this chapter, the results obtained in the previous studies are discussed. The chapter starts with a general discussion about the technique of TCD and other neurological measures of brain activity, and with a justification of the experimental designs that have been followed in the studies included in the present PhD Thesis. Then, the chapter continues with a separate analysis of the results obtained in the different studies.

  There is a section about the study of BFV in different navigation conditions. This section starts with a discussion about the differences in presence as measured by questionnaires in the different experimental conditions. Then, the kind of analysis that has been made in the BFV signal is justified, and possible explanations to the differences observed between the different experimental conditions are proposed. The results from the analysis of BFV during BIPs and during the recovery from BIPs are also discussed and possible interpretations about the observed behavior are explained.

  The chapter continues with another section about the study of BFV in different immersive conditions. This section analyzes the possible factors that can justify the observed differences in SUS-responses and

BFV variations between the various experimental conditions that are considered in this study.

The next section of the chapter is focused on the study about a simple visual perception task. The importance of the signal processing methods that have been applied to obtain a more reliable analysis of the BFV responses to visual perception is highlighted. The contributions of this work to the VR field are also commented.

Finally, the last section of the chapter analyzes the results from the study about simple motor tasks (moving the joystick). Possible interpretations of the differences observed in the non-linear features that have been calculated in repose and in the moments associated with hand movements are proposed and commented.

- **CHAPTER 7: Conclusions**. This is the last chapter of the document. It describes the relevance of the results from the present PhD Thesis in different fields such as virtual therapy and augmented cognition. A list of the publications that have been generated from the different studies of this PhD Thesis is included. Finally, future works and analyses are described in the last section.

- **APPENDIXES**. Six appendixes have been included:

  1. **List of acronyms**. In this appendix, the equivalences of the different acronyms and abbreviations used during the present work are detailed.
  2. **SUS Questionnaires**. In this appendix, the SUS questionnaire is included, as used in the experimental sessions with VR.
  3. **BFV analysis in different navigation conditions. Analysis of Normality** . The normality of the different variables included in this study was analyzed to decide if parametric or non-parametric tests should be applied in the statistical analysis. The results from this analysis of normality are included in the different tables of this appendix.
  4. **BFV analysis in different immersive conditions. Analysis of Normality**. In this case, the analysis of normality in the

study about BFV in different immersive conditions is included.

5. **BFV Analysis during a Visual Perception Task. Analysis of Normality**. Analogous analysis for the study in which BFV data during a visual perception task were analyzed.
6. **BFV Analysis during Motor Tasks. Analysis of Normality**. Finally, the analysis of normality about the variables of the study about BFV during the performance of motor tasks is included.

Chapter 2

Presence

2.1 Concept of presence

Immersive Virtual Environments (VE) are being used successfully in many fields [39]. As described in chapter 1, VE take advantage of people's imaginative ability to psychologically transport them to another place. In order to study the psychological mechanisms underlying experiences in VE, one of the concepts that are analyzed is presence [1, 2, 3, 4].

A comprehensive explication of the concept of presence can be found in the web page from the International Society for Presence Research (http://www.ispr.info). It is based on a discussion that took place via the presence-l listserv during the spring of 2000 among members of a community of scholars interested in the presence concept. *Presence (a shortened version of the term "telepresence") is a psychological state or subjective perception in which even though part or all of an individual's current experience is generated by and/or filtered through human-made technology, part or all of the individual's perception fails to accurately acknowledge the role of the technology in the experience. Except in the most extreme cases, the individual can indicate correctly that s/he is using the technology, but at some level and to some degree, her/his perceptions overlook that knowledge and objects, events, entities, and environments are perceived as if the technology was not involved in the experience. Experience is defined as a person's observation of and/or interaction with objects, entities, and/or*

events in her/his environment; perception, the result of perceiving, is defined as a meaningful interpretation of experience [40].

Although there is still a lack of concise definitions of the construct of presence, a commonly used definition considers that presence is the subjective experience of being in one place, even when you are physically located in another [7, 41, 3, 42].

Although the concept of presence is also applied to non-immersive and non-interactive media, this work will focus on VEs. Presence in VEs can be described as the sense of being in a VE instead of being in the room where the virtual reality (VR) experience is taking place. It is the process of discerning and validating the existence of self in the natural world, a process humans have engaged in since birth. A sense of presence in a VE derives from feeling as if you exist within, but as a separate entity from, a virtual world that also exists [43].

Other definitions avoid the need for a subjective sense of presence by suggesting that the effectiveness of the coupling of perception and action between the user and the (virtual) environment defines presence [14]. This perspective has generated body-centered definitions which look at several components to determine presence, such as the plausibility of the VE and the sensory motor contingencies [44].

2.2 Dimensions of presence

Presence is a multi-dimensional concept. Researchers in this field state that there are different types or dimensions of presence. Little is currently known concerning which types exist, but several dimensions have been proposed by different researchers.

Major proposed dimensions are included in the International Society for Presence Research website (http://www.ispr.info). We include here a summary of the main dimensions:

- **Spatial Presence**. It occurs when part or all of a person's perception fails to accurately acknowledge the role of technology that makes it appear that s/he is in a physical location and environment different from the actual location and environment in the physical

world. In these cases, the user will forget that the environment is created by the technology and will feel as being somewhere else.

- **Sensory Presence**. It occurs when part or all of a person's perception fails to accurately acknowledge the role of technology that makes it appear that s/he is in a physical location and environment in which the sensory characteristics correspond to those of the physical world. In this case, the user perceives the objects, events and people as they do in the physical world (visual, auditory, tactile). It does not mean that they are exactly as in the real world, but the user perceives them like that. The user will feel as if the VE was real.

- **Social Realism**. It occurs when part or all of a person's perception fails to accurately acknowledge the role of technology that makes it appear that s/he is in a physical location and environment in which the social characteristics correspond to those of the physical world. The user perceives that the objects, events, and people in the VE could exist in the physical world, and they act and respond the same way as the would do in the physical world. All the environment will see realistic.

- **Engagement**. It occurs when part or all of a person's perception is directed toward objects, events, and people created by the technology, and away from objects, events, and people in the physical world. The user will not pay attention to other events (such as sounds or movements) that may be occurring in the experimental laboratory while navigating in the VE. The user will feel that the VR experience was really involving.

- **Social Presence** (distinct from social realism). It occurs when part or all of a person's perception fails to accurately acknowledge the role of technology that makes it appear that s/he is communicating with one or more other people or entities. There are several aspects that can be considered when talking about social presence:

  - **"Social actor within the medium"**. It occurs when part or all of a person's perception fails to accurately acknowledge

the role of technology in her/his perception of being engaged in two-way communication with another person or people, or with an artificial entity, when the communication is in fact one-way. The user thinks s/he is interacting with the virtual character.

- **"Co-presence"**. It occurs when part or all of a person's perception fails to accurately acknowledge the role of technology in her/his perception that the people with whom s/he is engaged in two-way communication are in the same physical location and environment, when in fact they are in a different physical location. The user thinks that the virtual characters are all with him/her in the virtual space.
- **"Medium as social actor"**. It occurs when part or all of a person's perception fails to accurately acknowledge the role of technology in her/his perception of being engaged in communication with another entity when in fact the other entity is merely a technology or medium (e.g., computer, television, etc.). The user will feel that the computer with which is interacting seems like a person.

2.3 Causes and consequences of presence

2.3.1 Causes of presence

A large number of possible causes of presence have been proposed. Presence can be generated individually by one of these causes, or may be based on a complex interaction of several circumstances. Most authors agree that presence is determined by two general categories of variables [45, 46, 47, 48, 8, 49]:

- **Media Characteristics**. Media characteristics are divided into media form and media content variables.
  - **Media form**. Media form includes the properties of a display medium (e.g., the extent of sensory information presented, the degrees of control that users have over positioning their sensors

within the environment, or users' ability to modify aspects of the environment).

  - **Media content**. Media content includes the objects, actors and events represented by the medium.

- **User Characteristics**. They refer to relevant individual aspects ranging from age, gender or cultural variables to users' perceptual, cognitive, motor abilities, prior experience with mediated experiences, willingness to suspend disbelief, and personality differences.

2.3.2 Consequences of presence

As has already been stated, presence in VE is studied to understand the psychological mechanisms underlying VR experiences. It is important to analyze the consequences that are observed when a user is present in a VE. These consequences may occur individually or in various combinations, and depend on a large number of complex interacting factors. They include but are not limited to:

- Increases or decreases in physiological arousal.
- A number of different emotional responses.
- Empathy and connectedness with other people.
- Feelings of self-motion
- Learning, improved task performance and skill training.

2.4 Relationship of presence with other factors of the VE experience

In the following points, results from previous studies that analyze the relationship of presence with other factors of the VE experience will be described: performance, emotions and technology. In some of the studies, references to questionnaires or other techniques to measure presence will be mentioned. These techniques will be described in detail in section 2.5.

2.4.1 Presence and performance

There is not a proven evidence that a higher presence in a VE is related with a higher performance of the tasks presented during the exposure to that VE. Contradictory conclusions can be extracted from previous studies.

There are studies that have obtained a positive correlation between presence and performance. For example, Biocca et al. [50] studied the response of 96 subjects that were exposed to an infomercial on TV and found a significant correlation between the parts of the presence questionnaire related with "departure" and the average recognition speed and factual memory from the infomercial.

However, other studies found no correlation between presence and performance. For example, Mania and Chalmers [51] compared lectures given in three different conditions (with 18 subjects in each condition): the real world, a virtual classroom, and an auditory-only environment. They found that presence was not correlated with the acquisition of knowledge during the lecture.

There are even authors that argue that, in some cases, it is observed precisely the opposite behavior: less presence might generate a better performance [52], for instance, when a more abstract view of an environment is more helpful for completing the task.

2.4.2 Presence and emotional state

Scientific literature has frequently paid more attention to the environmental determinants of presence than to other issues such as user characteristics or media content. As Schubert et al. [53] pointed out, in some theoretical models, the sense of presence had been seen as the outcome, or a direct function of immersion. However, the other characteristics (media content and user characteristics) have to be also taken into account. Some VR studies have proven that users can feel present even in the impoverished environments world that some VEs provide [54]. Emotions are an essential part of how people experience the world, and their study could have important implications for a better understanding of the virtual experience [55].

2.4.2.1 Fear of heights

Some studies have used stressful VE associated with the fear of heights and have analyzed presence in the participants of the study and the emotional reactions of these participants during their exposure to those VE.

Regenbrecht et al. [56] investigated the relationship between presence and fear of heights, both measured by questionnaires. In an experiment with 37 non-phobic subjects they did not find a significant correlation between presence and fear. A regression analysis showed that presence was the best predictor of fear.

In an explorative study with 10 subjects being treated for fear of heights, Schuemie et al. [57] found a significant correlation between fear and presence reported on questionnaires, but no significant correlation between presence and reduction of acrophobia (also measured through questionnaires).

Usoh et al. [58] compared three different kinds of navigation in a VE that contained a virtual pit used to generate emotional reactions related to fear of heights in participants (complementing a previous study from Slater et al. [59]):

- Locomotion by walking-in-place (virtual walking).
- Locomotion by flying (advance in the gaze direction).
- Real walking (participants were free to walk around the entire virtual scene in the same manner as in a real environment).

The VE was divided in two rooms: a training room and an experimental room, each of 5 x 4 meters. The training area was a room with several pieces of furniture and a door in the opposite wall. When the user went through the door, s/he entered in the experimental room, which contained a virtual pit. The user was on a 0.7 m wide ledge 6 m above the floor of the room. The ledge went all the way around the room and there was a chair on the ledge on the far side. The floor below contained living room furniture. A direct path from the doorway to the chair would mean walking out onto “empty space”.

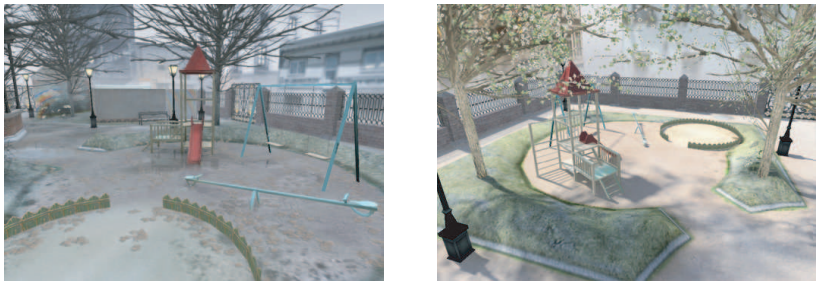

(a) (b)

Figure 2.1: (a) Screen capture of the sad park. (b) Screen capture of the happy park.

Their results related to the mode of locomotion showed that real walking was significantly better than both virtual walking and flying in simplicity and naturalness. Furthermore, subjects felt present in the VE and their subjective presence was higher in the case of real walkers than in the case of virtual walkers. Finally, it was also found that real walking through the VE generated a highly compelling virtual experience. Emotional reactions were observed when participants found themselves at the open door to the ledge above the pit. Posterior studies [11] have found physiological reactions in response to this stressful VE.

2.4.2.2 VR Mood Induction Procedures

VR Mood Induction Procedures were developed in LabHuman during the EMMA project. The VE used for these procedures is a park whose appearance changes depending on the emotion to be induced. For example, in the case of sadness, the park is grey, it is a cloudy day, the trees have no leaves and the music that is heard is a very sad piece. Images from the happy and sad parks are shown in Fig. 2.1.

Inside the park, there is a band stand where a virtual and interactive version of the statements of the Velten procedure is included [60]. Participants have to order the sentence and think about its meaning, while related images are visualized. There is also a summer cinema where a

movie related to the emotion can be visualized. During the exposure to the environment, the system will measure mood with Visual Analogue Scales (VAS) in different moments, after different key events.

These VEs were tested in an experiment with 80 university students [61]. The environments were retro-projected in a big screen (400x150 cm) and participants used a wireless pad to navigate. Data from subjective mood state measurements showed that the four emotional environments (sad, joy, anxiety, and relax) were able to produce mood changes in the users. No changes were observed for the neutral environment. Regarding the role of mood on the sense of presence, the results showed differences between emotional and neutral environments in some presence measurements. The participants reported a higher degree of realism, they also judged the experience as more real, they felt more present, and they experienced a higher emotional involvement. It seems that sense of presence is determined by the emotions that a virtual environment is able to provoke in the user, and emotional issues are important variables in order to enhance presence.

2.4.2.3 Other kinds of emotional VE

Other studies have analyzed other kinds of stressful VE, for example, related to the emotional reaction generated when talking to an audience of people. Slater et al. [62] made a between-subject study with 10 subjects and 2 conditions (positive and negative audience) and showed that, in a regression analysis, people experiencing a higher level of presence were prone to report more negative reactions to a negative audience and more positive reactions to a positive audience.

Riva et al. [63] analyzed the efficacy of VR as an affective medium. The results confirmed its efficacy: the interaction with anxious and relaxing virtual environments produced anxiety and relaxation. Furthermore, it was found a circular interaction between presence and emotions: on one side, the feeling of presence was greater in the emotional environments; on the other side, the emotional state was influenced by the level of presence.

Bouchard et al. [64] made a study to investigate the direction of the causal relationship between anxiety and presence. The participants of the

study were 31 people who suffered from snake phobia and were immersed in a virtual Egyptian desert. It was a within-subject design. In one condition, they were told that the environment was safe and contained no snakes. In the second condition, they were told that dangerous snake could appear at any moment during the exposure to the environment. Brief measures of presence were taken during the exposure. State anxiety appeared to have a direct impact on the subjective feeling of presence. However, large changes in anxiety were associated with smaller changes in presence. The influence of a ceiling effect that restricts the range of potential change in presence would be one plausible explanation for this.

2.4.3 Presence and technology

Presence is a property of an individual and varies across people and time; it is not a property of a technology commonly referred to as a medium, although technologies with specific characteristics are likely to evoke a similar set of presence responses across individuals and across time (for example, an IMAX 3D presentation typically produces greater presence in viewers than a small television presentation).

An important aspect pointed out by Slater and Wilbur [42] is the distinction between "presence" and "immersion":

- **Immersion**: an objective description of aspects of the system such as field of view and display resolution.

- **Presence**: a subjective phenomenon such as the sensation of being in a VE.

Likewise, Kalawsky [48] states that presence is essentially a cognitive or perceptual parameter, whilst immersion essentially refers to the physical extent of the sensory information and is a function of the enabling technology.

Next, some technical variables and their relationship with presence will be described.

2.4.3.1 Stereoscopy

Stereoscopy is a technique for creating the illusion of depth and 3D imaging while presenting a different image to each eye. Several previous studies have focused on the relationship of this variable with presence; most of them found that the use of stereoscopic presentation increased presence ratings.

Hendrix and Barfield [26] found significant effects for stereoscopy in a study with a within-subject design. Subjects participated in three consecutive experiments in which one of three variables was manipulated: stereoscopy, head tracking, and geometric field of view of 10°, 50°, or 90°. Presence was measured using a two-item questionnaire. Results showed that the reported levels of presence were significantly higher when head tracking and stereoscopic cues were added and when wider fields of view were presented (50° and 90°).

Other studies were conducted to analyze the role of stereoscopy, image motion, and screen size on the sense of presence using subjective and objective measures of presence. These studies [65, 66] found that participants experienced higher subjective levels of presence in scenes of a film that were presented stereoscopically. However, in these experiments, the presentation of stereoscopic and monoscopic sections of the film was not randomly varied. In a later study, Freeman et al. [67] adapted methods of continuous assessment of TV picture quality to monitor presence. While viewing a VE, subjects could manipulate a handheld slider indicating their sense of presence. The study manipulated stereoscopic and motion parallax cues within video sequences (containing monoscopic and stereoscopic segments). The results showed that the presentation of both stereoscopic and motion-parallax cues was associated with higher presence ratings.

In a more recent study [27], participants in a within-subject design were exposed to four conditions based on two variables: stereoscopy and moving or still images. Results showed that stereoscopy had a positive effect on the magnitude of the participant's automatic postural responses (which were measured via a magnetic tracking device). Post-test subjective ratings of presence, vection, and involvement were also higher for the stimuli presented stereoscopically. Authors concluded that increasing the

realism of a moving display by adding stereoscopic information increased both postural responses to the display and subjective ratings of presence.

IJsselsteijn et al. [68] employed a large projection display with a 50° horizontal field of view and manipulated image motion and stereoscopic presentation in a within-subjects factor and screen size in a between-subjects factor. Results demonstrated a positive effect of stereoscopic presentation on the lateral postural responses and on post-test subjective ratings of presence.

Finally, LabHuman has also analyzed the influence of stereoscopy on the sense of presence [69]. This study investigated how stereoscopy affects the sense of presence and the intensity of the positive mood that users feel in VEs (which were the parks developed in the EMMA project). A between-group design was used, and 40 volunteers were randomly assigned to one of two experimental conditions (stereoscopy vs. no stereoscopy) and to one of two emotional VEs (relaxation or joy). The participants' emotions were assessed before and after the VR experience. Presence was measured with two post-experiment questionnaires (ITC-SOPI and SUS). Results showed that there were no differences between stereoscopic and monoscopic presentations in VEs (neither in the subjective sense of presence nor in the emotional reactions). The results do not replicate findings from previous studies that show that subjective feelings of presence are enhanced by stereoscopic stimuli presentation. However, in those previous works neutral VEs were used. In this study, emotion inducing environments were used, and it may be that stereoscopic presentation is not as critical for this specific purpose.

2.4.3.2 Type of display

Another technological factor that may have an influence in presence ratings is the type of visual display that is used in the VR system. Examples of visual displays include desktop VR systems, head-mounted displays (HMD), CAVE-like environments and other projection screen systems.

Examples of real displays can be visualized in Fig. 2.2 (photograph of a 4-wall CAVE-like system) and Fig. 2.3 (images of a single projection screen system and an HMD).

Figure 2.2: User navigating inside a CAVE

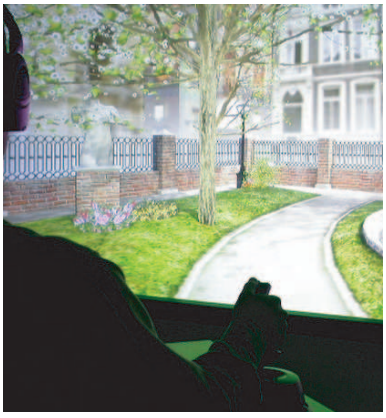

(a)

(b)

Figure 2.3: (a) Virtual environment projected on a single screen. (b) Head Mounted Display for visualizing virtual environments.

Previous studies have compared several types of visual displays to analyze their influence on the presence variable. These studies have found that a higher degree of immersion can contribute positively to achieve a greater level of presence.

In a study from Axelsson et al. [25], the sense of presence in a CAVE-like system was compared to the sense of presence a desktop VR system. The task that the 44 users that participated in the experience had to perform was to solve a 3D puzzle together. Half of them used a CAVE-like system, and the other half used desktop VR. Presence was measured using a single question at the end of the experience, and it was found that subjects had a significantly higher sense of presence in the CAVE-like system.

In a study from our group [70], the role of immersion (using different kinds of visual display) and media content on the sense of presence was analyzed. The experiment compared three immersive systems (a PC monitor, a rear projected video wall, and a head-mounted display) and two virtual environments, one involving emotional content and the other not. Two self-report presence measurement questionnaires were used to compare among six groups of 10 people each. The results suggest that both immersion and affective content have an impact on presence. However, immersion was more relevant for non-emotional environments than for emotional ones. According to data, the sense of presence in the non-emotional environment depends mainly on immersion. Both the HMD and the big screen elicited a higher sense of presence than a non-immersive system, namely, a PC monitor. However, in an emotional environment, a PC monitor was able to elicit a high sense of presence, in the same way as the big screen. On the other hand, the HMD condition was not the most presence-enhancing technology, possibly because of the less comfortable HMD setup.

Sutcliffe et al. [71] have also analyzed presence, memory and interaction in three different virtual environments: a CAVE-like system, an Interactive WorkBench and a Reality Room. Eighteen undergraduate students took part in the study. It was found that the CAVE was remembered better, had better usability, and provided a better sense of presence to its users.

Finally, Juan and Pérez [72] made a comparison of presence and anxiety

in an acrophobic environment that was viewed using a CAVE-like system and a HMD. Twenty-five participants took part in the study. After each visualization, participants answered the SUS questionnaire. It was found that the CAVE-like system induced higher levels of presence and anxiety in users. A correlation was found between the level of presence and the level of anxiety.

2.4.3.3 Field of view

Other studies have focused on the analysis of the field of view (FOV), defined as the effective horizontal and vertical angles through which the world can be seen. Most of them found that wider FOVs were associated with increased presence ratings.

Prothero and Hoffman [73] made a study with 38 subjects (within-subject design) and two conditions: visual scene masking at the eye (60° FOV) and an unmasked screen (105° FOV). Presence was measured using a 5-item questionnaire. A significantly higher presence was found for the wider FOV.

Lin et al. [74] studied the effects of FOV in a VE on presence, enjoyment, memory, and simulator sickness. A scale designed to assess subjects' engagement, enjoyment, and immersion (E2I) was developed. Items to examine subjects' memory of the VE were included. Simulator sickness was examined using the Simulator Sickness Questionnaire [75]. Using a within-subjects design, data were collected from 10 subjects at four FOVs (60°, 100°, 140°, and 180°). The VE, Crayoland, was presented in a driving simulator. Results indicated that presence, enjoyment, and simulator sickness varied as a function of display FOV. Subjects exhibited higher presence subscale scores with increasing FOV. Presence and simulator sickness were positively correlated.

Kim and Biocca [50] performed an experiment with 96 subjects that were exposed to a infomercial on television (between-subject design), with six conditions based on two variables: FOV and illumination of the VE. In this case, the viewing angle levels selected were 9.8 degrees, 21.5 degrees, and 33.7 degrees. Screen sizes of television sets were manipulated, while the viewing distance remained constant. Presence was measured using

their own telepresence scale. In this study with television, no significant effect was found for the FOV. Illuminating the real environment, making it more distracting, did not have either any significant effect on presence.

Hendrix and Barfield [26] analyzed stereoscopy, head tracking and geometric Field of View (geometric FOV), defined as the viewing-angle used to design the visual display, which can be independent of the regular FOV. It was a within-subject design with 12 subjects. Two aspects of presence were evaluated: (1) the sense of 'being there' and (2) the fidelity of the interaction between the virtual environment participant and the virtual world. It was found that the geometric FOV used to design the visual display highly influenced the reported level of presence, with more presence associated with a 50^o and 90^o geometric FOV when compared to a narrower 10^o geometric FOV.

2.4.3.4 Other visual aspects

Other visual aspects have also been studied.

Welch et al. [28] analyzed the influence of pictorial realism, delay of visual feedback and interactivity on presence. It was a within-subject design with 20 subjects and eight conditions. The subjects were exposed to two VEs (a simulated driving task) and they were asked to indicate which one generated a higher sense of presence (paired comparison procedure), scoring the difference by means of a 1-100 scale. As predicted, realism and interactivity increased presence while delay of visual feedback diminished it.

Barfield et al. [76] studied the type of input device used for navigating within the VE, the display update rate, and their influence on presence. Eight subjects participated in the study. Three different update rates were analyzed: 10, 15 and 20 Hz. It was found that an update rate of at least 15 Hz was critical for the user feeling present in the VE.

Stanford et al. [77] analyzed the effects of latency. The VE used in the study included two rooms: the first was normal and non-threatening; the second was designed to evoke a stressful response (the pit room previously described). Participants were assigned to two groups with different latency: low latency (around 50 ms) or high latency (around 90 ms). Participants in

the low latency condition had a higher self-reported sense of presence and a statistically higher change in heart rate between the two rooms than did those in the high latency condition. There were no significant relationships between latency and simulator sickness

In another study which used the same VE (the pit room) [78], it was examined the influence of visual realism on presence. Two different renderings of the VE were visualized by 33 participants, in a head-tracked HMD, with a random order. In one of the conditions ray casting was used achieving a result equivalent to OpenGL based per-pixel local illumination, and in the other condition full recursive ray tracing was used. Reported presence was obtained by questionnaires following each session. The results indicate that reported presence was significantly higher for the ray tracing than for the ray casting condition.

2.4.3.5 Other sensorial inputs

Although frequently undervalued, sounds and other sensorial inputs clearly are important in generating presence. Multimodal VE create richer, more complete and coherent experiences that may contribute to an enhanced sense of presence [79].

Dihn et al. [80] performed a study with 322 subjects to analyze the effects of tactile, olfactory, audio and visual sensory cues on a participant's sense of presence in a VE, and on their memory about that environment. Results show that if the modalities of sensory input are increased, it is possible to increase sense of presence and memory. The addition of tactile, olfactory and auditory cues to a VE increases the sense of presence and the memory of the VE. The increase of the level of visual detail did not result in an increase in the user's sense of presence or memory.

In a previous study, Hendrix and Barfield [81] had analyzed the effect of spatialized sound, and compared it with no sound, or non-spatialized sound. Sixteen subjects participated in two within-subject studies, which compared spatialized sound with no sound, and spatialized sound with non-spatialized sound. The users were allowed to navigate freely throughout several VEs. Survey questions were used to evaluate their level of presence, the VE realism, and the interactivity between the participant and the

environment. The results indicated that the addition of spatialized sound significantly increased the sense of presence but not the realism of the virtual environment.

Lärsson et al. [82] analyzed the influence of realistic auditory stimuli on the creation of a sensation of self-motion. Twenty-six participants took part of a within-subjects design with three factors: type of sound source (moving, still, artificial), velocities (20, 40, 60 deg/s) and acoustic rendering (marketplace, anechoic). Results related to presence showed that the still and moving sounds induced higher presence than the artificial. For velocity, the 60 deg/s induced higher presence than the other velocities. Finally, it was shown that the marketplace environment generated a higher presence that the anechoic.

On another study, Bormann [83] analyzed the impact of the utility of audio spatialization (and not fidelity of audio spatialization) on presence. Subjects performed a searching task. In some conditions, they looked for a music-playing radio (active sound source), and in other conditions, they searched for another object, while the playing radio was stationary. Independently of this, the music that was played on the radio was fully spatialized or directional but non-attenuated. It was found that the utility of the audio had an influence on presence, but in an unexpected way. When searching for the sound source, a lower fidelity of audio increased presence while decreasing performance.

2.4.3.6 Interaction

Interactivity has been described as the extent to which users can participate in modifying the form and content of a mediated environment in real time [84]. Several studies have analyzed the influence of interactivity on presence, finding that presence is usually increased when interactivity is provided.

In a study from Welch et al. [28] (previously described in the section about other visual effects), the influence of interactivity on presence was one of the factor analyzed. Two levels of interaction were allowed: the user could be the active driver of a car, or s/he could be a passive observer. It was found that interactivity increased presence.

In another work by Schubert et al. [85], they continued the analysis of the influence of interaction on reported presence. They performed three studies. In the first one, they were interested in whether the sense of presence, and especially spatial presence, would correlate with an assessment of the interaction possibilities. They surveyed players of computer games, asking them first to describe their possible interactions with the game world, and their comprehension of these interaction possibilities. Then, they presented them the IPQ presence questionnaire [53]. In the second study, the participants experienced a VE by means of a fully tracked HMD. Participants could either move freely through the VE or they were shown a prerecorded interaction sequence from a first-person perspective. In the third study, the goal was to test if the mere illusion of interaction could generate an increase of spatial presence. In one condition, participants were told that they could interact with virtual characters, and that they would react. In the other condition, participants were told that virtual characters would not react to their actions. A correlative study showed that self-reported interaction possibilities correlated significantly with spatial presence. It was found that possible self-movement significantly increased spatial presence and realness. Furthermore, even the illusion of interaction, with no actual interaction taking place, significantly increased spatial presence.

Barfield et al. [76] analyzed the display update rate and the type of input device used for navigating within the VE (in a study also described in the section about other visual aspects). Regarding navigation, two different devices were used: a joystick or a SpaceBall. The task was to search for an object hidden within a VE that represented a virtual Stonehenge. It was found that the type of input device had no effect on the user's sense of presence.

In another study, Slater et al. [44] analyzed the influence of body movement on presence. Twenty subjects participated in the study. They had to walk through a virtual field of trees and count the number of trees with diseased leaves. A 2x2 between-subjects design was used. One factor was tree height variation, and the second factor was the complexity of the task. Tree height variation was associated with body movement, as long as the VE with greater variation in tree height required subjects

to bend down and look up more than the other condition. The results showed a significant positive association between reported presence and the amount of body movement, in particular head yaw, and the extent to which subjects bent down and stood up.

Other aspect related with interaction is head tracking. In a study already explained in the previous section about FOV, Hendrix and Barfield [26] found a highly significant effect for head tracking.

2.5 Presence measurement

But how can presence be measured? Some possible measures have been mentioned in the previous points. However, in this section the possible options for presence measurements will be described in detail.

A good presence measurement should be [81, 86, 41]:

- Relevant, having a direct connection with presence and its components.
- Reliable, having proven test-retest repeatability.
- Sensitive, having sensitivity to variations in the variables affecting presence.
- Non-intrusive, avoiding unintentional degradation of performance and/or sense of presence.
- Convenient/portable, low cost and easy to learn and administer.

Different techniques and their combinations have been proposed and used to measure presence in VEs [5, 6]. As has been stated in chapter 1, some techniques have been based on the application of psychological measurement instruments like rating scales and subjective reports [7, 8, 9] and other techniques have been based on the monitoring of physiological and behavioral responses to stimuli in an immersive VE [10, 11, 12, 13, 14]. Although no measure of presence has been universally accepted, in the following sections the most important approaches will be summarized.

2.5.1 Subjective measures

Subjective measures, specially, questionnaires, have been developed to analyze presence and its components as a result to the exposure to a VE. Some of these questionnaires include:

- **Igroup Presence Questionnaire - IPQ** [87]. It was constructed from previous questionnaires, generating a 75-item questionnaire. A factor analysis revealed eight factors. Three of them were related with presence itself, and the other five were identified as immersion factors. The presence factors were: spatial presence (relation between the VE as a space and the own body), involvement (awareness devoted to the VE) and realness (sense of reality attributed to the VE). The immersion factors were: quality of immersion (richness and consistency of the multimodal presentation), drama (perception of dramatic content and structures), interface awareness (awareness of interfaces that distract from the VE experience), exploration of VE (possibility of exploring the VE) and predictability (ability to predict and anticipate what will happen next).

- **ITC Sense of Presence Inventory - ITC-SOPI** [8]. It focuses on users' experiences of media, with no reference to objective system parameters. Initially, 63 items were proposed. Exploratory analysis (principal axis factoring) revealed four factors: sense of physical space (which includes items related to a sense of physical placement in the mediated environment, and interaction with and control over parts of the mediated environment), engagement (which is related to the feeling of being psychologically involved and enjoying the contents of the environment), ecological validity (which is associated with the perception of the mediated environment as lifelike and real), and negative effects (which include adverse physiological reactions such as dizziness). After the validation, 44 items were retained which loaded on one of these factors.

- **Kim and Biocca's Questionnaire** [50]. This is a questionnaire thought for measuring presence in the context of television viewing. Telepresence is defined here as a television viewer's feeling of being

present in the mediated environment created by the auditory-visual information emitted from the television. Eight items were included in the questionnaire, based on the definition of telepresence and other presence measures used in previous studies. Two component factors were found for telepresence: departure (not being present in the unmediated environment) and arrival (being present in the mediated environment).

- **Lombard and Ditton's Questionnaire** [88]. This questionnaire was based on the definition of presence as the perceptual illusion of non-mediation. A questionnaire containing 103 items measuring presence and additional items measuring subjects' tendency to suspend disbelief were included. The factor analysis revealed seven dimensions: immersion (immersion, involvement and engagement in the mediated environment), parasocial interaction (crossing the border between physical and mediated environment to interact with people in real time), parasocial relationships (related to feelings of frienship toward people in the mediated environment), physiological responses (including items from the Simulator Sickness Questionnaire [75], which measures physiological responses to the mediated environment), social reality (comparisons between how events could occur in the non-mediated world and in reality), interpersonal social richness (how well the media user can observe various interpersonal communication cues) and general social richness (emotional, responsive, personal)

- **Presence Questionnaire - PQ** [9]. This questionnaire measures the degree to which individuals experience presence in a VE and the influence of possible contributing factors on the intensity of this experience. Thirty-two items were included in the definitive version. Three subscales were identified from the cluster analysis of the PQ data: involved/control (perceived control of events in the VE, responsiveness of the VE to user-initiated actions, how involving were the visual aspects of the VE, and how involved in the experience the participant became), natural (extent to which the interactions felt natural, extent to which the VE was consistent with reality, and how

natural was the control of locomotion through the VE), and interface quality (whether control devices or display devices distract from task performance, and extent to which the participants felt able to concentrate on the tasks).

- **Presence and Reality Judgement Questionnaire - PRJQ** [7]. This questionnaire was designed to assess presence and reality judgement. Items were based on other questionnaires present in the literature and on the definitions of presence and reality judgement. The final result was a 77-item questionnaire in Likert scale ranging from 0 to 10. Items were related to different concepts: reality judgement, presence, emotional involvement, interaction, control, attention, realism, perceptual congruence and expectations. Factor analysis revealed three factors, which were called: reality judgement, interaction/external correspondence, and attention/absorption.

- **SUS questionnaire** [22]. This questionnaire has evolved over different studies. It is based on several Likert scale items ranging from 1 to 7. These questions are variations on three themes [89]: the subject's sense of being there, the extent to which the VE becomes more real or present than actual reality, and the locality, or the extent to which the VE is thought of as a place that was visited rather than just a set of images. The presence score is taken as the mean of all the answers (SUS Mean) or as the number of answers that have a high score (SUS Count).

Questionnaires have also been proposed to predict a person's tendency to experience the cognitive state of presence [90].

However, measurements based on questionnaires have received some criticism. Freeman et al. [67] showed their inherent instability. Furthermore, Slater [91] discussed the possibility that the concept of presence was brought into by the fact of asking questions about it. Finally, presence questionnaires can only be used after the exposure to the VE, so it is not possible to have data about the temporal evolution of the participant's presence during the session.

In order to avoid this limitation, some studies have tried to adapt questionnaires in order to monitor different variables during the virtual

experience. For example, IJsselsteijn and de Ridder [92] used a continuous registration of measures during the exposure to the VE; a control was shown in the screen and users could move it in real time to indicate their level of presence. As previously explained, Freeman et al. [67] proposed a handheld slider as a new form of direct subjective presence evaluation. Slater and Steed [93] used a virtual counter that measured the transitions from the VE to the real one.

Other qualitative measures, such as thinking aloud, interviews and group discussions have already been proposed [94].

2.5.2 Objective measures

In order to avoid the problems inherent to subjective measurements, objective techniques have been suggested. There are two main kinds of objective techniques to analyze presence: behavioral measures and physiological measures. These measures are usually obtained during the VR experience rather than following it, so they can be used for real-time monitoring during the exposure. However, although they are called objective, they do not generate a direct measure of presence. Instead, presence is assumed to be related in some way with the degree of change in parameters that can be obtained from physiological measures or from behavioral observation.

In the following paragraphs, studies that have used behavioral or physiological measures in presence research will be summarized.

2.5.2.1 Behavioral measures

Behavioral measures analyze how the user acts when navigating in a VE, in order to estimate the level of presence that s/he is feeling. Several studies have been made focused on different behavioral aspects:

- **Postural responses**. Freeman et al. [27] stated that users in a mediated environment that makes them feel present will respond to stimuli within the environment as they would to stimuli in the real world. They measured postural responses to a video sequence from a car in a rally track, presented to 24 volunteers using both monoscopic and stereoscopic presentation. They found that the magnitude

of the postural responses observed was higher in the stereoscopic presentation. Furthermore, presence estimated by questionnaires after the experience was also higher in this kind of presentation, although postural and subjective measures were not significantly correlated.

- **Conflicts between real and virtual cues**. Slater et al. [89] analyzed the effects of dynamic shadows in an immersive VE. Eight subjects had to perform tasks in a VE. Two measurements of presence were used: a questionnaire, and a behavioral measure. Each method gave similar results, and the two measures were significantly correlated. In order to take the behavioral measure, an extra task was given to the users during the VR experience: they were told that a radio will appear in the VE in four different moments during the VR experience. Whenever they heard a sound from the radio, they had to look for it and point towards it, pressing a button on the hand-held mouse to switch it off. The sound came from a real radio which was moved to four different positions during the experience, but the virtual radio was always in the same place. Therefore, the subject would hear the sound coming from a different location compared to the visible position of the radio. The idea was that a high degree of presence would lead to the subject pointing towards the virtual radio rather than the real one. A numeric value for presence was obtained as the ratio of angles of real to virtual pointing directions. This value was significantly correlated with the results from the presence questionnaire that was used in the experiment. Furthermore, it was found that the angular ratio increased with exposure to shadows in visually dominant people. This effect was not observed for people who were dominant on the auditory scale.

- **Reflex responses**. Nichols et al. [12] performed two experiments, one of them focused on the comparison between direct performance measures and rating scales to assess presence. The VE display medium (HMD vs desktop) and the presence or absence of sounds were varied in the experience. Direct performance measures were made analyzing reflex responses. The VE was programmed with a startle event that occurred randomly. Participants' reactions were classified

into three categories: no reaction, a verbal report of a reaction, or a physically noticeable reaction. There was compatibility between reflex responses and rating scales.

- **Facial analysis**. Huang et al. [55] proposed that the concept of presence had to be reexamined in terms of people's emotional engagement with reality and their environment. Any theory of presence had to take emotional factors into account. Validated psychological techniques for assessing emotions by subjective report, behavioral observations, and facial analysis could all be applied to increase the understanding of the concept of presence.

Another group of measures estimates the quality of actions made in the VE, such as the completion time and the error rate [95], the number or actions required to finish a task [96] and the transfer of abilities to the real world [97].

The main disadvantage of all these behavioral measures is that they are closely related to the contents of the VE and are usually not generalizable for any kind of VE.

2.5.2.2 Peripheral physiological measures

The objective measures that are most commonly used are based on peripheral physiological signal monitoring. Dillon et al. [98] argued that, compared to conventional media, highly immersive mediated experiences are expected to elicit greater subjective ratings of presence and more intense physiological responses. The relationship between the two variables has to be systematically investigated.

Examples of physiological measures that have been analyzed include:

- **Cardiovascular parameters and skin conductance**. Several studies have performed analysis of cardiovascular parameters and skin conductance during the exposure of subjects to VE, and have tried to analyze the relationship of these measures with presence.

  Skin conductance is measured by passing a small current through a pair of electrodes placed on the surface of the skin [99]. The technique

is based on the Ohm's law, which states that skin resistance (R) is equal to the voltage (V) applied between two electrodes placed on the skin surface, divided by the current (I) that passes through the skin (R = V/I). Skin conductance recordings are typically taken from locations on the palms of the hands. Results have shown that within normal ranges of ambient room temperature and thermoregulatory states of subjects, there is a high correlation between sympathetic system activity and skin conductance [100].

On the other hand, the **cardiovascular system** is under control of both the sympathetic and parasympathetic branches of the autonomic nervous system [101]. Electrocardiography (ECG or EKG) is a transthoracic interpretation of the electrical activity of the heart over time captured and externally recorded by skin electrodes (leads). The extremity leads include the unipolar leads of the right arm, left arm, and left leg and the bipolar leads I (left arm – right arm), II (left leg – right arm), and III (left leg – left arm), with the right leg serving as ground. These leads are often approximated by electrodes placed on the torso, rather than the limbs. For most psychophysiological applications, a lead II or comparable configuration works well. Heart period, or the time in ms between adjacent heart beats, is typically measured between successive R spikes in the ECG. It is usually converted to heart rate in beats/min. On the other hand, measures of heart rate variability (HRV) have been deeply analyzed, including two international committee reports on the origins and implications of heart rate variability [102, 103]. High frequency HRV reflects variations in vagal control, and has been applied as an index of parasympathetic cardiac control.

A photograph of a self-made system to monitor skin conductance and ECG is shown in Fig. 2.4.

In the following points, some of the studies that used skin conductance and cardiovascular parameters to study presence will be summarized:

- Meehan et al. [11, 104] conducted several experiments that com-

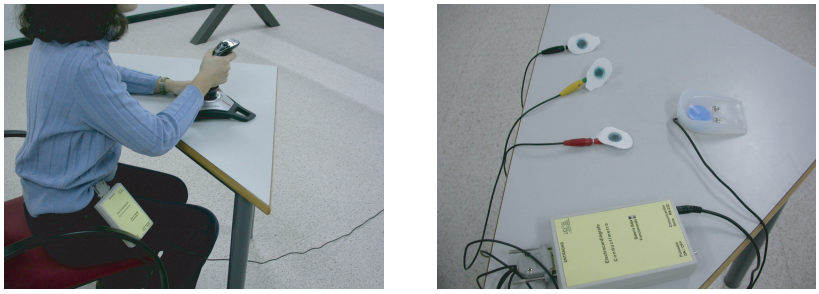

(a) (b)

Figure 2.4: (a) User navigating while ECG and skin conductance are recorded using a self-made system developed for LabHuman during the EMMA project. (b) Detail of the device used for monitoring ECG and skin conductance.

pared participants' physiological reactions to a non-threatening virtual room and their reactions to a stressful virtual height situation (the pit room previously described). Basically, their analysis is based in the following premise: a VE will evoke physiological responses similar to those evoked by the corresponding real environment, and greater presence will evoke a greater response; if so, these responses can serve as objective surrogate measures of subjective presence.

Changes in heart rate consistently differentiated among conditions with more sensitivity and more statistical power than the other physiological measures. Authors considered that heart rate can be used as a measure of presence: it is reliable (heart rate was higher in the pit room for 90% of the exposures to the VE), valid (hear rate was the signal that correlated best with the reported presence), sensitive (heart rate reliably distinguished between subjects reaction in the pit room and the training room, which assured at least a minimal sensitivity) and objective (physiological measures are inherently better shielded from both subject bias and experimenter bias than either re-

ported measures or measures based on behavior observations).

The same aspects were studied for skin conductance. It was found that skin conductance satisfied the conditions to be used as a measure of presence, but to a lesser extent than heart rate.

Moreover, the results showed that significant increases in heart rate measures of presence appeared with the inclusion of a passive haptic element in the VE, with increasing frame rate and when end-to-end latency was reduced.

- Ravaja examined the effects of a small talking facial image on emotional responses [105]. Respiratory sinus arrhythmia (RSA, activity corresponding to respiratory-locked oscillations in HR), which is a non-invasive index of parasympathetic nervous system function [106], was used to index attention and engagement. The results showed that the talking facial image (when compared to a static facial image) was considered more pleasant and arousing. In addition, it was associated with a decrease in RSA in individuals with high dispositional behavioral activation system sensitivity. It was suggested that a small talking facial image contributes to sustained attention and engagement given that it may increase the sense of presence. These findings also suggest that RSA may be a particularly useful and easily applicable psychophysiological measure in presence research.
- Wiederhold et al. [107] analyzed the relationship between subjective ratings of presence and physiological responses to a VE. Heart rate and skin resistance were monitored. Seventy-two participants were exposed to a VE about an airplane flight. The percentage variation of heart rate and skin resistance between baseline and exposure were calculated. Results showed a correlation between Presence Questionnaire scores and both heart rate and skin resistance parameters.

- **Other measures**. Although heart rate and skin conductance are the most common measures used in combination with VR systems, other measurements have also been proposed.

- Laarni et al. [108] proposed the use of eye tracking technology. Their starting point was the assumption that the degree to which people attend to a continuous stimulus flow is related to their state of presence. They proposed several ways of using eye tracking to measure presence: to measure the degree to which the user's attention is distracted away from the media stimuli, to analyze which aspects of the mediated information the user looks at and the order in which different areas of media stimuli are processed, and to classify attentional states to focused attention and distributed attention on the basis of eye fixation duration.
- Antley et al. [109] analyzed the onsets of muscle activity using surface electromyography (SEMG) in different conditions. In one condition, SEMG was captured in real world situations, while subjects were walking on a normal floor, on a narrow ribbon along the floor, and on a narrow beam platform elevated from the floor. In another condition, the same situations were reproduced in a CAVE-like environment. Twelve participants did the three types of walking in a within-groups design. The mean number of SEMG activity onsets per unit of time followed the same pattern in the virtual environment as in the physical environment. Usually, studies which analyze physiological responses are based on the premise that if the user is present in the VE, the physiological responses observed during the exposure would be similar to those observed during a similar situation in the real world. This analysis has usually been related to stressful situations [11, 23]. However, this work from Antley et al. [109] has used a non-stressful environment in which whole body sensory motor contingencies are used, opening the door to new studies that may deepen in this kind of analysis.

2.5.2.3 Neurological measures

VE have opened up many new research possibilities and applications in behavioral neuroscience, cognitive science and psychology [110]. For ex-

ample, VR has been used as a tool to help to understand brain mechanisms related to body ownership [111, 112]. Moreover, it has been argued recently that VR is not only a tool for neuroscience, but that presence is also an object of study [15].

The brain activity measures that have been proposed for presence measurement are the electroencephalogram (EEG) and the functional magnetic resonance imaging (fMRI).

EEG

EEG reflects the brain's electrical activity, and in particular post-synaptic potentials in the cerebral cortex. Scalp-recorded EEG signals are thought to be generated by the addition of excitatory and inhibitory post-synaptic potentials in the cortical pyramidal neurons [113]. EEG signals always represent the potential difference between two electrodes, an active electrode and the reference electrode. This technique has a temporal resolution of milliseconds, making it possible to analyze both fluctuations of EEG dependant of task demand, and differentiate between functional inhibitory and excitatory tasks. In general, low frequencies (delta and theta) show large synchronized amplitudes, whereas high EEG frequencies (beta and gamma) have small amplitudes due to a high degree of desynchronization in the neuronal activity [114]. Different placements for the electrodes are used: the International 10-20 system [115], the 10-10 system [116] and the 5-5 system [117]. In recent years, high-resolution EEG systems with numbers of electrodes ranging from 64 up to as many as 256 have been introduced, with the goal of increasing the spatial sampling of the EEG. The main goal of any EEG source imaging technique is to draw reliable conclusions about sources underlying scalp recorded signals, that is, to solve the inverse problem.

EEG has been described as a possible tool for obtaining objective indicators of presence, to detect brain states and detect transitions in the user, who can feel present in the virtual world and then change to feel present in the real world [118]. It was speculated that adaptive autoregressive parameters can be used to discriminate between states.

Some studies have been made investigating EEG responses to VE ex-

periences, but without relating them to the concept of presence [119, 120]. Baumgartner et al. [16] were the first to use EEG to analyze neural correlates of spatial presence in arousing virtual environments without interaction. The VE used was a virtual roller coaster scenario. Twelve children and eleven adolescents participated in the study. There was a control session, with a horizontal roundabout track, and several realistic rides (with ups, downs and loops). EEG and skin conductance were captured during the experience. It was found in both groups that spatial presence was higher in the realistic rides (when compared with the control condition). Furthermore, this was accompanied by increased electrodermal reactions and activations in parietal brain areas known to be involved in spatial navigation. Parietal processing centers in turn stimulated the insula as the core region for generating body sensations and the posterior cingulate which is strongly involved in emotion processing. On the other hand, children showed higher spatial presence, but less activity in some prefrontal areas than adolescents. These prefrontal areas are involved in the control of executive functions. The higher increase in spatial presence observed in children can have its origin on the fact that their frontal cortex function is not fully developed. Recently, preliminary results from a study to analyze the parietal activity in interactive VR were presented [121]. The goal of the study was to analyze if the parietal activity that was found in the study from Baumgartner et al. [16] would also appear during a free navigation in a virtual environment. The environment was a virtual maze in which the participant performed a wayfinding task while EEG activity was monitored. Results showed that parietal activation also occurred in this interactive VR.

fMRI

The other tool that has been proposed for presence measurement is fMRI. This technique is used for the study of metabolic and vascular changes that accompany changes in neural activity. It has a spatial resolution of about $1mm^3$ but often is around $3mm^3$ for whole-brain functional studies. A sample of the MRI signal in the whole brain is obtained around each 2-3 seconds (which is called repetition time of image acquisition), de-

pending on how data were acquired and on the needed spatial resolution [122]. fMRI has its own temporal limitation due largely to the latency and duration of the hemodynamic response to a neural event, which begins within a second and peaks 5-8 seconds after the neural activity peaked [123, 124]. It is mandatory that the participant does not move during the whole length of the experimental session.

fMRI is based on the Blood Oxygen Level Dependend method (BOLD), which measures the ratio of oxygenated to deoxygenated hemoglobin in the blood across regions of the brain. As neural activity increases, so does metabolic demand for oxygen and nutrients. A T2-weighted signal that depends on the oxygenation of hemoglobin is used. As neural activity increases, so does metabolic demand for oxygen and nutrients. As oxygen is extracted from the blood, increases in deoxyhemoglobin can lead to a initial decrease in BOLD signal. However, this is followed by an increase, due to an overcompensation in blood flow that tips the balance towards oxygenated hemoglobin. It is this that leads to a higher BOLD signal during neural activity [125]. The BOLD signal corresponds relatively closely to the local electrical field potential surrounding a group of cells – which is itself likely to reflect changes in post-synaptic activity – under many conditions.

fMRI contains sources of signal variation due to noise, including a slow drift of the signal in time and higher frequency changes in the signal due to physiological processes accompanying heart rate and respiration. That is why most fMRI experiments use discrete events that can be repeated many times.

fMRI is not a tool that can be easily combined with VR environments. First of all, a test platform has to be developed to allow the exposition to the VE while capturing the fMRI images without altering in a significant way any of both technologies. The user has to be inside the magnetic resonance machine in supine position and with minimum head movement, and devices used to navigate and interact in the VE have to work inside high magnetic fields with minimum electromagnetic interference. An image of a fMRI machine can be visualized in Fig. 2.5.

fMRI was used in a study related to VR and presence [126]. Subjects reported experiencing an illusion of presence in VR via a magnet-friendly

Figure 2.5: Varian 4T fMRI, part of the Brain Imaging Center, in: Helen Wills Neuroscience Institute at the University of California, Berkeley.

VR image delivery system despite the constraint of lying down with their head immobilized in an enclosed environment. fMRI results were not reported in the study. Other related studies only presented preliminary results [127].

Recent works [17, 18] have complemented the study with the roller coaster scenario that has been previously described [16]. In the first study [16], EEG was used to monitor brain activity. However, the most recent works [17, 18] have analyzed fMRI data captured during the exposure to the same VE. Each ride lasted 102 s in total, whereas the different phases where divided into the following time scheme: anticipation phase 30 s, dynamic phase 60 s and end phase 12 s. In total, eight different roller coaster rides were presented, four High Presence and four Low Presence roller coaster rides. Results from the fMRI analysis show that the presence experience evoked by the virtual roller coaster scenario is associated with an increase in activation in a distributed network, which comprises extrastriate areas, the dorsal visual stream, the superior parietal cortex (SPL) and inferior parietal cortex (IPL), parts of the ventral visual stream, the premotor cortex (PMC), and the brain structures located in the basal and mesiotemporal parts of the brain. The network is modulated by the dorso-

lateral prefrontal cortex (DLPFC). The DLPFC activation strongly correlates with the subjective presence experience (the right DLPFC controlled the sense of presence by down-regulating the activation in the egocentric dorsal visual processing stream, the left DLPFC up-regulated widespread areas of the medial prefrontal cortex known to be involved in self-reflective and stimulus-independent thoughts). In contrast, there was no evidence of these two strategies in children. This difference is most likely attributable to the prefrontal cortex that is not fully matured in children.

Neural correlates of presence appear to be a promising measure because they potentially provide data that is not influenced by the participant's interpretation as it happens with subjective measures. However, the analysis of brain processes' data can be extremely difficult since very little is known about the neural processes that are involved in the complex experience of presence.

2.5.3 Breaks in presence (BIPs)

The concept of break in presence (BIP) has been proposed to contribute to the analysis of presence during the VR experience. The BIPs approach is based on the idea of analyzing presence during the VR experience itself, instead of only using a post-experience questionnaire to assess presence.

The use of BIPs to analyze presence was first proposed by Slater and Steed [93]. A BIP occurs when the participant stops responding to the virtual stream and instead responds to the real sensory stream [128]. At different times during a VR experience, the participant would switch between interpreting the sensory inputs as coming from the VE or as coming from the real world. Participants in the study by Slater and Steed [93] were asked to report transitions from virtual to real. A probabilistic Markov chain model was constructed to model these transitions, and this model was used to estimate the equilibrium probability of being present in the VE. A positive correlation was found between questionnaire-based presence and presence as estimated by the number of reported BIPs. A simplified version of this model was used in a posterior study about BIPs [129] in which the number of BIPs was counted as reported by subjects, without using the Markov Chain analysis. This simplified analysis also found a

relationship between presence and BIPs: the reported presence variable was negatively correlated with the number of BIPs.

After the first studies about BIPs, it was proposed that it would be interesting to analyze jointly physiological measures and BIPs [130, 128]. The idea was to search for a common pattern of physiological response to a BIP independently of the actual event that caused it.

Following this proposal, some studies were conducted in order to study the responses to BIPs during the exposure to VE [131, 23]. Twenty volunteers participated in the study in a four-walled CAVE-like system. The VE was a bar in which there were five virtual characters who could spoke and gesticulate towards the participant. The total experience lasted about 5 minutes. BIPs were forced by the experimental design: the projections were forced to go white, generating identifiable anomalies in the audiovisual experience. Four BIPs were forced during the whole experience, at approximately evenly spaced intervals during the bar experience.

Garau et al. [131] focused on a qualitative analysis of interviews from these experiments. Analysis of these interviews clearly showed that these anomalies were subjectively experienced by subjects as breaks in presence. The interviews also revealed that BIPs experienced by subjects had different causes (not only the whiteouts, but also environmental factors and the interaction with virtual characters). These different types of BIPs could range in intensity resulting in varying recovery times as indicated by subjects in these interviews. In general, participants experienced a longer recovery after whiteouts than after character-related BIPs.

Slater et al. [23] made an analysis of physiological responses to BIPs. Physiological measures including ECG and skin conductance were recorded during the whole experiment. The skin conductance waveform was extracted for $\pm$ 10s around each BIP point, and averaged over all BIPs over all participants to find a characteristic GSR response to the induced BIPs. Regarding heart rate, a decrease was observed in the forced BIPs.

Chapter 3

Transcranial Doppler Monitoring

3.1 Doppler Ultrasound

Doppler ultrasound is a non-invasive diagnosis technique that can be used to measure blood flow and blood pressure by transmitting high-frequency sound waves (ultrasound) and receiving the echoes of those waves that come from the red blood cells. In the following paragraphs, the Doppler Effect, which is the basis of the technique, and the Doppler Ultrasound principles will be described.

3.1.1 Doppler Effect

3.1.1.1 Introduction

Let us suppose that there is a sound focus in a point of space (perturbation focus) and an observer in another point of space. Both the focus and the observer are in repose. For simplicity, we will consider that the focus is emitting at a single frequency f_0. The emission focus F vibrates and generates a perturbation in the environment. A wave surface is generated ($S1$) which advances a distance $\lambda = c \cdot T$ in a period T, being c the propagation velocity. At this moment, an analogous and new wave surface is generated

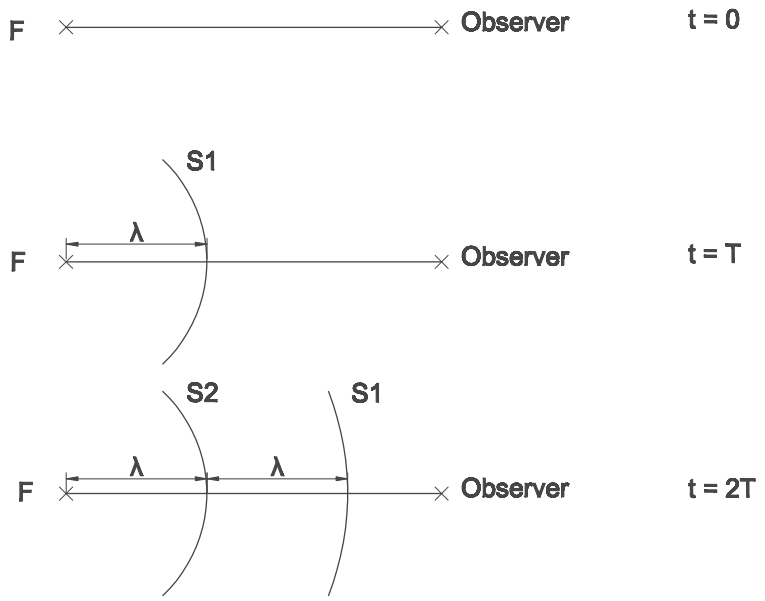

Figure 3.1: Both the emission focus and the observer are in repose. The wave surface advances λ in a period T. The focus position and wave surface at 0, T, and 2T are represented.

in the focus ($S2$). As both wave surfaces are propagating at the same velocity, the distance between them (λ) will remain constant The frequency that the observer will receive will be the original frequency: $f_r = f_0$. No Doppler Effect occurs. The process can be visualized in Fig. 3.1.

3.1.1.2 Emission focus in movement

What happens when there is relative movement between the observer and the perturbation focus? Let us consider first the case in which the emission focus is moving with a velocity v' smaller that the wave propagation velocity c, approaching to an observer in repose. In the time T that happens between the generation of the wave surface $S1$ until the emission of the analogous $S2$, the emission focus advances to a new position F'. The

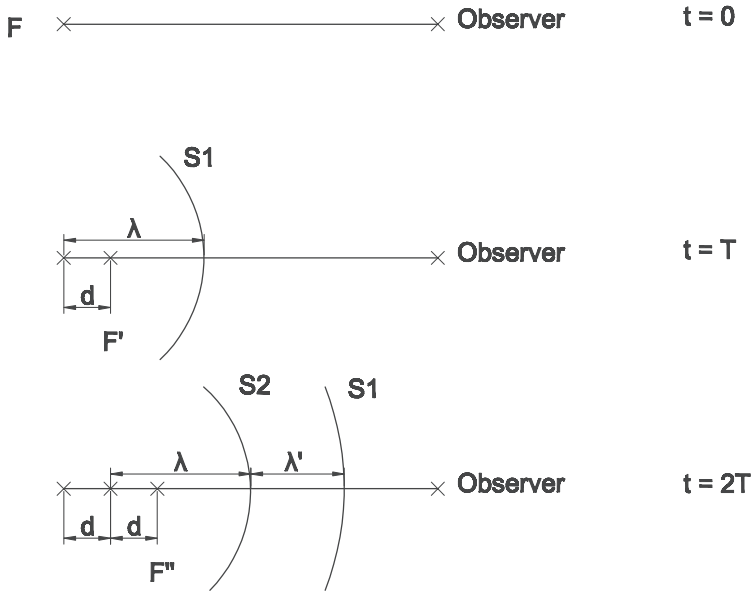

Figure 3.2: The observer is in repose, but the emission focus is in movement, and advances d each period T. The wave surface advances λ in a period T. The focus position and wave surfacez at 0, T, and 2T are represented.

distance between the original position and the new one will be: $d = v' \cdot T$. The distance between $S1$ and $S2$ will be reduced precisely by this value [132] (equation 3.1).

$$\lambda' = \lambda - v' \cdot T \tag{3.1}$$

Expressing the previous equation in terms of frequency, it results 3.2:

$$\frac{c}{f_r} = \frac{c}{f_0} - \frac{v'}{f_0} \Rightarrow f_r = f_0 \cdot \frac{c}{c - v'} \tag{3.2}$$

The evolution at different moments can be visualized in Fig. 3.2.

The observer will perceive a frequency f_r different from the original one f_0. If the focus is approaching the observer, the perceived frequency will be higher than the original. On the contrary, if the focus is moving away from the observer, the perceived frequency is lower than the original. That is why when we hear a siren from a car coming the sound is perceived as more high-pitch and when it goes away, we perceive it as more low-pitch.

3.1.1.3 Observer in movement

Let us consider now the opposite case. The emission focus is in repose, but the observer is moving towards the emission focus with a velocity v''.

When both the observer and the focus are in repose, the observer perceives f_0 identical wave surfaces per second. As in this case the observer is moving towards the focus, s/he will perceive in a second the same f_0 waves as in repose, plus the number of times that λ is contained in the distance that the observer covers in one second (which is $d = v'' \cdot 1 = v''$). Taking this into account, the perceived frequency is given in equation 3.3:

$$f_r = f_0 + \frac{v''}{\lambda} \Rightarrow f_r = f_0 \cdot \frac{c + v''}{c} \tag{3.3}$$

The conclusion is that the frequency perceived by the observer will be higher when s/he moves towards the source, and will be lower when s/he moves away from the source.

The difference between the emitted frequency and the received one is called Doppler Shift (equation 3.4):

$$f_d = f_0 - f_r \tag{3.4}$$

3.1.2 Doppler Ultrasound principles

3.1.2.1 Blood cell velocity

In ultrasonography, the Doppler Effect is used to evaluate blood cells velocity. In order to apply the measurement, a probe is required. The probe is a piezoelectric transducer. When electrical energy is applied to transducer,

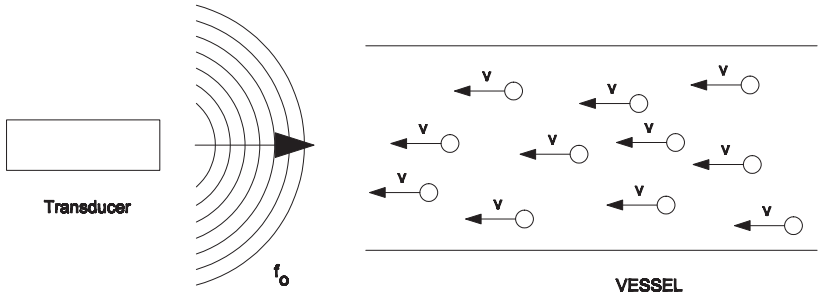

Figure 3.3: An ultrasound wave of frequency f_0 is emitted from the transducer towards the vessel where blood cells are moving.

its shape changes as a function of the polarity of the applied electrical energy. As the crystal expands and contracts it produces compressions and expansions, and creates ultrasound waves. On the other hand, when this material receives ultrasound waves, it creates electrical currents.

The Doppler Effect appears twice during the process of emission and reception of ultrasound waves from blood cells. The first Doppler shift (equation 3.5) occurs when the transducer emits waves towards the vessels where blood cells are moving with velocity v_{BC} (in this case, the emission focus is in repose and the observer in movement). A schema of this part of the process can be seen in Fig. 3.3.

$$f_{r1} = f_0 \cdot \frac{c + v_{BC}}{c} \tag{3.5}$$

The second Doppler shift occurs when the ultrasound wave is reflected in the blood cells towards the transducer (equation 3.6). In this case, blood cells act as an emission focus in relative movement towards the transducer, which acts as an observer in repose. A schema of this second part of the process has been represented in Fig. 3.4

$$f_{r2} = f_0 \cdot \frac{c + v_{BC}}{c} \cdot \frac{c}{c - v_{BC}} = f_0 \cdot \frac{c + v_{BC}}{c - v_{BC}} \tag{3.6}$$

The global Doppler Shift is represented by the following equation (3.7):

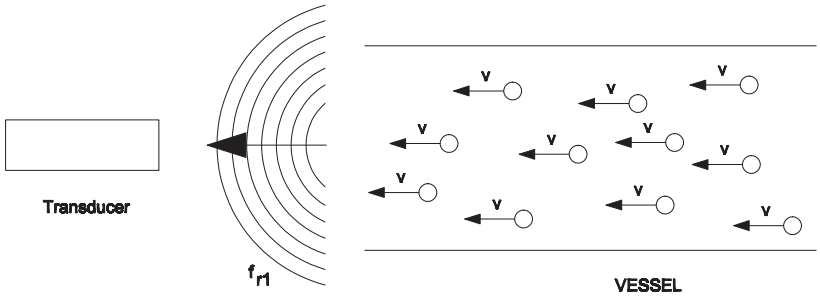

Figure 3.4: The ultrasound wave is reflected in the blood cells and returns towards the transducer.

$$f_d = f_{r2} - f_0 = f_0 \cdot \frac{c + v_{BC}}{c - v_{BC}} - f_0 = f_0 \cdot \frac{2 \cdot v_{BC}}{c - v_{BC}} \approx f_0 \cdot \frac{2 \cdot v_{BC}}{c} \tag{3.7}$$

Analyzing the resulting equation, it can be seen that the global Doppler shift is proportional to the velocity of the blood cells, multiplied by some constants. f_0 is the frequency of the transducer, and c is the propagation constant. The average propagation speed in soft tissue is approximately 1540 m/s [133]. The Doppler equipment will calculate the Doppler shift and, consequently, the blood flow velocity (BFV) from the echoes that return to the transducer.

3.1.2.2 Insonation angle

In the previous pictures, it has been assumed that the insonation angle is 0º. The insonation angle (or incidence angle) is the angle that is formed between the BFV vector and the imaginary line that represents the direction of the ultrasound beam. Only the component of the BFV in the direction of the ultrasound beam is responsible of the appearance of the Doppler effect that generates the Doppler shift in the reflected ultrasound wave. Let us consider several cases that may occur:

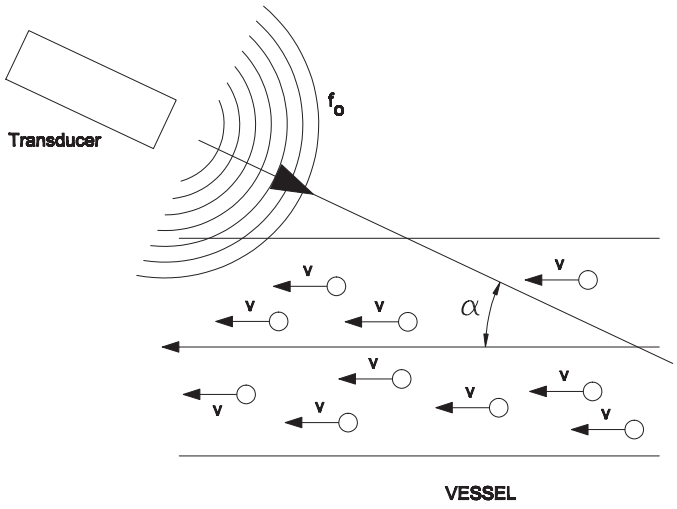

Figure 3.5: When the probe is not aligned with the vessel, there is an attenuation effect on the Doppler signal due to the angle of incidence.

- If the insonation angle is 0^o, the blood cells are approaching the transducer. The Doppler shift will be positive and its absolute value will be represented by equation 3.7.
- If the insonation angle is 180^o, it means that the blood cells are moving away from the transducer. The Doppler shift will be negative and its absolute value will be the absolute value of equation 3.7.
- If the insonation angle is 90^o, the transducer is perpendicular to the BFV vector. In this case, there is no component of the velocity in the direction of the ultrasound beam, so no Doppler effect appears.
- If the insonation angle is comprised between 0^o and 90^o (which is the general case, which is represented in Fig. 3.5), the component of the velocity in the direction of the ultrasound beam has to be calculated in order to obtain the Doppler shift.

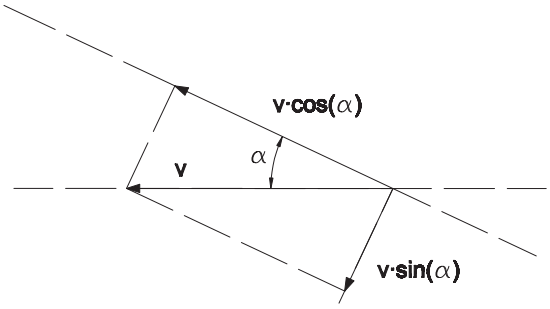

Figure 3.6: Decomposition of the BFV vector in its two orthogonal components. One of the velocity components is parallel to the ultrasound beam, and can be used to calculate the Doppler shift.

The decomposition of the BFV vector in its two components (parallel and perpendicular to the ultrasound beam) can be visualized in Fig. 3.6.

The magnitude of the velocity vector parallel to the ultrasound beam is given by equation 3.8:

$$v_{parallel} = v \cdot cos(\alpha) \tag{3.8}$$

So, equation 3.9 will give us the Doppler shift in this general case:

$$fd = 2 \cdot \frac{f_0}{c} \cdot v \cdot cos(\alpha) \tag{3.9}$$

It is important to remak that the existence of an incidence angle greater than zero only affects to the Doppler shift. The intensity of the echo signal that returns to the Doppler unit is not affected by this angle.

Doppler equipments calculate the Doppler shift from equation 3.7, assuming that the ultrasound beam is parallel to the BFV vector. When the incidence angles are smaller than 20º, this approximation would generate errors smaller than 5%. The neurosonologist can apply a correction factor from the Doppler software for higher incidence angles. In any case, it is not advisable to use incidence angles higher than 60º.

3.1.2.3 Spectral analysis

Another simplification that has been made in the previous analysis is that there is not a single velocity for all the blood cells that are moving through a vessel. In fact, each blood cell will have its own velocity and will generate a Doppler shift in the reflected ultrasound signal. The Doppler equipment will receive a complex signal generated by the Doppler shifts caused by the different blood cells that are moving in the monitored vessels.

In order to analyze the received signal, the frequency information (which is related to the blood cell velocities by means of equation 3.9) has to be analyzed. The Doppler units usually apply a Fast Fourier Transform to do this analysis.

Each frequency that appears in the frequency spectrum of the received signal will correspond to a single velocity. Furthermore, the higher the amplitude associated to that frequency, the higher will be the number of blood cells moving at that velocity.

The Fast Fourier Transform is calculated continuously, because the velocity information can change over time, and consequently the frequency spectrum will also be dynamic. The conclusion of this is that we will not have a single frequency spectrum, but an instantaneous frequency spectrum for each moment of time (which is called a spectrogram). The most common format for the spectrogram is a 2D graph:

- The horizontal axis represents time.
- The vertical axis is velocity in cm/s (each velocity is associated to a single frequency by equation 3.9).
- A third dimension indicates the amplitude of a particular velocity/frequency (which is proportional to the number of blood cells moving at that velocity) at a particular time by means of the intensity or color of each point in the image.

There is a baseline in the representation that separates positive velocities from negative velocities. Positive velocities represent BFV of cells that are approaching to the transducer, while negative velocities are occasioned

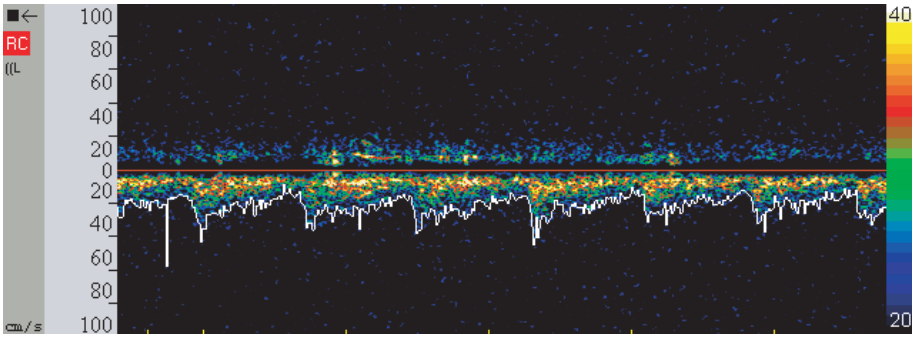

Figure 3.7: Example of spectrogram from the right posterior cerebral artery as represented by DWL® Doppler software (QL software).

by flows that move away from the transducer. An example of a spectrogram as represented by DWL® Doppler software (QL software) is shown in Fig. 3.7.

3.1.2.4 Ultrasound Doppler techniques

There are two main ways to generate the ultrasound waves that are used in TCD measurement:

- **Continuous Wave Doppler (CWD)**. In this technique, the transducer has two sets of piezoelectric crystals: one of them is the responsible of the transmission of the ultrasound wave. The other one receives the echoes that contain the information about the Doppler shifts. Both sets of crystals are working simultaneously and without interruption.

  The advantage of this method is that it imposes no practical limits in the range of velocities that can be measured. However, as the echoes are received continuously, there is no temporal information that can be used to obtain the depth where the Doppler shifts have their origin. Consequently, this method does not have resolution in depth.

- **Pulsed Wave Doppler (PWD)**. In order to obtain depth resolution, this other technique is used. The ultrasound waves are generated in burst mode. The echo reception is only possible in the time period between bursts. That way, there is a commutation of functions between transmission and reception (pulsed mode). The frequency with which bursts are repeated receives the name of Pulse Repetition Frequency (PRF).

  The Doppler unit is ready to receive echoes after the emission of a burst. But that is no possible during the whole period between bursts. In fact, the unit will only allow the reception during a short period of time, so that only the echoes that will be received during that period will be considered. Let us explain this in more detail. Assuming that a specific vessel is located a depth z, and knowing that the propagation velocity is c, the time T_s that will take to the ultrasound wave to arrive to the vessel and go back to the transducer can be deduced:

$$2 \cdot z = c \cdot T_s \rightarrow T_s = \frac{2 \cdot z}{c} \tag{3.10}$$

  Depending on the T_s that is used in the Doppler unit (that has to be smaller than the PRF), the depth that will be monitored will be different.

  In order to calculate the velocities that can be measured without ambiguity with the system, the Nyquist theorem has to be taken into account: the maximum Doppler shift has to be equal or less than half the PRF (equation 3.11).

$$f_{d_{max}} \leq \pm\frac{PRF}{2} \rightarrow v_{max} \leq \pm\frac{c}{2 \cdot f_0} \cdot PRF \tag{3.11}$$

  In order to measure velocities from deeper vessels, the PRF has to be reduced, so it is possible to have time to receive the echoes to come from those deeper zones. However, a reduction in PRF implies also a reduction in the range of velocities that can be measured. This has to be taken into account when configuring the Doppler unit to monitor a specific vessel.

Depending on the operating frequency of the equipment f_0 (which is the frequency of the waves sent in each burst and varies in commercial diagnostic instruments between 2 an 10 MHz), the Doppler frequency shift for physiologic blood flow is between 0.5 KHz and 15.0 KHz [133].

3.2 Transcranial Doppler Ultrasound

Transcranial Doppler (TCD) is a Doppler Ultrasound diagnosis technique which is used to analyze the hemodynamical variations in the brain. As all these techniques, it is secure and non-invasive. It was first used in 1982. It was then when Aaslid et al. [19] introduced a transcranial Doppler device based on a pulsed emission of 2 MHz bursts that could penetrate the skull and measure direction and velocity of blood flow in cerebral vessels.

The bases of the technique have been described in the generic section about Doppler Ultrasound techniques (section 3.1). Some details specific to the monitoring of brain vessels are described below.

3.2.1 TCD unit and probes

The commercially available TCD units that are used in functional studies usually have an ultrasound intensity of 100 mW/cm^2 and one or two 2-MHz transducers (probes).

One probe has to be used to monitor blood flow velocity (BFV) from the vessels of each brain hemisphere. In the early 1990, it was only possible to measure BFV unilaterally. If information from both sides of the brain was important, the arteries on each side had to be measured separately, one at a time. However, advances in the technique allow today the simultaneous bilateral measurement using two probes [21].

In standard clinical TCD instruments, the probe is held in the hand of the examiner and is placed in the correct location. In functional studies, each probe is placed in its correct location by attaching it to a user headband or headpiece that the user has to wear during the whole experiment.

In Fig. 3.8, a subject is seated with the TCD probes places in their correct location with the help of a probe holder.

Figure 3.8: Subject with TCD probes placed in their correct location with the help of a probe holder.

3.2.2 Windows

The ultrasound beam can only cross the skull at certain points known as windows. There are three ultrasonic windows in the cranium, located in positions where the bone is thin enough to allow the penetration of the ultrasound beam, or where natural foramina can serve to this purpose.

For the insonation of the major intracranial arteries, the natural ultrasonic cranial windows are used:

- **Transtemporal window**. It corresponds to the thinnest portion of the squamous part of the temporal bone. It can be located anteriorly (close to the vertical portion of the zygomatic bone) or posteriorly (close to the pinna of the ear).
- **Transforaminal or suboccipital window**. The ultrasound beam is introduced between the atlas and the base of the skull, and through the foramen magnum.
- **Transorbital window**. In this case, the transducer is located in a lateral fashion, directing the beam of ultrasound medially.

Functional TCD studies use the transtemporal window [20]. This window makes it possible to register directly the information about the Middle Cerebral Artery (MCA), Anterior Cerebral Artery (ACA) and Posterior Cerebral Artery (PCA). The location of the different vessels can be visualized in Fig. 3.9 [1]. A schematic representation of the circle of Willis (which includes, between other vessels, ACAs and PCAs), and other arteries of the brain (including MCAs) is shown in Fig. 3.10 [2]. The probe direction, the reference volume depth and the flow direction identify each cerebral artery [134].

Ultrasound gel is applied to the skin in the area of the window. In general population, satisfactory signals can be obtained in an area around the window. However, in some patients and elder people, the transtemporal window can be quite small, and shifting the probe a few millimeters may result in a loss of signal.

3.2.3 Blood flow velocity measures

As in other Doppler Ultrasound techniques, the probes emit an ultrasound beam that is reflected by the blood cells that are moving through the blood vessels in the brain. The probes receive the reflected signal with modifications in the original frequency that are proportional to the velocities of the blood cells. The FFT of the received signal is calculated and the spectrogram is represented in the Doppler unit monitor. As has been explained previously, the abscises axis represents the time, the ordinates axis indicates the velocities (or frequencies) and the brightness of each point is an indicator of the amplitude of the signal. The envelope of the signal represents the maximum velocity of the cardiac cycle.

Maximum BFV represents the instantaneous velocity of the quickest blood cells. It varies during each cardiac cycle, reaching a maximum shortly after the cardiac contraction and falling to a minimum just before the next. Most TCD studies do not use directly this maximum BFV.

[1] Adapted from http://commons.wikimedia.org/wiki/File:Gray516.png (Wikimedia Commons)

[2] Downloaded from http://en.wikipedia.org/wiki/File:Circle_of_Willis_en.svg (Wikimedia Commons)

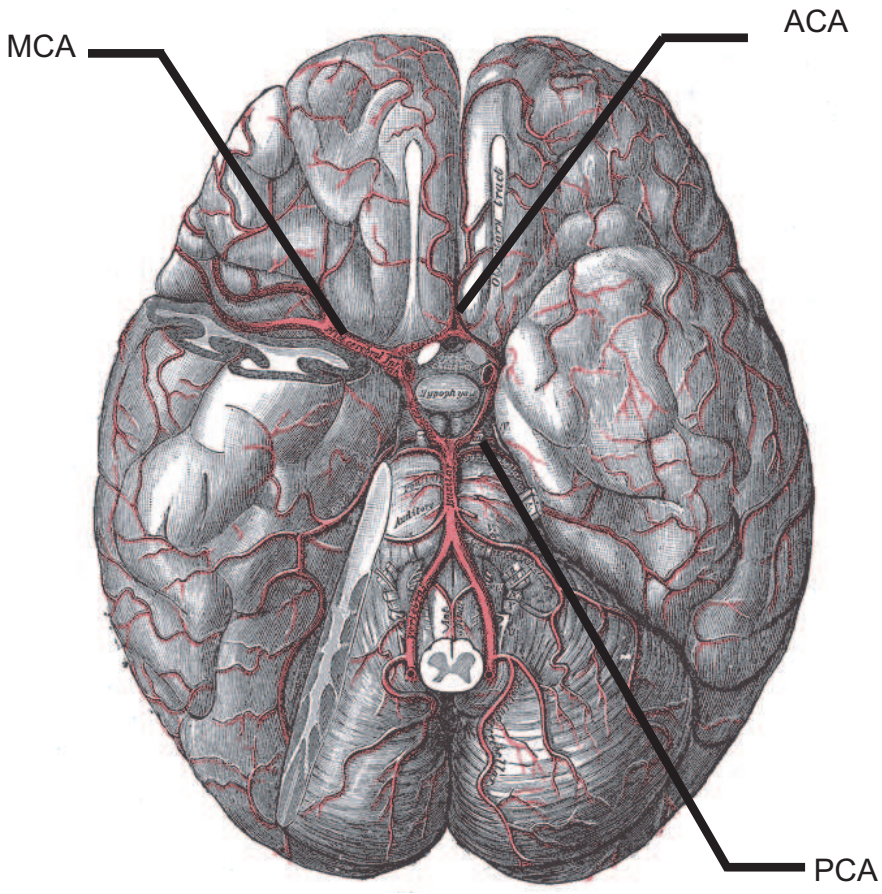

Figure 3.9: Location of the middle cerebral artery (MCA), anterior cerebral artery (ACA) and posterior cerebral artery (PCA).

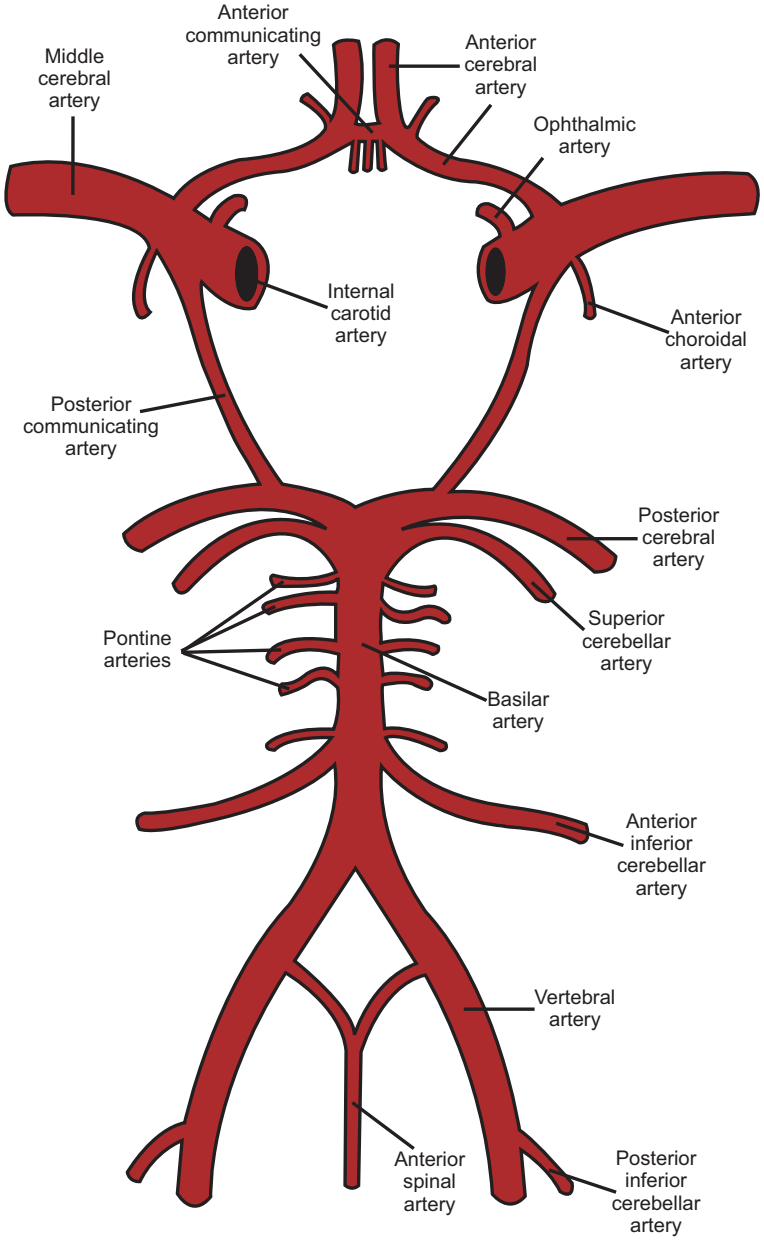

Figure 3.10: A schematic representation of the circle of Willis and arteries of the brain.

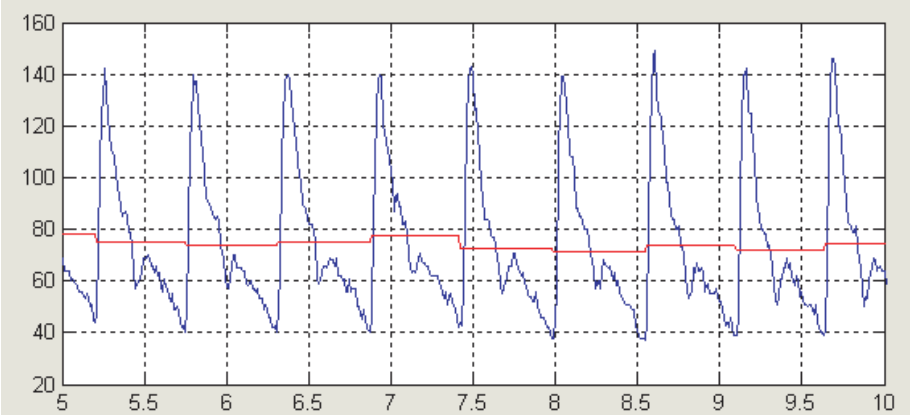

Figure 3.11: Some seconds of the MCA maximum and mean velocity signals (in cm/s) from a subject.

Instead, they use an averaged version of it (the mean BFV), which is calculated from the maximum BFV value as the mean velocity value during one complete cardiac cycle. It has been described as a time-averaged, area-averaged mean velocity value that results when a line is placed on the horizontal axis of the maximum velocity signal achieving that the area above the line is the same as the area below it [134]. In Fig. 3.11, some seconds of the MCA maximum and mean velocity signals (in cm/s) from a subject are represented.

3.2.4 Blood flow velocity and cerebral blood flow

Previous studies have proven that regional cerebral blood flow (rCBF) increases when performing mental activities [135]. Because of its quantitative characteristics, the flow, in principle, is a more suitable measure for cerebral activation studies than the velocity [136]. Nevertheless, in TCD, BFV is used. Let us analyze the relation between rCBV and BFV measured by TCD [20].

The definition of blood flow indicates that blood flow through an artery (Q), in ml/s, is equal to the instantaneous average blood cell velocity

(BFV), in cm/s, multiplied by the cross-sectional area of the vessel (A), in cm^2 (equation 3.12) [137].

$$Q = BFV \cdot A \tag{3.12}$$

On the other hand, blood flow through cerebral tissues (rCBF) can be defined as the quantity of blood (ml) perfusing a volume of brain tissue ($100\,g$) per unit of time (min). Arterial blood flow (Q), in ml/min, is equal to the product of rCBF and the perfusion territory T ($100\,g$ brain tissue) for the given artery (equation 3.13) [137].

$$Q = rCBF \cdot T \tag{3.13}$$

From the previous two formulae (equations 3.12 and 3.13) it can be demonstrated that blood cells velocity can be directly related to rCBF by equation 3.14:

$$BFV = \frac{1}{60} \cdot rCBF \cdot T \cdot A^{-1} \tag{3.14}$$

where BFV represents blood flow velocity, rCBF represents the regional Cerebral Blood Flow, T represents the size of the brain region being perfused by the artery under study and A represents the cross-sectional area of this vessel in cm^2 [137]. In order to calculate rCBF in a precise way, it is required to know the cross-sectional area of the vessel, the perfusion territory and the angle of incidence between the ultrasound beam and the insonated arteries, as long as the TCD technique only registers the component of the velocity which is parallel to the ultrasound beam. If there are no variations in any of these parameters between two experimental conditions, the modification in BFV that can be observed by TCD is directly related with the rCBF modifications occasioned by the differences between the experimental conditions.

Brain activity, metabolism and blood flow are closely related. Mental activity is associated with an increment in regional cerebral metabolism, which generates a local increase in pCO_2 that causes a dilation of the precapillary bed. Consequently, it occurs an increase in blood flow in the cortical sites where there is activity, associated with a reduced local vascular resistance. This reduction in resistance will finally generate an

increase in BFV in the artery that supplies that particular cortical site [138].

When the neurovascular coupling (mechanism that adapts CBF to the metabolic demands and the activity of the brain cortex [139]) is adequate, the velocity variations that are detected by TCD reflect changes in regional CBF due to brain activation [140]. Most functional TCD studies directly use BFV measurements instead of CBF, assuming that the diameter of the main cerebral vessels that are analyzed using TCD does not significantly change under a variety of physiological conditions [141, 142].

3.2.5 Cortical areas supplied by the cerebral vessels.

The division of the brain in lobes is represented in Fig. 3.12 [3]. A description of each lobe is detailed below [143]:

- **Frontal lobe**. It represents one third of the hemispheric surface and it is located in front of the central sulcus. A great part of the frontal lobe is responsible of the planning, prediction and programming of the subject's necessities. The lower part, specially in the left hemisphere, is specialized in speech articulation. A narrow band of the frontal lobe in front of the central sulcus is the motor area, which controls the movements of the body.

- **Temporal lobe**. It is located below the lateral sulcus. Its superior part is related to audition. The internal part is related to the memory processing. The other parts of the temporal lobes can be implied in the integration of different sensory functions: audition, touch, vision.

- **Parietal lobe**. It is located behind the central sulcus, but its exact limits are difficult to establish. A portion of the parietal lobe located just behind the central sulcus (the primary somatosensorial area) receives nerve impulses associated to pain, temperature, touch and pressure.

[3] Downloaded from http://en.wikipedia.org/wiki/File:Lobes_of_the_brain_NL.svg (Wikimedia Commons)

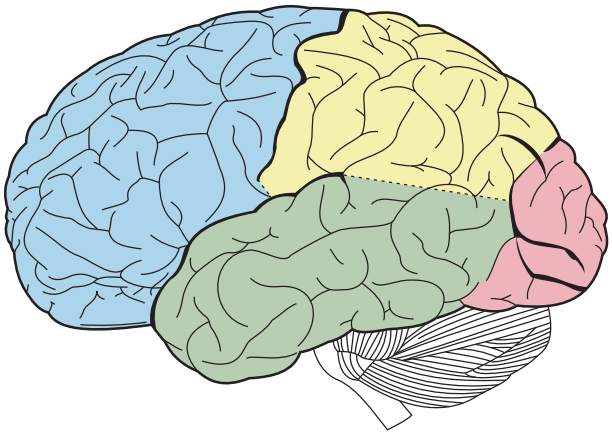

Figure 3.12: Division of the brain in lobes: frontal lobe (blue), parietal lobe (yellow), occipital lobe (pink) and temporal lobe (green).

- **Occipital lobe**. It is located behind the temporal and parietal lobes. Visual information is processed in this area.

In this section, the areas supplied by each cerebral artery that can be monitored with TCD are going to be described. In Fig. 3.13 [4] the areas supplied by each cerebral artery are represented over the outer surface of a cerebral hemisphere.

3.2.5.1 Middle cerebral arteries

The arteries that supply blood to the greater part of the brain are MCAs. Each MCA carries 80% of the blood flow within its cerebral hemisphere [144]. Their perfusion territory includes subcortical areas, large fractions of the frontal and parietal lobes, as well as the temporal lobes [145].

As they supply blood to big areas of the brain, modifications in MCAs BFV can be produced by different kinds of brain activity (related to aspects such as motor tasks, attention tasks, language processing or emotional

[4] Downloaded from http://en.wikipedia.org/wiki/File:Gray517.png (Wikimedia Commons)

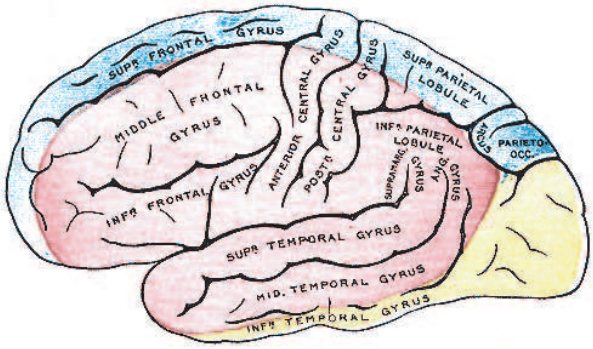

Figure 3.13: Outer surface of cerebral hemisphere, showing areas supplied by cerebral arteries. Pink is the region supplied by middle cerebral artery. Blue is the region supplied by the anterior cerebral artery. Yellow is the region supplied by the posterior cerebral artery.

states). For example, parts of the parietal and frontal lobe are involved in the processing of emotions, as well as areas of the temporal lobe with the limbic system, so that would justify an increment in MCAs BFV when somebody is experiencing an emotion [146].

3.2.5.2 Anterior cerebral arteries

Other vessels that can be monitored with TCD can provide more specific information about the exact areas that may be active at each moment, as long as their perfusion territory is smaller. ACAs supply most of the medial areas of the brain, including the medial frontal cortex and most parts of the limbic system particularly the cingulated [144].

BFV variations in ACAs can be closely related with the emotional state of the subject who is being monitored and with the activity of the frontal cortex (for example, for the cognitive processing of decision-making).

3.2.5.3 Posterior cerebral arteries

Finally, PCAs are the blood vessels that supply oxygenated blood to the posterior part of the brain (occipital lobe).

They are responsible for the irrigation of the primary visual cortex as well as the lateral geniculate body and some of the visual association regions in the occipital cortex [29], so they are useful to analyze brain activity related with visual stimuli.

3.2.6 TCD advantages and disadvantages

The main disadvantage of TCD is its spatial resolution, which is limited by the size of the cortical areas supplied by the arteries under study. Velocity increments in small vessels could not generate a noticeable increment in the bigger artery, so activations of small groups of neurons in areas of the brain that can be visualized with fMRI cannot be detected using TCD. Another problem is that some individuals are not suitable for this kind of analysis because of the lack of an ultrasonic window. Up to 10% of subjects in the elderly population have to be excluded because of this reason [21]. Finally, it has to be taken into account that the data obtained from blood flow sensitive imaging techniques (which includes both fMRI and TCD) is always affected by the reaction times of the vascular system (around 1 s) [136]. Changes in the extracellular currents that are measured with EEG are substantially lower (around 1 ms) [147].

However, TCD has important advantages when compared to other techniques:

- **Temporal resolution**. TCD has a high temporal resolution. In usual experimental designs, other neuroimaging techniques do not allow for the continuous study of changes in cerebral blood perfusion because the duration of the necessary scanning procedures is at least of several seconds.

- **Non-invasiveness and simplicity**. TCD is non-invasive, so it is possible to use it in an ecological way in a great variety of environments. It only requires to place two probes in the outer part of the temporal window of the skull, and it imposes fewer limitations to

the user. That constitutes its main advantage when compared with other techniques such as fMRI, which imposes serious restrictions to the experiments in which it is used, as long as the subject has to remain in supine position inside the magnetic resonance machine with minimum head movement while hearing annoying noises. The simple technical requirements of the TCD technique make easier the presentation of a wide range of stimulus presentations.

3.3 TCD in psychophysiological studies

TCD has been widely used to monitor cerebral hemodynamics during the performance of cognitive tasks in psychophysiological research. These studies have shown that mean BFV obtained from TCD signals increases if users are doing a cognitive activity when compared to baseline periods [20, 21].

Changes in mean BFV or maximum BFV that can be observed between a baseline period and a phase in which a cognitive task is performed can be analyzed as an absolute change (in cm/s) or as a relative change (in percentage change from baseline). Different cognitive tasks have been considered in these studies, such as reading, arithmetic operations, visual perception, attention, verbal tasks, motor tasks, visuospatial tasks and memory.

In Fig. 3.14, some seconds of the maximum and mean BFV from a subject during a baseline period and during a period with cognitive activity are shown. BFV remains stable during the baseline period, but during the period with cognitive activity, there is an increment in BFV that can be clearly observed in the graph.

In the following sections, studies using TCD to analyze cerebral hemodynamics during the performance of different kinds of tasks will be described.

3.3.1 Visual perception tasks

Visual perception tasks were one of the first activities to be analyzed using functional TCD.

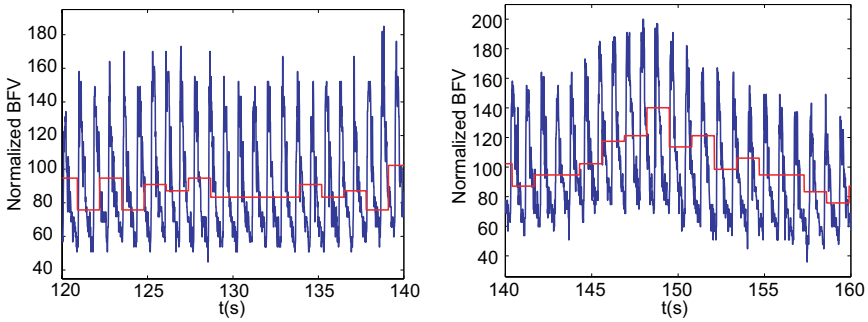

(a) (b)

Figure 3.14: (a) Some seconds of maximum and mean BFV of a subject during a repose (baseline) period in a experimental design. (b) Some seconds of maximum and mean BFV of a subject during an activation period in a experimental design.

In 1987, Aaslid et al. [29] analyzed the effects of visual stimulation on cerebral blood flow. They recorded changes in BFV under simple light stimulation (rectangular bright white surface alternating with total darkness) in PCAs (the vessels responsible for the irrigation of the primary visual cortex as well as the lateral geniculate body and some of the visual association regions in the occipital cortex) and, as control measurements, in MCAs and the superior cerebellar artery (SCA, unrelated to visual brain areas). For each of the ten subjects included in the study, data was averaged from a series of dark/light cycles (each half cycle lasting 20 seconds) in order to extract response from random variations. The averaging algorithm calculated the arithmetic mean over all cycles for each sample time. BFV in PCA achieved a value 16.4% higher during visual stimulation than during darkness. In MCA, the increment was only 3.3%. The study also concluded that BFV changes occur very rapidly after changes in the visual cortical function, with a 90% response time of 4.6 seconds.

Later studies have focused on the analysis of the reaction to visual stimuli of different complexity. For example, Harders et al. [31] analyzed BFV responses to different mental tasks, with a specific analysis of visual

cortex activity, studying BFV in the PCA. Different stimuli with increasing complexity were used (such as illumination, illumination of both visual fields or looking at 6 pictures). They obtained similar velocity increases to the study from Aaslid et al. [29], with differences depending on the visual stimulus (more complex stimuli generated greater differences). In this case, the maximum velocity increase was reached after 18 s. They considered that the difference to the previous study could be caused by the time required by the cones of the retina to adjust to colored pictures. Sitzer et al. [33] also used stimuli with increasing degrees of complexity (diffuse white light, alternating checkerboard patterns and a video movie) and obtained similar increases in PCA to previous studies. The first maximum of the BFV during the testing phase was achieved 6.2 seconds after the presentation of the visual stimulus. Posteriorly, Panczel et al. [148] completed this study with the analysis of age and stimulus dependency of visually evoked BFV. A total of 60 healthy participants were exposed to different experimental conditions: the three environments with different levels of visual complexity (diffuse light, checkerboard image and movie), with different stimuli durations (5, 10, 20 and 30 seconds) and at different recording sites (P1 vs. P2 segments of the PCA). It was found that the greater responses were in the conditions with a duration of 20 s, in P2 segments of PCA, and in the environments with greater visual complexity.

Njemanze et al. [32] used dark, light and color conditions to examine BFV response, but focused on the analysis of side-to-side differences between left and right PCA (PCA-L and PCA-R). Significant differences were found during the dark and color stimulation, but not in the light condition. They also observed differences between colors.

Sturzenegger et al. [34] analyzed PCA evoked flow responses to different visual stimuli combining room light and stimulation using goggles with light diodes. Similarly to the study from Aaslid et al. [29], data was averaged from a series of dark/light cycles, although in this case each half cycle lasted 10 seconds. The observed increment in PCA velocities was greater than in basilar arteries and MCA (that were also included in some experimental conditions). They observed a trend toward a greater right-sided activation. Gomez et al. [30] monitored PCA using TCD during intermittent photic stimulation at frequencies from 5 to 60 Hz. Maximal

change (expressed as percentage from baseline) was obtained when the frequencies were of 10 and 20 Hz.

More recently, Trkanjec and Demarin [35] measured PCA with opened and closed eyes, and while watching colored light for 1 minute. The increment in PCA-R was significantly higher than the corresponding increment in PCA-L, which can indicate a greater metabolism of visual cortex in the right occipital lobe while watching colors.

3.3.2 Language

TCD has been widely used to analyze brain lateralization during language tasks. One of the first studies that included language tasks was performed by Rihs et al. [149] in 1995. They analyzed BFV in six different tasks (synonyms, faces, syntaxis, design, reading and baseline). There were 10 successive cycles of each task, consisting of 20 s of repose and 20 s of activity. The percentage variation between repose and activation was calculated. It was found that language related tasks generated a left lateralization, while visuospatial tasks generated a lateralization to the right hemisphere.

Posteriorly, several experiments related to language using TCD were performed in the Department of Neurology of the University of Muenster (Germany). In one of these studies [150], the reproducibility of TCD sonography in determining hemispheric language lateralization was analyzed. The task used to determine language lateralization was performed once, and then repeated one hour later, and one year later of the initial task. The task consisted of saying as many words as possible beginning by a letter that is shown in the monitor. The letter appeared, there was a repose period of 15 s, and a sound was heard to indicate that the user could start to say words in loud voice. This process was followed by 30 s of relaxation. MCAs were monitored. In order to analyze the BFV signal, a specific software called AVERAGE [151] was used (it will be described in more detail in following sections). Ten subjects participated in the study. It was found a high level of reproducibility.

Knecht et al. [152] made a study with 326 subjects. The same task as in the previous study was used with 20 repetitions with a separation of 60 s between them. Most subjects (264) had a left hemispheric language repre-

sentation, while 31 subjects had a bilateral language representation and 31 subjects had a right hemisphere language representation. However, there were no significant differences between groups with different hemisphere language representation with respect to mastery of foreign languages, academic achievement and other linguistic processing abilities. The authors concluded that atypical hemispheric specialization for language is not associated with linguistic difficulties in healthy subjects.

They also studied the relationship between handedness and language dominance [153]. It was found that the incidence of right hemisphere language dominance increases linearly with the degree of left handedness.

In another study [154], they analyzed the possible combinations of cerebral lateralization and attention of healthy subjects. They investigated 75 participants (37 right-handed and 38 left-handed) with a visual attention task and the previous word generation task. Although the neural systems that support language and spatial attention usually dissociate in healthy individuals (left dominance for language, and right dominance for attention), language and visuospatial attention were found associated with the left hemisphere in five subjects, and within the right hemisphere in eight subjects. All these combinations may exist in a healthy brain.

Finally, in a study with 14 volunteers from Dräger et al. [155], three different levels of difficulty in the generation of words were compared. It was found that incrementing the task difficulty did not change the BFV in the dominant or subdominant hemisphere.

3.3.3 Motor tasks

Different studies have been conducted related to motor tasks. These studies have mainly found increments in BFV in the MCA contralateral to the hand or arm that is performing the task. Some results will be summarized in the following paragraphs.

Sitzer et al. [156] analyzed MCA BFV in 38 right-handed volunters in different experimental tasks: 10 subjects performed a somatosensorial discrimination task, 10 subjects made a complicated sequence of finger movements with the right hand, 10 subjects received vibrations in the right hand, and 6 subjects received the three kinds of stimuli. In two subjects,

the PCA was analyzed instead. In each session, there was a initial repose stage (5 minutes) followed by three stages of stimulation alternated with repose (2 minutes each) and a final repose stage of 2 minutes. It was found that the mean BFV in the left MCA (MCA-L) during a period of 90 s was increased only in the somatosensorial task, but not in motor and vibratory stimulation. A maximum in BFV was found about 3.3 s after the beginning of the stimulation. A previous study that also applied vibration to the hand [157] did not find either any difference in BFV between the activation period and the repose.

Orlandi and Murri [158] performed a study with fifty-five right-handed volunteers. BFV in right MCA (MCA-R) and left MCA (MCA-L) were investigated at rest (30 s), during a motor task performed by the hand (60 s), and in the following rest condition (30 s). In all cases, the motor task induced an increase in bilateral BFV which was significantly greater in the contralateral hemisphere. The percentage BFV variation when compared with the repose condition was significantly greater in the contralateral MCA of young participants when compared with the elderly.

In a study from Klingelhöfer et al. [159], lateralization in MCA was analyzed during various tasks. One of the tasks consisted of simple sequential finger movements. A more pronounced increase in BFV was observed in the hemisphere contralateral to the performing hand.

Matteis et al [160] designed an experiment in which 20 right-handed volunteers had to perform passive and active elbow and hand movements. There was a repose period of one minute before starting the task. It was followed by a minute of active and passive elbow flexion-extension movement for both arms. After that, there was a minute of passive and active hand extension movement for both arms. A greater increment in MCA BFV was found in the hemispheric brain contralateral to the arm with which the movement was made (when compared to the ipsilateral hemisphere).

In the study with 14 volunteers from Dräger et al. that was described in the section about visual perception studies [155], a motor task condition was also included. A sound was heard and, after 5 s, the participant had to move fingers at the frequencies indicated by a disc (0.5, 1, 2.5, and 4 Hz) during 10 s. The task was followed by 20 s of relax. An increment in

the bilateral perfusion was found when fingers' velocity was increased.

Silvestrini et al. [161] analyzed the activation of the healthy hemisphere in post-stroke recovery. They compared 12 normal people and 12 patients who had recovered from a stroke. The participants had to do a thumb-finger opposition task during two minutes, alternatively with the normal and the recovered hand. There was a two-minute repose period followed by a two-minute task and a one-minute recovery period. It was found an MCA BFV increment in the contralateral hemisphere both for patients and controls. However, a significant increment in the ipsilateral MCA was only found in the patients who moved the recovered hand. Another study with 45 patients from the same group [162] achieved similar results.

3.3.4 Emotions

Some studies have analyzed emotion-related changes in BFV. These studies have found an emotion-related cerebral asymmetry, observing a significantly higher increase in the right than in the left MCA during emotional processing.

Troise et al. [163] designed a study with three tasks: visualizing 15 non-emotional slides, visualizing 15 negative emotional slides and visualizing 15 non-emotional slides. Each slide was seen during 4 s, which gives a total of 60 s of activation. Between 10 and 15 minutes were left between phases. Sixteen subjects participated. Percentage variations between repose and activation were calculated. It was found that, during the non-emotional tasks, the increment in BFV was similar in both vessels. However, in the negative emotional task, a significantly higher increment was found in MCA-R with respect to MCA-L.

Stoll et al. [164] studied BFV in the MCA during emotional stimulation using videos in 24 volunteers. The videos consisted of an erotic scene and a violent scence shown in contrast to a calming scene. Mean BFV during the erotic scene significantly increased when compared with the baseline in the MCA-R. Also in the violent scene there was a significant increment in MCA-R. Furthermore, BFV time course showed a close relationship to the video sequence.

Vingerhoets et al. [165] made a functional TCD study in which vol-

unteers had to indicate the emotion of the semantic or prosodic part of a sentence. Four different conditions were used (1- Neutral content; emotional tone. 2- Emotional content; neutral tone. 3- Neutral content and tone. 4- Emotional content and tone). The user gave the response making an indication with two fingers. MCA BFV percentage variation was calculated, and it was found a significant lateralization to the left hemisphere when the semantic emotion was indicated. When attention was given to the prosody, the lateralization effect disappeared, due to an increment in BFV in the right hemisphere.

In a recent study, Stegagno et al. [166] analyzed BFV during emotional activation in two groups of women (20 hypotensives and 20 normotensives). Three series of 20 images from the IAPS [167] (neutral, pleasant and unpleasant) were shown. Both groups showed greater increases in MCA-R than in MCA-L during emotional stimulation. The increases were lower in hypotensives, although they rated the emotional pictures as more arousing. Furthermore, hypotensives exhibited lower MCA BFV at rest than normotensives.

3.3.5 Vigilance and attention tasks

TCD has also been used in studies closely related with the Augmented Cognition (AugCog) field. There are two main aspects that should be controlled in an AugCog system. Firstly, the system should be able to detect the instantaneous cognitive state of the user, in order to find limitations such as overload, cognitive lockup, and underload [168]. Secondly, depending on the user's detected state, the system has to adapt the computational interface in order to improve the user's performance.

Several experiences have been related to the study of brain activity measured by TCD during vigilance tasks [169, 170]. Some studies [171, 172] have found that the vigilance decrement in detection rate over time was accompanied by a decrease in BFV in both MCAs. This reduction only happens when the observers are asked to actively monitor the stimuli, and not when they are asked just to look at the vigilance displays with no task to be performed. However, other studies [173] have focused on abbreviated vigilance tasks and, although there was a significant decline in performance

over time, there was no significant change in BFV measures over time. This finding does not coincide with earlier findings from long-duration tasks.

TCD has also been used to monitor the influence of automation cues of varying reliability on vigilance performance in a 40 minute simulated air traffic control task [174]. Performance effects for cueing found in the experiment were closely followed by changes in BFV just in the right MCA in conjunction with low salience signals.

3.3.6 Video games

No studies have been conducted up to now which used TCD to monitor brain activity during the navigation in a VE. The most similar study can be found in a research from Kelley et al. [175], who analyzed brain activity using TCD while participants played a commercial video game using a joystick. Although a video game is not VR, at least it has some of the characteristics that VEs have, mainly, the engagement and the interaction with a computer generated world. Twenty-one normal volunteers participated in the study. Eight minutes in repose were compared with 8 minutes of playing. MCAs, ACAs and PCAs were monitored. Serial measurement of the right and left sides were made with a headband with two probes. It was observed a global increase in BFV above baseline measurement during task performance. During the video game, both MCAs and PCA-L had a significant increase in BFV compared with the ipsilateral ACA. No statistically significant differences were found between right and left MCA. The mean percentage increment in the different vessels (calculated from the data provided in their work) is:

- Left MCA (MCA-L): 9.83 %
- Right MCA (MCA-R): 11.86 %
- Left ACA (ACA-L): 4.34 %
- Right ACA (ACA-R): 4.08 %
- Left PCA (PCA-L): 18.75 %
- Right PCA (PCA-R): 11.76 %

Authors interpret these increments as an activation of different areas of the cerebral cortex, because game playing required attention, visual input, visuospatial orientation, and fine motor activity.

In another study from Vingerhoets and Stroobant [176], brain lateralization in 13 different tasks was analyzed by means of TCD. Six of the tasks were verbal, and the other seven were visuospatial. The experimental design alternated repose periods (120 s) with activation periods (performing of one of the tasks during 120 s). It was found a significant lateralization in all but three tasks. In language tasks, greater activity was found in the left hemisphere. In visuospatial tasks, a right lateralization was found. One of the visuospatial tasks was a video game playing. Participants had to use a steering wheel and pedals to drive a car in a race circuit. An increment of 18.3 % in MCA-L and of 21.6 in MCA-R were found.

3.3.7 Other tasks

Some examples of studies about other kinds of tasks will be summarized in this point. For example, Schmidt et al. [177] used a visual discrimination task that was expected to activate mainly the right hemisphere. MCAs BFV was monitored using TCD and results were cross-validated by fMRI. A greater activation of the right hemisphere was found with both techniques.

Matteis et al. [178] analyzed the influence of the meaning of an action on BFV changes. MCAs were monitored in 26 volunteers. There was a repose period of 1 minute before each task. The tasks included in the experimental design consisted of a meaningful action (pouring sugar on a cup) and a meaningless action (make the same movement, but without sugar, cup or spoon). The actions were performed with both arms. It was found that during the meaningless action there was a higher increment in BFV in the contralateral MCA. However, during the meaningful action, an increment in the contralateral MCA was found when making the movements with the right arm; when the movements were made with the left arm, a bilateral increment was observed.

Bäcker et al. [179] compared MCAs BFV when two different kinds of acupuncture stimulation were applied: high frequency and low amplitude

vs. low frequency and high amplitude. It was found that the high frequency and low amplitude condition is perceived as more intense and induces a more marked increase in BFV in the right hemisphere.

3.4 Blood flow velocity signal analysis

3.4.1 BFV signal analysis in functional studies

Usually, TCD commercial equipment can provide maximum BFV data and mean BFV data (as seen in Fig. 3.11) for off-line analysis. Functional TCD studies have mainly worked with mean BFV. However, there is not a standardized method to analyze the evolution of BFV during the experimental conditions. In the following paragraphs, the different approaches that have been followed will be summarized. It is important to note that the BFV absolute or relative variations that can be observed during cognitive tasks are studied in most functional TCD works. However, and although the high temporal resolution of TCD is one of the key advantages of this technique, the instantaneous temporal evolution of BFV signals in subjects performing cognitive tasks has only been analyzed in some of the functional studies [20], which have found a maximum peak in BFV between 4 [180] to 20 s [181] after the initiation of a cognitive task, with an average peak after 6-9 s [31, 158, 149].

There are two main kinds of experimental designs that have been applied in psychophysiological TCD studies, and this fact conditions the kind of signal analysis that can be performed off-line. The two kinds of experimental designs are:

- **One execution of the experimental task**. Each experimental task is performed only once. BFV in each experimental task is compared with baseline values.

- **Repetitive executions of the experimental task**. The same experimental task is repeated several times alternating with repose periods. A time-locked averaging of BFV signals during repose and during activity periods is usually applied during the analysis. This

kind of analysis is similar to the analysis of EEG evoked potentials (EPs).

3.4.1.1 One execution of the experimental task

In this kind of experimental design, one or several tasks can be studied, but each of them is performed only once. If there is more than one task, there are usually several baseline periods. One example of this kind of study is the already described work by Vingerhoets and Strootbant [176]. In that case, 13 different tasks were performed. The experiment started with 120 s of repose, continued with 120 of a task, and that schema (repose-activation) was repeated 12 times more for the other 12 tasks that were analyzed in the study.

The interesting point is that, for each task that is being analyzed, there is experimental data only about a single performance. BFV during this single performance has to be compared with BFV during repose.

In this kind of studies, the most simple analysis consists of calculating the mean value of the mean BFV during the repose period and during the activation period (in absolute BFV values). These values are then compared to check if there are significant differences between them. This analysis has been used in some of the previous studies [175, 163, 182, 35].

Another approach consists of calculating percentage variations between repose and activation. When percentage variations are used, one of the problems of the use of absolute values is solved: the dependance of absolute BFV values on the probe angle. Although using absolute values it is possible to compare data from the same vessel corresponding to different periods of the experimental design (for example, repose vs. activation), an error could be introduced if left and right hemisphere vessels were compared because probe angles may be different in each hemisphere. Using percentage variations, the BFV dependance on the probe angle is eliminated. It is possible to compare (without error) the percentage variation that is observed in the left hemisphere with the percentage variation in the right hemisphere.

The most common formula used to calculate the BFV percentage variation is the following (equation 3.15):

$$BFV_{var}(\%) = 100 \cdot \frac{BFV_{act} - BFV_{rep}}{BFV_{rep}} \tag{3.15}$$

BFV_{act} is a BFV representative value for the activation period (during the performance of the task) and BFV_{rep} is a BFV representative value for the repose period (during the baseline period).

Let us prove that using this formula the angle dependance is eliminated. Equation 3.16 shows the results of substituting equation 3.9 in equation 3.15:

$$BFV_{var}(\%) = 100 \cdot \frac{\frac{f_{d_{act}} \cdot c}{f_0 \cdot 2 \cdot cos(\alpha)} - \frac{f_{d_{rep}} \cdot c}{f_0 \cdot 2 \cdot cos(\alpha)}}{\frac{f_{d_{rep}} \cdot c}{f_0 \cdot 2 \cdot cos(\alpha)}} \rightarrow BFV_{var}(\%) = 100 \cdot \frac{f_{d_{act}} - f_{d_{rep}}}{f_{d_{rep}}} \tag{3.16}$$

As can be observed, the resulting $BFV_{var}(\%)$ is no longer dependant of the incidence angle.

BFV_{act} is usually taken as the mean value of the mean BFV during the whole activation period. Similarly, BFV_{rep} is usually taken as the mean value of the mean BFV during the whole repose period. This approach has been followed in some of the previous studies [163, 160, 178].

Other studies have selected part of the repose or the activation period to obtain the representative BFV value. For example, Vingerhoets et al. [176, 165] used only the middle part of the activation section to calculate the mean of the activation, and the last half of the repose period to calculate the mean of the repose.

Finally, there are studies that have focused specially on the analysis of the temporal evolution of the signal during the activation period. In those cases, it is not enough to have a single representative value for each experimental condition. Let us discuss some examples about studies which have analyzed the temporal evolution of the BFV signal during the different experimental conditions.

In the previously described study from Orlandi and Murri [158], BFV percentage variations were analyzed. Temporal evolution was also studied, and it was found that elderly subjects achieved the maximum variations later than young subjects and returned to repose values more slowly. In a study from Harders et al. [31] they calculated the mean of the maximum

BFV every three seconds, and the evolution during the performance of different visual tasks was analyzed. It was found a maximum after 18 s, and a decrease 5 s after finishing the task. A study from Vardanore et al. [183] also analyzed the temporal evolution calculating a mean BFV each 3 seconds. In this case, the cognitive task consisted of solving anagrams or constructing new words using letters. Time-course patterns showed elevations in MCA velocity at the beginning and the end of the periods, while PCA velocity typically slowed below baseline in the middle of the periods.

3.4.1.2 Repetitive executions of the experimental task

In this kind of studies, the same experimental task is repeated several times alternating with repose periods. It is logical that the kind of analysis that is applied in this case is similar to the analysis of evoked potentials in EEG studies.

A time-locked averaging of all the BFV signals during the repose and during the activity periods is usually applied during the analysis. After this averaging, the resulting signal is analyzed. In some studies, the BFV percentage variation can be calculated from a representative BFV value of the repose period to a representative BFV value of the activation period. For example, in the study from Gomez et al. [30], there were 70 mean BFV measurements per condition. The measurements during the total darkness condition were considered baseline, and the mean BFV corresponding to each illumination condition was calculated as a percentage change from baseline. Similarly, Sturzenegger et al. [34] also used stimulus-triggered velocity averaging in a visual perception study. There were 14 repetitions of each cycle (10 s of stimulus off, and 10 s of stimulus on) that were averaged. The percentage change from baseline (stimulus off) to activation (stimulus on) was calculated. In another study with 14 subjects, Rihs et al. [149] analyzed BFV lateralization induced by language and visuospatial tasks. Periods of 20 s of activity alternated with periods of 20 s of repose. In the analysis of lateralization, the first 5 s of the activation or the repose period were not taken into account, because the maximum/minimum BFV during the period was always observed later.

In order to avoid the dependance with the incidence angle, another approach that has been followed has been the normalization of the BFV signal, that is, to express the BFV in relative units. For example, in the study from Sitzer et al. [33], after averaging BFV data between the different observations of the same experimental task, BFV relative to the mean BFV during the whole experiment were calculated. Equation 3.17 indicates the normalization procedure that is followed in this kind of studies:

$$BFV_{norm} = 100 \cdot \frac{BFV}{BFV_{mean}} \tag{3.17}$$

It can be observed that, as the factor $cos(\alpha)$ affects both BFV variable in the numerator and BFV_{mean} in the denominator (see equation 3.9), the influence of this factor is eliminated.

In the same study from Sitzer et al. [33], once relative values have been obtained, the maximum variation in each condition is obtained as the difference between the maximum normalized BFV in the activation period and the minimum value in the repose period.

Schmidt et al. [177] also used an average of 10 alternating periods of activation and rest, and all BFV data were transformed to percentages for subsequent data evaluation. The BFV value at the end of the resting phase of each cycle was considered 100%. The temporal evolution of the percentage BFV signal was studied.

Schnittger et al. [181] analyzed BFV during an attention task with 16 subjects. Forty runs of each attention level were administered during two experimental sessions. The data was averaged and expressed in percentage BFV changes. The temporal evolution during the 35-s periods of passive stimulation and the 65-s periods of active tasks were analyzed. A highly significant increase of blood flow was detected upon initiation of the active task, which was clearly present after 4 s. The BFV reached a maximum after 20 s and remained stable during the rest of the active condition.

Panczel et al. [148] expressed the amplitude of response as percentage of BFV increase from baseline during stimulation. Furthermore, they also analyzed the adaptation (percent decline of the response at the end of the activation phase relative to the maximal value).

Other studies have based their analysis on the use of AVERAGE [151],

which is a software developed in the University of Muenster focused specifically on the analysis of TCD signals. It supports several processes such as data transformation, heart beat analysis, noise reduction, trigger signal and marker modification, artefact analysis and artefact rejection, and also data reduction. One of the first steps of the processing that AVERAGE performs is the normalization of the maximum BFV signal. The transformation is given by equation 3.17, although, in opposition to the approach from Sitzer et al. [33], they calculate the BFV_{mean} as the mean value of the baseline periods that is not affected by the evoked BFV responses.

Although AVERAGE works with the maximum BFV signal (what they call "raw data envelope curve"), after the averaging process, this signal is reduced to a step function where the width of the steps corresponds to the cardiac intervals and the height represents the mean blood flow velocity within these intervals.

The evolution of the averaged BFV signal during an epoch (which can be defined by the software as a period of time before and after an event) can be graphically visualized with the software. Furthermore, the software supplies the possibility of automatically averaging across BFV data from a group of participants.

The software allows the calculation of a lateralization index defined by the authors [136] to indicate differences of the relative BFV changes between the left and right vessels.

Using an initial version of the software, Knecht et al. [180] analyzed a language task, and observed that first BFV increase started immediately after a cuing tone that indicated the beginning of the task. Approximately 4 s later, it reached its maximum, which was on average 2 % above baseline. The second increase began during letter presentation and had a peak 4 s later on average and approximately 5 % above baseline.

In a different approach to the analysis of BFV signal during functional studies, Rosergarten et al. [184] proposed a control system method to analyze the time course of BFV responses to cognitive tasks. The relative BFV response after an event is analyzed as a "step response of a second-order linear system". A standard evolution of the BFV response is assumed, with an initial acceleration phase and a velocity stabilization at a constant level after an overshoot. Fitting this step response enables quantification of the

measured BFV response by a specific set of system parameters (gain, natural frequency, rate time, damping and time delay). The method has been applied in some posterior studies to analyze physiological or pathological conditions [185, 186].

Finally, in a recent study, Schuepbach et al. [187] examined the relation between BFV responses and performance in a non-routine planning task. They used an analysis of the steepness of the slope of the signal (previously integrated to one value per heart beat) after an event occurs. The steepness of the increasing slope was calculated as percentage BFV change per second.

3.4.2 Other analyses of the BFV signal

The previous paragraphs detail the kind of analysis that have been made in functional studies. However, there are other possibilities of analyzing BFV signal that have not been used in psychophysiological studies about the performance of cognitive tasks. In the following paragraphs, these other kinds of BFV signal analysis will be summarized.

3.4.2.1 Spectral analysis

The spectral analysis allows the study of signals from a different point of view that provides information about the power of the signal at different frequencies [188]. Both representations of the signals (in the temporal domain and in the frequency domain) are equivalent, and only represent different ways of analyzing the same information. Signals with slow variations in the temporal domain are associated to frequency spectra with high content in the lower frequencies, and viceversa, signals with quick variations in the temporal domain are associated to frequency spectra with high content in the higher frequencies.

Frequency domain analysis has only been applied previously to the BFV signal to analyze its spontaneous changes (not stimulus-correlated) [136]. Kuo et al. [189] used this kind of analysis to study BFV correlation with arterial blood pressure. Thirty-three normal volunteers participated in the study. During 15 minutes, instantaneous arterial blood pressure was measured by plethysmography and bilateral BFV was monitored using

TCD. In this study, a classification of the fluctuations in MCA BFV in three different ranges was proposed:

- **Very low-frequency (0.016 to 0.04Hz)**. These variations of BFV have been associated with B-waves of intracranial pressure [190, 191], so they are also known as B-wave equivalents (BWE). It has been proposed that they can be caused by a phasic contraction and dilatation of small arteries, which produces fluctuations in cerebral blood volume. Cross-spectral analysis [189] revealed low coherence between the VLF components of MCA BFV and those of the arterial blood pressure. VLF fluctuations of BFV are not correlated to arterial blood pressure nor respiration.

- **Low-frequency (0.04 to 0.15 Hz)**. LF fluctuations had been described in arterial blood pressure and heart rate signals. However, they were rarely reported in BFV [192]. These components showed high coherence with those of arterial blood pressure [189]. Authors proposed that the observed LF fluctuations of BFV were secondary to LF fluctuations of arterial blood pressure which originated from peripheral vasomotor activity and are additionally modified by cerebral autoregulation with a time delay. However, there is currently no consensus on the origin of these waves [136].

- **High-frequency (0.15 to 0.4 Hz)**. These variations in BFV are correlated with respiration rate. The respiration-related fluctuations in BFV were found to be more pronounced when respiratory movements were deep and slow [193]. Coherence analysis revealed great similarity between HF components of MCA BFV and those of the arterial blood pressure [189]. HF fluctuations of BFV are secondary to HF fluctuations of arterial blood pressure induced by respiration.

Even higher frequencies are also present in the BFV spectrum due to rhythmic modulations of BFV caused by the heart beat. They typically appear in the BFV spectrum as a peak whose center corresponds to the mean heart rate and its harmonics [136].

3.4.2.2 Non-linear analysis

The origin of the behaviors of biological signals like the heart beat, the number of leucocytes in the blood or brain signals can be found in dynamical systems of great complexity that have to be studied. Although temporal series can have an appearance of noise, in many occasions, behind them, it can be found a determinist mechanism that can explain their disordered appearance. This is known as deterministic chaos [194, 195].

It is important to distinguish random sequences from deterministic chaos. Let us explain this more in detail. The series of numbers obtained when throwing successively the dice is an example of completely random sequence. It is impossible to predict what number will appear next. It is an unpredictable and aperiodic system. However, temporal series with the same appearance of these numbers can be generated in a deterministic way. These temporal series are generated by dynamical systems, that is, deterministic processes in which a function's value changes over time according to a rule that is defined in terms of the function's current value. Bornàs [195] points out two aspects of this definition of dynamical systems:

- Dynamical systems are deterministic, their behavior is guided by a rule.
- The future state of a dynamical system is a function of its present state.

At any given time a dynamical system has a state given by a set of real numbers (a vector) which can be represented by a point in an appropriate state space. The state space or phase space can be described as a mathematical space in which the coordinates represent the variables that are required to describe the state of the system. The evolution rule of the dynamical system is a fixed rule that describes what future states follow from the current state. The rule is deterministic: for a given time interval only one future state follows from the current state.

It is not always easy to distinguish a completely random series from a deterministic one. For example, the temporal series represented in Fig. 3.15 has the appearance of a random series. However, it has been generated using a rule called the logistic equation. This is a mathematical model

that has been used to model the evolution in the number of members of a population. The mathematical equation that describes this model is the following (equation 3.18):

$$x_{t+1} = k \cdot x_t \cdot (1 - x_t) \tag{3.18}$$

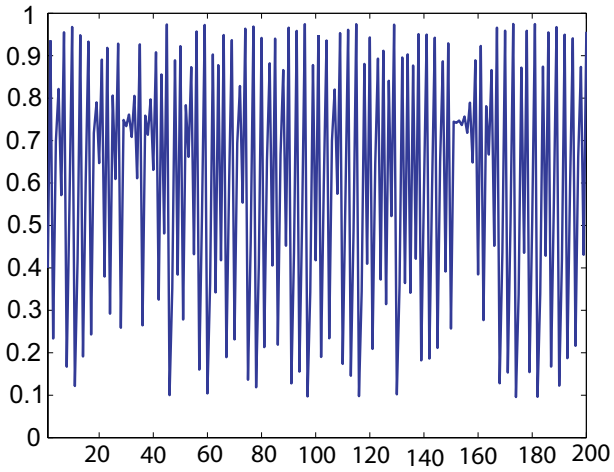

Figure 3.15: Temporal series of length 200 generated using the logistic equation with k=3.9 and $x_1 = 0.4$.

When applying this equation to describe the behavior of populations, x_{t+1} will represent the number of members in a future time $t+1$, which is a function of the number of members in the present time x_t. The behavior of a temporal series defined by this equation heavily depends on the exact value of k. For example, with $k < 2.9$, the system will have a transient behavior at the beginning and will stabilize in a single value. If $k \approx 3$, after the transient behavior, the system will oscillate between two values. However, for k=3.9, which is the value used to generate Fig. 3.15, the behavior that is observed is deterministic chaos.

TCD signals have also been analyzed from the perspective of non-linear dynamic systems. However, this kind of analysis has not been used in

the functional TCD studies previously described, in which only a linear perspective has been used.

Different approaches have been taken to study the non-linear features of the TCD signals:

- Some studies have analyzed the original signal received in the Doppler unit (without calculating the spectrogram to obtain velocity information) [196].
- There are also studies that have analyzed the BFV signal averaged over each cardiac cycle [197, 198, 199, 200, 201].
- Finally, other studies have analyzed the instantaneous maximum BFV (envelop from the spectrogram) [36, 37, 38, 202].

Ozturk et al. [196] analyzed MCA BFV of 82 patients with different brain diseases (cerebral aneurism, brain hemorrhage, cerebral oedema and brain tumor) and 24 healthy people. It was found using the surrogates method that all of the TCD signals presented non-linear dynamics and had an underlying low-level determinism. Maximum Lyapunov exponent was found to be positive for all TCD signals. The correlation dimension was found to have a fractional value higher than 2 for all TCD signals. This result indicates that the non-linear dynamics of TCD correspond to a strange attractor in the phase space with a low-level chaotic behavior. Besides, the non-linear parameters were approximately the same for the TCD signals of the patients with the same brain disease.

Regarding the studies that have analyzed the mean BFV signal, West et al. [201] showed that TCD has both a systematic and random component. Six healthy subjects participated in the study. Relative dispersion (ratio of the standard deviation to the mean) was used to show that the correlation in the beat-to-beat BFV signal is a modulated inverse power law, which indicates the existence of a long-time memory in the underlying control process. This analysis was posteriorly applied to compare between healthy humans and people who suffered from "severe" migraines [197, 200] and it was found that the multifractality that can be observed in the BFV of healthy people is almost entirely lost for people who suffer from these migraines.

In the study from Rossitti and Stephensen [198], the fractal dimension and the temporal correlation of the mean BFV at the MCA of 4 subjects was calculated. It was concluded that the temporal heterogeneity of the MCA BFV in the normal human has fractal properties.

More recently, Soehle et al. [199] analyzed complexity in 31 patients after subarachnoid hemorrhage. The spectral index β_{low} and the Hurst coefficient H_{bdSWV} were analyzed as fractal measures. The standard deviations and coefficients of variation were also calculated as measures of variability. BFV had significantly higher variability and Hurst coefficient as compared with arterial blood pressure. Better outcome correlated significantly with higher standard deviation of BFV and arterial blood pressure, as well as with a higher Hurst coefficient of arterial blood pressure.

Regarding the studies that have analyzed the maximum BFV signal, Vliegen et al. [38] proved that the maximum BFV had non-linear characteristics applying the surrogates technique. Previously to this confirmation, Keunen et al. [36] had already analyzed the correlation dimension of the maximum velocity. Their results had shown that this value was significatively greater during hypocapnia than during normocapnia (in both cases, it was a non-integer value).

In another study by the same group [37], the correlation dimension and the maximum Lyapunov exponent were obtained. An increment of the correlation dimension and a decrement in the maximum Lyapunov exponent in elder people were observed. The decrement in the maximum Lyapunov exponent was interpreted as a greater periodicity in the signal, explained by the reduction in heart rate variability and an alteration in the baroreceptor reflex. On the other hand, the increment in the correlation dimension could be related with oscillations in the most prominent vascular walls due to greater rigidity in elder people.

Finally, in another study with the maximum BFV [202], the fractal dimension was estimated by dispersional analysis in subjects with different head rotation angles, without obtaining significant differences between conditions.

Chapter 4

Methods

As described in the chapter 1, several experimental designs have been proposed to analyze the different hypotheses of the present PhD Thesis. These experiments are:

- **BFV analysis in different navigation conditions.** Monitoring of BFV during the exposure to a VE in a CAVE-like configuration in different navigation conditions.
- **BFV analysis in different immersive conditions.** Monitoring of BFV during the exposure to a VE in a projection system with a single screen. Comparison with the CAVE-like configuration results.
- **BFV analysis during a visual perception task.** Monitoring of BFV during simple visual tasks.
- **BFV analysis during motor tasks.** Monitoring of BFV while the participants perform simple motor tasks.

4.1 BFV analysis in different navigation conditions

This study was designed to analyze BFV responses during different moments of a VR experience, including the free navigation through the envi-

ronment, an automatic navigation guided by the system and forced ruptures of the VR experience.

4.1.1 Participants

Thirty-two right-handed volunteers (24 men, 8 women) aged between 17 and 51 years (mean age, 29.93 years; standard deviation, 6.35) participated in the study. Handedness was established by an experienced neurologist during the previous interview. Only right-handed subjects were included in the study in order to have a homogeneous group, because BFV differences in response to cognitive tasks have been observed between right- and left-handed users [20]. All the participants gave their informed consent prior to their inclusion in the study.

4.1.2 Apparatus

A commercially available 2-MHz pulsed-wave TCD unit (Doppler-Box^{TM}, DWL® Compumedics Germany GmbH, Singer, Germany) was used. This device was chosen mainly due to its portability. It has dimensions of 27x10.5x9 cm and weighs 1.8 Kg. The technique used is Pulsed Wave Doppler.

The apparatus was connected to a PC in which DWL® Doppler software (QL software) was installed. This software was used to receive the data from the Doppler Box and save the selected variables in the hard disk of the PC. Two dual 2-MHz transducers were connected to the Doppler Box, and were used to simultaneously monitor both brain hemispheres through the temporal window. The probe frequency determines the frequency of the sound wave in each burst. Probes can be attached to their location using the probe holder provided with the device. This probe holder can be regulated to be adapted to the user's head dimensions while holding the two probes in their correct position.

4.1.3 Virtual reality setting

The study was carried out in the Universidad Politécnica de Valencia, in a four-wall Reality Center. Any Reality Center requires at least the following

components:

- An image generator.
- High-brightness projectors.
- Projection screens.
- Software to control the system.

Furthermore, these systems usually include also optional modules required for additional features:

- A central system for the control of data, audio, illumination.
- Systems for the emission of audio/video.
- Stereoscopic visualization devices (such as transmitters or glasses).
- Interaction devices such as a joystick, a tracker, a mouse, or a keyboard.

Several configurations are possible for the projection screens that configure a Reality Center. The Reality Center that was used in this study has a CAVE-like configuration. As already explained, a CAVE is an immersive VR environment where projectors are directed to three, four, five or six of the walls of a room-sized cube. The first CAVE was developed in the Electronic Visualization Laboratory at University of Illinois at Chicago and was presented at the 1992 SIGGRAPH [203]. CAVE is a registered trademark of the University of Illinois Board of Regents. Several commercial and self-made systems have been developed based on the initial concept of CAVE. The Reality Center in the Universidad Politécnica has four sides: three walls and the floor. The dimensions of the floor were 2.5 x 2.5 m, and the height of the walls was 2.35 m. A photograph of the room with the Reality Center during the preparation of one of the experimental sessions can be visualized in Fig. 4.1.

Figure 4.1: Image of the room with the Reality Center during the preparation of one of the experimental sessions.

In order to deliver the images to the different screens, four Barco 909 (Barco, Kortrijk, Belgium) projectors were used combined with four big mirrors that reduce the required space to focus the image from the projectors on the screens. All images are retro-projected, except from the floor, in which the image is generated in a projector which is placed in the upper side of the room (frontal projection). The Barco 909 projectors are based on CRT technology, which uses small, high-brightness CRT (cathode ray tubes) as the image generating elements. The image is then focused and enlarged onto a screen using a lens kept in front of the CRT face. Most modern CRT projectors (including Barco 909) are color projectors with three separate CRTs and their own lenses to achieve color images. Barco

909 projectors are compatible with workstations that generate a resolution up to 3,200 by 2,560 pixels.

The machine used to generate the images was an SGI Prism (SGI, Sunnyvale, USA), which includes 16 Itanium2 1500MHz 4MB L3 CPUs, 16 GB of main memory (NUMA) and 8 graphic pipes. This machine allows the simultaneous processing of real-time 3D graphics, 2D images and text. Furthermore, it has good features for immersive applications, such as anti-aliasing and tools for stereo configuration. Finally, it allows multi-pipe rendering, which is required to generate the images corresponding to the different screens.

The system uses active stereoscopy. Stereoscopy is used to create depth perception in the brain, by providing the eyes of the viewer with two different images. These images represent two slightly different perspectives of the same scene, with a minor deviation similar to the perspectives that both eyes naturally receive in binocular vision. In active stereoscopy, alternate-frame sequencing is used. First, the left-eye image is projected, then the corresponding right-eye image, followed by the next left-eye image, the next right-eye image and so on. Glasses containing liquid crystal that blocks or pass light through in synchronization with the images generated by the graphics cards are required to obtain the expected effect (LCD shutter glasses). In the Reality Center, LCD shutter glasses, CrystalEyes3 (Real D, StereoGraphics, Beverly Hills, USA), were used for the visualization. They were synchronized with the output of the graphic cards by infrared technology.

In CAVE-like systems, the user's head position and orientation are monitored using a head-tracking device. As the participant in the VE experience moves within the limits of the CAVE, the instantaneous position and orientation are detected by the head tracking device, and the correct perspective and stereo projections of the environment are calculated and projected on the different display screens. In the Reality Center, an optical tracking system is used to monitor user's head and hand position and orientation. In optical tracking systems, the body part that has to be tracked is equipped with markers, which can be passive (light reflectors, retroreflectors) or active (light emitters, LEDs). In the room, several cameras are distributed to scan a certain volume, detect the light that is

reflected in the markers and calculate the marker position and orientation. In fact, each camera calculates a 2D marker position and this data is sent to a central PC which calculates 3D positions of a single marker, or 3D position and orientation of combinations of several markers forming a rigid body (also called constellations of markers). The position and orientation of the markers represent the position and orientation of the part of the body which carries the markers.

In the Reality Center, a commercial tracking system is used: ARTtrack1 (Advance Realtime Tracking GmbH, Weilheim, Germany). The tracking system is controlled from a PC which is placed in the control room. It is composed by 4 infrared cameras that are placed in the upper side of the screens. These cameras detect the reflections of the infrared light in targets. Some of the reflective targets were attached to the CrystalEyes3 to monitor the instantaneous position and orientation of the user's head so the visual perspective in the CAVE-like system could be adapted dynamically to this position and orientation.

On the other hand, a wireless joystick with 8 buttons was used to navigate (Flystick, Advance Realtime Tracking GmbH, Weilheim, Germany) and reflective markers were also attached to this device in order to monitor the hand position and orientation. This information was used in the navigation system that was programmed for the experiment. Only two buttons of the joystick were used for the navigation. The front button was used to advance towards the direction in which the Flystick is pointing to, and the rear button was used to move in the opposite direction (backwards). The CrystalEyes3 with the reflective targets can be visualized in Fig. 4.2 and the Flystick can be observed in Fig. 4.3.

The selection of a CAVE-like environment was made to maximize participants' presence, because previous studies [71] have shown that these systems have better usability and provide a better sense of presence to its users.

4.1.4 Software

The VE displayed in the Reality Center was a maze composed of several rooms and corridors. The virtual maze was designed specifically for this

Figure 4.2: Image of the shutter glasses (CrystalEyes3, Real D, StereoGraphics, Beverly Hills, USA) used to visualize the VE inside the CAVE. Reflective targets are attached to them in order to detect their position and orientation while the subject navigates in the VE.

Figure 4.3: Image of the wireless joystick (Flystick, Advance Realtime Tracking GmbH, Weilheim, Germany) used to navigate. Reflective targets are attached to it in order to detect its position and orientation while the subject navigates in the VE.

task. One important objective in the design of the virtual environment was to simplify the navigation, so the distribution of the environment was chosen to minimize the user's movements towards the laterals, forcing users to advance through long corridors in which lateral displacements have no sense.

The contents of this VE were generated using Autodesk 3ds Max 8 (Autodesk, Inc., San Rafael, California, USA). The environment was programmed using Brainstorm eStudio software (Brainstorm Multimedia, Madrid, Spain). This software allows the creation of interactive real-time 3D graphic solutions. Both the environment geometry and programming were carefully reviewed in order to avoid inconsistencies or problems that could generate spontaneous BIPs (not controlled by the experimental design) in the users. A cenital view of the whole environment can be visualized in Fig. 4.4 and some detailed captures of the VE can be visualized in Fig. 4.5.

The participants could not make any interaction with the VE, apart from navigation.

4.1.5 Procedure

4.1.5.1 Preliminary phase

All users had to follow the same protocol. When they arrived to the experimental room, they read a short description of what they were supposed to do during the experiment. First of all, they were told that the purpose of the experiment was to analyze some physiological measures that were going to be monitored during the exposure to a virtual environment in an immersive system. The word *presence* was not included in the description. After that, the different stages of the experiments were briefly described. A paragraph was also included with some comments about the Transcranial Doppler technique. Personal data related to age and sex were collected

Once in the Reality Center room, the probe holder with the two ultrasound probes was adjusted. Both hemispheres were simultaneously monitored through the temporal window using two probes capable of simultaneous exploration at two different depths, which were connected to the Doppler Box. An experienced neurosonologist adjusted the measurement

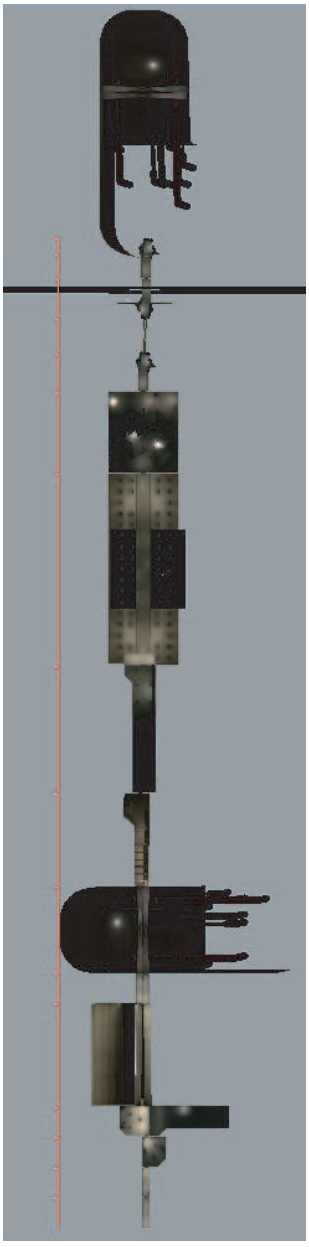

Figure 4.4: Cenital view of the virtual environment used during the experimental sessions.

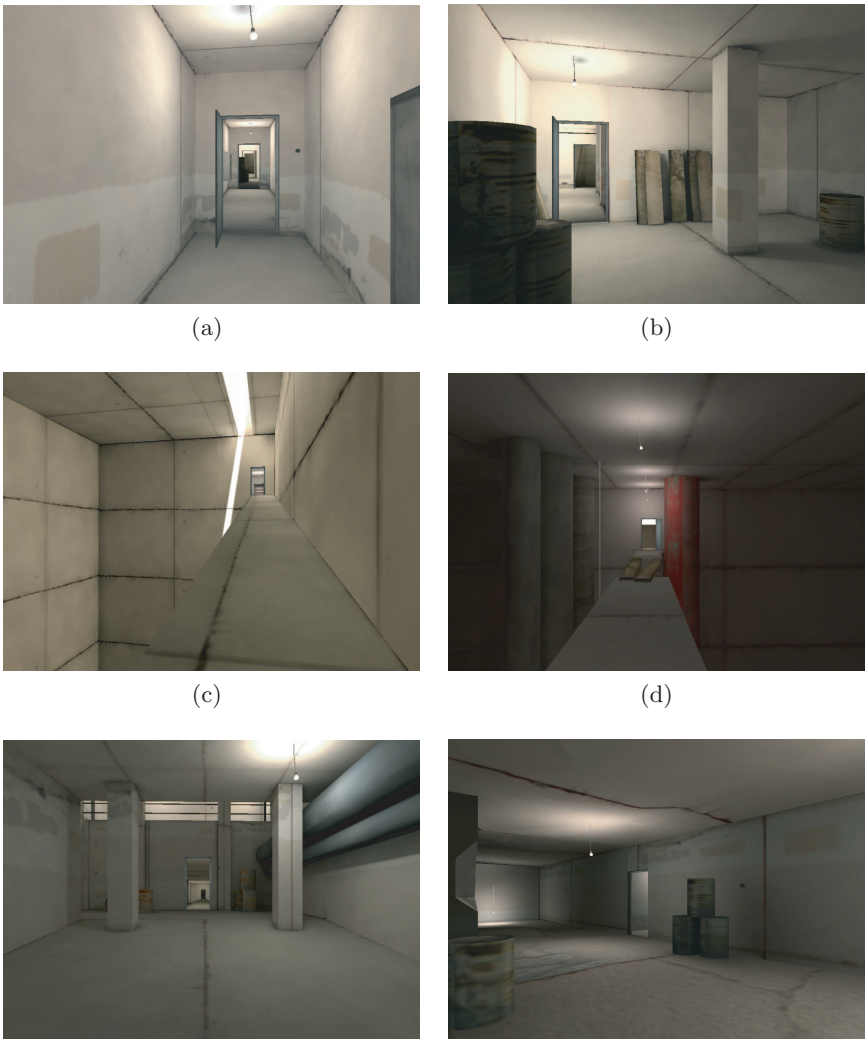

(a) (b)

(c) (d)

(e) (f)

Figure 4.5: Screen captures of several rooms of the maze displayed in the Reality Center during the sessions.

settings in order to guarantee the signal quality using QL software. Details about the insonation technique can be found in different studies [204]. First gate of each probe was located between 50-55 mm depth in order to register MCA-L and MCA-R flow. Second gate was located deeper, between 65-70 mm, to take ACA-L and ACA-R flow signals. The probes were adjusted to capture simultaneously data from as many vessels as possible, although for most of the subjects, the simultaneous recording was limited to only some of the vessels. Mean BFV signal were registered by QL Software.

Once the probes have been placed, the CrystalEyes3 shutter glasses were also adjusted in their correct location, as can be seen in Fig. 4.6. As has been explained in the previous section, the subjects had to wear the shutter glasses, because they were required to visualize correctly with stereoscopy the 3D environment, and because they had attached the markers to detect the position of the user's head during the whole duration of the exposure to the VE.

Figure 4.6: User with TCD probes and shutter glasses for visualizing VE with stereoscopy.

4.1.5.2 Exposure to the VE

The subjects remained standing up in the middle of the Reality Center for the entire duration of the experiment. They did not make any special movements during the different periods, apart from right arm movements and rotations to indicate the direction towards which they wanted to advance inside the virtual environment during the free navigation condition. Involuntary or reflex movements might have occurred, but they were equally possible in the different conditions.

The different phases during the exposure to the VE can be visualized in Fig. 4.7

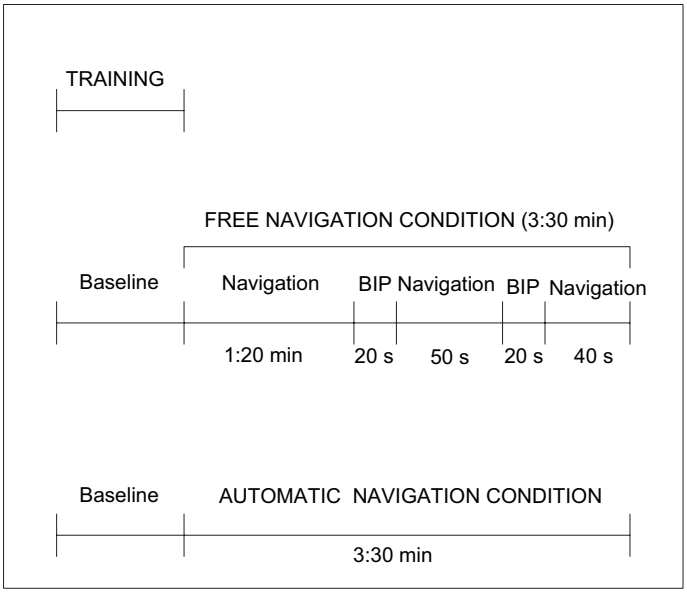

Figure 4.7: Schema representing the different phases of the experiment.

4.1.5.3 Training stage

There was a training stage, during which the subject learnt to navigate inside the VE (pointing in the correct direction with the Flystick, and

Figure 4.8: Screen capture of the training environment.

pushing the forward and backward buttons of this device). A simplified environment consisting only of a surface with a chessboard texture was used (Fig. 4.8). The user had to move on this surface following some instructions that appeared on screen.

It was confirmed that the user felt comfortable and the cardiac frequency was stable prior to the beginning of the experiment.

4.1.5.4 Free navigation condition

Subjects had to navigate in the same virtual environment in two different navigation conditions. The free navigation condition consisted in a free navigation in the virtual environment using the Flystick, for a total time 3:30 minutes. The Flystick was held with the right hand during the whole duration of the free navigation condition.

Before this condition, there was a baseline period used to obtain reference values. During baseline periods, the subjects did not see anything. The screens were completely black. Users were instructed to be relaxed during the baseline until navigation started.

Fig. 4.9 shows an image of a subject during a real session during the free navigation condition.

Figure 4.9: Image of one user navigating during the free navigation condition

4.1.5.5 Automatic navigation condition

The automatic navigation condition, consisted in watching an automatic navigation through the same virtual environment. Users were completely passive. They only had to watch the automatic navigation that was presented to them. No device was held with their right hand during this period. The display lasted 3:30 minutes.

The automatic navigation condition was also preceded by a baseline period.

Fig. 4.10 shows an image of a subject during a real session in the automatic navigation condition.

4.1.5.6 BIPs

Following a similar approach to previous studies [23, 131], two interruptions or anomalies were forced during the free navigation condition at two

times at approximately evenly spaced intervals during the free navigation condition.

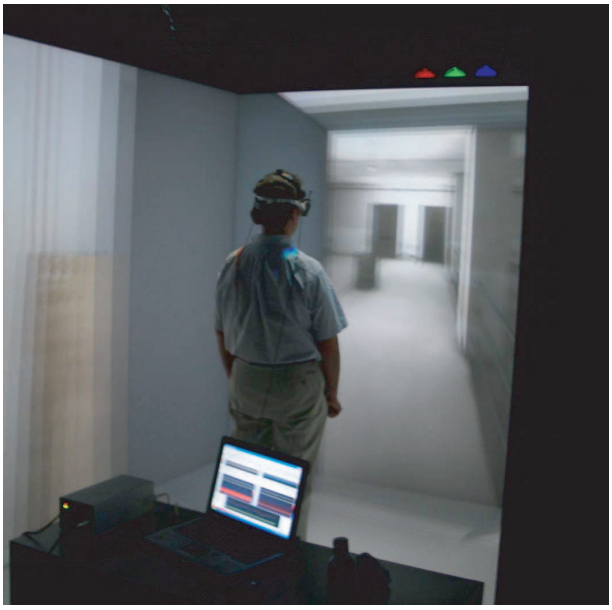

Figure 4.10: User visualizing the automatic navigation in the Reality Center. The probes are placed on the user's head and connected to the Doppler Box, which is connected to a PC that runs QL software.

In one of the interruptions, the four projection walls became completely black. In the other interruption, the lateral and floor walls also became completely black, but the frontal wall remained active, so the VE could be visualized in the frontal wall. However, navigation was blocked, so the user could not advance nor go backwards in the VE for the duration of this interruption. Each of these anomalies lasted 20 s, and after this period, the normal navigation and visualization conditions were restored. These interruptions were used to force BIPs in the participants of the VR experience, as supported by the conclusions of the study by Garau et al. [131].

4.1.5.7 Presence questionnaires

The users' level of presence during the experiment was checked by means of one sufficiently validated method: subjective reports. Once the experiment had finished, users had to answer SUS questionnaires [22]. This questionnaire includes six 7-point Likert-like questions that were adapted to the contents of the virtual environment including references to the maze. Annex B contains a copy of the questionnaire that was given to the subjects that participated in the experiment. The user had to answer the questionnaire twice, once for the free navigation, and the other for the automatic navigation condition. Subjects were ignorant of the goals of the experiment in order to minimize expectation bias.

4.1.6 Data analysis

The data that were obtained with this experiment were:

- Responses to the different items of the SUS questionnaire corresponding to the free navigation condition, and responses to the different items of the SUS questionnaire corresponding the automatic navigation condition.
- Mean BFV signal. The original Doppler signal was captured using the Doppler Box with a sampling frequency of 100 Hz. A Fast Fourier Transform (FFT) algorithm included in QL software was used to automatically obtain the spectrogram. The mean of the envelope of this velocity spectrum (in centimetres per second) was recalculated by the software every 1.3 s. An example of a captured signal with the calculated mean can be visualized in Fig. 4.11. In this experiment, mean BFV signal was registered for the analysis.

Different analyses were performed based on the available data in order to check the hypotheses of this study. These analyses include:

- Comparison of SUS questionnaire responses between the free navigation condition and the automatic navigation condition.
- Comparison of BFV parameters between baseline periods and VE exposure periods.

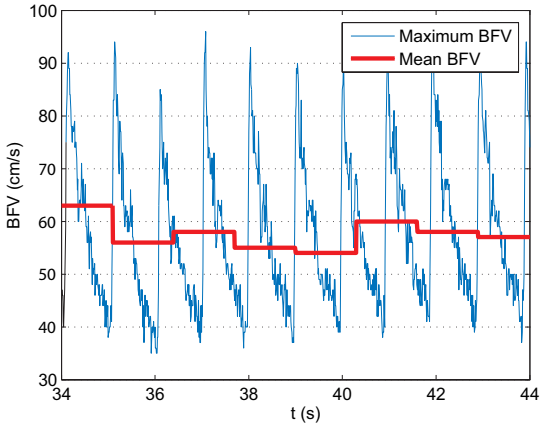

Figure 4.11: Maximum and mean Blood Flow Velocity in the left middle cerebral artery in a sample subject as calculated by QL software.

- Study of correlation between SUS responses and BFV parameters in the different navigation conditions.
- Comparison of changes in BFV parameters between the free navigation condition and the automatic navigation condition.
- Analysis of BFV responses during BIPs.

In the following paragraphs, the different analyses will be described in detail.

4.1.6.1 Comparison of SUS questionnaire responses between the free navigation condition and the automatic navigation condition

The data available for this analysis are the individual responses to the six questions associated with each of the periods (free and automatic navigation). Two additional measures, which had been used in previous studies [22], were also calculated as follows:

- **SUS Count.** It is calculated as the number of the SUS responses with "6" or "7" scores amongst the six questions.

- **SUS Mean**. It is the mean score across the six questions.

As responses to questionnaires are ordinal variables, a non-parametric test, the Wilcoxon Signed-Rank Test, was used to compare between individual SUS responses, SUS Mean and SUS Count (dependent variables) in the different experimental conditions (independent variable): free vs. automatic navigation.

4.1.6.2 Comparison of BFV between repose periods and VE exposure periods

The purpose of this analysis was to compare BFV during repose periods (baseline) with BFV during VE exposure periods in the different vessels that were monitored: MCA-L, MCA-R, ACA-L and ACA-R.

Only data from the last 20 s (and at least 15 cardiac cycles) of the baseline periods were included in the analysis in order to guarantee that the signal was stable and that the obtained value was representative of the situation. Similar approaches have been used to calculate the baseline value in other studies [153, 205].

As long as the neurovascular coupling occurs a few seconds after the beginning of a mental task [31, 180, 158, 149, 181] and velocity remains relatively constant while the activity is maintained, only a section of the period (both in the free navigation condition and the automatic navigation condition) was included in the analysis. This procedure can contribute to avoid BFV variations caused by factors different to the VE exposure (for example, a possible fatigue effect).

In the case of the automatic navigation condition, data from the first half of the period (1:45 minutes) were included in the analysis. In the case of the free navigation condition, only the first 1:20 minutes of the free navigation condition were included, in order to avoid any interference from the forced BIPs included in the experiment.

The mean of BFV values corresponding to the selected data in each period (baselines, free and automatic navigation conditions) were calculated

and used as a reference value for that period. Instantaneous BFV remains relatively stable while the activity is maintained.

Summarizing, the four BFV parameters that were calculated were:

- Mean BFV during the last 20 s of the baseline previous to the free navigation condition.
- Mean BFV during the first 1:20 minutes of the free navigation condition.
- Mean BFV during the last 20 s of the baseline previous to the automatic navigation condition.
- Mean BFV during the first 1:45 minutes of the automatic navigation condition.

A parametric test (repeated measures ANOVA) was used to compare BFV measurements in each vessel between the different experimental conditions. The mean BFV was selected as the dependent variable and the experimental period (baseline previous to the free navigation, free navigation condition, baseline previous to the automatic navigation, and automatic navigation condition) as the independent variable. No comparisons between vessels were made. If Mauchly's test indicated that the assumption of sphericity had been violated, Greenhouse Geisser corrections were applied. As post-hoc tests were needed to obtain paired comparisons, the Bonferroni correction was applied to adjust for multiple comparisons.

Results of applying the Kolmogorov-Smirnov test to the mean BFV variables corresponding to the different periods, in order to check their normality, can be found in Annex C.

4.1.6.3 Correlation between SUS responses and BFV values during the different navigation conditions

In order to analyze whether there are correlations between SUS answers (the individual answer to each question, SUS Mean and SUS Count) and BFV values (in MCA-L, MCA-R, ACA-L and ACA-R) in the different periods (free and automatic navigation conditions), non-parametric Spear-

man's rank correlation coefficient (Spearman's rho) was calculated for the different combinations of SUS answers and BFV parameters at each period.

4.1.6.4 Comparison of BFV variations in the free navigation condition and the automatic navigation condition

As described before, each activation period (free navigation or automatic navigation) is preceded by a baseline period, and the BFV of each activation period can be compared with the BFV of the preceding baseline [206, 207, 20]. In order to compare the BFV variations observed in the automatic navigation condition (with respect to its preceding baseline) with the BFV variations observed in the free navigation condition (when compared to its preceding baseline), the percentage variation in BFV between the baseline and the activation period was calculated (4.1) [160, 178, 163, 176, 165].

$$BFV(\%) = 100 * \frac{BFV_{activation} - BFV_{baseline}}{BFV_{baseline}} \tag{4.1}$$

Percentage variations between activation and baseline had been used in previous studies to eliminate any variability associated with changes in the insonation angle or the vessel diameter [151, 177]. In the present study, these values were calculated just to compare between mean BFV variations in the different experimental conditions.

Parametric tests were applied to compare the percentage variations obtained in the different conditions. The percentage variations in the free navigation and in the automatic navigation conditions for the different vessels were compared using a two-tailed Student's t test for paired samples.

Results of applying the Kolmogorov-Smirnov test to the percentage variation variables corresponding to the different periods can be found in Annex C.

4.1.6.5 Analysis of BFV signal when BIPs occur

Each BIP lasts only a short period of time (20 s). The BFV signal is not stable during this period. On the contrary, it is expected to vary in

response to the occurrence of the BIP. Furthermore, when the normal navigation and visualization are restored, new variations in BFV are expected

Calculating a mean BFV as a representative of a period had sense in the previous analyses about long periods of exposure to VEs, in which BFV was stabilized during the period of activation / baseline. However, in the BIPs and in the recovery from the BIPs, the signal is on a transient state, so it was decided to analyze the temporal evolution of BFV signal during the BIP, instead of obtaining a mean BFV, which represents less faithfully the behavior of BFV signal during the period.

The term *Total BIP* will be used to refer to the most intense BIP caused by the interruption in which the four projection walls became black. The term *Partial BIP* will be applied to the less intense BIP caused by the interruption in which only lateral walls and floor became black and navigation was blocked.

The temporal evolution will also be analyzed in the period following the moment in which the normal visualization and navigation are restored (recovery period from the BIP). In order to analyze the recovery from each BIP, only the 20 s that follow the end of the BIP will be considered. The term *Total Recovery* will be used to refer to the period of 20 s that follows the end of *Total BIP*, and the term *Partial Recovery* to refer to the period of 20 s that follows the end of *Partial BIP*.

In order to analyze the temporal evolution of BFV signals during the BIPs and their recoveries, some signal processing methods were programmed using Matlab (The MathWorks, Natick, Massachusetts, USA).

Prior to other processing, BFV signals were lowpass filtered to smooth them using a moving average FIR filter of 250 coefficients.

After the filtering, the signal was transformed to normalized units, simply dividing BFV by the mean BFV measured during the whole examination time and multiplying by 100 [33], as indicated by the following formula:

$$X[n] = 100 * \frac{x[n]}{\frac{1}{N} \cdot \sum_{n=0}^{N-1}(x[n])} \tag{4.2}$$

being n the sample, X[n] the normalized signal, x[n] the original BFV signal and N the length of the data captured during the whole examination time.

There are several reasons for performing this normalization. First of all, BFV values have important interindividual variations if described using absolute units [204]. In addition, absolute values are sensitive to the insonation angle between the ultrasound beam and the course of the insonated artery [19]. The normalization process solved these problems, making possible the comparisons between vessels in both hemispheres without any influence from the angles of the two probes [151].

Two parameters have been obtained from the normalized signal in order to characterize the temporal evolution of the BFV signal during the BIPs and during the recovery periods:

- **The maximum BFV percentage variation.** It is calculated as the percentage difference between the peak value of BFV signal during the period (which can be a maximum or a minimum) and its initial value.

- **The response time.** It is calculated as the time that has elapsed between the beginning of the period and the moment in which the peak value is achieved.

A statistical analysis has been applied to check if the response time and the maximum BFV percentage variation show significant differences between both BIPs and between both vessels considered in the study (MCA-L and MCA-R).

Two-way ANOVAs with repeated measures were applied to analyze the effects on the response time and on the percentage variation (dependent variables) of the within-subjects factors (vessel and kind of BIP / recovery).

Results of applying the Kolmogorov-Smirnov test to the variables corresponding to the different periods can be found in Annex C.

4.2 BFV analysis in different immersive conditions

The goal of this study was to analyze if the results of the previous study about navigation are generalizable to VR systems with other degrees of immersion. The same experimental design as in the previous study was

used, but in this case the VR system was less immersive, and only a reduced number of volunteers participated in the study.

4.2.1 Participants

Ten right-handed volunteers (5 men and 5 women) aged between 23 and 55 years (mean age, 34.10 years; standard deviation, 8.87) participated in the study. All the participants gave their informed consent prior to their inclusion in the study.

4.2.2 Apparatus

As in the previous study, BFV was monitored using the Doppler-Box^{TM}, DWL® Compumedics Germany GmbH, Singer, Germany), connected to a PC where DWL software was installed.

Analogously, other physiological measurements such as blood pressure, CO_2 and respiratory rate were not controlled during the experiments.

4.2.3 Virtual reality setting

The environment was retro-projected in a 2 x 1.5 m metacrilate screen. Monoscopic vision was used in this case. A single Sony VPL - CX5 (Sony, Minato, Tokyo, Japan) projector was used to project the image in this case. The device that was used to navigate inside the VE was an Attack^{TM} 3 Joystick from Logitech (Logitech, Fremont, CA, USA).

4.2.4 Software

The same VE as in the previous study was used (a maze composed of several rooms and corridors).

In order to advance in the VE, the joystick was moved forwards, and in order to go back in the VE, the joystick was moved backwards. No additional interaction was allowed apart from navigation.

4.2.5 Procedure

The procedure followed during the experimental sessions in this study is summarized in the following points:

- Preliminary phase
  - Subjects read a short description of what they had to do during the experiment. Personal data related to age and sex were collected.
  - The probe holder with the two probes was adjusted by the neurosonologist. MCA-L and MCA-R BFV values were monitored in this study.
- Exposure to the virtual environments. In this study, the user remained seated in front of a table where the joystick was placed during the whole duration of the exposure to the VE.
  - Training stage. Users learnt to navigate inside a VE using the joystick.
  - Free Navigation Condition. Subjects navigated freely inside the VE using the joystick during 3:30 minutes. The period was preceded by a repose period used as baseline.
  - Automatic Navigation Condition. Users visualized a system-guided navigation inside the VE during 3:30 minutes. The period was preceded by a repose period used as baseline.
- SUS Questionnaires. Subjects answered the SUS questionnaires corresponding to the free navigation condition and to the automatic navigation condition.

4.2.6 Data Analysis

The data from this study (SUS questionnaire responses and BFV data) were compared with the data obtained in the study about navigation, in order to analyze the influence of the VR configuration (degree of immersion) on the observed results.

The different experimental conditions and the duration of the periods included for the analysis are summarized in Table 4.1.

Table 4.1: Summary of the different experimental conditions.

		NAVIGATION	
		Free	Automatic
IMMERSION	STUDY 1: CAVE-like	Baseline (20 s) VE exposure (1:20 min)	Baseline (20 s) VE exposure (1:45 min)
	STUDY 2: Single screen	Baseline (20 s) VE exposure (1:20 min)	Baseline (20 s) VE exposure (1:45 min)

4.2.6.1 SUS-questionnaires analysis

As responses to questionnaires are ordinal variables, parametric tests could not be used, and a robust two-way ANOVA was selected for the statistical analysis (data were α-Winsorized with α=0.2). The dependent factors were the answers to each of the six SUS questions, as well as the SUS Count and SUS Mean values. Navigation (free vs. automatic) was the within-subjects factor and immersion (CAVE-like vs. single screen environments) was the between-subjects factor. Homocedasticity (or equality of variances between the levels of the between-subjects factor) was analyzed with the Levene statistic.

4.2.6.2 Comparison of BFV variations in the free navigation condition and the automatic navigation condition

BFV percentage variations between each activation period and its preceding baseline were calculated to allow comparisons between BFV variations in the different experimental conditions.

BFV percentage variations for the different vessels were compared by means of a two-way ANOVA (dependent factor: percentage of BFV change) with navigation (free vs. automatic) as within-subjects factor. Immersion (CAVE-like vs. single screen configuration) was evaluated by adding it as between-subjects factor to the ANOVA. Homocedasticity was also analyzed by the Levene statistic.

4.3 BFV analysis during a visual perception task

There are several aspects that change between baseline and the exposure to the VE including visual perception, motor tasks, attention, emotions and presence, which complicates the analysis of the BFV registers. In order to facilitate the interpretation of BFV responses during VR experiences, simpler experiments were designed to study individual variables that contribute to the VR experience. In this one, visual perception aspects were analyzed.

4.3.1 Participants

Twenty-three right-handed volunteers (13 men, 10 women) aged between 19 and 66 years (mean age, 33.52; standard deviation, 13.17) participated in the study.

All the participants gave their informed consent prior to their inclusion in the study. Handedness was established using the Edinburgh Handedness Inventory [208]. All the participants had normal or corrected-to-normal vision.

4.3.2 Apparatus

As in the previous studies, a commercially available 2-MHz pulsed-wave TCD unit (Doppler-Box^{TM}, DWL® Compumedics Germany GmbH, Singer, Germany) was used to obtain a bilateral continuous measurement of the Doppler signal.

Blood pressure was measured before and after the visual tasks using a wrist blood pressure monitor (R3 Intellisense, Omrom Healthcare Co., Ltd., Kyoto, Japan).

A Sony VPL-CX5 (Sony, Minato, Tokyo, Japan) projector was connected to a PC to provide the visual stimulation in a 2.40 x 1.80 m screen.

4.3.3 Procedure

4.3.3.1 Preliminary phase

The tests were performed in a quiet, dark room. In the preparatory stage, the subjects received written instructions about the experiment and answered the Edinburgh Handedness Inventory Questionnaire [208]. Once finished, they sat down on a chair in front of the screen.

Distal segments of the PCA-L and PCA-R were monitored during the experiment through the temporal window using two symmetrically attached probes held in place by the probe holder provided with the device. An experienced neurosonologist adjusted the angle and the insonation depth of each probe once the subject was seated in front of the screen in order to monitor the PCA. The insonation depth varied between 58 and 65 mm, depending on the subject, and the insonated volume was fixed to 10 mm^3. Further details about the insonation technique can be found in other studies [204].

Once the probes had been adjusted, the subject was told to relax and blood pressure was measured.

4.3.3.2 Visual stimulation

Following this, the visual stimulation stage started. Visual stimulation was provided using a presentation developed in Microsoft Office PowerPoint

(Microsoft, Redmond, Washington, EEUU) that was projected into the screen.

Subjects were exposed to short periods of obscurity and illumination (20 s length each period). The presentation lasted globally 6 minutes and 40 s. It showed empty black and white slides alternatively, each of them appearing for a fixed duration of 20 s. This length has been selected in accordance with the methodology applied in other previous studies that also used alternating 20 s periods of repose and activation [29]. This duration is long enough to guarantee that the temporal maximum after the onset of the mental task is located inside the period of analysis. When black slides were projected, the room was completely dark (repose periods). When white slides were projected, the screen in front of the subject was illuminated (activation periods). The appearance of each slide was marked acoustically with a beep sound that indicated to the subject that the slide had changed. The experiment consisted of ten repetitions of repose-activation cycles. The user closed and opened their eyes alternatively, coinciding with the repose and activation periods.

4.3.3.3 Final stage

Finally, when the visual stimulation stage finished, the subject's blood pressure was measured again, just to confirm that the experience did not alter the subject's blood pressure significantly.

4.3.4 BFV signal analysis

Maximum BFV signals corresponding to the maximum velocity of blood cells at each instant were registered in this study. These signals vary following each cardiac cycle. They were stored during the experiment on the PC hard disk for off-line analysis. Their sampling rate was 100 Hz.

A neurologist validated the registries for the different vessels. Seven subjects' measurements were discarded because a clear enough quality signal could not be obtained for both PCA.

4.3.4.1 Data normalization

Prior to other steps, the maximum BFV signal was transformed to percentage relative units, simply dividing each sample by the arithmetic mean of the full set of data during the whole examination time and multiplying by 100 [33], as indicated in equation 4.2.

This normalization is useful to minimize the interindividual variations that are observed in the BFV signal if described using absolute units [204] and to eliminate the influence of the insonation angle a between the ultrasound beam and the course of the insonated artery [19, 151].

4.3.4.2 Spectral analysis

Spectral analysis was performed separately for the repose and activation periods, as long as it cannot be assumed that the signal characteristics remain stationary between them.

The spectral estimator that was used is the Modified Periodogram [209]. This method applies the Fourier Transform to a signal fragment, which is selected using an arbitrary window $w[n]$ of length L. The spectral estimation given by the modified periodogram is:

$$\widehat{\Phi}_x(e^{j\cdot\omega}) = \frac{1}{L\cdot U}\cdot|\sum_{n=0}^{L-1} X[n]\cdot w[n]\cdot e^{-j\cdot\omega\cdot n}|^2, \tag{4.3}$$

where $X[n]$ is the signal, $w[n]$ is the window used to select the samples, L is the length of this window and U is a constant used to compensate the attenuation effect in the window extremes, so the signal power is not underestimated. It can be calculated as:

$$U = \frac{1}{L}\cdot\sum_{n=0}^{L-1}(w[n])^2 \tag{4.4}$$

The modified periodogram of the normalized BFV signal is calculated for each of the ten activation periods and for each of the ten repose periods. The spectral leakage that could appear in the spectral estimation caused by the extraction of the temporal data sequence was reduced using a Hamming window, which has an important attenuation in the side lobe levels when

compared with the main lobe level (-41 dB). The length of the window was 2000 samples (20 s sampled at 100 Hz), value that coincides with the length of each repose / activation period. All the data available from each period were used to obtain the modified periodogram, because that way the frequency resolution of the spectral estimation is maximized and it is guaranteed that the segment of the signal over which the modified periodogram is calculated is large enough to be representative.

In order to reduce the excessive variance of the modified periodogram estimation, the WOSA (Weighted Overlapped Segment Averaging) method was used [209]. Assuming that we have a signal of length L_T, this method consists of averaging a number of periodograms of length L (being $L < L_T$), instead of using only one periodogram of length L_T. That way, the estimation variance will be reduced. The original WOSA method allows an overlap between the different periods that are selected to calculate the periodograms used to average. The WOSA estimator can be described as:

$$\widehat{\Phi}_x^{WOSA}(e^{j\cdot\omega}) = \frac{1}{K} \cdot \sum_{k=1}^{K} \widehat{\Phi}_x^{(k)}(e^{(j\cdot w)}) \tag{4.5}$$

where K represents the number of periodograms that are averaged. In the analysis that was performed, 10 modified periodograms corresponding to the 10 repose periods were averaged in order to obtain a global spectral estimation for the repose periods. Obviously, as long as different periods were used to calculate the different modified periodograms, no overlapping was applied. The same procedure was applied for the activation periods, obtaining a global spectral estimation corresponding to activation times.

4.3.4.3 Low-frequency estimation

In order to study the influence of the visual stimuli in the BFV signal, the low-frequency band of the spectral estimation was analyzed. The peak of the spectral estimation in the low-frequency band was calculated for each subject in both vessels (PCA-L and PCA-R) and in both experimental conditions (repose and activation).

The instantaneous average of the signals corresponding to the different repose periods was calculated for each subject and the component of this

signal at the peak frequency in the low-frequency band was estimated [210, 211]. This component is given by:

$$\widehat{x} = C \cdot \cos\left(2 \cdot \pi \cdot f_0 \cdot n\right) + D \cdot \sin\left(2 \cdot \pi \cdot f_0 \cdot n\right) + E, \tag{4.6}$$

where f_0 is the frequency of the peak observed in the low-frequency band of the spectral estimation, n represents the sample, and C, D and E are three parameters that have to be estimated to minimize the quadratic error (4.7) between the normalized BFV signal ($X[n]$) and the estimation ($\widehat{X}[n]$).

$$\xi = \sum_{n=0}^{L-1} \left(\widehat{X}[n] - X[n]\right)^2, \tag{4.7}$$

The same procedure was applied for the activation periods.

4.3.4.4 Calculus of BFV parameters

Several parameters were calculated in the repose and activation periods corresponding to each of the PCA-R and PCA-L valid measurements.

After normalizing the signals, mean BFV values corresponding to the normalized BFV during repose periods, and to the normalized BFV during activation periods, both in PCA-R and PCA-L, were obtained. These values can be used to analyze global differences in BFV between vessels (PCA-R vs. PCA-L) and between periods (repose vs. activation), as in previous studies [175, 153, 160, 176, 165].

Apart from this, two additional parameters were obtained from the low-frequency estimation in order to characterize the temporal evolution of the BFV signal during repose and during activation periods: the percentage variation and the response time. The percentage variation was calculated as the percentage difference between the peak value of the estimation signal during its temporal evolution inside the period (which can be a maximum or a minimum) and its initial value. The response time was calculated as the time in which the peak value of the low-frequency estimation signal is achieved.

4.3.5 Statistical analysis

A statistical analysis was applied to check if the differences in the BFV calculated parameters (mean, percentage variation and response time) between repose and activation periods and between vessels were significant. Prior to the analysis, the variables were checked for normality using the Kolgomorov-Smirnov test. Two-way analysis of variance (ANOVAs) with repeated measures were applied to analyze the effects on the previous parameters (dependent variables) of the within-subjects factors:

- The vessel under study (PCA-R vs. PCA-L).
- The presence of visual stimulus (repose versus activation periods).

Only those cases in which measurements from both vessels were available (16 subjects) were included in the statistical analysis to allow the comparison between vessels.

Results of applying the Kolmogorov-Smirnov test to the different variables can be found in Annex E.

4.4 BFV analysis during motor tasks

Continuing with the simpler experiments in which single aspects of the VR experience were analyzed, this study focused on motor aspects (specifically, the motor movements required to control a joystick).

4.4.1 Participants

Eleven volunteers (4 men, 7 women) aged between 22 and 45 years (mean age, 29.09; standard deviation, 8.117) participated in the study.

All the participants gave their informed consent prior to their inclusion in the study. Handedness was established using the Edinburgh Handedness Inventory [208].

4.4.2 Apparatus

As in the previous studies, a commercially available 2-MHz pulsed-wave TCD unit (Doppler-Box^{TM}, DWL® Compumedics Germany GmbH, Sin-

ger, Germany) was used to obtain a bilateral continuous measurement of the Doppler signal.

Blood pressure was measured before and after the visual tasks using a wrist blood pressure monitor (R3 Intellisense, Omrom Healthcare Co., Ltd., Kyoto, Japan).

The motor tasks performed during the experience consisted in the manipulation of a joystick as it would be done when navigating inside a VE. A joystick from Logitech (Logitech, Fremont, CA, USA) was used during the experiment: the Attack^{TM} 3 model.

A Sony VPL-CX5 (Sony, Minato, Tokyo, Japan) projector was connected to a PC to project the instructions about the different phases of the experiment in a 2.40 x 1.80 m screen.

4.4.3 Procedure

4.4.3.1 Preliminary phase

The tests were performed in a quiet room. In the preparatory stage, the subject received written instructions about the experiment and answered the Edinburgh Handedness Inventory Questionnaire. Once finished, they sat down on a chair looking to the screen. The Logitech Attack^{TM} 3 joystick was put on a table that was in front of them. The joystick was not connected to a computer.

Two symmetrically attached probes held in place by the probe holder provided with the Doppler unit were used to monitor maximum BFV in the MCA-L and MCA-R. An experienced neurosonologist adjusted the angle and the insonation depth of each probe to monitor those vessels. The insonation depth varied between 50 and 55 mm, depending on the subject. Further details about the insonation technique can be found in other studies [204].

Once the probes had been adjusted, the subject was told to relax and blood pressure was measured.

4.4.3.2 Motor tasks

Following this, the motor tasks stage started. These motor tasks consisted of arm movements with the purpose of moving the joystick in different directions and as fast as possible (similarly to what would happen when navigating in a VE). As there were different phases in the experiments, the transition from one phase to the following was indicated in the following way:

- A text with a short description of the stage that was beginning was projected on the screen, so the participant could read (and remember from the initial written description) the action that had to perform. These texts were integrated in a presentation developed in Microsoft Office PowerPoint (Microsoft, Redmond, Washington, EEUU).
- A beep sound indicated the transition between experimental conditions.

There were two experimental conditions:

- Joystick movements with the dominant hand.
- Joystick movements with the non-dominant hand.

Joystick movements in each of the experimental conditions were performed during a period of 2:30 minutes. Each condition was preceded by a repose period of 2:30 minutes.

The different experimental conditions and the associated repose periods are summarized in Table 4.2

Two different orders of presentation of the two active conditions (dominant hand movements and non-dominant hand movements) were used in the study. Nine subjects were exposed first to the dominant hand movements condition, and two subjects were exposed first to the non-dominant hand movements condition.

4.4.3.3 Final stage

Finally, when the motor tasks finished, the subject's blood pressure was measured again, just to confirm that the experience did not alter the subject's blood pressure significantly.

Table 4.2: Summary of the different experimental conditions.

EXPERIMENTAL CONDITION	DURATION
(a) REPOSE: Hands reposing on the legs	2:30 minutes
(b) DOMINANT HAND MOVEMENTS: Subjects perform quick and uninterrupted joystick movements with their dominant hand	2:30 minutes
(c) REPOSE: Hands reposing on the legs	2:30 minutes
(d) NON-DOMINANT HAND MOVEMENTS: Subjects perform quick and uninterrupted joystick movements with their non-dominant hand	2:30 minutes

4.4.4 Registering and pre-processing BFV signals

4.4.4.1 BFV signal features

Maximum BFV signals corresponding to the maximum velocity of blood cells at each instant were registered in this study. They were stored during the experiment on the PC hard disk for off-line analysis with a sampling rate of 100 Hz.

A neurologist validated the registries for the different vessels. MCA-L measurements from two subjects and MCA-R measurements from other two subjects were discarded because a clear enough quality signal could not be obtained.

4.4.4.2 Pre-processing

As non-linear methods were applied to analyze the BFV in the different experimental conditions, some pre-processing was required to adapt the data to this kind of analysis. This pre-processing consisted basically of two steps:

- Data extraction to select the relevant information from each period.
- Lowpass filtering to eliminate high-frequency noise.

In the first step, the central 1:30 minute-period of each condition (both in repose and activation conditions) was selected, to avoid any transitory which could appear when changing from one condition to another. As phase transitions in the non-linear parameters are expected between the different experimental conditions, the periods just before and after the transition from one condition to another were eliminated. All the non-linear methods that will be described below can only be applied when the dynamics of the system have converged [194].

Once the data of interest have been selected, in the second and final step of the pre-processing, a lowpass filter was applied to the selected data in order to reduce high-frequency noise before calculating non-linear parameters. The window method was applied for the calculus of the coefficients of the filter.

The basis of the window method is the fact that the frequency response of a filter $H_F(w)$ and the corresponding impulse response $h_F(n)$ are related by the inverse Fourier transform, as indicated in equation 4.8:

$$h_F(n) = \frac{1}{2\pi} \int_{-\pi}^{\pi} H_F(2) e^{jwn} dw \tag{4.8}$$

The window method is composed of the following steps:

1. The ideal frequency response of the filter, $H_F(w)$ is specified.
2. The impulse response of the filter, $h_F(n)$, is obtained applying the inverse Fourier transform (equation 4.8). The impulse responses for ideal lowpass, highpass, bandpass and bandstop filters have a practical limitation: they are not finite. Although $h_F(n)$ decreases as we

move away from $n = 0$, it theoretically continues to $n = \pm\infty$. This impulse response is not from a FIR (Finite Impulse Response) filter.

3. In order to solve the previous limitation, the ideal impulse response is truncated (forcing their values to be zero if n is greater than a specified threshold). A direct truncation is equivalent to multiplying the ideal impulse response by a rectangular window $w(n)$, which is equivalent to convolving $H_F(w)$ and $W(w)$ in the frequency domain, where $W(w)$ is the Fourier transform of $w(n)$. As the Fourier transform of a rectangular window is a *sinc* function, overshoots and ripples appear in the frequency response. In order to reduce the ripples, other windows different to the rectangular one are usually applied to truncate the ideal impulse response (such as the Hamming, Hanning, Blackman or Kaiser windows). The specific characteristics of these windows have been described elsewhere [212]. The impulse response $h_F(n)$ is multiplied by one of these windows, $w(n)$, with finite duration. This way, the resulting impulse response decays smoothly towards zero. The window is selected so that it satisfies the passband or attenuation specifications. For example, in the case of the Hamming window, the maximum stopband attenuation is 53 dB, and the main lobe relative to side lobe is 41 dB. The passband ripple is 0.0194 dB [212]. The number of filter coefficients is selected using the appropriate relationship between the filter length and the transition width, δf. Continuing with the example of the Hamming window, the normalized transition width is 3.3/N Hz. Once the window has been selected, the values of the actual FIR coefficients, $h(n)$, are obtained by multiplying $h_F(n)$ by $w(n)$, as indicated in equation 4.9.

$$h(n) = h_F(n)w(n) \tag{4.9}$$

In this study, a FIR filter of order 40 was designed in Matlab using the window method. A Hamming window was selected. The cut-off frequency was fixed at 10 Hz, as in previous studies about non-linear analysis of the Doppler signal [37]. The normalized gain of the filter at the cut-off frequency was -6 dB. The filter obtained with this method was linear and

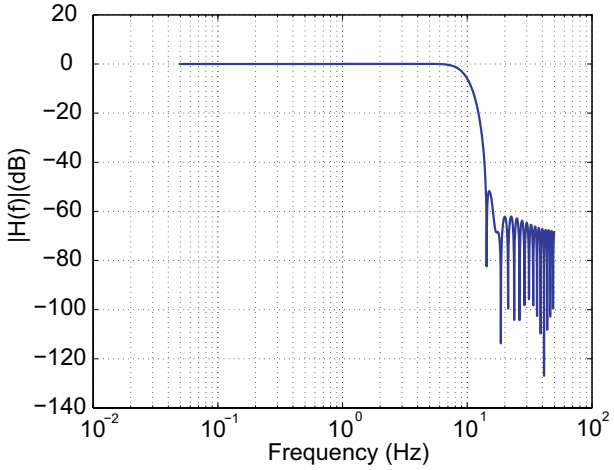

Figure 4.12: Frequency response of the designed FIR filter.

had linear phase. The frequency response of the applied filter can be observed in Fig. 4.12.

4.4.5 Non-linear Analysis of BFV signals

4.4.5.1 Introduction

In the present study about motor tasks, non-linear analysis is applied to study if there is any change in the dynamics of the system between periods corresponding to different activities (repose / hand movements). Several methods have been applied in previous studies about physiological measures from the perspective of non-linear dynamical systems. Some of these methods require a minimum number of samples to obtain reliable results. This requirement is not a problem in this study, because the experimental design has been prepared taking this into account, so large periods corresponding to different activities (repose / hand movements) are available. In the following sections, the different non-linear parameters that have been calculated for each period are described.

4.4.5.2 Surrogates method

In order to apply all the methods that will be described in the following sections, the existence of non-linearity in the available data (in this case, maximum BFV data measured using TCD) has to be proven. One of the methods most commonly used to check the existence of non-linearity is the generation of surrogate data. This is a procedure that was developed by Theiler et al. [213].

The method consists of generating, from the original series, a set of random series that maintain some of the properties of the original series (mean, variance, spectrum, self-correlation structure), but in which any non-linear dependence has been eliminated [214, 215]. Once the new set has been generated, a statistical index sensitive to the non-linear dependence in the original time series is calculated both in the original series and in the surrogate series. If using a statistical test it is possible to reject the null hypothesis (indexes have their origin in a linear system), it would be proven (with a certain confidence level) the non-linearity of the original data, because the surrogates are the result of a random linear process.

In this study, the surrogates were generated using the procedure developed by Schreiber and Schmitz [216]. This method is based in amplitude adjusted Fourier transform (AFFT) proposed by Theiler et al. [213]. The surrogate series generated with the Schreiber and Schmitz's method have the same histogram of the original series, and practically the same spectral power.

Once the significance level for the statistical analysis is decided, $\frac{2}{\alpha}$ surrogate series have to be generated for a bilateral test. In the present study, $\alpha = 0.05$, so 39 surrogate series were generated applying the algorithm from Schreiber and Schmitz [216], with the implementation of the TISEAN 2.1 [217]. Previously to the generation of the surrogates, sub-sequences of the original series were selected using the programs *endtoend* and *choose*, implemented in TISEAN 2.1. These programs select the maximum number of consecutive samples in the original time series with the condition that the sub-sequence starts and ends with data that approximately coincide in value and phase [217]. An erroneous rejection of the null hypothesis can be generated due to periodicity artifacts [218].

The irregularity measure that was applied to the original series and to each of the surrogate series was SampEn (a measure of entropy that will be described in the following section). If the original signal is non-linear, the SampEn of the surrogates will be higher than the SampEn found in the original signal [219].

4.4.5.3 Multiscale entropy

Several algorithms have been developed to calculate the complexity of physiological time series. Multiscale Entropy (MSE) is one of these algorithms, which is based on previous proposals: the approximate entropy (ApEn) and a refinement of this parameter known as sample entropy (SampEn). ApEn and SampEn will be described in the following paragraphs, before explaining the improvements that the use of MSE offers when compared with these previous approaches.

Approximate entropy (ApEn)

ApEn is a method for quantifying regularity and complexity that works well with relatively short series (greater than 100 points) and noisy time-series data [220]. $ApEn(m, r, N)$ is approximately equal to the negative average natural logarithm of the conditional probability that two sequences that are similar for m points remain similar (within a tolerance r) at the next point [221]. When it is likely that the two sequences remain close for the next point (regular series), small ApEn values are obtained.

The exact mathematical procedure to calculate ApEn is going to be described. Let us assume that we have a vector v of N data points:

$$v = [v(1), v(2), ..., v(N)] \tag{4.10}$$

Different data sequences can be formed from these values selecting m consecutive v values starting with the ith component. The formula that describes this is:

$$x(i) = [v(i), ..., v(i + m - 1)] \tag{4.11}$$

Possible values of i range from 1 to $N - m + 1$. In Fig. 4.13 the process for generating the different sequences for m=5 in a sample signal is shown.

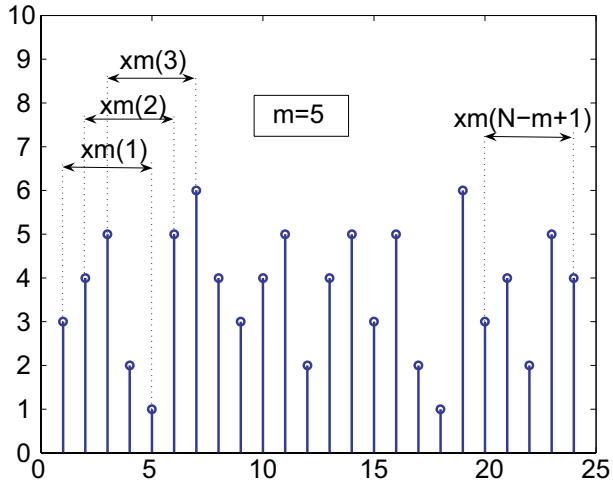

Figure 4.13: The process followed to generate the different sequences for m=5 from the original signal is shown in the figure.

The distance between two of these sequences can be defined as the maximum difference between their respective scalar components: $d[x(i), x(j)]$ would represent the difference between vectors $x(i)$ and $x(j)$.

A new parameter $(C_i^m(r))$ can be defined for each $i \leq N - m + 1$:

$$C_i^m(r) = \frac{\sum_{j=1}^{N}(\theta(r - d[x(i), x(j)]))}{N - m + 1} \tag{4.12}$$

where $\theta(y)$ is the Heaviside function: $\theta(y) = 0$, if $y < 0$; $\theta(y) = 1$, if $y > 0$. This formula counts the number of j in which the distance between sequences is smaller than the tolerance r.

Another parameter can be calculated, as the mean of the natural logarithm of the functions $C_i^m(r)$:

$$\phi^m(r) = \frac{\sum_{i=1}^{N-m+1}(ln(C_i^m(r)))}{N - m + 1} \tag{4.13}$$

where ln is the natural logarithm.

Finally, the ApEn parameter can be defined as:

$$ApEn(m,r) = \lim_{N\to\infty}[\phi^m(r) - \phi^{m+1}(r)] \tag{4.14}$$

Given N data points, the $ApEn$ parameter is estimated by the statistic:

$$ApEn(m,r,N) = \phi^m(r) - \phi^{m+1}(r) \tag{4.15}$$

Operating with the previous formula, the following results can be obtained:

$$ApEn(m,r,N) = \frac{\sum_{i=1}^{N-m+1} ln[C_i^m(r)]}{N-m+1} - \frac{\sum_{i=1}^{N-m} ln[C_i^{m+1}(r)]}{N-m} \tag{4.16}$$

When N is large, the following approximation is valid:

$$ApEn(m,r,N) \approx \frac{\sum_{i=1}^{N-m}(-ln[\frac{A_i}{B_i}]}{N-m} \tag{4.17}$$

where B_i can be defined as the number of vectors $x_m(j)$ which are within a distance r of $x_m(i)$ and A_i can be defined as the number of vectors $x_{m+1}(j)$ which are within a distance r of $x_{m+1}(i)$.

The number of input data points (N) required for calculating ApEn is typically between 75 and 5000 [220].

The algorithm used to calculate ApEn counts each sequence as matching itself to avoid the occurrence of $ln(0)$. That is why ApEn is influenced by the record length, giving lower values for short records. On the other hand, it can result in a lack of consistency [221]. For these reasons, other measures of complexity such as SampEn were proposed.

Sample Entropy (SampEn)

$SampEn(m,r,N)$ is the negative natural logarithm of the conditional probability that two sequencies similar for m points remain similar at the next point, without including self-matches in the calculus of the probability. As happened with ApEn, a low value of SampEn indicates more self-similarity (less complexity). However, SampEn is mostly independent of the record length and is relatively consistent under circumstances where ApEn is not.

In order to describe SampEn mathematically, two new parameters have to be defined. If we take $B_i^m(r)$ as $\frac{1}{N-m-1}$ times the number of vectors $x_m(j)$ which are within a distance r of $x_m(i)$, where j ranges from 1 to $N-m(j \neq i)$, $B^m(r)$ can be defined as indicated in equation 4.18:

$$B^m(r) = \frac{\sum_{i=1}^{N-m} B_i^m(r)}{N-m} \tag{4.18}$$

Similarly, $A_i^m(r)$ can be defined as $\frac{1}{N-m-1}$ times the number of vectors $x_{m+1}(j)$ which are within a distance r of $x_{m+1}(i)$, where j ranges from 1 to $N-m(j \neq i)$. A_m can be defined as indicated in equation 4.19:

$$A^m(r) = \frac{\sum_{i=1}^{N-m} A_i^m(r)}{N-m} \tag{4.19}$$

These equations can be interpreted in the following way: $B^m(r)$ represents the probability that two sequences match for m points; and $A^m(r)$ represents the probability that two sequences match for $m+1$ points. Taking this into account, the $SampEn$ parameter can be defined as:

$$SampEn(m,r) = \lim_{N\to\infty}[-ln[\frac{A^m(r)}{B^m(r)}] \tag{4.20}$$

which can be estimated by the statistic:

$$SampEn(m,r,N) = [-ln[\frac{A^m(r)}{B^m(r)}] \tag{4.21}$$

This quantity represents the conditional probability that two sequences within a tolerance r for m points remain within r of each other at the next point.

Multiscale Entropy (MSE)

The Multiscale entropy (MSE) analysis was first proposed by Costa et al. [222, 223, 224]. It is a method that can be used to measure the complexity of finite length time series. In particular, it is applicable to physiological signals of finite length.

One of the basic hypothesis that supports the MSE method is that biological systems need to operate across multiple spatial and temporal

scales, and consequently, their complexity is also multiscaled. Complexity is associated with "meaningful structural richness" [225] and correlations over multiple scales are incorporated.

The process for calculating MSE is divided in two steps:

- Firstly, a "coarse-graining" process is applied to the time series. Given a one-dimensional discrete time series $([x_1, x_2, ...x_i, ...x_N])$, the new coarse-grained time series (y^τ) are constructed by averaging the data points within non-overlapping windows of increasing length τ. This parameter represents the multiple scales of the process (scale factor). The length of each coarse-grained time series is $\frac{N}{\tau}$.

  The formula that represents this is:

$$y_j^\tau = \frac{1}{\tau} \cdot \sum_{i=(j-1)\tau+1}^{j\tau} x_i, \qquad 1 \leq j \leq \frac{N}{\tau} \tag{4.22}$$

  For scale 1, the coarse-grained time series is simply the original time series. For scale 2, y_1 is calculated as the mean of x_1 and x_2; y_2 is calculated as the mean of x_3 and x_4; and the process continues until the data points from the original series end. For scale 3, three data points of the original series are averaged to obtain each of the points in the scale 3 data series.

  An example of the calculus of the different points of the coarse-grained time series for scale 2 in a sample original series is represented in Fig. 4.14.

- Secondly, the SampEn method for entropy calculation is applied for each coarse-grained time series.

As MSE finally is based on the calculus of SampEn for several scales, the following parameters are required to calculate it:

- m. This parameter defines the pattern length.
- r. This value defines the similarity criterion.

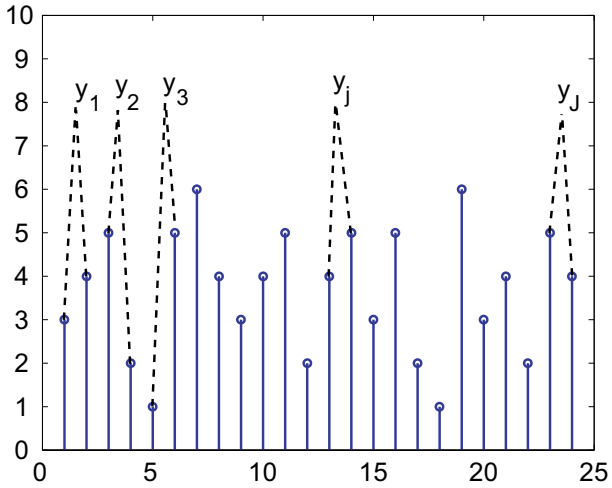

Figure 4.14: Calculus of the different points of the coarse-grained time series for scale 2.

- n. It indicates the number of scales that are going to be included in the analysis.

- N. It is the total length of data that are going to be included in the analysis.

Traditional entropy measures quantify only the regularity of time series on a single scale. In these measures, there is no a clear correspondence between regularity and complexity. Completely ordered signals (for example, periodic signals) have minimum entropy. On the other hand, completely random signals (for example, uncorrelated noise) have maximum entropy. However, neither of them are truly complex. One of the main advantages of the MSE method is that its results are consistent with the consideration that both completely ordered and completely random signals are not really complex.

Results of applying SampEn to the multiple time series corresponding to the different scales can be plotted as a function of the scale factor.

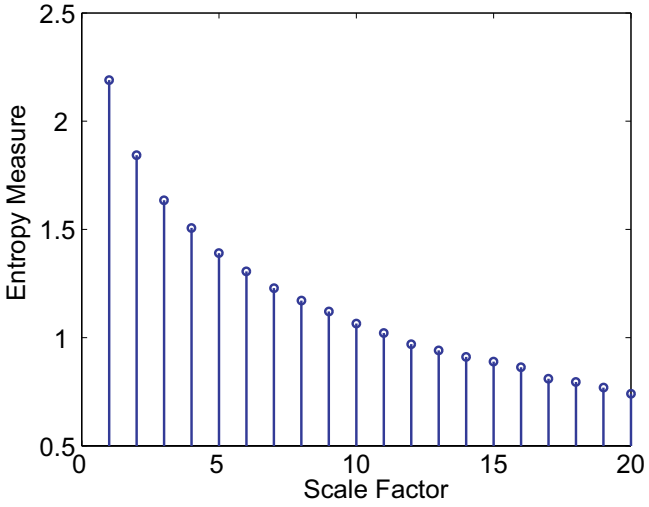

Figure 4.15: MSE analysis of Gaussian distributed white noise (mean zero, variance one).

This process can help in the analysis of the evolution of the complexity of the signal in the different time scales. Some considerations can be made regarding the interpretation of the obtained data.

- If two series are being compared, and for the greater part of the scales the entropy values are higher for one time series than for another, the first one is considered more complex.
- If a monotonic decrease of the entropy values when the scale increases is observed, that would mean that the original signal contains information only in the smaller scale. An example of this behavior can be observed in Fig. 4.15, where the MSE analysis of Gaussian distributed white noise (mean zero, variance one) is shown (m=2, r=0.2, N=40000, n=20).

In this study, the MSE implementation from PhysioNet was used for the calculus of the entropy of the maximum BFV signal in the different experimental conditions [226].

The different parameters of the algorithm were selected as follows:

- m(pattern length) = 2.
- r(similarity criterion) = 0.15. This means that it is set at a 15 % value of the original time series standard deviation.
- n(number of scales) = 9. The number of scales have been selected so that there is a minimum of 1000 data points in the shortest coarse-grained time series, as recommended by Costa et al. [222]
- N(total length of the data) = 9000 data points.

4.4.5.4 Correlation dimension

In order to understand the meaning of the correlation dimension, several concepts have to be explained. Let us start with a more detailed analysis of the phase space.

Phase space and attractors

The coordinates of this space represent the variables that are required to describe the state of a system. The state vector is a vector of length n, where n is the number of variables necessary for a complete description of the current status of the system [227].

For example, let us imagine that the system that is being analyzed is the motion of a simple harmonic oscillator. In this case, two possible variables required for describing the system are the horizontal position (x) and horizontal velocity (v). These two variables will constitute the state vector.

If ideal conditions (no friction) are assumed, the equations that describe the evolution of both variables are the following:

$$x = acos(t); y = -asin(t) \tag{4.23}$$

In order to obtain the state space corresponding to the behavior of the harmonic oscillator, two axes will be represented, one corresponding to the position and one to the velocity. For each discrete time that is considered, a pair of values (x_i, y_i) can be calculated, and represented as a point in the

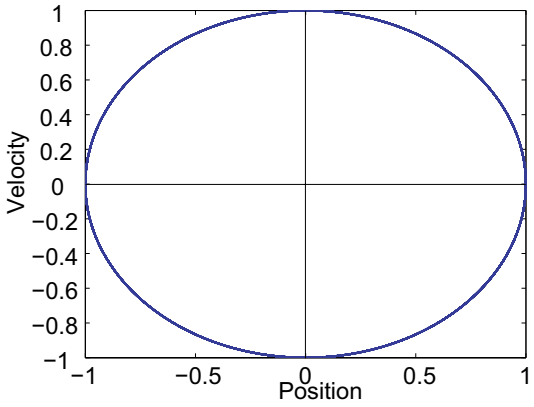

Figure 4.16: Representation of the state space of an ideal harmonic oscillator system.

axes corresponding to the state space. The results in the case of the ideal harmonic oscillator are represented in Fig. 4.16

In this simplified example, the system behavior is repeated over and over in time. However, the usual behavior of dynamic systems is that there is a transient period at the beginning that evolves / converges towards a stationary state (asymptotic behavior). The term asymptotic behavior refers to the stable behavior that remains once the initial transient behavior has died away. In the state space, this is represented as a sequence of points (which is called the trajectory of the system). Any possible trajectory in the system depends on the initial conditions, and evolves to a subset of the phase space which is called attractor. Three main kinds of attractors have been described:

- **Point attractor**. In this case, the asymptotic behavior of the system is a point in the state space. The temporal equivalence of this behavior in the phase space is that the different variables that describe the system do not vary with time once the asymptotic behavior has been achieved.

- **Limit-cycle attractor**. In this attractor, the asymptotic behavior

is a loop in the state space. The system will have a transient behavior that will gravitate toward the loop, and will remain in the loop once the stationary state has been achieved. The temporal equivalence of this behavior is that, in the asymptotic behavior, the variables repeat in a periodic way a series of values.

- **Strange attractor**. In this case, the asymptotic behavior will be attracted toward a finite region of the state space. Unlike the behavior of systems governed by point and limit-cycle attractors, the asymptotic state-space trajectory of a chaotic system never intersects itself. The only way to delimit these trajectories inside a finite volume is using a fractal (a rough or fragmented geometric shape that can be split into parts, each of which is, at least approximately, a reduced-size copy of the whole [228]) with non-integer dimension. The temporal equivalence of this behavior is that the exact values of the different variables that define the system are never repeated in the same way. The Lorenz attractor, which is a classic example of strange attractor, is represented in Fig. 4.17 [229].

Delay embedding theorem

The different variables that determine the state of a dynamic system are not always known. The most common situation in psychophysiological analysis is that only a physiological time series is known (for example, the heart rate, or the EEG, or in this case, the TCD BFV signal). Furthermore, it is not even known how many variables are required for a complete description of the system.

There is a theorem proposed by Withney and developed by Takens [230] which shows that it is possible to reconstruct the whole information about the system only from a single temporal series. The attractor associated to the system can be reconstructed working with the original time series, and other new time series that are generated by introducing in the original one a temporal delay τ.

The vector state will be given by the following expression:

$$v = [x(t), x(t+\tau), x(t+2\tau), ..., x(t+(n-1)\tau)] \tag{4.24}$$

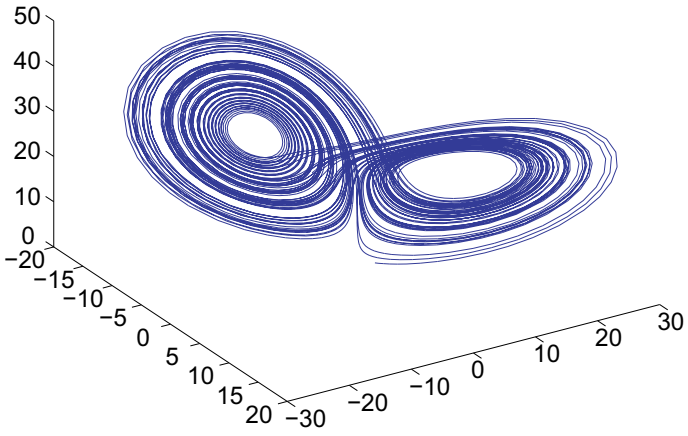

Figure 4.17: Representation of the Lorenz attractor.

assuming that $x(t)$ are values from the original time series.

The new attractor that is generated with these methods does not necessarily have the same shape as the original, but is topologically equivalent. That means that it conserves the properties of periodicity, stationarity and chaocity, and has the same dimension and Lyapunov exponents (parameters that will be described later). Takens proved that this is true as long as the phase space has at least a dimension of $2m + 1$, where m is the dimension of the space where the attractor is. However, practical results show that a lower number of dimensions is usually enough [231].

Correlation dimension

Some parameters have been used in the literature to characterize attractors in a more objective way than the simple visualization of them in the phase state. One of these procedures has been based in the calculus of a geometric property of the attractor: its fractal dimension.

There is a method to easily calculate an inferior cote for the fractal dimension. The technique is called correlation dimension, and it was first

proposed by Grassberger and Procaccia [232]. This method also allows that the reconstruction dimension (phase state dimension) can be obtained.

The procedure follows these steps:

1. The parameter corresponding to the delay (τ) in equation 4.24 has to be chosen. Rosenstein et al. [233] stated that for a given embedding dimension, the time lag is chosen so that the near-maximum expansion of the attractor in phase space is achieved (equivalent to minimum reconstruction error). If the delay is too small, there will be high redundancy error. On the other hand, if the delay is too long, the points may become unrelated, and a high irrelevance error will appear. The objective of the methods for selecting the delay are that both redundancy and irrelevance errors are minimized.

   The delay has been obtained in the literature in different ways [195]. Some approaches take it as the time where the minimum of the autocorrelation function of the original signal is achieved; other approaches select the delay as the time where the autocorrelation function gets to zero; and other researchers take it as the time where the autocorrelation function of the time series drops to 1/e of its original value [38]. In the present study, this last approach has been followed.

2. Different phase spaces with different dimensions n (with $n = 2$, 3, 4,...) have to be reconstructed. In each of these spaces, the following steps should be followed [194]:

   (a) The attractor is reconstructed using the Takens' Theorem with the delay τ previously decided.

   (b) The correlation sum is calculated for different ϵ values (the meaning of the ϵ value is explained following). The correlation sum gives us information about the degree of correlation between the different points of the state space. The equation used to calculate the correlation sum is equation 4.25:

$$C(\epsilon) = lim_{N\to\infty} \frac{1}{N(N-1)} \sum_{i\neq j=1}^{N} (\theta(\epsilon - \|\vec{v_i} - \vec{v_j}\|) \qquad (4.25)$$

ϵ is a arbitrary small distance, $\|\vec{v_i} - \vec{v_j}\|$ represents the euclidean distance between two points of the attractors, and $\theta(z)$ is the Heaviside function. To calculate $C(\epsilon)$, a point is chosen, the distances between this point and each of the other $N-1$ points are calculated, and the number of pairs that are within a distance smaller than ϵ are counted. This process is repeated for all the points of the attractor, so the correlation sum is calculated. The result can be interpreted as the percentage of distances that are within the parameter ϵ.

The previous equation 4.25 can only take values between 0 and 1. If ϵ is small, it can be said that (equation 4.26):

$$C(\epsilon) \alpha \epsilon^d \tag{4.26}$$

d is the dimension of the attractor.

(c) The dimension of the attractor can be calculated as the pendent of the function obtained when representing $Log(C(\epsilon))$ versus $Log(\epsilon)$ in the range of ϵ values where the points better adjust to a straight line (the self-similar structure of the attractor is clearer in this zone). The different ϵ values and the associated $C(\epsilon)$ are represented in a logarithmic scale. A regression line is adjusted to the data in the linear region, and the slope of this line (d) is calculated. This will be the dimension of the attractor for the actual phase space.

3. Once the dimensions of the attractors have been calculated for the different phase spaces of growing dimensions n (with $n = 2, 3, 4,...$), the behavior of the dimension d when n grows has to be observed. It may happen that d grows when the number of degrees of freedom of the phase space (n) is increased. This is the usual behavior when the input signal is just noise. However, when the system is chaotic, a low dimensionality can usually be observed. The usual behavior will be that d will grow at the beginning (with low values of n) and then it will stop growing in a value of n, usually a small value. This saturation value (d_s) is an estimation of the attractor dimension (*correlation dimension*). On the other hand, the n value over

which saturation is observed is an estimation of the number of variables which are necessary and sufficient to characterize the system (*reconstruction dimension*).

In this study, Matlab was used to program the algorithm and to represent the graphics that were needed for the interpretation of results. The correlation sum was obtained using the implementation contained in TISEAN 2.1 [217]. The algorithm has been applied to the BFV signal corresponding to the different experimental conditions.

The correlation dimension was obtained as the slope of the linear section of the function $\frac{log(C(\epsilon))}{log(r)}$. The linear section was taken in this study between ϵ_{min} and ϵ_{max}:

- ϵ_{max} was taken so that $C(\epsilon_{max}) = 0.001$ in the maximum reconstruction dimension analyzed (which was D=20).

- ϵ_{min} was obtained using the following equation:

$$\epsilon_{min} = \epsilon_{null} + 0.25 \cdot (\epsilon_{max} - \epsilon_{min}) \tag{4.27}$$

  where ϵ_{null} is taken as the minimum distance between two different points on the attractor. This procedure is similar to the procedure followed in the study by Vliegen et al. [38].

4.4.5.5 Fractal dimension using the Katz method

Different algorithms have been proposed to estimate the fractal dimension (FD) of the signal waveform in the time domain [234, 235, 236]. In this case, the concept is different, and it is not necessary to reconstruct the strange attractor.

In the present study, the Katz method was also applied.

As Katz explains [234], waveforms are planar curves that proceed forwards monotonically. The fractal dimensions of these waveforms range between D=1.0 (straight lines) to values close to D=1.5 (for certain highly spiked waves). True waveforms can never become sufficiently convoluted to fill a plane, so they will never achieve dimension D=2.0.

In the Katz method, FD is defined as (equation 4.28):

$$FD = \frac{ln(N)}{ln(N) + ln(\frac{d}{L})} \tag{4.28}$$

where N is the total number of data points in the data time series to be analyzed; L is the total length of the data section (which is calculated as the sum of the Euclidean distances between successive data points); and d is the diameter of the data (which is calculated as the Euclidean distance between the first data point and the point corresponding to the farthest distance).

The FD obtained applying this method is dependant on the units of the coordinates used for calculating the distances and lengths. A practical convention that Katz proposes is to define the standard unit to be the average step or convolution of a shape. For waveforms, this average step is a, the average distance between successive points (equation 4.29).

$$a = \frac{L}{N} \tag{4.29}$$

The data introduced in the formula for the calculus of the FD are scaled so that the average step size a is 1 unit.

In this study, the temporal units were 0.01 s and the units for the BFV values were dm/s. Forty-five non-overlapping periods of 200 samples were selected for the repose periods, and forty-five non-overlapping periods of 200 samples were selected for periods with hand movements. The FD was calculated applying the Katz method for each of the periods. A mean FD value for the repose period was calculated by averaging the forty-five FD values of the repose periods. Similarly, a mean FD value was calculated for the motor activity periods.

4.4.5.6 Maximum Lyapunov exponent

One of the most widely known aspects of the chaos theory is the butterfly effect. It is a metaphor that encapsulates the concept of sensitive dependence on initial conditions in chaos theory: small differences in the initial

condition of a dynamical system may produce large variations in the long term behavior of the system.

That means that two trajectories in the phase space, even if they are as close as required in a specific moment, will diverge in an exponential way. Consequently, the long-term prediction is almost impossible.

How can the sensibility to the initial conditions in a dynamic system be measured? One of the most common techniques to evaluate this are the Lyapunov exponents. The Lyapunov exponents measure the rate with which infinitesimally close trajectories diverge.

Let us assume that we have a point in the phase space x_0, and we select another point in the phase space really close to the first one $(x_0 + \Delta x_0)$. If the trajectories that the dynamic system will follow from the first and from the second points are drawn, different situations can be observed depending on the characteristics of the system [195]:

- Situation 1: The two trajectories come close to each other as time elapses.
- Situation 2: The two trajectories maintain their initial distance during all the path.
- Situation 3: The two trajectories diverge. As time elapses, the distance between them is increased, and the trajectories become really different between them. This last situation occurs in chaotic and unstable systems.

If the initial distance between two trajectories is Δx_0, and the distance between this two trajectories grows exponentially as time (t) is increased, this can be expressed mathematically as indicated in equation 4.30

$$|\Delta x_t| \approx e^{\lambda t} \cdot |\Delta x_0| \tag{4.30}$$

In fact, as the phase space is a multidimensional space, different Lyapunov exponents can be calculated, one in each dimension of the phase state. Each of these exponents characterizes the rate of divergence of the trajectories in a direction of the state space.

Usually, only the maximum Lyapunov exponent is calculated, because this one is enough to determine the predictability of the system [195]. Again, three different responses can be observed:

- If the maximum Lyapunov exponent is negative, the system is asymptotically stable. The trajectories converge to the attractor of the system.
- If the maximum Lyapunov exponent is zero, the system is in an equilibrium state.
- If the maximum Lyapunov exponent is positive, the system may be chaotic (this is a necessary condition for the system being chaotic).

In this study, the maximum Lyapunov exponent was calculated for BFV data corresponding to the different experimental conditions, applying the algorithm proposed by Rosenstein et al. [237] and using the TISEAN 2.1 [217] implementation. This algorithm is fast and robust with changes in the embedding dimension, the size of the data set, the reconstruction delay, and the noise level.

4.4.6 Statistical Analysis

In the case of the multiscale entropy (dependent variable), a parametric test (three-way ANOVA with repeated measures) was used to analyze the effects of the three within-subjects factors:

- Motor movements: active hand movements / repose.
- Active hand: dominant / non-dominant hand.
- Brain hemisphere: contralateral / ipsilateral to the active hand.

Comparisons between the period with active hand movement versus the period of repose were performed by means of t tests.

In the other calculated parameters (correlation dimension, fractal dimension with the Katz method,and maximum lyapunov exponent) differences between the period with active hand movement versus the period of

repose were analyzed directly by means of a t test or a Wilcoxon signed-rank test, depending on the normality of the variables. Results of applying the Shapiro-Wilk test to check the normality of the parameters in the different conditions can be found in Annex F. In the cases where normality tests failed, non-parametric methods were applied.

Chapter 5

Results

The following sections summarize the results obtained in the different experimental designs that were described in chapter 4.

5.1 BFV analysis in different navigation conditions

A neurologist validated the registries for the different vessels during the experiment. Some measurements were discarded because the recorded signals were not reliable (their values were not included in the typical range of BFV in the vessels) or because in the moment of measurement it was impossible to detect a good quality signal corresponding to the vessel. The number of valid measurements was 24 for MCA-L, 22 for MCA-R, 9 for ACA-L and 6 for ACA-R.

The different data analysis methods described in the chapter 4 were applied and the results of these analyses are shown in the following subsections.

5.1.1 Comparison of SUS questionnaire responses between the free navigation condition and the automatic navigation condition

Mean values of the responses to the different questions of SUS Questionnaire (Questions 1-6), and the values of SUS Count and SUS Mean are shown in Table 5.1.

Table 5.1: SUS responses corresponding to the free navigation condition and to the automatic navigation condition. The mean value and the standard error of the mean (mean ± s.e.m.) are shown. The number of subjects is 32 for the free navigation and 31 for the automatic navigation condition.

Measurement	Free Nav.	Automatic Nav.
SUS Count	2.46 ± 0.38	1.19 ± 0.33
SUS Mean	4.83 ± 0.23	3.89 ± 0.29
SUS Question 1	5.25 ± 0.21	4.19 ± 0.28
SUS Question 2	4.84 ± 0.28	4.06 ± 0.27
SUS Question 3	4.56 ± 0.34	3.80 ± 0.34
SUS Question 4	5.18 ± 0.27	3.80 ± 0.28
SUS Question 5	4.56 ± 0.25	4.00 ± 0.28
SUS Question 6	4.59 ± 0.24	3.67 ± 0.31

In the case of the free navigation condition, the mean value of the SUS Mean parameter was 4.83, and the mean values of the answers to each individual question were always greater than 4.50.

In the case of the automatic navigation condition, answers were slightly lower; the mean value of SUS Mean was 3.89, and the mean values of the answers to each question were always greater than 3.60.

The Wilcoxon Signed-Rank Test showed that the values of responses to the different questions were significantly greater in the case of the free navigation than in the case of the automatic navigation condition. The

exact Z values and significance values are shown in Table 5.2.

Table 5.2: Results of applying the Wilcoxon Signed-Rank Test to the different variables that summarize the responses to the SUS questionnaires in the free and automatic navigation conditions.

Measurement	Z	$p - value$
SUS Count	**3.65**	< 0.001
SUS Mean	**4.38**	< 0.001
SUS Question 1	**3.47**	0.001
SUS Question 2	**3.56**	< 0.001
SUS Question 3	**2.69**	0.007
SUS Question 4	**3.65**	< 0.001
SUS Question 5	**2.57**	0.010
SUS Question 6	**3.55**	< 0.001

5.1.2 Comparison of BFV between repose periods and VE exposure periods

The BFV signal has variations inside each repose and activation period. Just to show the behavior of the BFV signal in the different vessels that have been monitored in this study, BFV values corresponding to the last 20 s of the baseline previous to the beginning of the free navigation condition and the first 20 s of the free navigation condition of one of the subjects have been represented graphically. Fig. 5.1 shows data corresponding to MCA-L, Fig. 5.2 shows the mean BFV values in MCA-R, Fig. 5.3 represents the data from ACA-L and Fig. 5.4 contains the values corresponding to ACA-R mean BFV.

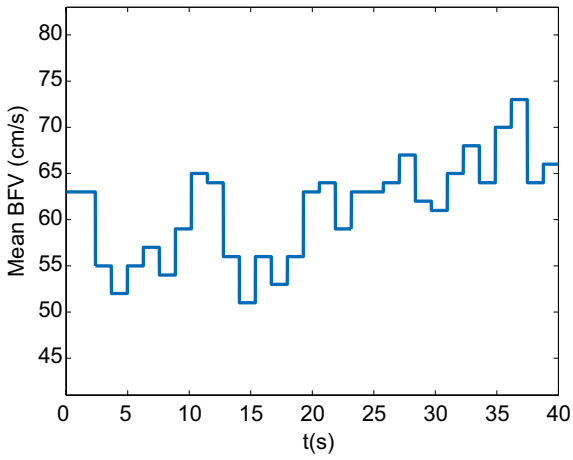

Figure 5.1: Mean BFV in MCA-L for one of the subjects during the last 20 s of the baseline and the first 20 s of the free navigation.

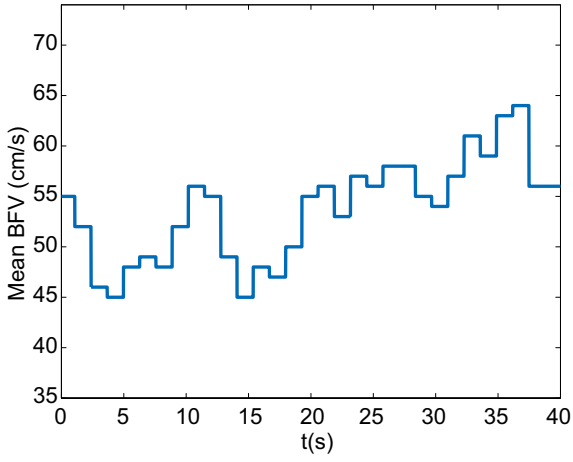

Figure 5.2: Mean BFV in MCA-R for one of the subjects during the last 20 s of the baseline and the first 20 s of the free navigation.

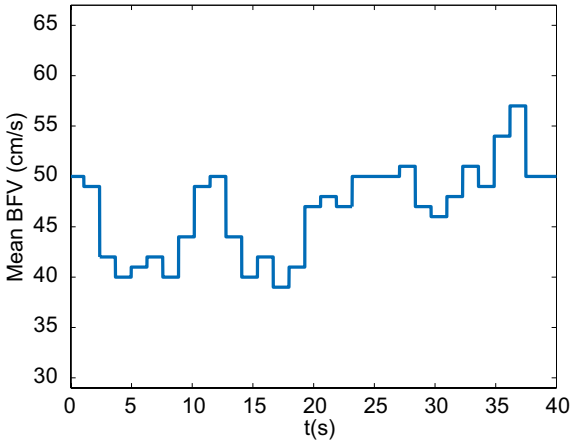

Figure 5.3: Mean BFV in ACA-L for one of the subjects during the last 20 s of the baseline and the first 20 s of the free navigation.

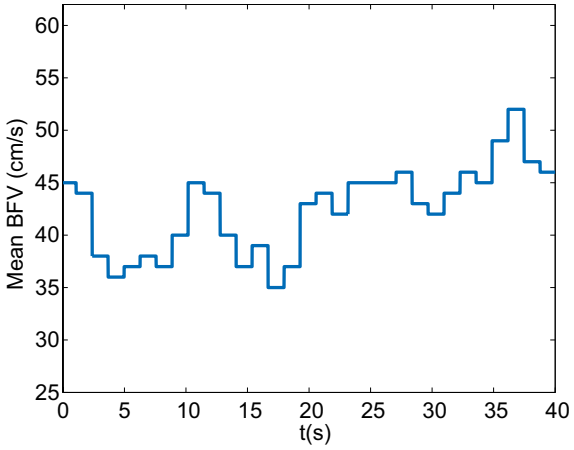

Figure 5.4: Mean BFV in ACA-R for one of the subjects during the last 20 s of the baseline and the first 20 s of the free navigation.

As can be observed in the previous figures, there is an increment in the

BFV signal when the navigation starts (corresponding to time t=20 s in the graphs).

In order to evaluate global differences between repose and activation periods, mean BFV values corresponding to the four different periods of the experiment (1- Baseline previous to the free navigation condition: baseline A. 2- Free navigation condition. 3- Baseline previous to the automatic navigation condition: baseline B. 4- Automatic navigation condition) have been calculated as described in chapter 4. Results can be found in Table 5.3.

Table 5.3: Baseline and activation values for mean BFV (cm/s) in the MCA-L, MCA-R, ACA-L and ACA-R (mean ± standard error of the mean).

	MCA-L	MCA-R	ACA-L	ACA-R
Baseline A	66.66±2.66	59.70±2.61	41.68±3.84	38.45±5.24
Free Nav.	73.09±2.95	65.71±3.11	48.68±4.65	39.59±5.12
Baseline B	62.58±2.46	55.84±2.17	42.96±2.96	36.00±4.63
Automatic Nav.	66.59±2.65	60.51±2.55	45.39±3.45	37.11±4.81

5.1.2.1 MCA-L results

In MCA-L, results of the ANOVA showed that mean BFV differed significantly between the four periods: $F(1.682,38.688) = 44.392$, $p < 0.001$. Post-hoc tests revealed that mean BFV during the navigation (73.091 cm/s) in the free navigation condition was significantly greater ($p < 0.001$) than during its previous baseline (66.660 cm/s). Moreover, during the automatic navigation condition (66.587 cm/s) mean BFV was also significantly greater ($p = 0.002$) than during the previous baseline period (62.583 cm/s). Mean values and standard errors of the mean are represented in Fig. 5.5.

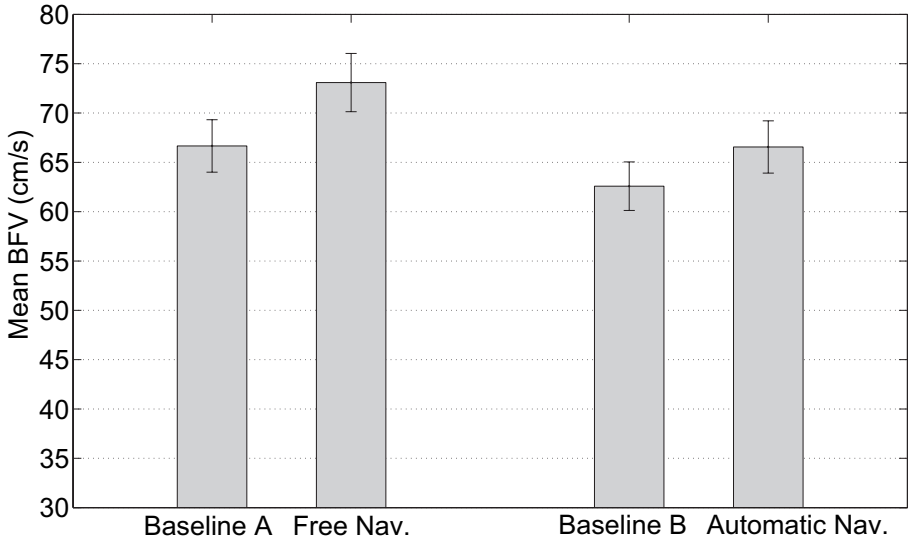

Figure 5.5: Mean MCA-L BFV values for the 2 experimental conditions and their preceding baseline: 1- Baseline preceding Free Navigation Condition (Baseline A). 2- Free Navigation Condition. 3-Baseline preceding Automatic Navigation Condition (Baseline B). 4-Automatic Navigation Condition. The error bars represent the s.e.m. The number of subjects is 24.

5.1.2.2 MCA-R results

In MCA-R, the ANOVA showed that the mean BFV differed significantly between the four periods: $F(1.947,40.896) = 33.917$, $p < 0.001$. Post-hoc tests revealed that mean BFV during navigation (65.712 cm/s) in the free navigation condition was significantly greater ($p < 0.001$) than during its previous baseline (59.702 cm/s). Moreover, mean BFV during the automatic navigation condition (60.514 cm/s) was significantly greater ($p < 0.001$) than during the preceding baseline period (55.840 cm/s). Mean values and standard errors of the mean are represented in Fig. 5.6.

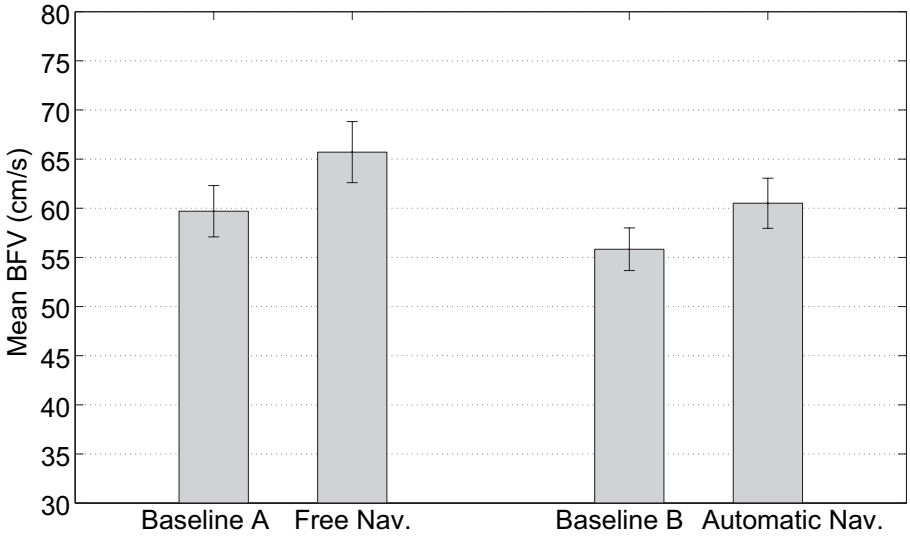

Figure 5.6: Mean MCA-R BFV values for the 2 experimental conditions and their preceding baseline: 1- Baseline preceding Free Navigation Condition (Baseline A). 2- Free Navigation Condition. 3-Baseline preceding Automatic Navigation Condition (Baseline B). 4-Automatic Navigation Condition. The error bars represent the s.e.m. The number of subjects is 22.

5.1.2.3 ACA-L results

The results of the ANOVA test for ACA-L showed that mean BFV differed significantly between the four periods: $F(1.710,13.679) = 6.843$, $p = 0.011$. Post-hoc tests concluded that mean BFV in the free navigation condition (48.683 cm/s) was significantly greater ($p = 0.012$) than during its previous baseline (41.681 cm/s). On the other hand, during the automatic navigation condition (45.390 cm/s), mean BFV only had a tendency to be greater than during the previous baseline period (42.967 cm/s). However, this tendency didn't reach significance. Mean values and standard errors of the mean are represented in Fig. 5.7.

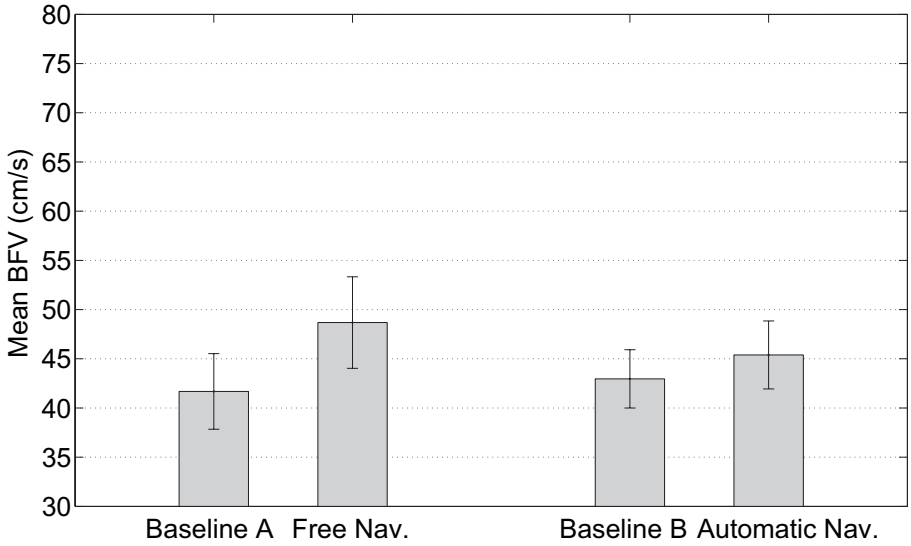

Figure 5.7: Mean ACA-L BFV values for the 2 experimental conditions and their preceding baseline: 1- Baseline preceding Free Navigation Condition (Baseline A). 2- Free Navigation Condition. 3-Baseline preceding Automatic Navigation Condition (Baseline B). 4-Automatic Navigation Condition. The error bars represent the s.e.m. The number of subjects is 9.

5.1.2.4 ACA-R results

The results obtained for ACA-R when applying the repeated measures ANOVA test did not support the hypothesis of having different mean velocities in the different periods: $F(1.453,7.263) = 5.049$, $p = 0.050$. Post-hoc tests did not show significant differences between the different periods. ACA-R mean BFV was not affected by presence measures differences obtained under different immersive conditions of the VE. Mean values and standard errors of the mean are represented in Fig. 5.8.

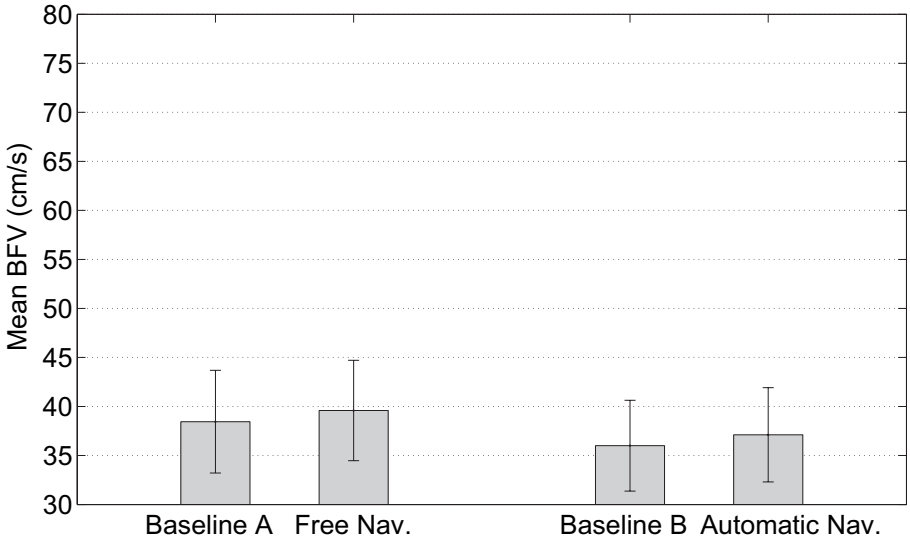

Figure 5.8: Mean ACA-R BFV values for the 2 experimental conditions and their preceding baseline: 1- Baseline preceding Free Navigation Condition (Baseline A). 2- Free Navigation Condition. 3-Baseline preceding Automatic Navigation Condition (Baseline B). 4-Automatic Navigation Condition. The error bars represent the s.e.m. The number of subjects is 6.

5.1.2.5 Global results

Summarizing the results from the statistical analysis, it can be concluded that there are differences between the mean BFV values for the different periods in some of the vessels. More specifically, mean BFV during the free navigation condition is significantly greater than the value observed during the baseline for MCA-L, MCA-R and ACA-L. On the other hand, while mean BFV during the automatic navigation condition is significantly greater than the value calculated in its previous baseline, this is only the case for the MCA-L and MCA-R.

5.1.3 Correlation between SUS responses and BFV values during the different navigation conditions

Interestingly, analyzing answers to SUS questionnaire for the free navigation condition and BFV during the free navigation, it was found that SUS-Mean and MCA-L BFV were significantly correlated ($r_s = 0.451$; $p = 0.027$). Besides, some answers to individual questions of SUS questionnaires also showed a significant correlation with MCA-L BFV (SUS Question 1: $r_s = 0.486$; $p = 0.016$; SUS Question 5: $r_s = 0.415$; $p = 0.044$).

On the other hand, when studying SUS answers in the automatic navigation and BFV during the automatic navigation, a correlation close to significance was found between SUS-Mean and MCA-L BFV ($r_s = 0.382$; $p = 0.065$). Significant correlations were found between the answers to some SUS questions and MCA-L BFV (SUS Question 2: $r_s = 0.428$; $p = 0.037$; SUS Question 5: $r_s = 0.611$; $p = 0.002$; SUS Question 6: $r_s = 0.425$; $p = 0.038$). Besides, a significant correlation was found also between some answers to SUS questions and MCA-R BFV (SUS Question 2: $r_s = 0.501$; $p = 0.021$; SUS Question 5: $r_s = 0.513$; $p = 0.018$). The correlation between SUS-mean and MCA-R BFV was close to significance ($r_s = 0.388$; $p = 0.082$). No significant correlations were found between the other combinations of variables. Results of the Spearman's Rho test are found in Tables 5.4, 5.5, 5.6 and 5.7.

Table 5.4: Correlation ($p - value$ in brackets) between SUS-Mean, SUS-Count, SUS Q1, SUS Q2, and mean BFV values (Free Navigation).

BFV	SUS-Mean	SUS-Count	SUS Q1	SUS Q2
MCA-L	**0.451(0.027)**	0.381(0.066)	**0.486(0.016)**	0.277(0.190)
MCA-R	0.188(0.402)	0.257(0.249)	0.152(0.499)	0.232(0.299)
ACA-L	0.083(0.831)	0.230(0.552)	0.312(0.414)	-0.053(0.893)
ACA-R	-0.257(0.623)	-0.334(0.518)	-0.353(0.492)	-0.530(0.280)

Table 5.5: Correlation between SUS Q3, Q4, Q5, Q6, and mean BFV values (Free Navigation).

BFV	SUS Q3	SUS Q4	SUS Q5	SUS Q6
MCA-L	0.341(0.103)	0.325(0.121)	**0.415(0.044)**	0.279(0.187)
MCA-R	0.219(0.328)	0.209(0.350)	0.173(0.442)	0.042(0.854)
ACA-L	-0.213(0.583)	0.070(0.858)	0.434(0.243)	-0.026(0.946)
ACA-R	-0.530(0.280)	-0.185(0.725)	-0.395(0.439)	-0.185(0.725)

Table 5.6: Correlation between SUS-Mean, SUS-Count, SUS Q1, SUS Q2 and mean BFV values (Automatic Navigation).

BFV	SUS-Mean	SUS-Count	SUS Q1	SUS Q2
MCA-L	0.382(0.065)	0.188(0.379)	0.321(0.126)	**0.428(0.037)**
MCA-R	0.388(0.082)	0.351(0.118)	0.339(0.133)	**0.501(0.021)**
ACA-L	0.357(0.385)	0.000(1.000)	0.196(0.641)	0.173(0.682)
ACA-R	-0.319(0.538)	-0.463(0.355)	-0.232(0.658)	-0.185(0.725)

Table 5.7: Correlation between SUS Q3, Q4, Q5, Q6, and mean BFV values (Automatic Navigation).

BFV	SUS Q3	SUS Q4	SUS Q5	SUS Q6
MCA-L	0.261(0.218)	0.299(0.155)	**0.611(0.002)**	**0.425(0.038)**
MCA-R	0.227(0.323)	0.348(0.122)	**0.513(0.018)**	0.424(0.055)
ACA-L	-0.170(0.688)	0.077(0.857)	0.430(0.288)	0.265(0.526)
ACA-R	-0.464(0.354)	0.058(0.913)	-0.441(0.381)	0.116(0.827)

5.1.4 Comparison of BFV variations in the free navigation condition and the automatic navigation condition

The percentage variations between mean BFV in the automatic navigation and its preceding baseline, and between mean BFV in the free navigation and its preceding baseline were calculated for the different vessels. The percentage variations obtained were always positive, indicating an increase when changing from baseline to the free navigation or the automatic navigation conditions.

Mean values and standard errors of the mean are represented in Fig. 5.9 and 5.10.

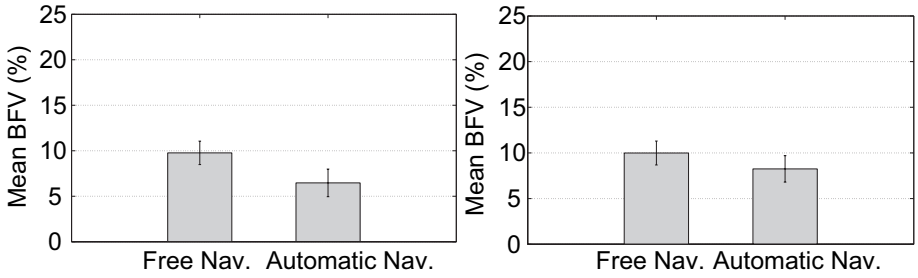

Figure 5.9: Percentage variation of mean BFV between the Free Navigation Condition and its preceding baseline, and between the Automatic Navigation Condition and its preceding baseline. The error bars represent the s.e.m. (a) MCA-L. 24 subjects. (b)MCA-R. 22 subjects.

A two-tailed Student's t test was applied to compare the BFV percentage variation in the free navigation with the BFV percentage variation in the automatic navigation in the four vessels. Results for MCA-L and ACA-L showed that there was a significant difference between the percentage variation observed in the free navigation and the automatic navigation conditions. The percentage increase was greater in the free navigation (MCA-L: $t(23) = 2.098$, $p = 0.047$; ACA-L: $t(8) = 5.725$, $p < 0.001$). However, there was not a significant difference between the percentage increase in the free navigation and the increase in the automatic navigation

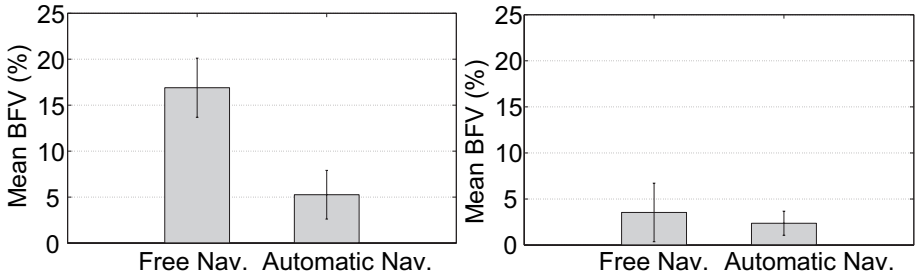

Figure 5.10: Percentage variation of mean BFV between the Free Navigation Condition and its preceding baseline, and between the Automatic Navigation Condition and its preceding baseline. The error bars represent the s.e.m. (a) ACA-L. 9 subjects. (b) ACA-R. 6 subjects.

for the right vessels.

Similar patterns were observed in SUS questionnaires and in BFV increases: BFV percentage variations in MCA-L and ACA-L and SUS questionnaire responses in the free navigation were significantly greater than percentage variations and SUS responses in the automatic navigation.

5.1.5 Analysis of BFV signal when BIPs occur

In the following paragraphs, the analysis made for the transitions from virtual to real (BIPs) and for the transitions from real to virtual that occur after each BIP (recovery periods) will be described.

As explained in the chapter 4, previously to the analysis, a filter is applied to smooth the squared signal corresponding to the mean BFV. The results of applying this filter to the squared signal can be observed in Fig. 5.11, where some seconds of the original mean BFV signal and the filtered one are represented.

The results described in the following subsections have been obtained analyzing the filtered BFV signal.

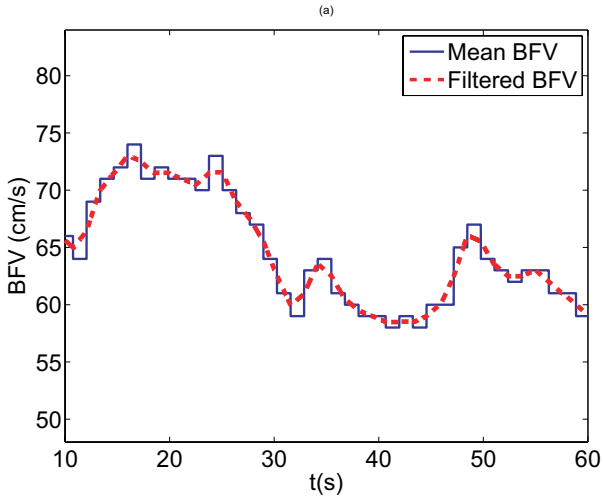

Figure 5.11: MCA-L mean BFV of one of the participants: original signal and filtered signal.

5.1.5.1 Evolution of the BFV signal during BIPs

During the *Total BIP*, it can be observed how the BFV signal of most subjects has a decreasing trend. The maximum variation that is observed in the period when compared with the initial value corresponds to a minimum.

On the other hand, the instantaneous temporal evolution during the *Partial BIP* has important interindividual differences. Usually, there are oscillations inside the period without a clear decreasing or increasing trend. In Fig. 5.12, the filtered MCA-L BFV signals corresponding to both BIPs (*Total BIP* and *Partial BIP*) of one of the subjects are shown.

As in previous studies [180, 181, 33], the grand average curves for each BIP (mean of the BFV signals from all the subjects during the BIP) have been calculated and are shown in Fig. 5.13. These grand average curves show the decreasing trend during the *Total BIP* and the oscillations during the *Partial BIP*.

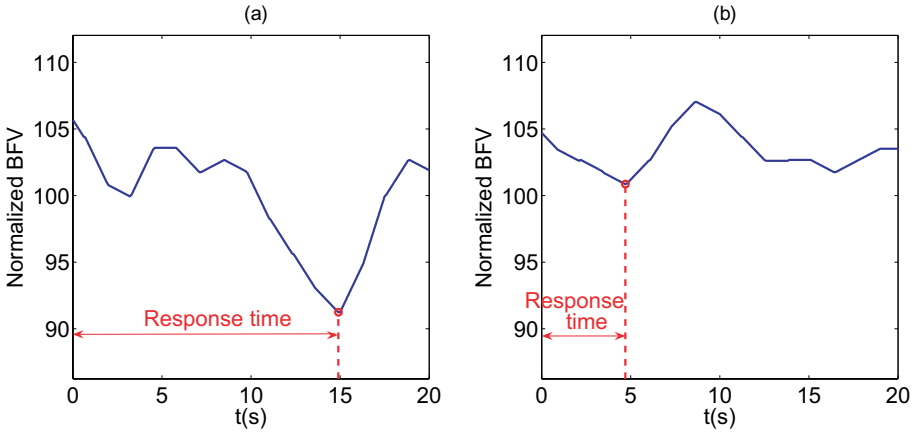

Figure 5.12: Filtered and normalized BFV in a sample subject during (a) the *Total BIP* and (b) the *Partial BIP*. The maximum variation is marked in the graphs with an 'o'. In this case, a decreasing trend can be observed for the *Total BIP* and an oscillating trend for the *Partial BIP*. The response time is indicated graphically.

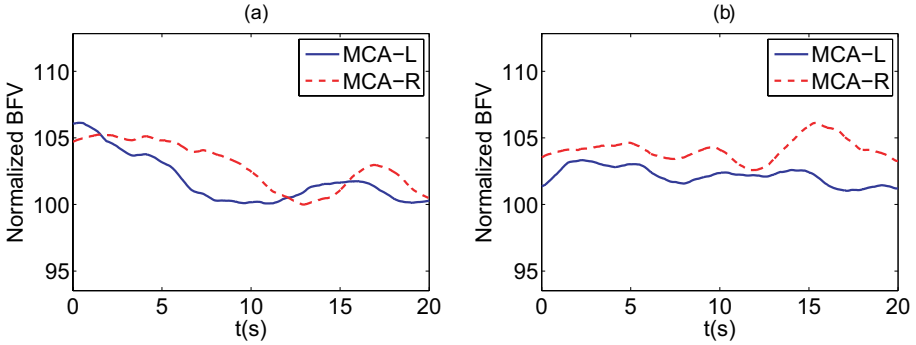

Figure 5.13: (a) Grand average of the 17 subjects MCA-L and MCA-R BFV signals during the *Total BIP* (b) Grand average of the 17 subjects MCA-L and MCA-R BFV signals during the *Partial BIP*

The response time and maximum percentage variation of each subject that participated in the study have been calculated both for the *Total BIP* and *Partial BIP*. Then, mean values of these parameters for the 17 subjects have been obtained. These mean values of the maximum percentage variation and response time are shown in Fig. 5.14 and 5.15, with their standard error of the mean (s.e.m.). Exact values are included in Table 5.8.

Results from the ANOVA applied to the maximum percentage variation showed a significant effect for the type of BIP ($F(1, 16) = 6.986$; $p = 0.018$). No significant effect was found for the vessel under study factor. Pairwise comparisons using the Bonferroni correction showed that there were significant differences between BIPs in MCA-L BFV ($p = 0.027$), but not in MCA-R BFV. The maximum percentage variation in MCA-L during the *Total BIP* is negative (mean -6.377) and significantly different to the maximum percentage variation in MCA-L during the *Partial BIP*, which has a mean of 2.994.

Results from the ANOVA applied to the response time showed no significant effect neither for the kind of BIP nor for the vessel under study.

Table 5.8: Response time and percentage variation in the different BIPs that are forced during the experiment. The mean value and the standard error of the mean - s.e.m. - (in brackets) are shown.

Moment	Vessel	Maximum Variation (%)	Response Time (s)
Total BIP	MCA-L	-6.377 (3.073)	12.774 (1.375)
	MCA-R	-2.020 (3.148)	12.224 (1.388)
Partial BIP	MCA-L	2.994 (2.619)	10.116 (1.425)
	MCA-R	3.512 (3.181)	11.425 (1.331)

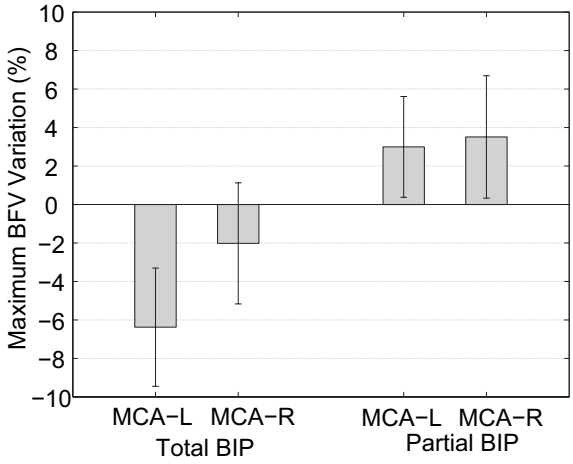

Figure 5.14: Percentage variation of MCA-L and MCA-R during the *Total BIP* and the *Partial BIP*.

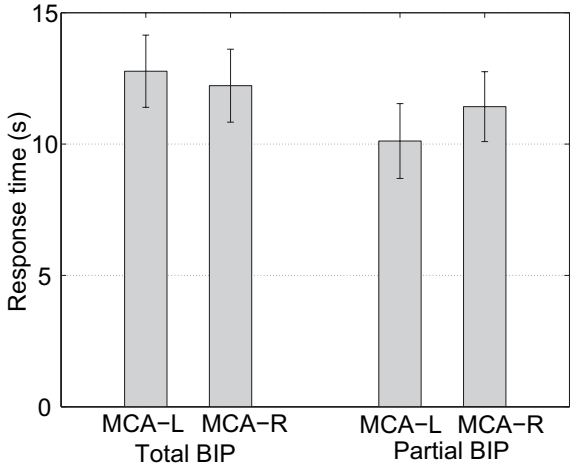

Figure 5.15: Response time in MCA-L and MCA-R during the *Total BIP* and the *Partial BIP*

5.1.5.2 Evolution of the BFV signal during recoveries from BIPs

The temporal evolution of BFV during recovery periods also presented important interindividual differences. Also in this case, the maximum percentage variation and response time were calculated for each subject both in the *Total Recovery* and the *Partial Recovery*. For most of the subjects, the maximum variation that was observed was positive in the recovery periods from both BIPs. The evolution depended on the subject and could have a continuous growing trend or oscillations. In Fig. 5.16, the filtered MCA-L BFV signals corresponding to both recovery periods (*Total Recovery* and *Partial Recovery*) of one of the subjects are shown.

The grand average curves corresponding to the recovery periods have been calculated and are shown in Fig. 5.17

The statistical analyses found no significant effect for any of the analyzed factors (vessel and kind of BIP that precedes the recovery) on the maximum percentage variation and response time values.

In Fig. 5.18 and 5.19, mean values of the maximum percentage variations and response times in the different BIPs for both vessels are shown, with their standard error of the mean (s.e.m.).

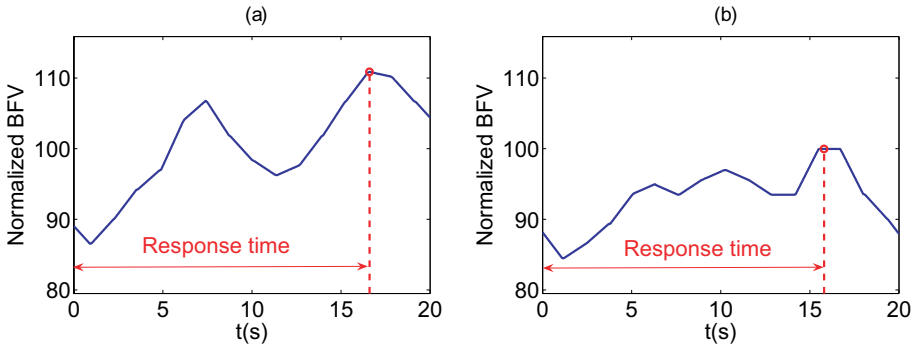

Figure 5.16: Filtered and normalized BFV in a sample subject during (a) the *Total Recovery* and (b) the *Partial Recovery*. The maximum variation is marked in the graphs with an 'o'. In this case, a growing trend is observed in both cases. The response time is indicated graphically.

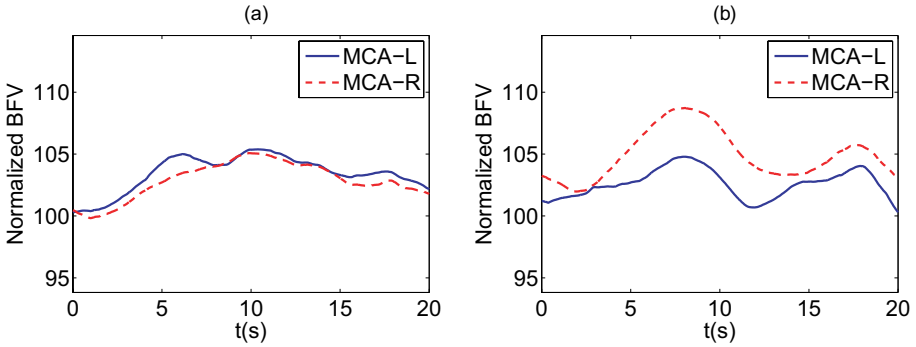

Figure 5.17: (a) Grand average of MCA-L and MCA-R BFV signals during the *Total Recovery* (b) Grand average of MCA-L and MCA-R BFV signals during the *Partial Recovery*

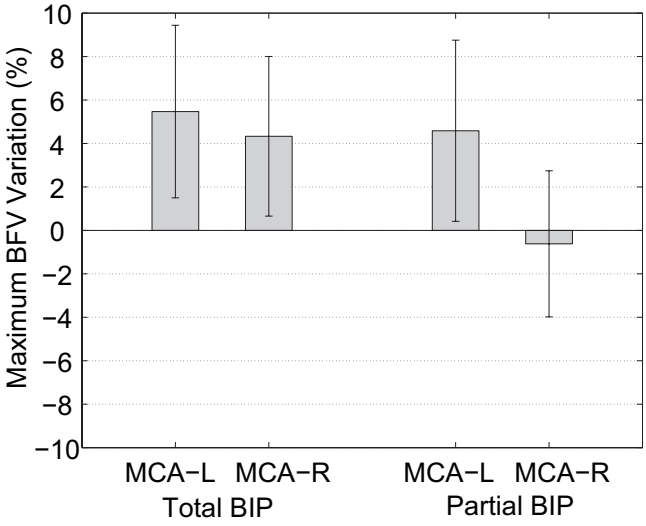

Figure 5.18: Percentage variation of MCA-L and MCA-R during the *Total Recovery* and the *Partial Recovery*.

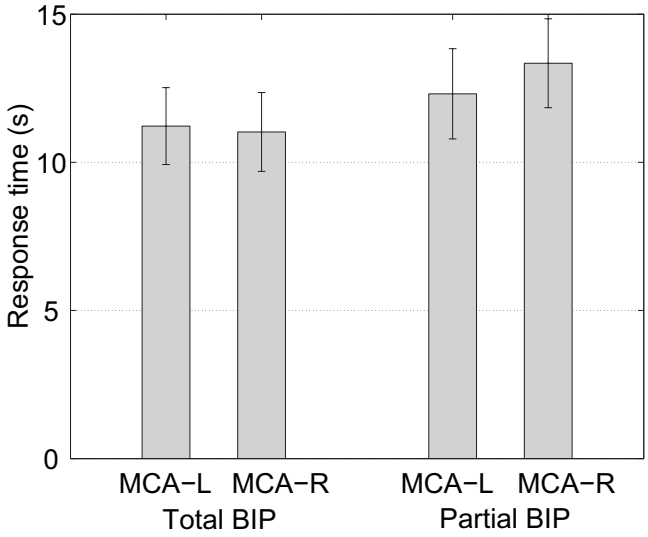

Figure 5.19: Response time in MCA-L and MCA-R during the *Total Recovery* and *Partial Recovery*.

Table 5.9 shows exact mean values and s.e.m. of the maximum BFV percentage variations and response times in the recovery periods for both vessels.

Table 5.9: Response time and percentage variation in the different BIPs that are forced during the experiment. The mean value and the standard error of the mean - s.e.m. - (in brackets) are shown.

Moment	Vessel	Maximum Variation (%)	Response Time (s)
Recovery A	MCA-L	5.469 (3.973)	11.224 (1.298)
	MCA-R	4.331 (3.675)	11.025 (1.330)
Recovery B	MCA-L	4.587 (4.171)	12.313 (1.524)
	MCA-R	-0.619 (3.364)	13.345 (1.500)

5.2 BFV analysis in different immersive conditions

As explained in the chapter 4, the data obtained in this study with a low-immersion VR configuration were compared with the data obtained in the study about navigation with a high-immersion VR configuration, in order to analyze if there is any influence of the immersion variable on the observed results.

In the following sections, the results obtained with the SUS questionnaire and the BFV registered in the different experimental conditions included in both studies are summarized.

5.2.1 SUS questionnaire analysis

The descriptive statistics for the different answers to the questionnaire and for SUS Count and SUS Mean are shown in Tables 5.10 and 5.11.

Table 5.10: SUS responses (SUS Mean, SUS Count, Q1 and Q2) after the free navigation condition and after the automatic navigation condition. The mean value and the standard error of the mean (s.e.m.) are shown. The number of subjects depends on the experimental condition: (a) CAVE-like configuration, free navigation: 32 subjects. (b) CAVE-like configuration, automatic navigation: 31 subjects. (c) Single screen configuration, free navigation: 8 subjects. (d) Single screen configuration, automatic navigation: 9 subjects.

Immersion	Navigation	SUS Mean	SUS Count	Q1	Q2
CAVE-like	Free	4.83(0.23)	2.48(0.38)	5.25(0.24)	4.87(0.31)
	Automatic	3.89(0.28)	1.19(0.30	4.19(0.26)	4.06(0.28)
Single screen	Free	4.10(0.41)	1.50(0.66)	4.20(0.42)	4.10(0.54)
	Automatic	3.00(0.49)	0.60(0.54)	3.00(0.47)	3.00(0.50)

Table 5.11: SUS responses (Q3-Q6) after the free navigation condition and after the automatic navigation condition. The mean value and the standard error of the mean (s.e.m.) are shown. The number of subjects depends on the experimental condition: (a) CAVE-like configuration, free navigation: 32 subjects. (b) CAVE-like configuration, automatic navigation: 31 subjects. (c) Single screen configuration, free navigation: 8 subjects. (d) Single screen configuration, automatic navigation: 9 subjects.

Immersion	Navigation	Q3	Q4	Q5	Q6
CAVE-like	Free	4.51(0.33)	5.16(0.29)	4.58(0.27)	4.61(0.26)
	Automatic	3.80(0.33)	3.80(0.32)	4.00(0.28)	3.67(0.31)
Single screen	Free	4.10(0.58)	4.70(0.52)	3.30(0.47)	4.20(0.46)
	Automatic	3.30(0.59)	3.20(0.57)	2.70(0.50)	2.80(0.55)

Results from the robust two-way ANOVA applied to the different variables showed that navigation is the only factor that has a significant effect on SUS Mean ($F(1,39) = 21.06$; $p = 0.02$), SUS Count ($F(1,39) = 12.28$; $p = 0.03$), question 1 ($F(1,39) = 21.36$, $p = 0.01$) question 3 ($F(1,39) = 10.52$; $p = 0.03$), question 4 ($F(1,39) = 27.74$; $p < 0.01$) and question 6 ($F(1,39) = 26.92$; $p = 0.01$), and a close to significant effect on question 2 ($F(1,39) = 10.81$; $p = 0.07$) and question 5 ($F(1,39) = 6.30$; $p = 0.07$). No significant effects were found for the immersion factor, or for the navigation x immersion factor. Nevertheless, results of the robust ANOVA for question 1 (*I had a sense of "being there" in the maze*), question 5 (*I think of the maze space as a place in a way similar to other similar places where I have been*) and SUS Mean showed a close to significant effect also for the immersion factor (question 1: $F(1,39) = 6.74$; $p = 0.09$; question 5: $F(1,39) = 4.33$; $p = 0.12$; SUS-Mean: $F(1,39) = 4.48$; $p = 0.10$). Taking into account these results, it can be concluded that the navigation variable has a significant effect in presence measures obtained from questionnaires, and the immersion variable has a close to significant effect in presence measures obtained from questionnaires. Mean values in the different con-

ditions for SUS Mean and SUS question 1 can be observed in Fig. 5.20 and 5.21.

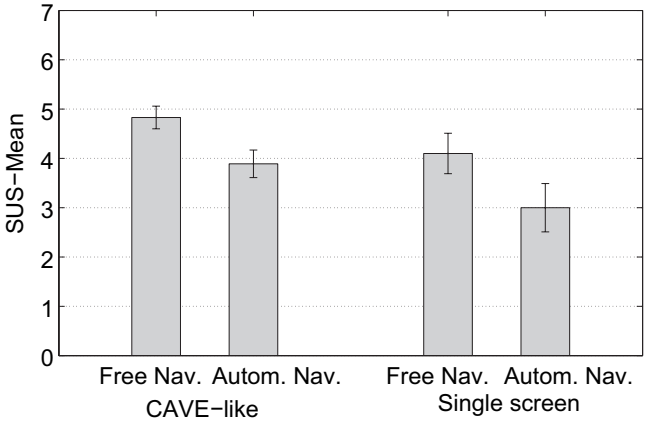

Figure 5.20: Mean values in the different experimental conditions for SUS Mean. Error bars represent s.e.m.

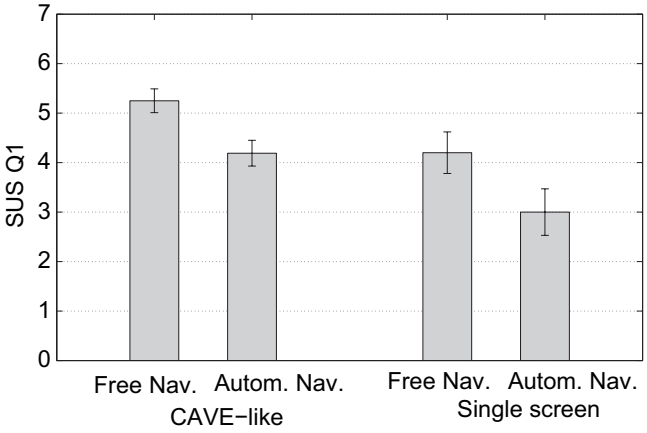

Figure 5.21: Mean values in the different experimental conditions for SUS question 1. Error bars represent s.e.m.

5.2.2 Comparison of BFV variations in the free navigation condition and the automatic navigation condition

The percentage variations between the mean BFV in the free navigation condition and its preceding baseline, and between the mean BFV in the automatic navigation and its preceding baseline have been calculated for the different vessels and the different immersive conditions. Their values have been indicated in Table 5.12.

Table 5.12: BFV Percentage Variations (%) in the different experimental conditions in MCA-L and MCA-R. The mean values and the standard error of the mean (s.e.m.) are shown.

Immersion	Navigation	MCA-L	MCA-R
CAVE-like	Free	9.77 (1.38)	9.99 (1.28)
	Automatic	6.47 (1.43)	8.25 (1.30)
Single screen	Free	8.27 (2.39)	9.04 (2.00)
	Automatic	5.18 (2.47)	3.54 (2.04)

The percentage variations were always positive, indicating an increase in BFV when changing from baseline to the VE exposure. BFV percentage variations have been represented graphically in Fig. 5.22 (for MCA-L) and Fig. 5.23 (for MCA-R).

Only the navigation factor seems to have a clear influence on BFV values. Results from the ANOVA applied to MCA-R showed a significant effect for the navigation factor ($F(1,29)=6,311$; $p=0.018$). Results from the ANOVA applied to MCA-L showed an effect for navigation factor which is close to significance ($F(1,30)=3.965$; $p=0.056$). There was no significant effect for the other factors (immersion and navigation x immersion) in any of the studied vessels. Nevertheless, if Fig. 5.22 and Fig. 5.23 are compared, it can be seen that the means do not follow exactly the same trend in the case of the MCA-L and in the case of the MCA-R.

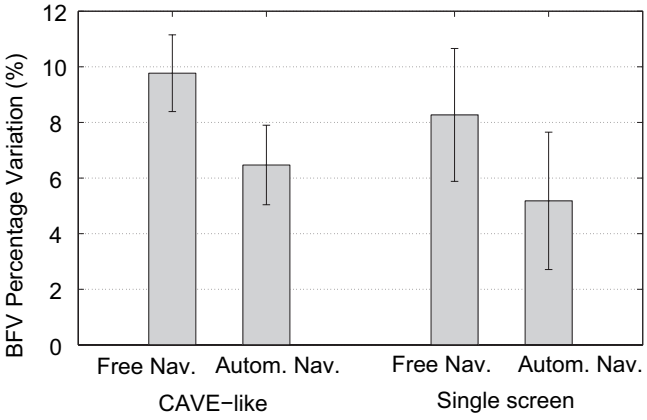

Figure 5.22: Percentage variations in MCA-L for different immersion and navigation conditions. The error bars represent s.e.m.

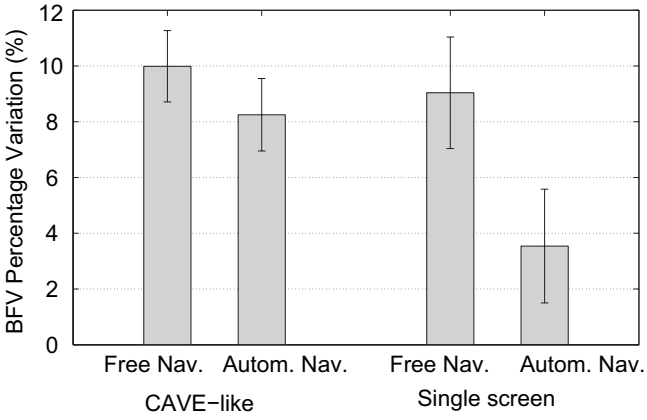

Figure 5.23: Percentage variations in MCA-R for different immersion and navigation conditions. The error bars represent s.e.m.

In MCA-L, the highest variations are observed in the free navigation condition. Moreover, if only the data from this navigation condition are

considered, the percentage variation that is observed in the CAVE-like environment is greater than the percentage variation in the single screen environment. In the automatic navigation condition, the variations are smaller, but the same trend is observed. The greatest variation occurs in the CAVE-like environment and the lowest in the single screen environment.

In MCA-R, these general considerations that have been described for MCA-L are also true. However, there are some differences. Analyzing only data from the free navigation condition, the variations observed in the single screen environment are close to the variations observed in the CAVE-like environment. However, in the case of the automatic navigation condition, the differences between variations in the CAVE-like environment and the single screen environment are greater. Analogously, the difference in the percentage variation between both navigation conditions in the single screen environment is greater than in the CAVE-like environment. The navigation x immersion factor seems to be having an influence in the measurements in the case of MCA-R. Nevertheless, these are no conclusive results as no statistical significance has been obtained.

5.3 BFV analysis during a visual perception task

Answers to the Edinburgh Handedness Inventory in the experiment about visual perception issues confirmed that all the participants of this study were right-handed.

The mean systolic blood pressure was 131.76 mmHg before the experiment and 133.85 mmHg after the experiment. A t test was applied just to confirm that no significant differences appear between the initial and final blood pressure ($t(20) = -1.013$, $p = 0.323$)

The mean diastolic blood pressure was 86.33 mmHg before the experiment and 87.57 mmHg after the experiment. The t test confirmed that there were no significant differences between these measures ($t(20) = -0.587$, $p = 0.563$).

Regarding BFV analyses, the results are going to be summarized in

the following subsections. Some seconds of maximum BFV signal (before and after normalization) in a sample subject are shown in Fig. 5.24.

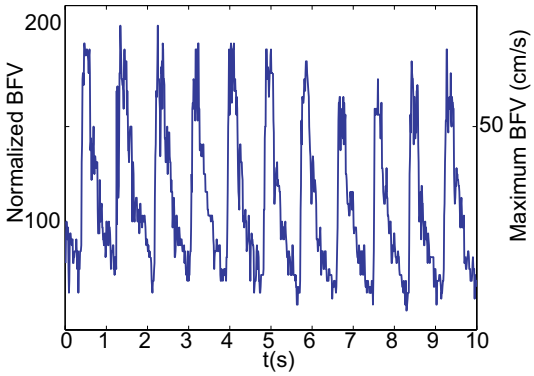

Figure 5.24: Some seconds of the PCA-L maximum BFV signal in one of the subjects. The original BFV signal (right y axis, in cm/s) and the normalized BFV signal (left y axis), as indicated in equation 4.2, are represented in the same graph.

5.3.1 Spectral Estimation

As expected, the spectral estimation of PCA-L and PCA-R BFV during repose and activation periods showed a peak around 1 Hz due to the heart rate and several harmonics were present at the corresponding multiple frequencies. A sample spectrum estimation corresponding to the PCA-L BFV of one of the subjects is represented in Fig. 5.25. As can be observed, the harmonics attenuate quickly. These peaks are not related to the objectives of the experiment.

Focusing on the low-frequency band of the spectrum, which is the band in which the slow changes in BFV signal that appear as a response to the cognitive stimuli can be reflected, it can be observed that an important peak is present in this frequency band. This peak appeared in PCA-L and PCA-R BFV from all the subjects in the study, both in repose and activation periods.

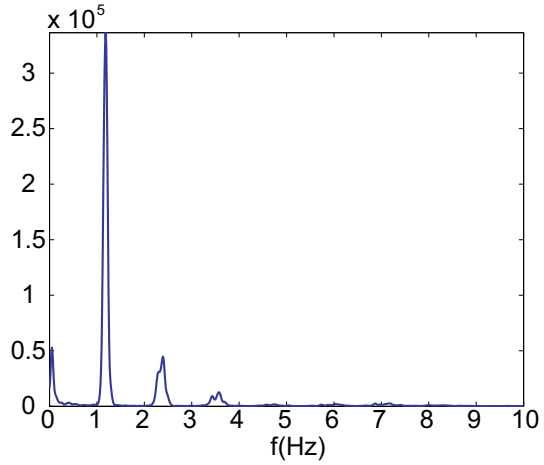

Figure 5.25: Spectral estimation of the PCA-L BFV of one of the subjects during the activation periods.

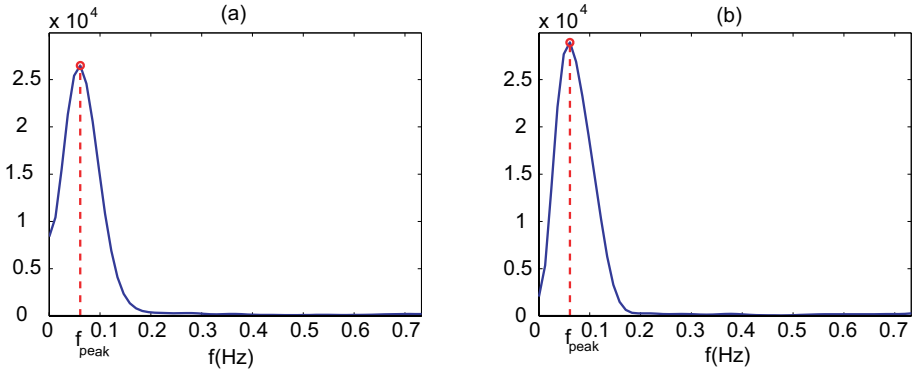

Figure 5.26: Spectral estimation of the low frequencies from a subject corresponding to (a) repose periods and (b) activation periods. The maximum value in the low-frequency band is marked with an 'o' and the frequency of this peak (f_{peak}) is indicated.

Fig. 5.26 shows a detail of the low-frequency band of the PCA-L BFV spectrum from one subject, during repose and activation periods.

Table 5.13 shows descriptive statistics corresponding to the low-frequency peak values in the different vessels and conditions. The frequency at which this peak occurs does not change significantly between vessels (PCA-L vs. PCA-R) or between periods (repose vs. activation).

Table 5.13: Descriptive statistics (mean, standard deviation -SD-, minimum value and maximum value) for the low-frequency peak. PCA-L and PCA-R BFV signals of repose and activation periods in the 16 subjects in which both vessels could be measured with enough quality have been included for this analysis.

Vessel	Stimulus	Mean (Hz)	SD (Hz)	Min. (Hz)	Max. (Hz)
PCA-L	Repose	0.059	0.015	0.049	0.098
	Activation	0.056	0.012	0.037	0.073
PCA-R	Repose	0.060	0.020	0.037	0.098
	Activation	0.055	0.009	0.037	0.073

5.3.2 Low-frequency estimation

A difference can be observed in the low-frequency estimation phase between repose and activation periods. Globally, in activation periods, the estimation starts the period with a low value and increases until it reaches a maximum after a few seconds. On the other hand, in repose periods, the estimation starts the period with a high value, which may increase a little until it achieves a maximum, and then decreases until it achieves a minimum after a few seconds. In Fig. 5.27, the low-frequency estimation corresponding to the PCA-L BFV during repose and activation periods of one of the subjects is shown. The phase differences between periods can be observed. The value in which the maximum percentage variation occurs and the response time are marked in the figure.

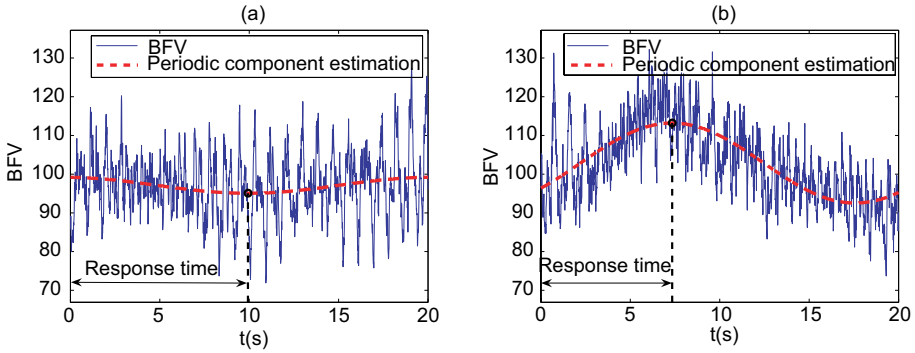

Figure 5.27: Instantaneous average BFV and low-frequency estimation in a sample subject during (a) repose and (b) activation periods. The value corresponding to the maximum variation during the period is marked with an 'o'. The response time is indicated graphically in both graphs.

5.3.3 BFV parameters

A statistical analysis was applied to check if the differences in the BFV-related parameters (mean BFV, percentage BFV variation and response time) between repose and activation periods and between vessels are significant.

Table 5.14: Mean BFV, response time and percentage variation for the different conditions and vessels. The mean value and the standard error of the mean (s.e.m.) are shown.

Vessel	Stimulus	Mean BFV	Resp. Time (s)	Variation(%)
PCA-L	Repose	97.689 (0.428)	10.146 (0.828)	-4.149 (1.080)
	Activation	102.311 (0.428)	8.974(0.748)	4.572(1.453)
PCA-R	Repose	97.762 (0.474)	10.726 (0.820)	-4.879 (1.019)
	Activation	102.238 (0.474)	8.544 (0.753)	4.114 (1.550)

Results from the ANOVA applied to mean BFV showed a significant

effect for the presence of visual stimulus factor ($F(1, 15) = 33.924$; $p < 0.001$). No significant effect was found for the vessel under study factor or for the interaction factor. In Fig. 5.28, the mean BFV values corresponding to the different experimental conditions and vessels are shown. Exact values are included in Table 5.14.

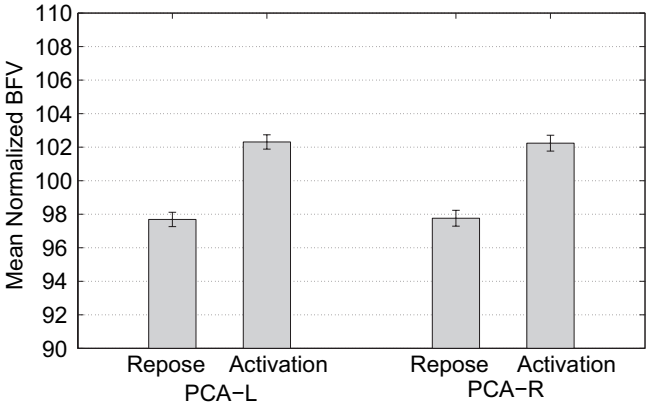

Figure 5.28: Mean BFV values in repose and activation periods for PCA-L and PCA-R. The error bars represent standard error of the mean.

On the other hand, the two-way ANOVA applied to the percentage variation showed a significant effect for the presence of the stimulus factor ($F(1, 15) = 18.303$; $p = 0.001$). No significant effects were found for the other factors. In Fig. 5.29, the percentage variation of the estimation in the different experimental conditions is shown. Exact values are included in Table 5.14. As BFV usually has a growing trend during activation periods, the maximum percentage variation is positive. On the other hand, during repose periods the usual trend in BFV signal is decreasing, so the maximum variation is negative.

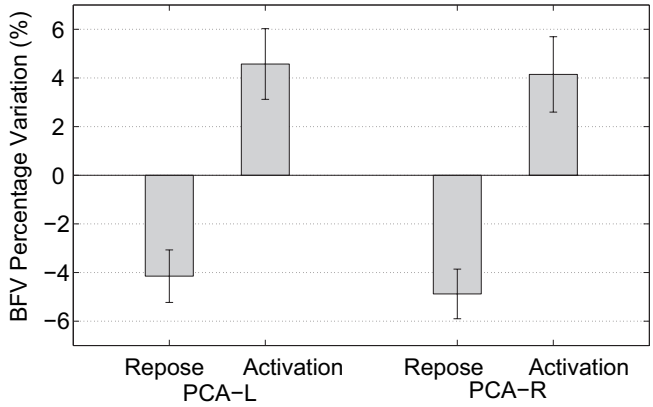

Figure 5.29: Mean PCA-L and PCA-R BFV percentage variation during repose and activation. The error bars represent standard error of the mean

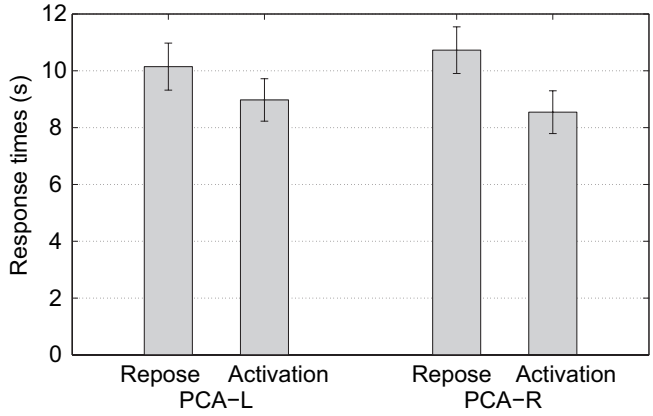

Figure 5.30: Mean PCA-L and PCA-R response times during repose and activation. The error bars represent standard error of the mean

Finally, results from the ANOVA applied to the response times show that these times did not differ significantly between repose and activation

periods. No significant effect was found either for the vessel under study or for the interaction between vessel and stimulus factors. In Fig. 5.30, the response times calculated from the estimation in the different experimental conditions are shown. Exact values corresponding to the different experimental conditions and vessels are included in Table 5.14.

5.4 BFV Analysis during motor tasks

Answers to the Edinburgh Handedness Inventory in the experiment about the performance of motor tasks to control the joystick showed that nine subjects were right-handed and two subjects were left-handed.

The mean systolic blood pressure was 113.55 mmHg before the experiment and 114.09 mmHg after the experiment. A t test was applied just to confirm that no significant differences appeared between the initial and final blood pressure ($t(10) = -0.215$, $p = 0.834$)

The mean diastolic blood pressure was 73.09 mmHg before the experiment and 72.00 mmHg after the experiment. The t test confirmed that there were no significant differences between these measures ($t(10) = 0.272$, $p = 0.791$).

On the other hand, focusing on BFV analysis, MCA-L and MCA-R BFV data were monitored in this study. Different non-linear parameters of the MCAs BFV were calculated in the different periods of the experiment to analyze if there are changes in the dynamics of the system when different activities are performed: the multiscale entropy (MSE), the correlation dimension, the fractal dimension (Katz Method), and the maximum Lyapunov exponent. The results of calculating these parameters in the different experimental conditions are summarized in the following subsections. First of all, the results obtained from the surrogates analysis, to check the non-linearity of the maximum BFV signal, are detailed.

5.4.1 Surrogates

As explained in the chapter 4, the irregularity measure that was applied to the original series and to each of the surrogate series was SampEn (with $m = 2$ and $r = 0.2$).

Table 5.15: SampEn values of the surrogates analysis in the condition with dominant hand movements and contralateral hemisphere monitoring.

Subject	BFV SampEn	Mean SampEn (surr.)	SD SampEn (surr.)
1	0.117	0.447	0.004
2	0.194	0.470	0.004
3	0.209	0.427	0.005
4	0.176	0.467	0.004
5	0.201	0.444	0.005
6	0.202	0.420	0.004
9	0.165	0.404	0.004
10	0.158	0.465	0.004
11	0.179	0.445	0.005

Table 5.16: SampEn values of the surrogates analysis in the condition with dominant hand movements and ipsilateral hemisphere monitoring.

Subject	BFV SampEn	Mean SampEn (surr.)	SD SampEn (surr.)
1	0.174	0.431	0.006
2	0.203	0.427	0.004
3	0.189	0.395	0.005
4	0.225	0.473	0.005
5	0.264	0.451	0.007
6	0.135	0.384	0.004
7	0.173	0.463	0.005
8	0.362	0.529	0.003
9	0.228	0.435	0.005

Table 5.17: SampEn values of the surrogates analysis in the condition with non-dominant hand movements and contralateral hemisphere monitoring.

Subject	BFV SampEn	Mean SampEn (surr.)	SD SampEn (surr.)
1	0.177	0.441	0.005
2	0.180	0.442	0.003
3	0.189	0.377	0.004
4	0.363	0.495	0.005
5	0.190	0.448	0.003
6	0.145	0.398	0.004
7	0.197	0.475	0.004
8	0.367	0.541	0.002
9	0.279	0.434	0.005

Table 5.18: SampEn values of the surrogates analysis in the condition with non-dominant hand movements and ipsilateral hemisphere monitoring.

Subject	BFV SampEn	Mean SampEn (surr.)	SD SampEn (surr.)
1	0.181	0.450	0.007
2	0.196	0.468	0.003
3	0.180	0.393	0.004
4	0.172	0.458	0.005
5	0.199	0.461	0.004
6	0.314	0.481	0.004
9	0.190	0.409	0.005
10	0.165	0.470	0.004
11	0.182	0.457	0.005

The results show that SampEn is higher in all the surrogates than in the original signals, which indicates that the original signal is non-linear. In tables 5.15, 5.16, 5.17 and 5.18, the SampEn value of the original time series are shown with the mean and standard deviation of the SampEn values of all the surrogates in the different experimental conditions.

5.4.2 Multiscale entropy

The MSE algorithm was applied to the selected data from each period of analysis as described in the chapter 4.

5.4.2.1 Descriptive statistics

In the following subsections, results of the MSE analysis in the different experimental conditions and the different vessels are detailed.

Dominant hand movements - Contralateral MCA

In one of the experimental conditions, the user controlled the joystick moving the dominant hand. In this paragraph, the results of applying the MSE analysis to the BFV data of the contralateral MCA are described. Data from two different periods have been included: the repose period, and the period with hand movements. Mean SampEn values corresponding to the different scale factors are represented in Fig. 5.31. Exact values can be found in table 5.19. There are valid data from 9 MCA-L and 9 MCA-R.

Dominant hand movements - Ipsilateral MCA

Continuing with the analysis of the experimental condition in which the user controls the joystick moving the dominant hand, the results of the MSE analysis of the BFV data of the ipsilateral MCA are described (both for the repose period and the period with hand movements). Mean SampEn values corresponding to the different scale factors are represented in Fig. 5.32. Exact values can be found in table 5.20. There are valid data from 9 MCA-L and 9 MCA-R.

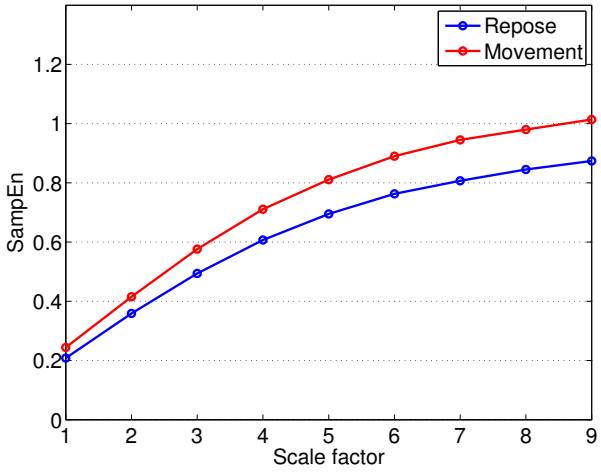

Figure 5.31: Dominant Hand - Contralateral MCA. SampEn values in the different scale factors.

Table 5.19: Dominant Hand - Contralateral MCA. SampEn values (mean and standard error of the mean -s.e.m.-) in the different scale factors.

Scale factor	Repose	Hand Movements
1	0.208 (0.010)	0.244 (0.009)
2	0.359 (0.016)	0.415 (0.016)
3	0.494 (0.023)	0.576 (0.023)
4	0.607 (0.031)	0.711 (0.029)
5	0.695 (0.038)	0.811 (0.035)
6	0.763 (0.045)	0.890 (0.043)
7	0.807 (0.051)	0.945 (0.049)
8	0.845 (0.057)	0.980 (0.054)
9	0.874 (0.060)	1.014 (0.059)

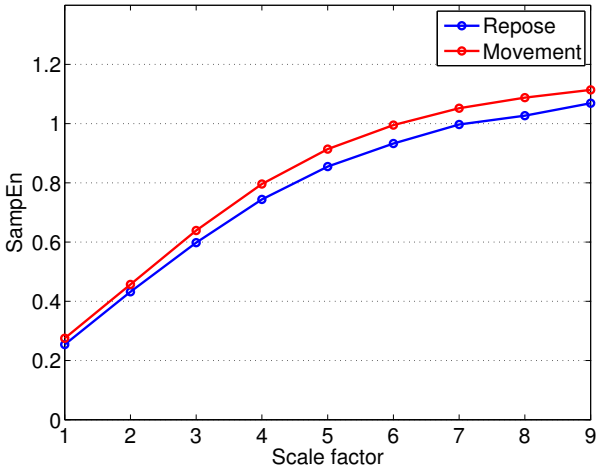

Figure 5.32: Dominant Hand - Ipsilateral MCA. SampEn values in the different scale factors.

Table 5.20: Dominant Hand - Ipsilateral MCA. SampEn values (mean and standard error of the mean -s.e.m.-) in the different scale factors.

Scale factor	Repose	Hand Movements
1	0.254 (0.025)	0.275 (0.027)
2	0.432 (0.036)	0.457 (0.040)
3	0.598 (0.053)	0.639 (0.059)
4	0.744 (0.066)	0.796 (0.075)
5	0.855 (0.073)	0.914 (0.086)
6	0.933 (0.075)	0.995 (0.092)
7	0.997 (0.079)	1.052 (0.100)
8	1.027 (0.078)	1.088 (0.100)
9	1.069 (0.085)	1.114 (0.108)

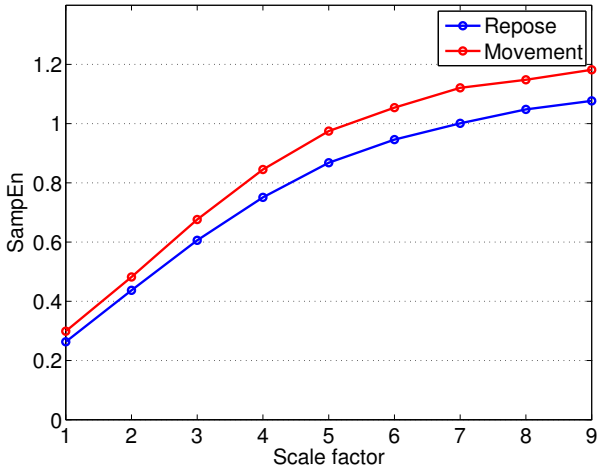

Figure 5.33: Non-Dominant Hand - Contralateral MCA. SampEn values in the different scale factors.

Table 5.21: Non-Dominant Hand - Contralateral MCA. SampEn values (mean and standard error of the mean -s.e.m.-) in the different scale factors.

Scale factor	Repose	Hand Movements
1	0.263 (0.030)	0.299 (0.034)
2	0.437 (0.045)	0.482 (0.048)
3	0.606 (0.067)	0.676 (0.072)
4	0.751 (0.085)	0.845 (0.091)
5	0.868 (0.097)	0.975 (0.105)
6	0.946 (0.103)	1.054 (0.113)
7	1.001 (0.105)	1.121 (0.114)
8	1.048 (0.107)	1.148 (0.109)
9	1.077 (0.106)	1.182 (0.109)

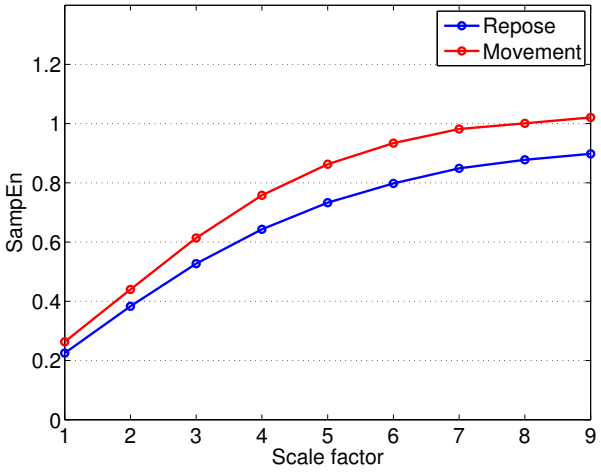

Figure 5.34: Non-Dominant Hand - Ipsilateral MCA. SampEn values in the different scale factors.

Table 5.22: Non-Dominant Hand - Ipsilateral MCA. SampEn values (mean and standard error of the mean -s.e.m.-) in the different scale factors.

Scale factor	Repose	Hand Movements
1	0.225 (0.021)	0.263 (0.020)
2	0.383 (0.033)	0.440 (0.032)
3	0.527 (0.049)	0.614 (0.048)
4	0.643 (0.064)	0.758 (0.063)
5	0.733 (0.075)	0.863 (0.073)
6	0.798 (0.084)	0.934 (0.079)
7	0.849 (0.090)	0.982 (0.084)
8	0.878 (0.092)	1.001 (0.086)
9	0.898 (0.092)	1.021 (0.084)

Non-Dominant hand movements - Contralateral MCA

In the other experimental condition, the user controlled the joystick moving the non-dominant hand. In this paragraph, the results of applying the MSE analysis to the BFV data of the contralateral MCA are described (both for the repose period and the period with hand movements). Mean SampEn values corresponding to the different scale factors are represented in Fig. 5.33. Exact values can be found in table 5.21. There are valid data from 9 MCA-L and 9 MCA-R.

Non-Dominant hand movements - Ipsilateral MCA

Continuing with the analysis of the experimental condition in which the user controls the joystick moving the non-dominant hand, the results of the MSE analysis of the BFV data of the ipsilateral MCA are described (both for the repose period and the period with hand movements). Mean SampEn values corresponding to the different scale factors are represented in Fig. 5.34. Exact values can be found in table 5.22. There are valid data from 9 MCA-L and 9 MCA-R.

5.4.2.2 Comparison between the different experimental conditions

As explained in the chapter 4, a three-way ANOVA with repeated measures was used to analyze the effects on the dependent variable (MSE in the different scale factors - S.F.) of the three within-subjects factors: (1) Motor movements (M.M.): Repose / Hand movements; (2) Active hand (A.H.): Dominant / Non-dominant; (3) Brain hemisphere (B.H.): Contralateral / Ipsilateral.

Results from the ANOVAs applied to the MSE values in the different scale factors are detailed in the tables 5.23, 5.24 and 5.25.

Table 5.23: Results from the ANOVA applied to the MSE values in scale factors from 1 to 3.

	S.F.=1		S.F.=2		S.F.=3	
	$F(1,6)$	p	$F(1,6)$	p	$F(1,6)$	p
A.H.	1.032	0.349	0.606	0.466	0.633	0.457
B.H.	0.008	0.931	0.065	0.807	0.065	0.808
M.M.	**8.145**	**0.029**	**6.017**	**0.050**	**6.882**	**0.039**
M.M.xA.H.	0.537	0.491	0.376	0.562	0.563	0.481
M.M.xB.H.	3.747	0.101	4.774	0.072	4.035	0.091
A.H.xB.H.	0.201	0.670	0.241	0.641	0.286	0.612
M.M.xA.H.xB.H.	0.004	0.950	0.049	0.833	0.016	0.902

Table 5.24: Results from the ANOVA applied to the MSE values in scale factors from 4 to 6.

	S.F.=4		S.F.=5		S.F.=6	
	$F(1,6)$	p	$F(1,6)$	p	$F(1,6)$	p
A.H.	0.521	0.498	0.508	0.503	0.299	0.604
B.H.	0.057	0.819	0.028	0.873	0.021	0.891
M.M.	**7.818**	**0.031**	**6.818**	**0.040**	4.791	0.071
M.M.xA.H.	0.649	0.451	0.554	0.485	0.439	0.532
M.M.xB.H.	3.501	0.111	3.086	0.129	1,768	0.232
A.H.xB.H.	0.335	0.584	0.389	0.556	0.340	0.581
M.M.xA.H.xB.H.	0.002	0.964	0.000	0.998	0.005	0.994

Table 5.25: Results from the ANOVA applied to the MSE values in scale factors from 7 to 9.

	S.F.=7		S.F.=8		S.F.=9	
	$F(1,6)$	p	$F(1,6)$	p	$F(1,6)$	p
A.H.	0.272	0.621	0.159	0.704	0.092	0.772
B.H.	0.003	0.961	0.002	0.964	0.031	0.867
M.M.	4.314	0.083	3.339	0.117	3.976	0.093
M.M.xA.H.	0.379	0.561	0.132	0.729	0.276	0.618
M.M.xB.H.	4.222	0.086	1.201	0.315	3.251	0.121
A.H.xB.H.	0.405	0.548	0.443	0.530	0.453	0.526
M.M.xA.H.xB.H.	0.002	0.969	0.000	0.997	0.046	0.837

The repeated-measures ANOVA revealed a main effect for the *Motor Movements* factor, for scale factors ranging from 1 to 5. No other significant main effect was found.

To analyze the differences between repose and motor movements, t tests were performed. All the subjects available in the following experimental conditions (N=9) were included in the analysis: (1) Dominant Hand - Contralateral hemisphere; (2) Dominant Hand - Ipsilateral hemisphere; (3) Non-Dominant Hand - Contralateral hemisphere; (4) Non-Dominant Hand - Ipsilateral hemisphere. The results of the statistical analysis are included in the tables 5.26, 5.27, 5.28 and 5.29.

It can be observed that, when the non-dominant hand was used to control the joystick, there were differences in the entropy of the BFV signal between the repose period and the hand movements period for all the scale factors. This happened both in the contralateral vessel BFV and in the ipsilateral vessel BFV. However, when the dominant hand is used to move the joystick, significant differences in the entropy of the BFV signal between the repose and the hand movements period can only be observed in the case of the contralateral MCA vessel, and only for the lower scale factors.

Table 5.26: Dominant Hand - Contralateral hemisphere. Results from the t test applied to SampEn values in the different scale factors.

	t	p
S.F. = 1	**-2.645**	**0.029**
S.F. = 2	**-2.357**	**0.046**
S.F. = 3	**-2.397**	**0.043**
S.F. = 4	**-2.359**	**0.046**
S.F. = 5	-2.253	0.054
S.F. = 6	-2.148	0.064
S.F. = 7	-2.145	0.064
S.F. = 8	-1.948	0.087
S.F. = 9	-2.113	0.068

Table 5.27: Dominant Hand - Ipsilateral hemisphere. Results from the t test applied to SampEn values in the different scale factors.

	t	p
S.F. = 1	-1.895	0.095
S.F. = 2	-1.440	0.188
S.F. = 3	-1.599	0.149
S.F. = 4	-1.535	0.163
S.F. = 5	-1.419	0.194
S.F. = 6	-1.317	0.224
S.F. = 7	-1.018	0.338
S.F. = 8	-1.078	0.312
S.F. = 9	-0.820	0.436

Table 5.28: Non-Dominant Hand - Contralateral hemisphere. Results from the t test applied to SampEn values in the different scale factors.

	t	p
S.F. = 1	**-4.451**	**0.002**
S.F. = 2	**-4.943**	**0.001**
S.F. = 3	**-4.709**	**0.002**
S.F. = 4	**-5.099**	**0.001**
S.F. = 5	**-4.906**	**0.001**
S.F. = 6	**-3.735**	**0.001**
S.F. = 7	**-4.579**	**0.002**
S.F. = 8	**-3.516**	**0.008**
S.F. = 9	**-3.545**	**0.008**

Table 5.29: Non-Dominant Hand - Ipsilateral hemisphere. Results from the t test applied to SampEn values in the different scale factors.

	t	p
S.F. = 1	**-2.714**	**0.026**
S.F. = 2	**-2.308**	**0.050**
S.F. = 3	**-2.483**	**0.038**
S.F. = 4	**-2.564**	**0.033**
S.F. = 5	**-2.528**	**0.035**
S.F. = 6	**-2.454**	**0.040**
S.F. = 7	**-2.438**	**0.041**
S.F. = 8	**-2.405**	**0.043**
S.F. = 9	**-2.708**	**0.027**

5.4.3 Correlation dimension

The Grasberger-Procaccia method was applied to calculate the correlation dimension ($D2$). The delay d of the different available signals was estimated first, as the delay in which a value smaller than $\frac{1}{e}$ is found in the autocorrelation function.

Just to show the procedure, in Fig. 5.35 the autocorrelation function of one of the BFV signals included in the experiment is represented.

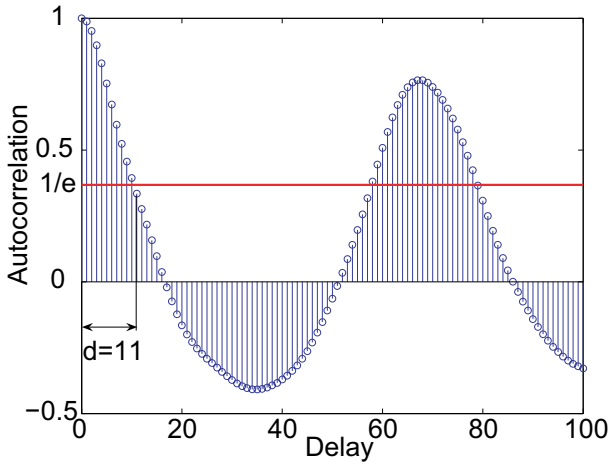

Figure 5.35: Autocorrelation of the maximum BFV signal of one of the subjects. The delay in which the autocorrelation falls below than $\frac{1}{e}$ has been marked graphically.

A delay $d = 11$ was selected for the calculus of the correlation dimension in all the signals because it was the most common value obtained with the previous procedure.

The correlation dimension has been calculated using the procedure described in the chapter 4:

- The correlation sum C is calculated for different reconstruction dimensions and different ϵ. In Fig. 5.36, the graphical representation of the correlation sum C corresponding to the BFV signal of one of

the subjects that participated in the experiment in the different reconstruction dimensions that have been tested (1-20) is represented.

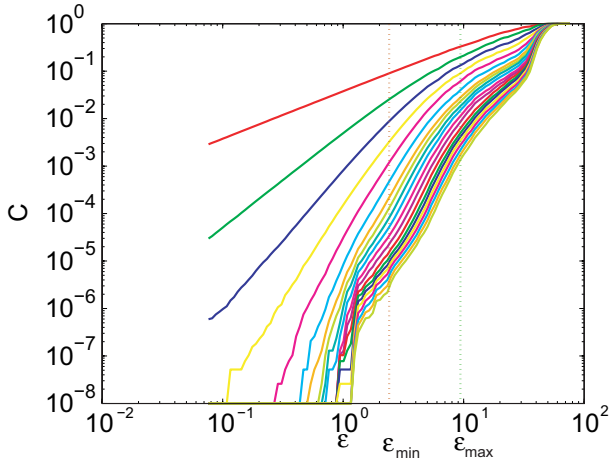

Figure 5.36: Correlation sum C in different reconstruction dimensions (1-20) corresponding to the BFV signal of one of the subjects that participated in the experiment. The values of ϵ_{min} and ϵ_{max} are represented graphically as vertical discontinuous lines.

- The values of ϵ_{min} and ϵ_{max} are fixed to the values detailed in the chapter 4. These values delimit the linear region of the C function. In Fig. 5.36 the values of ϵ_{min} and ϵ_{max} are represented graphically as vertical discontinuous lines

- The slope of the function in its linear region is calculated. This is the $D2$ value corresponding to the different reconstruction dimensions. The correlation dimension is the saturation value of $D2$ when scale grows. The $D2$ values of the BFV of one of the participants corresponding to the different reconstruction dimensions are represented graphically in Fig. 5.37.

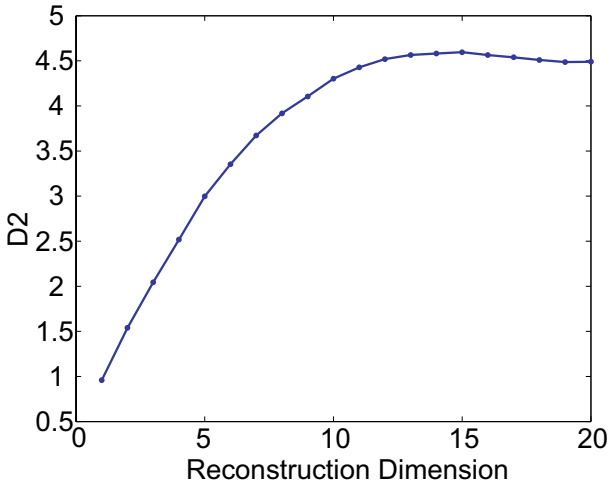

Figure 5.37: Correlation dimension $D2$ in different reconstruction dimensions (1-20) corresponding to the BFV signal of one of the subjects that participated in the experiment.

5.4.3.1 Descriptive statistics

The results for each of the BFV signals are detailed in the table 5.30.

5.4.3.2 Comparison between the different experimental conditions

A Wilcoxon signed-rank test was applied to compare between the different motor conditions (repose versus hand movements) in the different experimental conditions:

- Dominant Hand - Contralateral Hemisphere.
- Dominant Hand - Ipsilateral Hemisphere.
- Non-Dominant Hand - Contralateral Hemisphere.
- Non-Dominant Hand - Ipsilateral Hemisphere.

Table 5.30: Mean and standard error of the mean (s.e.m.) of the Correlation Dimension (calculated using the Grasberger-Procaccia method) in the different experimental conditions: (a) Dominant hand - Contralateral hemisphere. (b) Dominant hand - Ipsilateral hemisphere. (c) Non-Dominant hand - Contralateral hemisphere. (d) Non-Dominant hand - Ipsilateral hemisphere. N=9.

Condition	Repose	Hand Mov.
Dom. Hand - Contralat.	5.164 (0.386)	5.877 (0.560)
Dom. Hand - Ipsilat.	4.835 (0.221)	5.735 (0.412)
Non-Dom. Hand - Contralat.	4.931 (0.176)	5.597 (0.452)
Non-Dom. Hand - Ipsilat.	5.171 (0.316)	6.018 (0.567)

Results from the Wilcoxon test are shown in the table 5.31.

Table 5.31: Results from the Wilcoxon signed-rank test: comparison of the Correlation Dimension between the different motor conditions (repose versus hand movements). N=9.

Condition	Z	p
Dom. Hand - Contralat.	-1.718	0.086
Dom. Hand - Ipsilat.	**-2.547**	**0.011**
Non-Dom. Hand - Contralat.	**-2.073**	**0.038**
Non-Dom. Hand - Ipsilat.	**-2.310**	**0.021**

As can be observed, there are significant differences in the Correlation Dimension between the different motor conditions when the active hand is the non-dominant one (both in the left and right hemisphere) and in the ipsilateral hemisphere when the active hand is the dominant one. A close-to-significant difference is found in the contralateral hemisphere when the active hand is the contralateral one.

5.4.4 Fractal dimension using the Katz method

The Katz Method was applied to calculate the fractal dimension of the BFV waveform as indicated in the chapter 4.

5.4.4.1 Descriptive statistics

The obtained results for each of the BFV signals are detailed in the table 5.32.

Table 5.32: Mean and standard error of the mean (s.e.m.) of the Fractal Dimension (calculated using the Katz method) in the different experimental conditions: (a) Dominant hand - Contralateral hemisphere. (b) Dominant hand - Ipsilateral hemisphere. (c) Non-Dominant hand - Contralateral hemisphere. (d) Non-Dominant hand - Ipsilateral hemisphere. N=9.

Condition	Repose	Hand Mov.
Dom. Hand - Contralat.	1.00311 (0.00038)	1.00337 (0.00036)
Dom. Hand - Ipsilat.	1.00381 (0.00083)	1.00411 (0.00082)
Non-Dom. Hand - Contralat.	1.00415 (0.00082)	1.00445 (0.00084)
Non-Dom. Hand - Ipsilat.	1.00307 (0.00041)	1.00338 (0.00046)

5.4.4.2 Comparison between the different experimental conditions

To analyze the differences between repose and motor movements, t tests were performed. All the subjects available in the following experimental conditions (N=9) were included in the analysis: (1) Dominant Hand - Contralateral hemisphere; (2) Dominant Hand - Ipsilateral hemisphere; (3) Non-Dominant Hand - Contralateral hemisphere; (4) Non-Dominant Hand - Ipsilateral hemisphere.

The results of the statistical analysis are included in the table 5.33.

As can be observed, significant differences appear in the fractal dimension of the BFV waveform between the different motor conditions (repose

Table 5.33: Results from the t test: comparison between the Fractal Dimension (calculated applying the Katz method) different motor conditions (repose versus hand movements). N=9.

Condition	$t(8)$	p
Dom. Hand - Contralateral	**-3.811**	**0.005**
Dom. Hand - Ipsilateral	**-2.961**	**0.018**
Non-Dom. Hand - Contralateral	**-6.848**	**0.000**
Non-Dom. Hand - Ipsilateral	**-4.160**	**0.003**

versus hand movement).

5.4.5 Maximum Lyapunov exponent

The Maximum Lyapunov Exponent was calculated using a delay $d = 11$ and a reconstruction dimension of $m = 16$ (which is equal to the dimension in which the $D2$ saturation value was achieved for most of the subjects).

5.4.5.1 Descriptive statistics

The obtained results for each of the BFV signals are detailed in the table 5.34.

5.4.5.2 Comparison between the different experimental conditions

To analyze the differences between repose and motor movements, t tests were performed. All the subjects available in the following experimental conditions (N=9) were included in the analysis: (1) Dominant Hand - Contralateral hemisphere; (2) Dominant Hand - Ipsilateral hemisphere; (3) Non-Dominant Hand - Contralateral hemisphere; (4) Non-Dominant Hand - Ipsilateral hemisphere.

The results of the statistical analysis are included in the table 5.35.

Table 5.34: Mean and standard error of the mean (s.e.m.) of the Maximum Lyapunov Exponent in the different experimental conditions: (a) Dominant hand - Contralateral hemisphere. (b) Dominant hand - Ipsilateral hemisphere. (c) Non-Dominant hand - Contralateral hemisphere. (d) Non-Dominant hand - Ipsilateral hemisphere. N=9.

Condition	Repose	Hand Mov.
Dom. Hand - Contralat.	0.0847 (0.0088)	0.0873 (0.0061)
Dom. Hand - Ipsilat.	0.0669 (0.0140)	0.0737 (0.0151)
Non-Dom. Hand - Contralat.	0.0719 (0.0156)	0.0689 (0.0156)
Non-Dom. Hand - Ipsilat.	0.0847 (0.0102)	0.0791 (0.0086)

Table 5.35: Results from the t test: comparison between maximum Lyapunov exponent in the different motor conditions (repose versus hand movements). N=9.

Condition	$t(8)$	p
Dom. Hand - Contralateral	-0.265	0.798
Dom. Hand - Ipsilateral	-1.129	0.292
Non-Dom. Hand - Contralateral	0.878	0.406
Non-Dom. Hand - Ipsilateral	0.961	0.365

As can be observed, no significant differences appear in the Maximum Lyapunov Exponent of the BFV between the different motor conditions (repose versus hand movement).

Chapter 6

Discussion

In this chapter, the results obtained in the different studies will be analyzed. In the first section, general aspects about the studies that have been conducted and the conclusions that can be extracted from them will be commented. In the other sections of the chapter, specific aspects of each of the different studies will be discussed.

6.1 General comments

In this section, general aspects are discussed. First, the conclusions about the use of TCD in comparison with other brain imaging techniques will be detailed. Then, some aspects about the experimental designs used in the different studies that have been conducted will be analyzed.

6.1.1 Comparison of TCD with other brain imaging techniques

Although fMRI and EEG had already been used in previous studies to study presence during the exposure to VE [118, 16, 121, 126, 17, 18], in this work an alternative brain activity measurement technique (TCD) that has never been used before in conjunction with virtual environments has been proposed. TCD constitutes a complementary neuroimaging tool to measure cerebral perfusion changes due to neural activation and has been

widely used to monitor hemodynamic variations in brain activity during the performance of cognitive tasks [20].

Results from the studies included in this PhD Thesis show that:

1. TCD is a tool that can be easily integrated in VR settings, so it is possible to obtain reliable TCD signals during the exposure to VEs.

2. The use of TCD does not interfere with the capability of the subjects to focus their attention on the VE.

When compared with fMRI, TCD has important advantages. It can be used as a measure of brain activity avoiding the exposure of the user to the VE in an uncomfortable way. It is ecological, it has a lower cost and it does not impose mobility restrictions [238]. Furthermore, when compared with fMRI, TCD usually provides a higher temporal resolution that allows the continuous monitoring of fast changes in BFV values caused by neural activity. Finally, TCD does not require any special adaptation of the VR hardware that is used while brain activity is monitored.

One of the main disadvantages of TCD is its low spatial resolution, which is delimited by the size of the cortical areas supplied by the vessel under study. Velocity increases in small vessels could not generate a noticeable increase in the bigger artery, so activations of small neuron groups in areas of the brain that can be visualized with fMRI cannot be detected using TCD.

TCD and fMRI can be complementary tools to analyze brain activity during presence experiences. The reasons are the following:

- fMRI has a high spatial resolution and can provide specific information about brain areas that are activated during the exposure to a VE. However, it imposes restrictions to the VR and presence experience, because the VE has to be shown while the user is in supine position inside the fMRI unit.

- TCD can obtain less detailed information about the brain areas that are being activated, but it can be easily integrated in more immersive versions of the VE and with different kinds of interaction techniques.

The results that have been obtained with TCD analysis in this PhD Thesis are coherent with the brain activity patterns obtained in fMRI and EEG studies, as will be described later. Further research with both techniques may contribute to a deeper understanding to the neural processes that are involved in the complex experience of presence.

6.1.2 Comments about the experimental design of the different studies

6.1.2.1 Physiological measurements

Blood pressure, CO_2, respiratory rate and other physiological measurements were not controlled during the first two studies (with different immersion and navigation conditions of the same virtual environment). There are several reasons for not measuring them:

- Including these kinds of measures would have a negative influence on the ecological validity of the experiment.

- Several studies have proven that these variables do not significantly change while performing cognitive tasks in psychophysiological experiments [207, 175, 182].

In the studies about simple tasks (visual perception and motor movements), blood pressure was controlled, but just before and after the experience. As expected, no significant differences were found in the blood pressure of the participants between these two moments.

Other kinds of physiological measurements (such as ECG or skin conductance) for presence monitoring were discarded in all the studies. Although these measurements can be closely related to presence and are an object of study [98, 128, 239], some authors consider that results from these experiments are frequently unreliable [41] to reflect the subtle construct of presence. Moreover, using these measurements would result in an additional source of invasiveness for subjects. Consequently, it was decided that it was not worth including these measurements in the present studies. Presence questionnaires were used instead for validation purposes.

6.1.2.2 Position of the subjects during the experience

Subjects were seated or stood up during the experimental task depending on the study. However, this factor does not impose any restriction to the conclusions of this work. In fact, although most of the experiments using TCD have focused on simple and controlled tests with seated patients, it has recently been published that in healthy subjects with intact cerebral autoregulation the neurovascular coupling works in an independent way to adapt flow demand to the activity in the different orthostatic situations [185].

6.2 BFV analysis in different navigation conditions

Results from the study about BFV in the different navigation conditions (free navigation versus automatic navigation) in the CAVE-like configuration show that there are BFV variations in every monitored vessel when subjects are exposed to a VE. Furthermore, BFV differences depending on presence measures obtained under different navigation conditions of the same VE have been found. In the following paragraphs, different aspects related with the experiment and the obtained results will be discussed.

6.2.1 Vessel selection

The election of the vessels is of great importance during TCD studies, as long as they determine the brain area that will be analyzed. In this case, as global responses of the brain in each hemisphere could be expected, MCAs were selected, as long as these vessels supply blood to the greater part of the brain. Their perfusion territory includes subcortical areas, large fractions of the frontal and parietal lobes, as well as the temporal lobes [145]).

ACAs were also included. They supply most of the medial areas of the brain, including the medial frontal cortex and most parts of the limbic system particularly the cingulated [144], so their BFV variations are closely

related with the emotional state of the subject who is being monitored and with brain activity related to decision making.

Posterior cerebral arteries (PCAs) were not included in the experiment because it was assumed that an increase in cerebral blood flow velocity in the PCA will occur when the user is exposed to visual stimulation [148], as occurs during VE exposure.

6.2.2 Presence Questionnaires

As already explained, the SUS questionnaire [22] was used for presence measurement.

Results from questionnaires about the free and the automatic navigation periods show that users feel present while experiencing the VE, both when they navigate through it freely and when they are just passive spectators (automatic navigation). However, the level of presence that is induced during the automatic navigation is significantly lower than the level of presence that is induced during the free navigation. That is coherent with the results of previous studies about the influence of interactivity and navigation on presence [28]

6.2.3 Selected features for BFV analysis

Two different features of the mean BFV signal were calculated to compare between the different periods in this study about navigation conditions:

- Mean BFV during a complete experimental condition.
- BFV percentage variation between the mean BFV in the preceding baseline period and the mean BFV in the free / automatic navigation condition.

Mean BFV values in the different experimental conditions were used to allow the comparison between the different periods (repose versus free / automatic navigation).

On the other hand, percentage variations between baseline and activation periods were also calculated to compare the magnitude of the BFV

variation that occurs in the free navigation and in the automatic navigation conditions with respect to their previous baseline. As indicated in the chapter 4, this procedure eliminates any variability associated with changes in the insonation angle or the vessel diameter [151, 177]. In this study, it has been used to estimate the BFV change that occurs when the situation changes from repose (baseline) to activation (free / automatic navigation in a VE). This approach has also been followed in previous studies: each activation period is preceded by a baseline period, and the BFV of each activation period is estimated in comparison with the BFV of the preceding baseline [206, 207, 20]

6.2.4 Comparison of BFV between repose periods and VE exposure periods

In this point, the discussion will focus on the interpretation of the results related to mean BFV values in the different periods of the experience: baseline previous to free navigation, free navigation, baseline previous to automatic navigation and automatic navigation.

Results from this analysis show that BFV values were significantly greater during the free navigation than during the preceding baseline in three vessels: MCA-L, MCA-R and ACA-L. Mean BFV absolute values were also significantly greater during the automatic navigation than during the preceding baseline, but in this case only in two vessels: MCA-L and MCA-R.

There are several factors that can potentially explain the BFV variations observed between the baseline period and the VE exposure:

- **Complex interaction between visuospatial interaction tasks, attention tasks, and the creation and execution of a motor plan**. When users navigate or passively watch a VE, they have an active role in the experience which is the creation of a motor plan [240]. This active role does not occur during the baseline. Measures in MCAs were significantly greater during the VE exposure than during the baseline. These vessels supply mainly the lateral parts of the brain [145]. The creation of a motor plan during the VE exposure could be contributing to the increase in MCAs BFV that is

observed, in accordance with the previous results obtained in studies about navigation in videogames [176, 175].

- **Emotional state changes induced by the VE**. BFV differences may also reflect changes in the limbic system activation. The medial frontal cortex and most parts of the limbic system are supplied by anterior vessels [145]. No significant differences have been found in BFV between the baseline and the VE exposure for ACA-R. This could be due to the reduced number of subjects, which makes it difficult to observe significant differences. In the case of ACA-L, a significant increase of BFV is observed in the free navigation with respect to the preceding baseline. However, there is not a significant increase in the case of the automatic navigation condition.

  Moreover, taking into account that middle cerebral arteries also supply areas of the parietal and frontal lobe involved in the processing of emotion [146], any variation in the emotions that the user is feeling can also have an influence in the BFV in middle cerebral arteries [164, 163]. This could potentially explain the observed variations in BFV in MCA-L and MCA-R.

- **Decision taking**. Since the user is actively participating in the creation of a complex motor plan, the frontal lobe could be used to take decisions about how to respond to stimuli and this can be the origin of the BFV variations in ACA-L. There is scarce experience about ACA BFV measurements and their correlates with cerebral functions. In any case, it can be emphasized that the percentage variation observed in ACA-L in the present study was much greater than the percentage variation that had been reported in one of the videogame studies that also analyzed ACA-L measurements [175].

- **Presence variations**. It can be argued that the presence that the user is feeling during the free and automatic navigation conditions could be an additional factor that influences the observed increases. Correlations between answers to SUS Questionnaire and BFV values have been found as previously described. In this context, presence could be explained as an activity that affects several brain regions

simultaneously and that is difficult to separate from other states. Perhaps presence can be considered a high level cognitive state that is the result of an integration of, among other things, visuospatial interaction tasks, attention tasks, the creation and execution of a motor plan and emotional states.

The order of stimuli presentation to the subjects may be a factor that could be having an influence on the results. However, previous cognitive studies with TCD have not found any influence for this factor [31].

These hypotheses about the origin of BFV variations are coherent with the results of studies with fMRI. In fact, the observed increment in MCA BFV may be related with the increment of brain activity in some parts of the distributed network (which comprises extra-striate areas, the dorsal visual stream, the superior parietal cortex (SPL) and inferior parietal cortex (IPL), parts of the ventral visual stream, the premotor cortex (PMC), and the brain structures located in the basal and mesiotemporal parts of the brain) that has been associated with the presence experience in previous studies [17, 18].

6.2.5 Comparison of BFV variations in the free navigation condition and the automatic navigation condition

In this point, the discussion will focus on the interpretation of the results related to mean BFV percentage variations in the two navigation conditions: free navigation versus automatic navigation.

Results show that the only significant differences in BFV percentage variations between the free and the automatic navigation conditions occur in the case of left vessels: MCA-L and ACA-L.

The significant difference between the percentage variations in the automatic and in the free navigation conditions that is observed in MCA-L could be related to the different navigation states. Given that the user had to navigate and control a joystick in the environment (with right arm movements), the differences could have their origin in these motor tasks (as subjects are right-handed, they move the right arm to control the joystick and variations in BFV are generated in the left hemisphere) [160, 178, 158].

The percentage variation in ACA-L is highly significant ($p < 0.001$). A possible explanation of this variation may be that subjects experience a different emotional state in the free and automatic navigation conditions. However, in these conditions, the VR setting is the same and the only difference is that users can navigate in the free navigation condition, so, in principle, no differences in the emotional state are expected. Decision taking during the free navigation condition can also be the origin of the observed changes. Further analysis would be required to obtain conclusions.

An alternative explanation would rely on the level of presence. Since the user feels more present in the free navigation than in the automatic navigation condition, as supported by the presence questionnaires, a possible relationship between presence level and BFV variations could be considered.

In the case of MCA-R and ACA-R, there are no differences in BFV that can be related to different presence ratings in both situations (free and automatic navigation conditions).

6.2.6 Analysis of BFV signal when BIPs occur

This part of the study was focused on the analysis of the neurological responses (BFV in MCAs measured using TCD) of the participants in the VR experience during breaks in presence.

6.2.6.1 Responses during BIPs

The first general conclusion that has been obtained from this study is about the kind of response that can be expected in MCAs BFV during BIPs. Initial hypotheses were not made because it was not clear if brain activity would increase or decrease during a BIP. A possibility was that the BIP would generate an increase of brain activity, occasioned by the possible surprise and rise in the level of attention due to an unexpected event. Another possibility was that the BIP would generate a decrease in brain activity due to the sudden disappearance of stimuli and navigation from the VE that generated a decrease in presence.

As can be observed from the experimental data, a different evolution is observed depending on the kind of BIP. The most frequent pattern observed during the *Total BIP* is a decrease in BFV (negative maximum percentage variation). However, during the *Partial BIP*, there are oscillations inside the period without a clear decreasing or increasing trend.

Response times had a mean which ranged between 10.116 s and 12.774 s depending on the vessel and on the kind of BIP, in accordance with BFV response times observed in previous studies that analyzed other kinds of cognitive activity [31, 158, 149].

As already pointed out by Slater et al. [23], there are several factors that may be having an influence in the responses observed during a BIP. Possible factors are summarized in the following points.

- **Interruption in the cognitive tasks associated with the navigation in a VE**. During the normal navigation in a VE environment, there is a complex interaction between visuospatial interaction tasks, attention tasks, and the creation and execution of a motor plan. Users are actively participating in the creation of the motor plan, focusing their attention on this task. However, this active role is suddenly interrupted when a BIP occurs, which could justify a decrement in BFV.

- **Interruption of the hand movements to control the joystick**. During the VR experience users have to make movements with their right arms and hands to control the joystick and navigate. The interruption of hand movements during the BIPs can contribute to a decrement in MCA-L BFV. However, MCA-R BFV is not influenced by the interruption of hand movements, as no movements are made in any case with the left arm (neither during the navigation nor during the BIP).

- **Breaks in presence (BIPs)**. There are presence changes when the BIPs occur. Users are suddenly aware that they are in a laboratory participating in an experiment and not in the VE. These presence modifications can also be contributing to the changes in MCAs BFV.

All these factors can be having an influence on the observed decrease in BFV during the *Total BIP*.

The different behavior (oscillations) observed during the *Partial BIP* can have its origin in the kind of BIP (the *Partial BIP* is less traumatic than the *Total BIP*). The presence factor may be having less influence in the *Partial BIP* than in the *Total BIP* because, although subjects cannot navigate during the BIP, they can visualize in the front wall a projection of the VE, which constitutes a connection with the VR experience in which they were participating before the BIP occurred. Furthermore, as the VE is visible in the front wall of the CAVE-like system, they keep on trying to advance by pressing the front button of the Flystick. The movements with the right arm and hand to control the joystick do not completely stop. In fact, subjects may become more involved in the task of pressing the button, as long as the expected reaction (a movement in the VE) is not achieved. This greater involvement may justify that an oscillating trend (instead of a clear decrease) is observed during the *Partial BIP*.

6.2.6.2 Responses during recovery periods

The second general conclusion that has been obtained from this study is that, in general, when the interruption that causes the BIP finishes, an increase in BFV signal is observed (as a result of the return to the normal navigation and visualization conditions during the VR experience). The recovery time after a BIP has only been analyzed previously in a qualitative way using interviews [131]. In this work, a quantifiable and objective way has been proposed and implemented to analyze the behavior during the recovery period, based on the calculation of the response time and the maximum percentage variation in the BFV signal.

Maximum percentage variations were predominantly positive for all vessels and conditions. The same aspects that were discussed to explain BFV variations observed during BIPs could also be the origin of the changes in BFV that have been registered in the recovery from each BIP. When the recovery starts, the visuospatial interaction tasks begin again, and subjects recover their active role in the creation and execution of the motor plan. Furthermore, the BIP has finished, so subjects feel

present again in the VE. Finally, the hand movements recover their normal pattern during a navigation in the VE. All these aspects can justify an increment in BFV during the recovery periods.

Mean response times ranged between 11.025 s and 13.345 s depending on the vessel and recovery period studied. As happened with response times observed during the BIPs, these values are in accordance with the results of previous cognitive studies [31, 158, 149]. Although the previous study by Garau et al. [131] stated that users reported in the interviews to have experienced different recovery times depending on the kind of BIP, in the case of the present experience objective parameters obtained analyzing the BFV signal show that there is not a significant difference between both BIPs (neither in the response time nor in the percentage variation). Maybe the users can experience subjectively a different recovery time, although the response time measured from BFV is similar in all cases. Or perhaps the differences between kinds of BIP considered in this experience are not strong enough to generate different response times. Further research will help to clarify the causes.

6.3 BFV analysis in different immersive conditions

In this section, the discussion will focus on the comparison of the results from the study where the VE was visualized in the CAVE-like configuration with the results from the study where the VE was visualized in a single screen. The same VE was used, but with different levels of immersion

The first observation that can be made is that the percentage variations between baseline and VE exposure are positive in all the experimental conditions. This increment in the BFV that is observed in the different conditions in both vessels included in the study (MCA-L and MCA-R) can be explained by several factors.

- First of all, during a VE exposure there is a complex interaction between visuospatial interaction and attention tasks, and the creation and execution of a motor plan [240] that cannot be observed during the baseline.

- Besides, any variation in the user's emotions that may happen when the VR experience starts may also be having an influence in BFV measurements [164, 163], because the MCAs also supply areas of the parietal and frontal lobe involved in the processing of emotion [146].
- Finally, the presence that the user feels during the VE exposure could be an additional factor that is having an influence on the observed increase.

The second observation that can be made in this study is that there are measurable differences in SUS questionnaire responses and BFV percentage variations observed in different immersive and navigation conditions in the VE. In the following paragraphs, the effects of the different conditions, both in terms of BFV values and SUS responses, are discussed.

6.3.1 Effects of navigation

6.3.1.1 SUS questionnaires

SUS questionnaires have been used both in the free and automatic navigation conditions. Results from the analysis show that users feel present in both situations, when they navigate freely through the environment and when they are just passive spectators. However, the level of presence during the automatic navigation is significantly lower than the level of presence during the free navigation.

6.3.1.2 BFV percentage variations

Regarding MCA-R BFV percentage variations, results show a significant difference between both navigation conditions. In MCA-L, there is also a difference in the percentage variation which is close to achieving significance.

Given that the user had to navigate and control a joystick in the environment, differences observed in MCA-L could be mainly due to these motor tasks. Users that took part in the experiments were right-handed, and variations in BFV in right-handed users have been observed in the left hemisphere during motor tasks [160, 178, 158].

However, differences in MCA-R cannot be explained by this issue. A first factor that can explain them is the difference in the degree of involvement of the users in the creation of a motor plan in the free navigation and in the automatic navigation, which can generate a change in the BFV variations. In fact, the right hemisphere is more tightly related to spatial and attentional processes than the left one.

Presence is another factor which is different between the free navigation and the automatic navigation (greater scores in SUS results have been observed during the free navigation condition), so it may also be having an influence on BFV variations.

6.3.2 Effects of Immersion

6.3.2.1 SUS questionnaires

Results from the robust ANOVA applied to SUS questionnaires show a trend to a higher value of presence scores during the high immersion condition.

6.3.2.2 BFV percentage variations

Regarding MCA-L and MCA-R BFV variations, no significant differences were found between both immersive conditions. There is also only a trend to a higher variation in the case of the most immersive system. Further investigations with a higher number of users will help to clarify if this factor has a significant effect on BFV variations. In any case, there are several possible explanations for this trend, such as the higher degree of involvemement of the user in the visuospatial tasks of the VE or the higher level of presence in the CAVE-like system than in the single screen configuration.

6.3.3 Effects of navigation x immersion

6.3.3.1 SUS questionnaires

Finally, the possible influence of the interaction effect (navigation x immersion) on SUS measurements and on BFV percentage variations is going to be discussed. Taking into account results from the ANOVAs, it has to be

concluded that the level of presence (measured by SUS questionnaires) is not influenced by the interaction between navigation and immersion effects.

6.3.3.2 BFV percentage variations

The same conclusion can be achieved when analyzing BFV percentage variations in both MCA-L and MCA-R: no significant effect is found for the interaction factor.

However, in the case of MCA-R, a trend has been found for a possible influence of the interaction factor in BFV variations: the BFV percentage variation difference between free navigation and automatic navigation conditions is greater in the case of the single screen configuration than in the case of the CAVE-like configuration. It is also observed that the BFV percentage variation difference between the CAVE-like and single screen configurations is greater in the case of the automatic navigation condition than in the case of the free navigation condition.

A possible explanation can come from the features of the different experimental conditions that are being considered. In the CAVE-like configuration, the immersion is so high that the brain activity changes that occur when starting the VR experience are mainly influenced by this factor (ceiling effect). The influence of navigation may be masked by the strong effect of high immersion. On the other hand, in the single screen configuration, the immersion is not so high, so this effect is not so powerful to mask the effect of navigation. Brain activity variations may be more influenced in this case by the effect of navigation. Greater differences are observed in MCA-R BFV variations between navigation conditions in the single screen configuration.

Analogously, focusing on navigation aspects, in the free navigation condition, the user actively controls the navigation. This may also have a strong influence on BFV responses, and may mask the effect of the immersion factor.

Visuospatial and attention tasks (that can require more user involvement in the CAVE-like configuration and in the free navigation condition) may be the origin of the BFV percentage variations that are observed in these experimental conditions. Presence (that is also higher in the case of

the CAVE-like configuration and in the free navigation) may be another factor that is influencing this BFV percentage variation.

Both immersion and navigation are factors that have been studied as causes of presence [25, 27, 26, 28]. The observed trend may show that environments with high immersion or a self-controlled navigation can mask the influence of other factors.

6.3.4 Global comments about immersion and navigation

The significant differences between MCA-R percentage variations in the different navigation conditions did not appear in the first study with just the data obtained in the CAVE-like configuration. This is a factor that has to be further analyzed. In any case, it can be observed that differences between navigation conditions are higher in the case of the single screen than in the CAVE-like configuration, and this may be the origin of the significant differences that appear between navigation conditions when including also the data from the single screen configuration.

Perhaps in the CAVE-like environment the immersion is so high that brain activity changes that occur are mainly caused by the fact of visualizing the VE inside a CAVE-like configuration, and other aspects such as navigation do not have a big influence on MCA-R BFV. However, as in the single-screen condition the immersion is not so high, maybe the effect of navigation is not masked and higher differences in MCA-R BFV percentage variations between navigation conditions are observed.

6.4 BFV analysis during a visual perception task

6.4.1 General comments

The analyses of the previous studies have two limitations:

- Firstly, although TCD has a high temporal resolution, the temporal variations inside the different experimental conditions were not analyzed: mean BFV values for each whole period were considered for the analysis.

- Secondly, there are several aspects that change between baseline and the exposure to the VE including visual perception, motor tasks, attention, emotions and presence, which complicates the interpretation of the BFV variations that are observed.

In order to improve the analysis of BFV signals during VR experiences, simpler experiments have to be proposed to analyze the individual variables that contribute to the VR experience. Furthermore, the kind of analysis that is applied to the BFV signal should be modified to study also the temporal evolution of the signal. This has been taken into account in this present study where BFV responses to one of the main issues that contributes to the VR experience (visual perception) have been analyzed. The maximum BFV signal has been studied, without any averaging prior to the analysis. The high temporal resolution of the TCD technique can provide information on the rapid adjustment of the brain to a higher state of activity [31]. Furthermore, the signal processing techniques proposed for the analysis represent a new way of studying the effects of cognitive stimuli on TCD functional studies, in a more precise way.

6.4.2 Vessel selection

PCAs were included in this experiment. These vessels are the responsible for the irrigation of the primary visual cortex as well as the lateral geniculate body and some of the visual association regions in the occipital cortex [29], so they are useful to analyze brain activity related with visual stimuli.

6.4.3 BFV features analysis

Visual stimulation of the occipital cortex results in an increased BFV in the PCA. Results of the present work are in accordance with previous studies with visual stimuli (i.e., [29]). Mean BFV are significantly different between repose and activation periods (higher mean BFV values are obtained in the presence of visual stimuli).

The two-channel recording has allowed direct comparison of different vessels, in this case, PCA-L versus PCA-R. However, no significant differences have been found between vessels in response to the simple visual

stimuli presented in the experiment.

One of the main contributions of this study has been the analysis of the low-frequency band of the spectrum of the BFV signal during a functional study. Different frequency bands had been described in the BFV spectrum [189], which can be associated with different temporal fluctuations in the BFV signal. As described in chapter 3, the very low-frequency band (from 0.016 to 0.04 Hz) is associated with B-waves of intracranial pressure and the high frequency band (from 0.15 to 0.4 Hz) is correlated with respiration rate. These frequency bands have not been included in the analysis as long as the low frequency region (from 0.04 to 0.15 Hz) is the band that can be associated with the slow variations that are observed in BFV signals after the onset of a mental task.

Once the low-frequency band has been analyzed, the component of the BFV signal at the peak frequency present in this band has been calculated both for repose periods and activation periods. BFV low-frequency variations have their origin in the presentation of visual stimulation in activation periods, and in the disappearance of any visual stimulation in repose periods. The component of the signal at the peak frequency constitutes a reliable way to estimate the influence that the visual stimuli are having on the BFV variations, isolating them from the variations caused by other factors.

Usually, at the beginning of the activation phases, the velocity quickly rises to a maximum that is achieved after a few seconds. Two parameters of this increase have been considered to analyze the subject response:

- The time when this variation achieves a maximum value (response time).
- An estimation of the degree of variation (percentage variation in BFV between the initial value and the maximum value).

On the other hand, in the repose periods, the velocity decreases to a minimum value that is also achieved after a few seconds. In this case, the absence of stimuli (after an activation period) is the origin of this response. The time when the minimum value is achieved can be considered the response time for repose periods, and the percentage variation can be calculated between the initial value and this minimum value.

With the proposed methodology, the percentage variation and response time can be obtained automatically using the low-frequency estimation of the BFV signal at the peak frequency that appears in the low-frequency band of the BFV spectrum.

These parameters (response time and percentage variation) have a great importance in the BFV analysis during functional studies. The response time can be considered an indicator of the activation time required for the subject to respond to the stimulus, that is, a way to characterize the temporal response of each subject. Therefore, this feature can be used, in combination with other parameters such as the maximum percentage variation, to differentiate between groups of subjects with different characteristics that give different response times and percentage variations to the same stimuli. In a previous study, Orlandi and Murri [158] found a stronger increase of BFV in younger participants in a motor task with simple hand movements. Moreover, in older people, the maximum reaction amplitude was reached later. The authors suggested a slower arteriolar vasomotor reactivity in response to cerebral activation in elderly subjects resulting from an increased resistance in the small vessels. These parameters of maximum reaction amplitude and reaction time can be obtained in an automated and precise way using the low-frequency estimation method proposed here. These values can be helpful to characterize the velocity of the arteriolar vasomotor reactivity in subjects in response to cognitive tasks. Although in the previous study [158] a different methodology was followed, these parameters were also estimated and this helped them to make classifications between younger and older people groups. In other applications, these parameters can be useful to differentiate between groups of people, as long as they can constitute a footprint of the individual arteriolar vasomotor reactivity to cognitive tasks.

6.4.4 Final comments

This study is a contribution to the global research performed in this PhD Thesis about the possibilities of TCD to monitor brain activity in VR settings. One of the aspects that is common to all VR configurations is the presence of visual stimuli of different complexity that are shown to the

participant using different techniques. In this work, the visual stimulation was provided as a projection in a big screen, as occurs in many VR settings. That way, the variations in PCAs maximum BFV that are generated by a simple visual stimulation in this VR setting have been analyzed. In future studies using TCD, the contribution of the visual stimuli factor to the observed BFV variations during a VR experience can be estimated from the results of the developed work. This is a first step in the analysis of the different factors that are needed to generate a complete VR experience. The separate influence of each of the factors has to be analyzed to achieve a better understanding of the BFV variations that occur during VR experiences.

6.5 BFV analysis during motor tasks

6.5.1 General comments

Continuing with the analysis of the individual factors that contribute to the VR experience, this study has focused on the analysis of the motor tasks that are required to control a navigation device in the VE. Specifically, the BFV variations in response to hand movements to control a joystick have been analyzed.

As in the previous study, the maximum BFV signal has been registered and analyzed, without any averaging prior to the analysis. In this case, a new kind of analysis has been applied to the BFV signal. Non-linear characteristics of the signal in the different periods have been calculated to study if there are differences in these non-linear features in periods with different motor activity (repose versus hand movements).

6.5.2 Vessel selection

MCAs were included in this experiment. As already explained, they are arteries that supply blood to the greater part of the brain. Each MCA carries 80% of the blood flow within its cerebral hemisphere [144]. Their perfusion territory includes subcortical areas, large fractions of the frontal and parietal lobes, as well as the temporal lobes [145], so modifications in

MCAs BFV can be produced by different kinds of brain activity, including motor tasks such as the hand movements to control the joystick that are analyzed in the present study.

6.5.3 Non-linearity of the Doppler BFV signal

Before applying any non-linear technique to analyze a physiological signal, it is fundamental to check the existence of non-linear features in the signal [241]. Although any physiological signal may have a complex appearance and it can be supposed that it is generated by non-linear dynamics, the simplest explanation for any irregularity would be that it is just noise. So the existence of non-linearity has to be analyzed before applying a non-linear analysis.

The *surrogate data* analysis is one of the procedures that is commonly used in the analysis of non-linearity [213, 215]. In the case of the maximum BFV signal, as explained in the chapter 3, the non-linearity has already been studied in previous works using this methodology [38].

However, to reinforce the non-linear analysis of the maximum BFV signal that has been performed in this work, an analysis of surrogates has been made. The SampEn of the surrogate series were always higher than the original maximum BFV signals, in all the subjects and in all the conditions. These results indicate that the maximum BFV signal has non-linear properties, so it is adequate to analyze it using non-linear methods and calculating parameters such as their entropy in the different periods of analysis.

It is important to point out that the output of a system (in this study, the maximum BFV signal) must not be confused with the system itself (in this case, the brain and nervous system). Although one output of the system presents non-linearity, that is not a definitive prove of deterministic chaos in the system [214].

6.5.4 Selection of non-linear features for the analysis

The methods to calculate non-linear parameters of a signal are in many cases highly subjective. In fact, experts of non-linear analysis recommend

precaution when using measures of low-dimensional chaos to analyze physiological signals [241, 242, 243]. They indicate that biological systems are probably much more complex (that is, they have a greater dimensionality) than mathematical systems.

Measures such as SampEn (and its associated measure of entropy in multiple scales: MSE) have been selected in this study about biological signals following approaches of previous studies [219, 244, 245]. The main advantages of SampEn for the analysis of biological signals are that [221]:

- It is highly independent of the length of the measured signal.
- It is consistent with situations where other methods such as ApEn are not.

Apart from this method, other non-linear features have been estimated using other techniques, to analyze if the observed behavior in MSE is similar in other non-linear indexes. The Grasberger-Procaccia method [232] has been used to estimate the correlation dimension in the phase space. This method is highly subjective, and important differences can be found if different researchers estimate the correlation dimension applying the procedure. However, it has been applied because it is a classic method in the analysis of non-linearity, and other previous studies with TCD have applied this kind of analysis [36, 37]. Its results will be used to complement the analysis obtained with the MSE method.

The Lyapunov exponent has also been calculated, as in previous studies with TCD [37]. It is also a classic method in the analysis of non-linearity which focuses on a different concept to the correlation dimension. The exponent is used as a measure of the velocity with which infinitesimally separated trajectories diverge.

Finally, the Katz method [234] has been used to estimate the fractal dimension of the BFV waveform. It is a method based on a concept different from the previous approaches, as long as it does not calculate the fractal dimension of the attractor in the phase space. It calculates the fractal dimension of the waveform corresponding to the time series. It has been selected because it has been applied in previous studies about motor tasks [246] (although analyzing a different biological signal: EEG)

and because its application is more objective than other classic methods such as the Grasberger-Procaccia to calculate the correlation dimension. Furthermore, it is considered the most effective method to capture the dynamical changes in fractal dimension of waveform-like data and is relatively insensitive to noise [247].

6.5.5 Discussion about MSE results

The MSE graphs that have been shown in the chapter 5 show that the entropy measures grow in low temporal scales and then they stabilize in a constant value. These results are coherent with the observed in the study by Costa et al. [223] about the entropy measures with temporal series from healthy volunteers.

In all the cases, the MSE value is higher in the hand movement condition than in the repose condition. Statistical analysis of the results show that there are significant differences in MSE values between the repose period and the hand movement period in some of the experimental conditions. Specifically, there are significant differences in the following situations:

- In the contralateral vessel, when the hand movements are performed with the dominant hand (and only for scale factors from 1 to 4).
- Both in the ipsilateral and contralateral vessels, when the hand movements are performed with the non-dominant hand (and for all the analyzed scale factors: from 1 to 9).

Before discussing these data, it has to be remembered that the results are preliminary. The study has to be completed with a greater number of subjects to validate the results and discard any influence of factors such as the order of presentation of the experimental tasks. In any case, the obtained results are really interesting and promising. The implications of these data are going to be discussed in the following paragraphs.

The fluctuations of the complexity in a signal are the expression of multiple interactions between the components of a dynamical system. These interactions introduce multiple temporal scales and related structures of fluctuation. The higher value of MSE during motor activity is associated with a higher complexity and structural richness of the BFV signal. It is

a way to quantify the "irregularity" of the signal in different scales and to estimate the quantity of information required to predict future states of the system. If the entropy grows, fluctuations are more irregular, and the system is less predictable.

Although there have been previous studies using TCD monitoring during the performance of motor tasks (i.e., [161, 162]), these studies did not apply an analysis of non-linearity to the BFV signal registered during the experiments. This is the first study to analyze the non-linearity of TCD signals during the performance of motor tasks. Our initial hypothesis was that an increment in BFV entropy would be found in the hand movement condition when compared with the repose condition. This initial hypothesis was supported by analysis about motor tasks in which complexity measures of other signals such as the EEG were analyzed. For example, Liu et al. [246] calculated the fractal dimension of the EEG signal during a handgrip task with difference degrees of force. The EEG signals were taken in the five cortical areas related to motor tasks. Results showed that the fractal dimension was incremented linearly with the force during the hand movement and the subjection periods. In another study, Soe et al. [248] analyzed the EEG of 3 subjects while they performed motor movements (real and imaginary ones) which were compared with repose states. Parameters such as the correlation dimension and Lyapunov exponents were calculated. The fractal dimension obtained was greater in movement conditions than in baseline. However, not all the studies about changes in the complexity of the EEG between the baseline and the performance of a task have found changes in the same direction [249], so more studies about this issue should be performed to have more reliable information about the expected direction of complexity variations during cognitive tasks.

Vaillancourt and Newell [250] propose that there are three factors that may have an influence in the direction of the changes of the complexity of a system:

- The dimension and nature of the intrinsical dynamic of the system.

- The nature of the required change (with respect to the intrinsical dynamic) to perform a task or to answer to an environmental demand.

- The changes in the intrinsical dynamic that may occur in short and long time scales (age, disease).

They understand the intrinsical dynamic as the natural behavior of a physiological or behavioral system working in an environment with no specific demands or tasks. For example, in the case of the heart rate, the system operates around a stationary state corresponding to a fixed-point attractor (dimension 0). The output of the system fluctuates around this value. Other possibility is that the intrinsical dynamic is associated to a limit-cycle attractor (dimension 1), which occurs, for example, with the movement of a leg while the subject is walking. When due to a task or to a external demand the system leaves the intrinsical dynamic, there is a change in complexity with the objective of achieving an optimum performance / working.

The changes in the entropy of the BFV signal during the performance of hand movements to control the joystick can be analyzed from the perspective of Vaillancourt and Newell [250]. While there are no movements (hand in repose) the brain and nervous system are in their intrinsical state (at least, in the activity related hand movement tasks). When the participant starts to move the hand, there is a increase of complexity to adapt the system to the new task that has to be performed and to achieve an optimum performance.

It is important to point out that MSE differences when the dominant hand is moved can only be observed in the contralateral hemisphere to the active hand and with low scales. Although in the ipsilateral hemisphere a trend to an increment in the MSE value is observed, the differences are not statistically significant.

On the other hand, when the movement is performed with the non-dominant hand, the significant increment in MSE is observed in all the analyzed scales, and both in the contralateral and ipsilateral hemispheres.

Probably, the justification of the behavior is that, when the movement is performed with the non-dominant hand, more processes in the brain are activated, and this generates a greater and clear increment of complexity in both hemispheres when the non-dominant hand is moved.

6.5.6 Discussion about other non-linear measures

6.5.6.1 Correlation dimension

In the case of the correlation dimension, greater values are also observed during the hand movement condition than during the repose condition. In this case, significant differences are found:

- In the ipsilateral hemisphere, when movements are performed with the dominant hand.
- Both in the ipsilateral and contralateral hemisphere, when movements are performed with the non-dominant hand.

The results are preliminary, but, even then, they are coherent with the results obtained with the MSE method, that show a greater complexity in the BFV signal when the participant is performing a hand movement task when compared with repose.

In this case, significant differences appear only in the ipsilateral hemisphere when the movements are performed with the dominant hand. As the MSE and the Correlation Dimension measure different aspects of the non-linearity of the signal (the correlation dimension is a calculus of the fractal dimension of the attractor of the signal in the phase state), this result is compatible with the results from the MSE analysis.

6.5.6.2 Fractal dimension using Katz method

In this case, significant differences between repose and hand movement were found in all the experimental conditions (in both hemispheres, and with both hands). The fractal dimension was greater in the hand movement condition when compared with the repose condition.

As it has been stated previously, the fractal dimension is an estimation of the BFV signal complexity from a different perspective (it is calculated directly from the temporal waveform, and it does not require any transformation to the state space). These results are coherent and complementary to the results about MSE and correlation dimension described in the previous points.

6.5.6.3 Maximum Lyapunov Exponent

All the Maximum Lyapunov Exponents were positive. This is a necessary condition for the existence of deterministic chaos [195], so this analysis reinforces the previous analysis with surrogates.

No significant differences were found between the maximum Lyapunov exponents in the different experimental conditions.

6.5.7 Final comments

This study has analyzed another aspect of the VR experience: the motor tasks required to control the navigation inside the VE. Interactive VR requires that participants use a device to control the navigation (in this case, a joystick has been selected) and the hand movements made to control the device are the origin of changes in BFV. The contribution of hand movements to changes in entropy and other non-linear features has been analyzed, observing a greater entropy and complexity in conditions associated with hand movements.

In future studies using TCD, the contribution of hand movements to changes in entropy can be estimated from the results of the developed work. This study is another contribution to the individual analysis of the different factors that constitute a complete VR experience, necessary to achieve a better understanding of the BFV variations that can be monitored during the exposure to a VE.

Chapter 7

Conclusions

7.1 Contributions of the present PhD Thesis

This PhD Thesis is an important contribution to the field of objective measures in presence research, specifically, to the neurological measures. In fact, the use of neurological techniques to study presence has only been proposed recently [15] and the first works applying fMRI and EEG to study the neural correlates of presence have been published during the development of this PhD Thesis [16, 17, 18]. This is the first work to apply TCD to analyze brain correlates of presence in VE.

TCD was a technique that had never been used in conjunction with VE. However, during the different experiences that have been developed, it was shown that TCD can be easily used to monitor blood flow velocity changes secondary to brain activity during the exposure to VEs.

TCD has been applied in the described experiences to monitor BFV in different immersive and navigation configurations, during breaks in presence and during the performance of single tasks (such as visual perception and motor movements to control navigation devices) that constitute part of the VR experience.

The main advantage of TCD is that it provides a high temporal resolution that allows the monitoring of fast changes in BFV values caused by neural activity. The use of TCD may help researchers to have reliable information about the brain activity of the subjects and correlate its changes

with specific events and states in the VR session. Presence is one of the factors that can be having an influence on the observed patterns of brain activity.

Another important contribution of the present PhD Thesis relies on the signal processing techniques that have been applied to analyze the BFV signal, so more information can be obtained from this high temporal resolution signal. A methodology to obtain a low-frequency estimation of the maximum BFV signal has been proposed and applied, in order to isolate BFV variations that have their origin in the performance of cognitive tasks from other sources of variation. That way, parameters such as the percentage variation and the response time of the BFV signal have been obtained in a more reliable way. On the other hand, a non-linear analysis of the BFV signal has been conducted in the study about motor tasks. This kind of analysis constitutes a new approach to the study of BFV variations in periods corresponding to different kinds of activity (in the case of the study, repose vs. motor tasks). The results of this study open new possibilities for the analysis of the BFV signal during the performance of other simple or complex cognitive tasks.

Two research fields where the results of the present PhD Thesis can be applied are clinical therapy and augmented cognition. In the following paragraphs, the possible applications are summarized.

7.1.1 Virtual Therapy

Clinical Therapy is one of the most challenging applications of VR. During the exposure to VE in clinical therapy sessions, it is interesting to monitor as many information from the patient as possible. Some information can be collected using questionnaires that analyze different factors of the VR experience, such as presence, immersion or emotions [7, 22, 251]. However, the use of questionnaires to measure the different variables has limitations, such as the impossibility to have data about the temporal evolution of the patient during the session. In order to avoid this limitation of questionnaires, some studies have proposed the use of short questions which were included in the VE during the VR experience to collect information about the level of anxiety [252]. Some proposals for presence continuous moni-

toring were also described in chapter 2. These approaches can be useful to have information directly related with specific events. However, they can hardly interfere with the VR experience itself. That is why in many cases physiological measurements, such as ECG or skin conductance [253], and neurological measurements such as EEG [254] have been proposed as tools to monitor the evolution of the patient during the exposure to VE in clinical therapy applications.

Based on the results of the present PhD Thesis, TCD could be another brain activity measure that could be easily integrated in the VR settings that are used in clinical therapy sessions, and could be useful to monitor BFV variations related to changes in presence or in the emotional state during the exposure of patients to the VE used for therapy. The use of TCD may help therapists to have reliable information about the brain activity of their patients and correlate its changes with specific events in the VR session. Previous studies that have analyzed BFV to monitor emotions [163, 166] could be the basis of this kind of applications.

7.1.2 Augmented Cognition

The AugCog field has already been described in the chapter 3. In AugCog applications, the system has to detect the instantaneous cognitive state of the user, and adapt the computational interface depending on this state. VR can be used in AugCog systems because it provides users with a controlled environment where different abilities and exercises can be trained.

The logical evolution in this kind of systems is that the user's cognitive state can be predicted automatically by the system. Sensors are used to acquire "physiological and behavioral parameter(s) that can be reliably associated with specific cognitive states, which can be measured in real-time while an individual or team of individuals is engaged with a system" [255]. Different measurements have been proposed to be related with specific cognitive states of the users [256]. Some of them are based on physiological measurements, such as electrocardiography [257] and skin conductance [258]. Other techniques such as behavioral analyses, speech and facial expression [259, 260, 261] have also been used to obtain information about the cognitive state of users. Neurological measures have also

been used because they provide a more direct analysis of the cognitive state [262, 263]. As described in chapter 3, TCD has been used in studies closely related with the AugCog field and vigilance tasks [169, 170, 172, 173, 174].

One of the conclusions of the present PhD Thesis is that TCD can be used as a cognitive state sensor in AugCog systems in which VR settings are used to train different abilities and exercises, including memory tasks, attention tasks, motor skills training. VR can provide the virtual laboratory in which all these tasks can be performed and analyzed, and TCD would be the tool to analyze brain activity during task performance to detect changes in cognitive load, underloads and overloads. TCD information would be valuable for the AugCog system to adopt the adequate mitigation strategies and to allocate tasks in an adaptive way.

7.2 Publications

The results and conclusions from the different studies included in this PhD Thesis have been partially published in papers included scientific journals and presented in scientific conferences. The different publications will be listed in the following points.

7.2.1 Publications in journals included in the JCR Science Edition

- Mariano Alcañiz, Beatriz Rey, José Tembl, Vera Parkhutik (2009). A Neuroscience Approach to Virtual Reality Experience Using Transcranial Doppler Monitoring. *Presence: Teleoperators and Virtual Environments*, 18(2): 97-111.

  DOI: 10.1162/pres.18.2.97

  In this work, results from the study about different navigation conditions were described and discussed. The impact factor of the journal in 2009 was 1.241, and it was located in the second quartile of the Computer Science - Cybernetics category (9/19) and Computer Science - Software Engineering category (46/93).

- Beatriz Rey, Valery Naranjo, Vera Parkhutik, José Tembl, Mariano Alcañiz (2010). A New Visually Evoked Cerebral Blood Flow Response Analysis Using a Low-Frequency Estimation. *Ultrasound in Medicine and Biology*, 36(3), 383-391.

  DOI: 10.1016/j.ultrasmedbio.2009.11.001

  In this work, results from the study about BFV during a visual perception task were presented and discussed. The journal had an impact factor of 2.021 in the list of 2009 (which was the last available data in the moment of writing this document). It was located in the first quartile of the Acoustics category (4/28) and in the second quartile of the category Radiology, Nuclear Medicine & Medical Imaging category (46/104).

7.2.2 Publications in other journals

- Beatriz Rey, Mariano Alcañiz, José Tembl, Vera Parkhutik (2010). Brain activity and presence: a preliminary study in different immersive conditions using transcranial Doppler monitoring. *Virtual Reality*, 14(1), 55-65.

  DOI: 10.1007/s10055-009-0141-2

  In this work, results from the study about BFV during different immersive conditions were described. It was published as an invitation after presenting a preliminary version of this work in the conference Presence 2008, that will be listed below in the section about communications in conferences.

- Beatriz Rey, Mariano Alcañiz, José Tembl, Vera Parkhutik (2009). Transcranial Doppler Monitoring in Presence Research. *CyberTherapy & Rehabilitation Magazine*, 2, 21-22.

  This work summarizes the possibilities of Transcranial Doppler Monitoring in Presence Research, based on the conclusions from the studies about BFV in different navigation and immersive conditions.

7.2.3 Book chapters - Conference proceedings

- Beatriz Rey, Mariano Alcañiz, José Tembl, Vera Parkhutik (2008). Brain Activity and Presence: a Preliminary Study in Different Immersive Conditions Using Transcranial Doppler Monitoring. *Presence 2008. Proceedings of the 11th International Workshop on Presence*, pp. 209-218.

  This work was presented as an oral communication in the conference *Presence 2008*, in Padova (Italy), 16-18th October 2008. It is a preliminary version of the work published in the journal *Virtual Reality*.

- Beatriz Rey, Vera Parkhutik, Mariano Alcañiz, José Tembl, Valery Naranjo (2009). Transcranial Doppler: a Non-Invasive Tool for Monitoring Brain Activity in Virtual Reality Therapy. *Studies in Health Technology and Informatics* 144, pp. 133-137.

  DOI: 10.3233/978-1-60750-017-9-133

  This work was presented as an oral communication in the *CyberTherapy and CyberPsychology 2009* conference, held in Verbania (Italy), 21st -23rd June 2009. It proposed, based on the evidence of the studies combining VR and TCD, that this ultrasound technique can be a useful tool for monitoring brain activity in VR therapy.

  The conference abstract is available online: Beatriz Rey, Vera Parkhutik, Mariano Alcañiz, Jose Tembl and Valery Naranjo (2009). Transcranial Doppler: a Non-Invasive Tool for Monitoring Brain Activity in Virtual Reality Therapy. Frontiers in Neuroengineering. Conference Abstract: Annual CyberTherapy and CyberPsychology 2009 conference.

  DOI: 10.3389/conf.neuro.14.2009.06.083

- Beatriz Rey, Mariano Alcañiz, Valery Naranjo, Jose Tembl and Vera Parkhutik (2009). Transcranial Doppler: A Tool for Augmented Cognition in Virtual Environments. *Lecture Notes in Computer Science* 5638, pp. 427-436.

DOI: 10.1007/978-3-642-02812-0_51

This work was presented as an oral communication in the *HCI International 2009* Conference, held in San Diego (EEUU), 19-24th July. Augmented Cognition systems assess the cognitive state of individuals while they are engaged with a system, using different kind of sensors that can be associated with specific cognitive states. In this work, it was proposed the use of TCD as a tool to measure brain activity during the exposure to VE in the Augmented Cognition field.

7.2.4 Other conferences

- Beatriz Rey, Mariano Alcañiz, Vera Parkhutik, José Tembl (2010). Comparison of Transcranial Doppler with other Techniques to Monitor Brain Activity during the Exposure to Virtual Environments. *RAVE 2010 Workshop.* Held in Barcelona, 3rd March 2010.

  This work's goal was to compare the results obtained in the studies about BFV variations during VR experiences using TCD with the results about brain activity obtained by other authors applying other techniques such as fMRI. New interpretations about TCD results were discussed based on this comparison.

- Beatriz Rey, Mariano Alcañiz, Valery Naranjo, Vera Parkhutik, José Tembl (2010). Analysis of Visual Perception Aspects of the Virtual Reality Experience with Transcranial Doppler Monitoring. Conference Abstract: Annual CyberTherapy and CyberPsychology 2010 conference. Held in Seoul, Korea (13-15th June 2010).

  This work was presented as an oral communication. This paper points out the importance of separately analyzing the different factors that can have a influence on BFV variations during a VR experience. The results from the visual perception study are summarized and their contribution to the analysis of BFV variations during a VR experience are discussed.

7.3 Future work

Results from the BIPs analysis and from non-linear analysis of the BFV signal obtained during the performance of the simple motor task (hand movements to control the joystick) are in the process of publication in scientific journals.

Furthermore, several future works can be planned from the results of the present PhD Thesis. In the following points, some of the aspects that may be analyzed in these future studies are summarized:

- **BFV monitoring during emotional induction**. The use of VE to induce emotional states has been shown in previous studies [61]. In fact, there are some studies that have analyzed BFV changes during emotional induction [163, 166] without VR. Future studies can be made where VR will be used to induce emotional states in the subjects, while their brain activity is monitored using TCD.

- **BIPs analysis**. In future studies, the effects that other kinds of BIPs have on BFV can be analyzed, so a deeper understanding can be achieved about the nature of the BFV variations that are observed after different kinds of BIPs and about the factors that could be having an influence on these variations.

- **Comparison of groups of subjects depending on their response time and BFV percentage variations**. These parameters can be easily and reliably obtained applying the low-frequency estimation that has been proposed in the study about simple visual perception. VE specifically designed to generate a response in users can be used and applied to different groups of people. For example, let us take a VE designed to generate an anxiety response in spider phobia patients. The BFV response generated by the appearance of a spider in the VE will probably be different in a group of spider phobia patients, and in a control group. Temporal and magnitude differences between groups can be calculated obtaining the response time and the BFV percentage variation from the low-frequency estimation.

- **Non-linear analysis of the maximum BFV signal captured during the performance of other kinds of cognitive tasks**. The final study included in this PhD Thesis has analyzed changes in non-linear parameters of the BFV signal in different moments of the experiments related to different tasks (repose versus hand movements). It would be interesting to design new experiments where other simple tasks are performed, and a non-linear analysis of the BFV signal is performed. Results from the BFV signal obtained during motor tasks are promising, and open new kinds of analyses that are possible to study the BFV signal obtained during the performance of different kinds of cognitive tasks. Differences between different groups of people may also be detected using these parameters.

- **Studies that compare fMRI results with TCD results**. TCD and fMRI can be complementary tools to analyze brain activity during presence experiences. fMRI has a high spatial resolution and can provide specific information about brain areas that are activated during the exposure to a VE. However, it is imposes restrictions to the VR experience, because the VE has to be shown while the user is in supine position inside the fMRI unit. TCD can obtain less detailed information about the brain areas that are being activated, but it can be easily integrated in more immersive versions of the VE and with different kinds of interaction techniques. Further research with both techniques may contribute to a deeper understanding of the neural processes that are involved in the complex experience of presence. The studies in this line can include the presentation of the same VE to subjects whose brain activity is monitored using TCD and to subjects whose brain activity is monitored using fMRI. The increments in BFV that are observed using TCD would be occasioned by the increment of brain activity in the brain areas that are shown by fMRI results, so results from both techniques can be combined.

- **New presence studies that apply the proposed processing techniques to the BFV signals**. Both the linear and non-linear processing techniques that have been applied to analyze BFV signals

captured during the performance of simple tasks, can also be applied to maximum BFV signals captured during the exposure to VE. The results obtained during the VE exposure should be carefully analyzed and interpreted based on the results obtained during the performance of simple tasks.

Appendix A

List of acronyms

The equivalence of the acronyms and abbreviations that have been used in the text are detailed below:

ACA: Anterior Cerebral Artery
ACA-L: Left Anterior Cerebral Artery
ACA-R: Right Posterior Cerebral Artery
A.H.: Active Hand
ApEn: Approximate Entropy
AugCog: Augmented Cognition
BFV: Blood Flow Velocity
B.H.: Brain Hemisphere
BIP: Break in Presence
BOLD: Blood Oxygen Level Dependend
CAVE: Cave Automatic Virtual Environment
C: Correlation Sum
CBF: Cerebral Blood Flow
CRT: Cathode Ray Tube
CWD: Continuous Wave Doppler
D2: Correlation Dimension
ECG / EKG: ElectroCardioGram
EEG: ElectroEncephaloGram
EP: Evoked Potential
fMRI: funtional Magnetic Resonance Imaging

FIR: Finite Impulse Response
FOV: Field Of View
HF: High Frequency
HMD: Head Mounted Display
HRV: Heart Rate Variability
ITC-SOPI: ITC Sense of Presence Inventory
LF: Low Freqency
MCA: Middle Cerebral Artery
MCA-L: Left Middle Cerebral Artery
MCA-R: Right Middle Cerebral Artery
M.M.: Motor movements
MSE: MultiScale Entropy
PCA: Posterior Cerebral Artery
PCA-L: Left Posterior Cerebral Artery
PCA-R: Right Posterior Cerebral Artery
PQ: Presence Questionnaire
PWD: Pulsed Wave Doppler
PRF: Pulse Repetition Frequency
PRJQ: Presence and Reality Judgement Questionnaire
rCBF: regional Cerebral Blood Flow
RSA: Respiratory Sinus Arrhythmia
SampEn: Sample Entropy
SD: Standard Deviation
S.F.: Scale Factor
s.e.m.: Standard Error of the Mean
SEMG: Surface ElectroMyoGraphy
TCD: TransCranial Doppler
VAS: Visual Analogue Scale
VE: Virtual Environment
VLF: Very Low Frequency
VR: Virtual Reality
WOSA: Weighted Overlapped Segment Averaging

Appendix B

SUS Questionnaires

In the following paragraphs, the SUS questionnaire that has been used for the experiments is shown. It is the original SUS questionnaire [22], but adapted to the contents of the virtual environment that has been used during the experiments. A final open question was also added to obtain qualitative information from the users.

Now we are going to make you a series of questions. The goal is to know up to what point you have considered that the things that you have visualized are real or not, and to know up to what point you have felt that "you were there", in that situation. We want to know if the experience has been similar to watching an image, a movie, or it has been the reality that you were living.

1. Please, rate your sense of being in the maze, on the following scale from 1 to 7, where 7 represent your normal experience of being in a place.

I had a sense of "being there" in the maze:

1. Not at all ..... 7. Very much

2. To what extent were there times during the experience when the maze was the reality for you?

There were times during the experience when the maze was the reality for me...

1. At no time ... 7. Almost all the time

3. When you think back about your experience, do you think of the maze more as images that you saw, or more as somewhere that you visited?

The maze seems to me to be more like...

1. Images that I saw ... 7. Somewhere that I visited

4. During the time of the experience, which was strongest on the whole, your sense of being in the maze, or of being elsewhere?

I had a stronger sense of...

1. Being elsewhere ... 7. Being in the maze

5. Consider your memory of being in "the maze". How similar in terms of the structure of the memory is this to the structure of the memory of other similar places? By "structure of the memory" consider things like the extent to which you have a visual memory of the office space, whether that memory is in colour, the extent to which the memory seems vivid or realistic, its size, location in your imagination, the extent to which it is panoramic in your imagination, and other such structural elements.

I think of the maze as a place in a way similar to other similar places where I have been...

1. Not at all ... 7. Very much so.

6. During the time of the experience, did you often think to yourself that you were actually in the maze?

During the experience I often thought that I was really walking in the maze...

1. Not very often... 7. Very much so.

7. Please write any comment that you want to make about the experience, specially those things that helped you to feel that you were in a maze, and that it was real.

Appendix C

BFV analysis in different navigation conditions. Analysis of Normality

Different statistical analysis were conducted in the study about BFV in different navigation conditions. The normality of the different variables that were used was analyzed in order to decide if parametric or non-parametric tests should be applied.

The test applied to analyze the normality was the Kolmogorov-Smirnov test. The null hypothesis for this test states that the data come from a normal distribution. $p - values$ are detailed in the tables included in this Appendix.

Table C.1: **SUS QUESTIONNAIRES RESPONSES:** $p - values$ obtained when applying the Kolmogorov-Smirnov test to the different responses to the SUS questionnaires corresponding to the free navigation condition - N=32 - and to the automatic navigation condition - N=31.

Variable	Free Nav. $p - value$	Automatic Nav. $p - value$
SUS-Count	0.040	< 0.001
SUS-Mean	0.053	0.147
SUS Q1	0.040	0.001
SUS Q2	0.003	< 0.001
SUS Q3	< 0.001	0.011
SUS Q4	< 0.001	0.003
SUS Q5	0.068	0.058
SUS Q6	0.034	0.074

Table C.2: **BFV MEAN VALUES:** $p-values$ obtained when applying the Kolmogorov-Smirnov test to MCA-L mean BFV variables (N=24), to MCA-R mean BFV variables (N=22), to ACA-L mean BFV variables (N=9) and to ACA-R mean BFV variables (N=6).

Variable	MCA-L BFV $p-value$	MCA-R BFV $p-value$	ACA-L BFV $p-value$	ACA-R BFV $p-value$
Baseline A	0.097	> 0.200	> 0.200	> 0.200
Free Nav.	> 0.200	> 0.200	> 0.200	> 0.200
Baseline B	> 0.200	> 0.200	> 0.200	> 0.200
Automatic Nav.	> 0.200	> 0.200	> 0.200	> 0.200

Table C.3: **PERCENTAGE BFV VARIATIONS:** $p-values$ obtained when applying the Kolmogorov-Smirnov test to MCA-L percentage BFV variations (N=24), to MCA-R percentage BFV variations (N=22), to ACA-L percentage BFV variations (N=9) and to ACA-R mean BFV variations (N=6).

Variable	MCA-L BFV(%) $p-value$	MCA-R BFV(%) $p-value$	ACA-L BFV(%) $p-value$	ACA-R BFV(%) $p-value$
Free Nav.	0.132	> 0.200	0.156	0.145
Automatic Nav.	0.080	> 0.200	> 0.200	> 0.200

Table C.4: **PERCENTAGE BFV VARIATIONS - BIPs:** $p-values$ obtained when applying the Kolmogorov-Smirnov test to the maximum BFV percentage variations detected during BIPs. N=17.

Variable	MCA-L BFV(%) $p-value$	MCA-R BFV(%) $p-value$
Total BIP	0.047	0.015
Partial BIP	0.041	0.047

Table C.5: **RESPONSE TIMES - BIPs:** $p-values$ obtained when applying the Kolmogorov-Smirnov test to the response times during BIPs. N=17.

Variable	MCA-L BFV(%) $p-value$	MCA-R BFV(%) $p-value$
Total BIP	> 0.200	> 0.200
Partial BIP	0.075	0.125

Table C.6: **PERCENTAGE BFV VARIATIONS - RECOVERY PERIODS:** $p-values$ obtained when applying the Kolmogorov-Smirnov test to the maximum BFV percentage variations detected during recovery periods. N=17.

Variable	MCA-L BFV(%) $p-value$	MCA-R BFV(%) $p-value$
Total BIP	> 0.200	0.135
Partial BIP	> 0.200	0.086

Table C.7: **RESPONSE TIMES - RECOVERY PERIODS:** $p-values$ obtained when applying the Kolmogorov-Smirnov test to the response times during recovery periods. N=17.

Variable	MCA-L BFV(%) $p-value$	MCA-R BFV(%) $p-value$
Total BIP	0.144	0.136
Partial BIP	0.186	0.030

Appendix D

BFV analysis in different immersive conditions. Analysis of Normality

Different statistical analysis were conducted in the study about BFV in different navigation conditions. The normality of the different variables that were used was analyzed in order to decide if parametric or non-parametric tests should be applied.

The test applied to analyze the normality was the Kolmogorov-Smirnov test. The null hypothesis for this test states that the data come from a normal distribution. $p - values$ are detailed in the tables included in this Appendix.

Table D.1: **SUS QUESTIONNAIRES RESPONSES:** $p-values$ obtained when applying the Kolmogorov-Smirnov test to the different responses to the SUS questionnaire in the different navigation conditions: free navigation (N=42) vs. automatic navigation (N=41). Data corresponding to the CAVE-like and single screen configurations are included.

Variable	Free Nav. $p-value$	Automatic Nav. $p-value$
SUS-Count	< 0.001	< 0.001
SUS-Mean	0.021	0.074
SUS Q1	< 0.001	0.003
SUS Q2	0.001	< 0.001
SUS Q3	< 0.001	< 0.001
SUS Q4	< 0.001	< 0.001
SUS Q5	0.062	0.029
SUS Q6	0.009	0.001

Table D.2: **PERCENTAGE BFV VARIATIONS:** $p-values$ obtained when applying the Kolmogorov-Smirnov test to MCA-L percentage BFV variations (N=32) and to MCA-R percentage BFV variations (N=31)

Variable	MCA-L BFV(%) $p-value$	MCA-R BFV(%) $p-value$
Free Nav.	0.132	0.080
Automatic Nav.	> 0.200	0.169

Appendix E

BFV Analysis during a Visual Perception Task. Analysis of Normality

Different statistical analysis were conducted in the study about BFV during a visual perception task. The normality of the different variables that were used was analyzed in order to decide if parametric or non-parametric tests should be applied.

The test applied to analyze the normality was the Kolmogorov-Smirnov test. The null hypothesis for this test states that the data come from a normal distribution. $p - values$ are detailed in the tables included in this Appendix.

Table E.1: **PCA-L AND PCA-R MEAN BFV:** $p - values$ obtained when applying the Kolmogorov-Smirnov test to the PCA-L and PCA-R mean BFV values during repose and activation. N=16.

Variable	Repose	Activation
	$p - value$	$p - value$
PCA-L	> 0.200	> 0.200
PCA-R	0.060	0.060

Table E.2: **PCA-L AND PCA-R PERCENTAGE BFV VARIATION:** $p - values$ obtained when applying the Kolmogorov-Smirnov test to the PCA-L and PCA-R maximum percentage variation values during repose and activation. N=16.

Variable	Repose	Activation
	$p - value$	$p - value$
PCA-L	> 0.200	0.051
PCA-R	0.014	0.017

Table E.3: **PCA-L AND PCA-R RESPONSE TIMES:** $p - values$ obtained when applying the Kolmogorov-Smirnov test to the PCA-L and PCA-R response times during repose and activation. N=16.

Variable	Repose	Activation
	$p - value$	$p - value$
PCA-L	> 0.200	> 0.200
PCA-R	> 0.200	> 0.200

Appendix F

BFV Analysis during Motor Tasks. Analysis of Normality

Different statistical analysis were conducted in the study about BFV during motor tasks. The normality of the different variables that were used was analyzed in order to decide if parametric or non-parametric tests should be applied.

The test applied to analyze the normality was the Shapiro-Wilk test. The null hypothesis for this test states that the data come from a normal distribution. $p-values$ are detailed in the tables included in this Appendix.

Table F.1: **MSE - DOMINANT HAND MOVEMENTS - CONTRALATERAL MCA:** $p-values$ obtained when applying the Shapiro-Wilk test to the SampEn values in the different scale factors and the different motor conditions (repose vs. hand movements). N=9.

Variable	Repose	Hand mov.
	$p-value$	$p-value$
SampEn (S.F.=1)	0.565	0.882
SampEn (S.F.=2)	0.382	0.724
SampEn (S.F.=3)	0.486	0.699
SampEn (S.F.=4)	0.710	0.488
SampEn (S.F.=5)	0.780	0.337
SampEn (S.F.=6)	0.605	0.159
SampEn (S.F.=7)	0.597	0.238
SampEn (S.F.=8)	0.682	0.320
SampEn (S.F.=9)	0.687	0.482

Table F.2: **MSE - DOMINANT HAND MOVEMENTS - IPSILATERAL MCA:** $p-values$ obtained when applying the Shapiro-Wilk test to the SampEn values in the different scale factors and the different motor conditions (repose vs. hand movements). N=9.

Variable	Repose $p-value$	Hand mov. $p-value$
SampEn (S.F.=1)	0.374	0.561
SampEn (S.F.=2)	0.501	0.404
SampEn (S.F.=3)	0.552	0.362
SampEn (S.F.=4)	0.631	0.383
SampEn (S.F.=5)	0.714	0.366
SampEn (S.F.=6)	0.688	0.343
SampEn (S.F.=7)	0.509	0.235
SampEn (S.F.=8)	0.475	0.260
SampEn (S.F.=9)	0.269	0.140

Table F.3: **MSE - NON-DOMINANT HAND MOVEMENTS - CONTRALATERAL MCA:** $p - values$ obtained when applying the Shapiro-Wilk test to the SampEn values in the different scale factors and the different motor conditions (repose vs. hand movements). N=9.

Variable	Repose	Hand mov.
	$p - value$	$p - value$
SampEn (S.F.=1)	0.077	0.089
SampEn (S.F.=2)	0.034	0.020
SampEn (S.F.=3)	0.023	0.015
SampEn (S.F.=4)	0.019	0.023
SampEn (S.F.=5)	0.018	0.037
SampEn (S.F.=6)	0.045	0.043
SampEn (S.F.=7)	0.084	0.071
SampEn (S.F.=8)	0.125	0.061
SampEn (S.F.=9)	0.211	0.027

Table F.4: **MSE - NON-DOMINANT HAND MOVEMENTS - IPSILATERAL MCA:** $p-values$ obtained when applying the Shapiro-Wilk test to the SampEn values in the different scale factors and the different motor conditions (repose vs. hand movements). N=9.

Variable	Repose $p-value$	Hand mov. $p-value$
SampEn (S.F.=1)	0.018	0.010
SampEn (S.F.=2)	0.044	0.123
SampEn (S.F.=3)	0.025	0.110
SampEn (S.F.=4)	0.019	0.108
SampEn (S.F.=5)	0.034	0.098
SampEn (S.F.=6)	0.027	0.077
SampEn (S.F.=7)	0.047	0.084
SampEn (S.F.=8)	0.036	0.069
SampEn (S.F.=9)	0.038	0.092

Table F.5: **CORRELATION DIMENSION** $p-values$ obtained when applying the Shapiro-Wilk test to the Correlation Dimension values associated to the BFV data in the different vessels (contralateral vs. ipsilateral) with different active hand (dominant vs. non-dominant) and different motor activity (repose vs. hand movement). N=9.

Condition	Repose	Hand Mov.
Dominant hand - Contralateral hemisphere	0.000	0.005
Dominant hand - Ipsilateral hemisphere	0.150	0.501
Non-Dominant hand - Contralateral hemisphere	0.906	0.027
Non-Dominant - Ipsilateral hemisphere	0.107	0.001

Table F.6: **FRACTAL DIMENSION -KATZ METHOD** $p - values$ obtained when applying the Shapiro-Wilk test to the Fractal Dimension values associated to the BFV data in the different vessels (contralateral vs. ipsilateral) with different active hand (dominant vs. non-dominant) and different motor activity (repose vs. hand movement). N=9.

Condition	Repose	Hand Mov.
Dominant hand - Contralateral hemisphere	0.931	0.747
Dominant hand - Ipsilateral hemisphere	0.058	0.109
Non-Dominant hand - Contralateral hemisphere	0.610	0.613
Non-Dominant - Ipsilateral hemisphere	0.317	0.093

Table F.7: **MAXIMUM LYAPUNOV EXPONENT** $p - values$ obtained when applying the Shapiro-Wilk test to the Fractal Dimension values associated to the BFV data in the different vessels (contralateral vs. ipsilateral) with different active hand (dominant vs. non-dominant) and different motor activity (repose vs. hand movement). N=9.

Condition	Repose	Hand Mov.
Dominant hand - Contralateral hemisphere	0.837	0.142
Dominant hand - Ipsilateral hemisphere	0.417	0.635
Non-Dominant hand - Contralateral hemisphere	0.393	0.250
Non-Dominant - Ipsilateral hemisphere	0.339	0.064

List of Figures

List of Tables

Bibliography

[1] R. Held and N. Durlach, "Telepresence," *Presence: Teleoperators & Virtual Environments*, vol. 1, no. 1, pp. 109–112, 1992.

[2] M. Schuemie, P. van der Straaten, M. Krijn, and C. van der Mast, "Research on presence in virtual reality: A survey," *CyberPsychology & Behavior*, vol. 4, no. 2, pp. 183–201, 2001.

[3] T. B. Sheridan, "Musings on telepresence and virtual presence," *Presence: Teleoperators & Virtual Environments*, vol. 1, no. 1, pp. 120–126, 1992.

[4] K. Stanney, M. Mollaghasemi, L. Reeves, R. Breaux, and D. Graeber, "Usability engineering of virtual environments (VEs): Identifying multiple criteria that drive effective VE system design," *International Journal of Human-Computer Studies*, vol. 58, no. 4, pp. 447–481, 2003.

[5] B. E. Insko, "Measuring presence: Subjective, behavioral, and physiological methods," in *Being there: Concepts, effects and measurement of user presence in synthetic environments* (G. Riva, F. Davide, and W. IJsselsteijn, eds.), pp. 109–120, IOS Press, 2003.

[6] D. Friedman, A. Brogni, C. Guger, A. Antley, A. Steed, and M. Slater, "Sharing and analyzing data from presence experiments," *Presence: Teleoperators & Virtual Environments*, vol. 15, no. 5, pp. 599–610, 2006.

[7] R. M. Baños, C. Botella, A. García-Palacios, H. Villa, C. Perpiñá, and M. Alcañiz, "Presence and reality judgment in virtual environments: A unitary construct?," *CyberPsychology & Behavior*, vol. 3, no. 3, pp. 327–335, 2000.

[8] J. Lessiter, J. Freeman, E. Keogh, and J. Davidoff, "A cross-media presence questionnaire: The ITC-Sense of presence inventory," *Presence: Teleoperators & Virtual Environments*, vol. 10, no. 3, pp. 282–297, 2001.

[9] B. G. Witmer and M. J. Singer, "Measuring presence in virtual environments: A presence questionnaire," *Presence: Teleoperators & Virtual Environments*, vol. 7, no. 3, pp. 225–240, 1998.

[10] W. Barfield and S. Weghorst, "The sense of presence within virtual environments: A conceptual framework," in *Advances in Human Factors Ergonomics*, vol. 19, pp. 699–704, Amsterdam, Netherlands: Elsevier, 1993.

[11] M. Meehan, B. Insko, M. Whitton, and F. P. Brooks Jr, "Physiological measures of presence in stressful virtual environments," *ACM Transactions on Graphics (TOG)*, vol. 21, no. 3, pp. 645–652, 2002.

[12] S. Nichols, C. Haldane, and J. R. Wilson, "Measurement of presence and its consequences in virtual environments," *International Journal of Human-Computers Studies*, vol. 52, no. 3, pp. 471–491, 2000.

[13] J. R. Wilson, S. Nichols, and C. Haldane, "Presence and side effects: Complementary or contradictory?," in *Advances in Human Factors Ergonomics*, vol. 21B, pp. 889–892, Amsterdam, Netherlands: Elsevier, 1997.

[14] P. Zahorik and R. L. Jenison, "Presence as being-in-the-world," *Presence: Teleoperators & Virtual Environments*, vol. 7, no. 1, pp. 78–89, 1998.

[15] M. V. Sánchez-Vives and M. Slater, "From presence to consciousness through virtual reality," *Nature Reviews Neuroscience*, vol. 6, no. 4, pp. 332–339, 2005.

[16] T. Baumgartner, L. Valko, M. Esslen, and L. Jäncke, "Neural correlate of spatial presence in an arousing and noninteractive virtual reality: An EEG and psychophysiology study," *CyberPsychology & Behavior*, vol. 9, no. 1, pp. 30–45, 2006.

[17] T. Baumgartner, D. Speck, D. Wettstein, O. Masnari, G. Beeli, and L. Jäncke, "Feeling present in arousing virtual reality worlds: Prefrontal brain regions differentially orchestrate presence experience in adults and children," *Frontiers in Human Neuroscience*, vol. 2, pp. 1–8, 2008.

[18] L. Jäncke, M. Cheetham, and T. Baumgartner, "Virtual reality and the role of the prefrontal cortex in adults and children," *Frontiers in Neuroscience*, vol. 3, no. 1, pp. 52–59, 2009.

[19] R. Aaslid, T. M. Markwalder, and H. Nornes, "Noninvasive transcranial Doppler ultrasound recording of flow velocity in basal cerebral arteries," *Journal of Neurosurgery*, vol. 57, no. 6, pp. 769–774, 1982.

[20] N. Stroobant and G. Vingerhoets, "Transcranial Doppler ultrasonography monitoring of cerebral hemodynamics during performance of cognitive tasks: A review," *Neuropsychology Review*, vol. 10, no. 4, pp. 213–231, 2000.

[21] S. Duschek and R. Schandry, "Functional transcranial Doppler sonography as a tool in psychophysiological research," *Psychophysiology*, vol. 40, no. 3, pp. 436–454, 2003.

[22] M. Usoh, E. Catena, S. Arman, and M. Slater, "Using presence questionnaires in reality," *Presence: Teleoperators & Virtual Environments*, vol. 9, no. 5, pp. 497–503, 2000.

[23] M. Slater, C. Guger, G. Edlinger, R. Leeb, G. Pfurtscheller, A. Antley, M. Garau, A. Brogni, and D. Friedman, "Analysis of physiological responses to a social situation in an immersive virtual environment," *Presence: Teleoperators & Virtual Environments*, vol. 15, no. 5, pp. 553–569, 2006.

[24] F. Biocca and B. Delaney, "Immersive virtual reality technology," in *Communication in the age of virtual reality* (F. Biocca and M. Levy, eds.), p. 124, Lawrence Erlbaum Associates, 1995.

[25] A. S. Axelsson, A. Abelin, I. Heldal, R. Schroeder, and J. Widestrom, "Cubes in the cube: A comparison of a puzzle-solving task in a virtual and a real environment," *CyberPsychology & Behavior*, vol. 4, no. 2, pp. 279–286, 2001.

[26] C. Hendrix and W. Barfield, "Presence within virtual environments as a function of visual display parameters," *Presence: Teleoperators & Virtual Environments*, vol. 5, no. 3, pp. 274–289, 1996.

[27] J. Freeman, S. E. Avons, R. Meddis, D. E. Pearson, and W. IJsselsteijn, "Using behavioral realism to estimate presence: A study of the utility of postural responses to motion stimuli," *Presence: Teleoperators & Virtual Environments*, vol. 9, no. 2, pp. 149–164, 2000.

[28] R. Welch, T. Blackmon, A. Liu, B. Mellers, and L. Stark, "The effects of pictorial realism, delay of visual feedback, and observer interactivity on the subjective sense of presence," *Presence: Teleoperators & Virtual Environments*, vol. 5, no. 3, pp. 263–273, 1996.

[29] R. Aaslid, "Visually evoked dynamic blood flow response of the human cerebral circulation," *Stroke*, vol. 18, no. 4, pp. 771–775, 1987.

[30] S. M. Gomez, C. R. Gomez, and I. S. Hall, "Transcranial Doppler ultrasonographic assessment of intermittent light stimulation at different frequencies," *Stroke*, vol. 21, no. 12, pp. 1746–1748, 1990.

[31] A. G. Harders, G. Laborde, D. W. Dröste, and E. Rastogi, "Brain activity and blood flow velocity changes: A transcranial Doppler study," *International Journal of Neuroscience*, vol. 47, no. 1, pp. 91–102, 1989.

[32] P. C. Njemanze, C. R. Gomez, and S. Horenstein, "Cerebral lateralization and color perception: A transcranial Doppler study," *Cortex*, vol. 28, no. 1, pp. 69–75, 1992.

[33] M. Sitzer, R. R. Diehl, and M. Hennerici, "Visually evoked cerebral blood flow responses: Normal and pathological conditions," *Journal of Neuroimaging*, vol. 2, pp. 65–70, 1992.

[34] M. Sturzenegger, D. W. Newell, and R. Aaslid, "Visually evoked blood flow response assessed by simultaneous two-channel transcranial Doppler using flow velocity averaging," *Stroke*, vol. 27, no. 12, pp. 2256–2261, 1996.

[35] Z. Trkanjec and V. Demarin, "Hemispheric asymmetries in blood flow during color stimulation," *Journal of Neurology*, vol. 254, no. 7, pp. 861–865, 2007.

[36] R. Keunen, H. Pijlman, H. Visée, J. Vliegen, D. Tavy, and K. Stam, "Dynamical chaos determines the variability of transcranial Doppler signals," *Neurological Research*, vol. 16, no. 5, pp. 353–358, 1994.

[37] R. Keunen, J. Vliegen, C. Stam, and D. Tavy, "Nonlinear transcranial Doppler analysis demonstrates age-related changes of cerebral hemodynamics," *Ultrasound in medicine & biology*, vol. 22, no. 4, pp. 383–390, 1996.

[38] J. Vliegen, C. Stam, S. Rombouts, and R. Keunen, "Rejection of the 'filtered noise' hypothesis to explain the variability of transcranial Doppler signals: A comparison of original TCD data with gaussian-scaled phase randomized surrogate data sets," *Neurological research*, vol. 18, no. 1, pp. 19–24, 1996.

[39] R. Stone, "Applications of virtual environments: An overview," in *Handbook of Virtual Environments: Design, Implementation, and Applications* (K. Stanney, ed.), pp. 827–856, Lawrence Erlbaum Associates, 2002.

[40] International Society for Presence Research, "The concept of presence, explication statement," http://ispr.info/, 2000.

[41] W. Sadowski and K. Stanney, "Presence in virtual environments," in *Handbook of virtual environments: Design, implementation, and*

applications (K. Stanney, ed.), pp. 791–806, New Jersey: Lawrence Erlbaum Associates, 2002.

[42] M. Slater and S. Wilbur, "A framework for immersive virtual Environments (FIVE)- speculations on the role of presence in virtual environments," *Presence: Teleoperators & Virtual Environments*, vol. 6, no. 6, pp. 603–616, 1997.

[43] C. Heeter, "Being there: The subjective experience of presence," *Presence: Teleoperators & Virtual Environments*, vol. 1, no. 2, pp. 262–271, 1992.

[44] M. Slater, A. Steed, J. McCarthy, and F. Maringelli, "The influence of body movement on subjective presence in virtual environments," *Human Factors*, vol. 40, no. 3, pp. 469–478, 1998.

[45] W. Barfield, D. Zeltzer, T. Sheridan, and M. Slater, "Presence and performance within virtual environments," *Virtual environments and advanced interface design*, pp. 473–513, 1995.

[46] W. A. IJsselsteijn and G. Riva, "Being there: The experience of presence in mediated environments," in *Being There: Concepts, effects and measurement of user presence in synthetic environments* (G. Riva, F. Davide, and W. IJsselsteijn, eds.), Amsterdam, Netherlands: IOS Press, 2003.

[47] W. A. IJsselsteijn, H. de Ridder, J. Freeman, and S. E. Avons, "Presence: Concept, determinants and measurement," in *Proceedings-SPIE The International Society For Optical Engineering*, pp. 520–529, 2000.

[48] R. Kalawsky, "The validity of presence as a reliable human performance metric in immersive environments," in *Proceedings of Presence 2000, 3rd Annual International Workshop on Presence*, 2000.

[49] M. Lombard and T. Ditton, "At the heart of it all: The concept of presence," *Journal of computer-mediated communication*, vol. 3, no. 2, 1997.

[50] T. Kim and F. Biocca, "Telepresence via television: Two dimensions of telepresence may have different connections to memory and persuasion," *Journal of Computer-Mediated Communication*, vol. 3, no. 2, pp. 1–22, 1997.

[51] K. Mania and A. Chalmers, "A user-centered methodology for investigating presence and task performance," in *Proceedings of Presence 2000, 3rd Annual International Workshop on Presence*, 2000.

[52] S. R. Ellis, "Presence of mind," *Presence: Teleoperators & Virtual Environments*, vol. 5, no. 2, pp. 247–259, 1996.

[53] T. Schubert, F. Friedmann, and H. Regenbrecht, "The experience of presence: Factor analytic insights," *Presence: Teleoperators & Virtual Environments*, vol. 10, no. 3, pp. 266–281, 2001.

[54] G. Riva, P. Loreti, M. Lunghi, F. Vatalaro, and F. Davide, "Presence 2010: The emergence of ambient intelligence," in *Being There: Concepts, effects and measurement of user presence in synthetic environments* (G. Riva, F. Davide, and W. IJsselsteijn, eds.), pp. 59–84, Amsterdam, Netherlands: IOS Press, 2003.

[55] M. P. Huang and N. E. Alessi, "Presence as an emotional experience," in *Medicine Meets Virtual Reality: The Convergence of Physical & Informational Technologies: Options for a New Era in Healthcare* (J. Westwood, H. Hoffman, R. Robb, and D. Stredney, eds.), pp. 148–153, Amsterdam, Netherlands: IOS Press, 1999.

[56] H. T. Regenbrecht, T. W. Schubert, and F. Friedmann, "Measuring the sense of presence and its relations to fear of heights in virtual environments," *International Journal of Human-Computer Interaction*, vol. 10, no. 3, pp. 233–249, 1998.

[57] M. J. Schuemie, M. Bruynzeel, L. Drost, M. Brinckman, G. D. Haan, P. M. G. Emmelkamp, and C. V. der Mast, "Treatment of acrophobia in virtual reality: A pilot study," in *Conference Proceedings Euromedia*, pp. 8–10, 2000.

[58] M. Usoh, K. Arthur, M. C. Whitton, R. Bastos, A. Steed, M. Slater, and F. P. B. Jr, "Walking> walking-in-place> flying, in virtual environments," in *Proceedings of the 26th annual conference on Computer graphics and interactive techniques*, pp. 359–364, 1999.

[59] M. Slater, M. Usoh, and A. Steed, "Taking steps: The influence of a walking technique on presence in virtual reality," *ACM Transactions on Computer-Human Interaction (TOCHI)*, vol. 2, no. 3, pp. 201–219, 1995.

[60] E. Velten, "A laboratory task for induction of mood states," *Behaviour Research and Therapy*, vol. 6, pp. 473–482, 1968.

[61] R. M. Baños, C. Botella, V. Liaño, B. Guerrero, B. Rey, and M. Alcañiz, "Sense of presence in emotional virtual environments," in *Proceedings of Presence 2004, 7th Annual International Workshop on Presence*, pp. 156–159, 2004.

[62] M. Slater, D. P. Pertaub, and A. Steed, "Public speaking in virtual reality: Facing an audience of avatars," *IEEE Computer Graphics and Applications*, pp. 6–9, 1999.

[63] G. Riva, F. Mantovani, C. S. Capideville, A. Preziosa, F. Morganti, D. Villani, A. Gaggioli, C. Botella, and M. Alcañiz, "Affective interactions using virtual reality: The link between presence and emotions," *Cyberpsychology & Behavior*.

[64] S. Bouchard, J. St-Jacques, G. Robillard, and P. Renaud, "Anxiety increases the feeling of presence in virtual reality," *Presence: Teleoperators & Virtual Environments*, vol. 17, no. 4, pp. 376–391, 2008.

[65] J. Freeman, S. E. Avons, J. Davidoff, and D. E. Pearson, "Effects of stereo and motion manipulations on measured presence in stereoscopic displays," *Perception*, vol. 26, no. Abstract Supplement, 1997.

[66] W. IJsselsteijn, H. de Ridder, R. Hamberg, D. Bouwhuis, and J. Freeman, "Perceived depth and the feeling of presence in 3DTV," *Displays*, vol. 18, no. 4, pp. 207–214, 1998.

[67] J. Freeman, S. E. Avons, D. E. Pearson, and W. A. IJsselsteijn, "Effects of sensory information and prior experience on direct subjective ratings of presence," *Presence: Teleoperators & Virtual Environments*, vol. 8, no. 1, pp. 1–13, 1999.

[68] W. IJsselsteijn, H. Ridder, J. Freeman, S. E. Avons, and D. Bouwhuis, "Effects of stereoscopic presentation, image motion, and screen size on subjective and objective corroborative measures of presence," *Presence: Teleoperators & Virtual Environments*, vol. 10, no. 3, pp. 298–311, 2001.

[69] R. M. Baños, C. Botella, I. Rubió, S. Quero, A. García-Palacios, and M. Alcañiz, "Presence and emotions in virtual environments: The influence of stereoscopy," *CyberPsychology & Behavior*, vol. 11, no. 1, pp. 1–8, 2008.

[70] R. M. Baños, C. Botella, M. Alcañiz, V. Liaño, B. Guerrero, and B. Rey, "Immersion and emotion: Their impact on the sense of presence," *CyberPsychology & Behavior*, vol. 7, no. 6, pp. 734–741, 2004.

[71] A. Sutcliffe, B. Gault, and J. E. Shin, "Presence, memory and interaction in virtual environments," *International Journal of Human-Computer Studies*, vol. 62, no. 3, pp. 307–327, 2005.

[72] M. Juan and D. Pérez, "Comparison of the levels of presence and anxiety in an acrophobic environment viewed via HMD or CAVE," *Presence: Teleoperators & Virtual Environments*, vol. 18, no. 3, pp. 232–248, 2009.

[73] J. D. Prothero and H. G. Hoffman, "Widening the field-of-view increases the sense of presence in immersive virtual environments," Tech. Rep. TR-95, Human Interface Technology Laboratory, 1995.

[74] J. J. Lin, H. B. L. Duh, D. E. Parker, H. Abi-Rached, and T. A. Furness, "Effects of field of view on presence, enjoyment, memory, andsimulator sickness in a virtual environment," *Proceedings of IEEE Virtual Reality 2002*, pp. 164–171, 2002.

[75] R. S. Kennedy, N. E. Lane, K. S. Berbaum, and M. G. Lilienthal, "Simulator sickness questionnaire: An enhanced method for quantifying simulator sickness," *The International Journal of Aviation Psychology*, vol. 3, no. 3, pp. 203–220, 1993.

[76] W. Barfield, K. M. Baird, and O. J. Bjorneseth, "Presence in virtual environments as a function of type of input device and display update rate," *Displays*, vol. 19, no. 2, pp. 91–98, 1998.

[77] M. M. Stanford, M. Meehan, and S. Razzaque, "Effect of latency on presence in stressful virtual environments," *Proceedings Of The IEEE Virtual Reality 2003*, pp. 141–148, 2003.

[78] P. Khanna, I. Yu, J. Mortensen, and M. Slater, "Presence in response to dynamic visual realism: A preliminary report of an experiment study," in *Proceedings of the ACM symposium on Virtual reality software and technology*, (Limassol, Cyprus), pp. 364–367, ACM, 2006.

[79] D. Hecht, M. Reiner, and G. Halevy, "Multimodal virtual environments: Response times, attention, and presence," *Presence: Teleoperators & Virtual Environments*, vol. 15, no. 5, pp. 515–523, 2006.

[80] H. Q. Dinh, N. Walker, C. Song, A. Kobayashi, and L. F. Hodges, "Evaluating the importance of multi-sensory input on memory and the sense of presence in virtual environments," in *Proceedings of the IEEE Virtual Reality*, pp. 222–228, IEEE Computer Society, 1999.

[81] C. Hendrix and W. Barfield, "The sense of presence within auditory virtual environments," *Presence: Teleoperators & Virtual Environments*, vol. 5, no. 3, pp. 290–301, 1996.

[82] P. Larsson, D. Västfjäll, and M. Kleiner, "Perception of self-motion and presence in auditory virtual environments," in *Proceedings of Presence 2004, 7th Annual International Workshop on Presence*, pp. 252–258, 2004.

[83] K. Bormann, "Presence and the utility of audio spatialization," *Presence: Teleoperators & Virtual Environments*, vol. 14, no. 3, pp. 278–297, 2005.

[84] J. Steuer, F. Biocca, and M. R. Levy, "Defining virtual reality: Dimensions determining telepresence," *Communication in the age of virtual reality*, pp. 33–56, 1995.

[85] H. Regenbrecht and T. Schubert, "Real and illusory interactions enhance presence in virtual environments," *Presence: Teleoperators & Virtual Environments*, vol. 11, no. 4, pp. 425–434, 2002.

[86] H. R. Jex, "Measuring mental workload: Problems, progress, and promises," in *Human mental workload* (P. Hancock and N. Meshkati, eds.), pp. 5–36, North-Holland: Elsevier Science Publishers, 1988.

[87] T. W. Schubert, F. Friedmann, and H. T. Regenbrecht, "Decomposing the sense of presence: Factor analytic insights," in *Proceedings of Presence 1999, 2nd Annual International Workshop on Presence*, pp. 3–23, 1999.

[88] M. Lombard, T. B. Ditton, D. Crane, B. Davis, G. Gil-Egui, K. Horvath, J. Rossman, and S. Park, "Measuring presence: A literature-based approach to the development of a standardized paper-and-pencil instrument," in *Proceedings of Presence 2000, 3rd Annual International Workshop on Presence*, p. 240, 2000.

[89] M. Slater, M. Usoh, and Y. Chrysanthou, "The influence of dynamic shadows on presence in immersive virtual environments," in *Selected papers of the Eurographics workshops on Virtual environments '95*, (Barcelona, Spain), pp. 8–21, Springer-Verlag, 1995.

[90] C. A. Thornson, B. F. Goldiez, and H. Le, "Predicting presence: Constructing the tendency toward presence inventory," *International Journal of Human-Computer Studies*, vol. 67, no. 1, pp. 62–78, 2009.

[91] M. Slater, "How colorful was your day? Why questionnaires cannot assess presence in virtual environments," *Presence: Teleoperators & Virtual Environments*, vol. 13, no. 4, pp. 484–493, 2004.

[92] W. A. IJsselsteijn and H. D. Ridder, "Measuring temporal variations in presence," in *Presence in Shared Virtual Environments Workshop*, (United Kingdom), 1998.

[93] M. Slater and A. Steed, "A virtual presence counter," *Presence: Teleoperators & Virtual Environments*, vol. 9, no. 5, pp. 413–434, 2000.

[94] R. Gilkey and J. Weisenberger, "The sense of presence for the suddenly deafened adult- Implications for virtual environments," *Presence: Teleoperators and Virtual Environments*, vol. 4, no. 4, pp. 357–363, 1995.

[95] C. Basdogan, C. Ho, M. Srinivasan, and M. Slater, "An experimental study on the role of touch in shared virtual environments," *ACM Transactions on Computer-Human Interaction (TOCHI)*, vol. 7, no. 4, pp. 443–460, 2000.

[96] M. Slater, V. Linakis, M. Usoh, and R. Kooper, "Immersion, presence, and performance in virtual environments: An experiment with tri-dimensional chess," in *ACM virtual reality software and technology (VRST)*, pp. 163–172, 1996.

[97] C. Youngblut and B. T. Perrin, "Investigating the relationship between presence and task performance in virtual environments," in *IMAGE 2002 Conference*, 2002.

[98] C. Dillon, E. Keogh, J. Freeman, and J. Davidoff, "Aroused and immersed: The psychophysiology of presence," in *Proceedings of Presence 2000, 3rd Annual International Workshop on Presence*, 2000.

[99] M. E. Dawson, A. M. Schell, and D. L. Filion, "The electrodermal system," in *Handbook of psychophysiology* (J. T. Cacioppo, L. G. Tassinary, and G. G. Berntson, eds.), vol. 2, pp. 159–181, Cambridge: Cambridge University Press, 2007.

[100] B. G. Wallin, "Sympathetic nerve activity underlying electrodermal and cardiovascular reactions in man," *Psychophysiology*, vol. 18, no. 4, pp. 470–476, 1981.

[101] G. Berntson, K. Quigley, and D. Lozano, "Cardiovascular psychophysiology," in *Handbook of psychophysiology* (J. T. Cacioppo,

L. G. Tassinary, and G. G. Berntson, eds.), vol. 2, pp. 182–210, Cambridge: Cambridge Universtiy Press, 2007.

[102] G. G. Berntson, J. T. B. Jr, D. L. Eckberg, P. Grossman, P. G. Kaufmann, M. Malik, H. N. Nagaraja, S. W. Porges, J. P. Saul, P. H. Stone, *et al.*, "Heart rate variability: Origins, methods, and interpretive caveats," *Psychophysiology*, vol. 34, no. 6, pp. 623–648, 1997.

[103] Task Force of the European Society of Cardiology and North American Society of Pacing and Electrophysiology, "Heart rate variability: Standards of measurement, physiological interpretation and clinical use," *Circulation*, vol. 93, no. 5, pp. 1043–1065, 1996.

[104] M. Meehan, S. Razzaque, B. Insko, M. Whitton, and F. P. Brooks, "Review of four studies on the use of physiological reaction as a measure of presence in Stressful Virtual environments," *Applied psychophysiology and biofeedback*, vol. 30, no. 3, pp. 239–258, 2005.

[105] N. Ravaja, "Presence-related influences of a small talking facial image on psychophysiological measures of emotion and attention," in *Proceedings of Presence 2002, 5th Annual International Workshop on Presence*, 2002.

[106] G. G. Berntson, J. T. Cacioppo, and K. S. Quigley, "Respiratory sinus arrhythmia: Autonomic origins, physiological mechanisms, and psychophysiological implications," *Psychophysiology*, vol. 30, pp. 183–196, 1993.

[107] B. K. Wiederhold, D. P. Jang, M. Kaneda, I. Cabral, Y. Lurie, T. May, I. Y. Kim, M. D. Wiederhold, and S. I. Kim, "An investigation into physiological responses in virtual environments: An objective measurement of presence," in *Towards CyberPsychology: Mind, Cognitions and Society in the Internet Age* (G. Riva and C. Calimberti, eds.), pp. 175–183, Amsterdam, Netherlands: IOS Press, 2003.

[108] J. Laarni, N. Ravaja, and T. Saari, "Using eye tracking and psychophysiological methods to study spatial presence," in *Proceedings of Presence 2003, 6th Annual International Workshop on Presence*, pp. 6–8, 2003.

[109] A. Antley and M. Slater, "The effect of lower spine muscle activation of walking on a narrow beam in virtual reality," in *2nd RAVE (Real Actions, Virtual Environments) Workshop*, (Barcelona), 2009.

[110] M. Tarr and W. Warren, "Virtual reality in behavioral neuroscience and beyond," *Nature Neuroscience*, vol. 5, pp. 1089–1092, 2002.

[111] B. Lenggenhager, T. Tadi, T. Metzinger, and O. Blanke, "Video ergo sum: Manipulating bodily Self-Consciousness," *Science*, vol. 317, no. 5841, pp. 1096–1099, 2007.

[112] M. Slater, D. Perez-Marcos, H. H. Ehrsson, and M. V. Sanchez-Vives, "Towards a digital body: The virtual arm illusion," *Frontiers in Human Neuroscience*, vol. 2, 2008.

[113] E. J. Speckman, C. E. Elger, and U. Altrup, "Neurophysiologic basis of the EEG," in *The treatment of epilepsy: Principles and practices* (E. Wyllie, ed.), Philadelphia: Lea and Febiger, 1993.

[114] D. Pizzagalli, "Electroencephalography and high-density electrophysiological source localization," in *Handbook of psychophysiology* (J. T. Cacioppo, L. G. Tassinary, and G. G. Berntson, eds.), vol. 2, pp. 56–84, Cambridge: Cambridge University Press, 2007.

[115] H. H. Jasper, "The ten-twenty electrode system of the international federation for electroencephalography: Appendix to the report of the committee on methods of clinical examination in electroencephalography," *The Journal of Eletroencephalography and Clinical Neuropsychology*, vol. 10, pp. 371–375, 1958.

[116] A. E. Society, "Guidelines for standard electrode position nomenclature," *Journal of Clinical Neurophysiology*, vol. 8, pp. 200–202, 1991.

[117] R. Oostenveld and P. Praamstra, "The five percent electrode system for high-resolution EEG and ERP measurements," *Clinical Neurophysiology*, vol. 112, no. 4, pp. 713–719, 2001.

[118] A. Schlögl, M. Slater, and G. Pfurtscheller, "Presence research and EEG," in *Proceedings of Presence 2002, 5th Annual International Workshop on Presence*, pp. 9–11, 2002.

[119] D. Strickland and D. Chartier, "EEG measurements in a virtual reality headset," *Presence: Teleoperators & Virtual Environments*, vol. 6, no. 5, pp. 581–589, 1997.

[120] L. Pugnetti, L. Mendozzi, E. Barbieri, F. D. Rose, and E. A. Attree, "Nervous system correlates of virtual reality experience," in *Proceedings of the First European Conference on Disability, Virtual Reality and Associated Technology*, pp. 239–246, 1996.

[121] S. Kober, "Cortical correlate of spatial presence in 2-D and 3-D interactive virtual reality: An EEG study," in *3rd RAVE (Real Actions, Virtual Environments) Workshop*, (Barcelona), 2010.

[122] J. J. T.D. Wager, L. Hernandez and M. Lindquist, "Elements of functional neuroimaging," in *Handbook of psychophysiology* (J. T. Cacioppo, L. G. Tassinary, and G. G. Berntson, eds.), vol. 2, pp. 19–55, Cambridge: Cambridge University Press, 2007.

[123] G. K. Aguirre, E. Zarahn, and M. D'Esposito, "The variability of human BOLD hemodynamic responses," *Neuroimage*, vol. 8, no. 4, pp. 360–369, 1998.

[124] K. J. Friston, C. D. Frith, R. Turner, and R. S. J. Frackowiak, "Characterizing evoked hemodynamics with fMRI," *NeuroImage*, vol. 2, no. 2PA, pp. 157–165, 1995.

[125] K. K. Kwong, J. W. Belliveau, D. A. Chesler, I. E. Goldberg, R. M. Weisskoff, B. P. Poncelet, D. N. Kennedy, B. E. Hoppel, M. S. Cohen, and R. Turner, "Dynamic magnetic resonance imaging of human brain activity during primary sensory stimulation," *Proceedings of*

the National Academy of Sciences of the United States of America, vol. 89, no. 12, pp. 5675–5679, 1992.

[126] H. G. Hoffman, T. Richards, B. Coda, A. Richards, and S. R. Sharar, "The illusion of presence in immersive virtual reality during an fMRI brain scan," *CyberPsychology & Behavior*, vol. 6, no. 2, pp. 127–131, 2003.

[127] A. Callan and H. Ando, "Neural correlates of imagery induced by the ambient sound," in *Proceedings of Presence 2007, 10th Annual International Workshop on Presence*, pp. 73–78, 2007.

[128] M. Slater, A. Brogni, and A. Steed, "Physiological responses to breaks in presence: A pilot study," in *Proceedings of Presence 2003, 6th Annual International Workshop on Presence*, pp. 157–160, 2003.

[129] A. Brogni, M. Slater, and A. Steed, "More breaks less presence," in *Proceedings of Presence 2003, 6th Annual International Workshop on Presence*, pp. 6–8, 2003.

[130] M. Slater, "Presence and the sixth sense," *Presence: Teleoperators & Virtual Environments*, vol. 11, no. 4, pp. 435–439, 2002.

[131] M. Garau, D. Friedman, H. R. Widenfeld, A. Antley, A. Brogni, and M. Slater, "Temporal and spatial variations in presence: Qualitative analysis of interviews from an experiment on breaks in presence," *Presence: Teleoperators & Virtual Environments*, vol. 17, no. 3, pp. 293–309, 2008.

[132] S. B. de Ercilla, E. B. García, and C. G. Muñoz, "Física general," 2006.

[133] "Physics and principles," in *Transcranial Doppler ultrasonography.*

[134] J. McCartney, K. Thomas-Lukes, and C. Gomez, *Handbook of transcranial Doppler.* Springer, 1997.

[135] J. Risberg, "Regional cerebral blood flow in neuropsychology," *Neuropsychologia*, vol. 24, no. 1, pp. 135–140, 1986.

[136] M. Deppe, E. B. Ringelstein, and S. Knecht, "The investigation of functional brain lateralization by transcranial Doppler sonography," *Neuroimage*, vol. 21, no. 3, pp. 1124–1146, 2004.

[137] W. Sorteberg, K. F. Lindegaard, K. Rootwelt, A. Dahl, D. Russell, R. Nyberg-Hansen, and H. Nornes, "Blood velocity and regional blood flow in defined cerebral artery systems," *Acta neurochirurgica*, vol. 97, no. 1, pp. 47–52, 1989.

[138] M. Reivich, "Arterial PCO_2 and cerebral hemodynamics," *American Journal of Physiology*, vol. 206, no. 1, pp. 25–35, 1964.

[139] C. Iadecola, "Regulation of the cerebral microcirculation during neural activity: Is nitric oxide the missing link?," *Trends in neuroscience*, vol. 16, no. 6, pp. 206–214, 1993.

[140] M. Daffertshofer, "Functional Doppler testing," in *Cerebrovascular ultrasound: Theory, practice and future development* (S. M. M.G. Hennerici, ed.), pp. 341–359, Cambridge: Cambridge University Press, 2001.

[141] C. A. Giller, G. Bowman, H. Dyer, L. Mootz, and W. Krippner, "Cerebral arterial diameters during changes in blood pressure and carbon dioxide during craniotomy," *Neurosurgery*, vol. 32, no. 5, pp. 737–742, 1993.

[142] H. Kontos, "Validity of cerebral arterial blood flow calculations from velocity measurements," *Stroke*, vol. 20, no. 1, pp. 1–3, 1989.

[143] M. C. Diamond, A. B. Scheibel, and L. M. Elson, *El cerebro humano. Libro de trabajo.* Barcelona: Ariel, 1996.

[144] J. F. Toole, K. Murros, and R. Veltkamp, *Cerebrovascular disorders.* Lippincott Williams and Wilkins, 1999.

[145] J. B. Angevine and C. W. Cotman, *Principles of Neuroanatomy.* Oxford University Press, 1981.

[146] L. Tatu, T. Moulin, J. Bogousslavsky, and H. Duvernoy, "Arterial territories of the human brain: Cerebral hemispheres," *Neurology*, vol. 50, no. 6, pp. 1699–1708, 1998.

[147] D. Regan, *Human brain electrophysiology*. Elsevier, 1989.

[148] G. Panczel, M. Daffertshofer, S. Ries, D. Spiegel, and M. Hennerici, "Age and stimulus dependency of visually evoked cerebral blood flow responses," *Stroke*, vol. 30, pp. 619–623, 1999.

[149] F. Rihs, K. Gutbrod, B. Gutbrod, H. J. Steiger, M. Sturzenegger, and H. P. Mattle, "Determination of cognitive hemispheric dominance by stereo transcranial Doppler sonography," *Stroke*, vol. 26, no. 1, pp. 70–73, 1995.

[150] S. Knecht, M. Deppe, E. B. Ringelstein, M. Wirtz, H. Lohmann, B. Drager, T. Huber, and H. Henningsen, "Reproducibility of functional transcranial Doppler sonography in determining hemispheric language lateralization," *Stroke*, vol. 29, no. 6, pp. 1155–1159, 1998.

[151] M. Deppe, S. Knecht, H. Henningsen, and E. B. Ringelstein, "AVERAGE: A Windows® program for automated analysis of event related cerebral blood flow," *Journal of neuroscience methods*, vol. 75, no. 2, pp. 147–154, 1997.

[152] S. Knecht, B. Dräger, A. Flöel, H. Lohmann, C. Breitenstein, M. Deppe, H. Henningsen, and E. B. Ringelstein, "Behavioural relevance of atypical language lateralization in healthy subjects," *Brain*, vol. 124, no. 8, pp. 1657–1665, 2001.

[153] S. Knecht, B. Dräger, M. Deppe, L. Bobe, H. Lohmann, A. Flöel, E. B. Ringelstein, and H. Henningsen, "Handedness and hemispheric language dominance in healthy humans," *Brain*, vol. 123, no. 12, pp. 2512–2518, 2000.

[154] A. Flöel, A. Buyx, C. Breitenstein, H. Lohmann, and S. Knecht, "Hemispheric lateralization of spatial attention in right-and left-hemispheric language dominance," *Behavioural brain research*, vol. 158, no. 2, pp. 269–275, 2005.

[155] B. Dräger and S. Knecht, "When finding words becomes difficult: Is there activation of the subdominant hemisphere?," *NeuroImage*, vol. 16, no. 3PA, pp. 794–800, 2002.

[156] M. Sitzer, U. Knorr, and R. J. Seitz, "Cerebral hemodynamics during sensorimotor activation in humans," *Journal of Applied Physiology*, vol. 77, no. 6, pp. 2804–2811, 1994.

[157] R. E. Kelley, J. Y. Chang, S. Suzuki, B. E. Levin, and Y. Reyes-Iglesias, "Selective increase in the right hemisphere transcranial Doppler velocity during a spatial task," *Cortex*, vol. 29, no. 1, pp. 45–52, 1993.

[158] G. Orlandi and L. Murri, "Transcranial Doppler assessment of cerebral flow velocity at rest and during voluntary movements in young and elderly healthy subjects," *International Journal of Neuroscience*, vol. 84, no. 1, pp. 45–53, 1996.

[159] J. Klingelhöfer, G. Matzander, D. Sander, J. Schwarze, H. Boecker, and C. Bischoff, "Assessment of functional hemispheric asymmetry by bilateral simultaneous cerebral blood flow velocity monitoring," *Journal of Cerebral Blood Flow & Metabolism*, vol. 17, no. 5, pp. 577–585, 1997.

[160] M. Matteis, C. Caltagirone, E. Troisi, F. Vernieri, B. C. Monaldo, and M. Silvestrini, "Changes in cerebral blood flow induced by passive and active elbow and hand movements," *Journal of Neurology*, vol. 248, no. 2, pp. 104–108, 2001.

[161] M. Silvestrini, C. Caltagirone, L. M. Cupini, M. Matteis, E. Troisi, and G. Bernardi, "Activation of healthy hemisphere in poststroke recovery. A transcranial Doppler study," *Stroke*, vol. 24, no. 11, pp. 1673–1677, 1993.

[162] M. Silvestrini, E. Troisi, M. Matteis, L. M. Cupini, and C. Caltagirone, "Involvement of the healthy hemisphere in recovery from

aphasia and motor deficit in patients with cortical ischemic infarction: A transcranial Doppler study," *Neurology*, vol. 45, no. 10, pp. 1815–1820, 1995.

[163] E. Troisi, M. Silvestrini, M. Matteis, B. C. Monaldo, F. Vernieri, and C. Caltagirone, "Emotion-related cerebral asymmetry: Hemodynamics measured by functional ultrasound," *Journal of neurology*, vol. 246, no. 12, pp. 1172–1176, 1999.

[164] M. Stoll, G. F. Hamann, R. Mangold, O. Huf, and P. Winterhoff-Spurk, "Emotionally evoked changes in cerebral hemodynamics measured by transcranial Doppler sonography," *Journal of neurology*, vol. 246, no. 2, pp. 127–133, 1999.

[165] G. Vingerhoets, C. Berckmoes, and N. Stroobant, "Cerebral hemodynamics during discrimination of prosodic and semantic emotion in speech studied by transcranial Doppler ultrasonography," *Neuropsychology*, vol. 17, no. 1, pp. 93–99, 2003.

[166] L. Stegagno, D. Patritti, S. Duschek, B. Herbert, and R. Schandry, "Cerebral blood flow in essential hypotension during emotional activation," *Psychophysiology*, vol. 44, no. 2, pp. 226–232, 2007.

[167] P. Lang, M. Bradley, B. Cuthbert, *et al.*, "International affective picture system (IAPS): Affective ratings of pictures and instruction manual," Tech. Rep. A-4, Gainesville, FL: University of Florida, 2005.

[168] T. D. Greef, K. van Dongen, M. Grootjen, and J. Lindenberg, "Augmenting cognition: Reviewing the symbiotic relation between man and machine," *Lecture Notes in Computer Science*, vol. 4565, pp. 439–448, 2007.

[169] J. S. Warm and R. Parasuraman, "Cerebral hemodynamics and vigilance," *Neuroergonomics: The brain at work*, pp. 146–158, 2007.

[170] J. Warm, G. Matthews, and R. Parasuraman, "Cerebral hemodynamics and vigilance performance," *Military Psychology*, vol. 21, pp. 75–100, 2009.

[171] D. Mayleben, *Cerebral blood flow velocity during sustained attention.* PhD thesis, University of Cincinnati, 1998.

[172] C. Schnittger, S. Johannes, A. Arnavaz, and T. F. Münte, "Relation of cerebral blood flow velocity and level of vigilance in humans," *NeuroReport*, vol. 8, no. 7, pp. 1637–1639, 1997.

[173] W. S. Helton, T. D. Hollander, J. S. Warm, L. D. Tripp, K. Parsons, G. Matthews, W. N. Dember, R. Parasuraman, and P. A. Hancock, "The abbreviated vigilance task and cerebral hemodynamics," *Journal of Clinical and Experimental Neuropsychology*, vol. 29, no. 5, pp. 545–552, 2007.

[174] E. M. Hitchcock, J. S. Warm, G. Matthews, W. N. Dember, P. K. Shear, L. D. Tripp, D. W. Mayleben, and R. Parasuraman, "Automation cueing modulates cerebral blood flow and vigilance in a simulated air traffic control task," *Theoretical Issues in Ergonomics Science, 4*, vol. 1, no. 2, pp. 89–112, 2003.

[175] R. E. Kelley, J. Y. Chang, N. J. Scheinman, B. E. Levin, R. C. Duncan, and S. C. Lee, "Transcranial Doppler assessment of cerebral flow velocity during cognitive tasks," *Stroke*, vol. 23, no. 1, pp. 9–14, 1992.

[176] G. Vingerhoets and N. Stroobant, "Lateralization of cerebral blood flow velocity changes during cognitive tasks. A simultaneous bilateral transcranial Doppler study," *Stroke*, vol. 30, pp. 2152–2158, 1999.

[177] P. Schmidt, T. Krings, K. Willmes, F. Roessler, J. Reul, and A. Thron, "Determination of cognitive hemispheric lateralization by functional transcranial Doppler cross-validated by functional MRI," *Stroke*, vol. 30, no. 5, pp. 939–945, 1999.

[178] M. Matteis, F. Federico, E. Troisi, P. Pasqualetti, F. Vernieri, C. Caltagirone, L. Petrosini, and M. Silvestrini, "Cerebral blood flow velocity changes during meaningful and meaningless gestures - A functional transcranial Doppler study," *European Journal of Neurology*, vol. 13, no. 1, pp. 24–29, 2006.

[179] M. Bäcker, M. G. Hammes, M. Valet, M. Deppe, B. Conrad, T. R. Tölle, and G. Dobos, "Different modes of manual acupuncture stimulation differentially modulate cerebral blood flow velocity, arterial blood pressure and heart rate in human subjects," *Neuroscience letters*, vol. 333, no. 3, pp. 203–206, 2002.

[180] S. Knecht, H. Henningsen, M. Deppe, T. Huber, A. Ebner, and E. B. Ringelstein, "Successive activation of both cerebral hemispheres during cued word generation," *Neuroreport*, vol. 7, no. 3, pp. 820–824, 1996.

[181] C. Schnittger, S. Johannes, A. Arnavaz, and T. F. Münte, "Blood flow velocity changes in the middle cerebral artery induced by processing of hierarchical visual stimuli," *Neuropsychologia*, vol. 35, no. 8, pp. 1181–1184, 1997.

[182] M. Silvestrini, L. M. Cupini, M. Matteis, E. Troisi, and C. Caltagirone, "Bilateral simultaneous assessment of cerebral flow velocity during mental activity," *Journal of Cerebral Blood Flow and Metabolism*, vol. 14, no. 4, pp. 643–8, 1994.

[183] A. Varnadore, A. Roberts, and W. McKinney, "Modulations in cerebral hemodynamics under three response requirements while solving language-based problems: A transcranial Doppler study," *Neuropsychologia*, vol. 35, no. 9, pp. 1209–1214, 1997.

[184] B. Rosengarten, O. Huwendiek, and M. Kaps, "Neurovascular coupling in terms of a control system: Validation of a second-order linear system model," *Ultrasound in Medicine & Biology*, vol. 27, no. 5, pp. 631–635, 2001.

[185] E. Azevedo, B. Rosengarten, R. Santos, J. Freitas, and M. Kaps, "Interplay of cerebral autoregulation and neurovascular coupling evaluated by functional TCD in different orthostatic conditions," *Journal of Neurology*, vol. 254, no. 2, pp. 236–241, 2007.

[186] E. Martens, L. L. H. Peeters, E. D. Gommer, W. H. Mess, F. N. van de Vosse, V. L. Passos, and J. P. H. Reulen, "The Visually-

Evoked cerebral blood flow response in women with a recent history of preeclampsia and/or eclampsia," *Ultrasound in Medicine & Biology*, vol. 35, no. 1, pp. 1–7, 2009.

[187] D. Schuepbach, H. Boeker, S. Duschek, and D. Hell, "Rapid cerebral hemodynamic modulation during mental planning and movement execution: Evidence of time-locked relationship with complex behavior," *Clinical Neurophysiology*, vol. 118, no. 10, pp. 2254–2262, 2007.

[188] W. van Drongelen, *Signal processing for neuroscientists: Introduction to the analysis of physiological signals*. Academic Press, 2006.

[189] T. B. J. Kuo, C. M. Chern, W. Y. Sheng, W. J. Wong, and H. H. Hu, "Frequency domain analysis of cerebral blood flow velocity and its correlation with arterial blood pressure," *Journal of Cerebral Blood Flow & Metabolism*, vol. 18, no. 3, pp. 311–318, 1998.

[190] T. Lundar, K. F. Lindegaard, and H. Nornes, "Continuous recording of middle cerebral artery blood velocity in clinical neurosurgery," *Acta neurochirurgica*, vol. 102, no. 3, pp. 85–90, 1990.

[191] D. Newell, R. Aaslid, R. Stooss, and H. Reulen, "The relationship of blood flow velocity fluctuations to intracranial pressure B waves," *Journal of neurosurgery*, vol. 76, no. 3, pp. 415–421, 1992.

[192] R. Diehl, B. Diehl, M. Sitzer, and M. Hennerici, "Spontaneous oscillations in cerebral blood flow velocity in normal humans and in patients with carotid artery disease," *Neuroscience letters*, vol. 127, no. 1, pp. 5–8, 1991.

[193] R. Diehl, D. Linden, D. Lucke, and P. Berlit, "Phase relationship between cerebral blood flow velocity and blood pressure: A clinical test of autoregulation," *Stroke*, vol. 26, no. 10, pp. 1801–1804, 1995.

[194] J. Bascompte, J. Flos, and E. Gutiérrez, *Ordre i caos en ecologia*. Edicions Universitat Barcelona, 1995.

[195] X. Bornàs, *Psicopatologia i caos.* Editorial Bubok, 2009.

[196] A. Ozturk, A. Arslan, and F. Hardalac, "Comparison of neuro-fuzzy systems for classification of transcranial Doppler signals with their chaotic invariant measures," *Expert Systems with Applications*, vol. 34, no. 2, pp. 1044–1055, 2008.

[197] M. Latka, M. Glaubic-Latka, D. Latka, and B. West, "Fractal rigidity in migraine," *Chaos, Solitons and Fractals*, vol. 20, no. 1, pp. 165–170, 2004.

[198] S. Rossitti and H. Stephensen, "Temporal heterogeneity of the blood flow velocity at the middle cerebral artery in the normal human characterized by fractal analysis," *Acta Physiologica Scandinavica*, vol. 151, no. 2, pp. 191–198, 1994.

[199] M. Soehle, M. Czosnyka, D. Chatfield, A. Hoeft, and A. Peña, "Variability and fractal analysis of middle cerebral artery blood flow velocity and arterial blood pressure in subarachnoid hemorrhage," *Journal of Cerebral Blood Flow & Metabolism*, vol. 28, no. 1, pp. 64–73, 2007.

[200] B. J. West, M. Latka, M. Glaubic-Latka, and D. Latka, "Multifractality of cerebral blood flow," *Physica A: Statistical Mechanics and its Applications*, vol. 318, no. 3-4, pp. 453–460, 2003.

[201] B. West, R. Zhang, A. Sanders, S. Miniyar, J. Zuckerman, and B. Levine, "Fractal fluctuations in transcranial Doppler signals," *Physical Review E*, vol. 59, no. 3, pp. 3492–3498, 1999.

[202] L. Vancsisin, B. Babel, I. Nyary, and O. Szentirmai, "Applying nonlinear dynamics to transcranial Doppler time-series analysis for assessing cerebral autoregulation," in *Proceedings of the 20th Annual International Conference of the IEEE Engineering in Medicine and Biology Society*, vol. 6, pp. 3016–3019, 1998.

[203] C. Cruz-Neira, D. J. Sandin, T. A. DeFanti, R. V. Kenyon, and J. C. Hart, "The CAVE: audio visual experience automatic virtual environment," *Communications of the ACM*, vol. 35, no. 6, pp. 64–72, 1992.

[204] E. B. Ringelstein, B. Kahlscheuer, E. Niggemeyer, and S. M. Otis, "Transcranial Doppler sonography: Anatomical landmarks and normal velocity values," *Ultrasound in medicine & biology*, vol. 16, no. 8, pp. 745–761, 1990.

[205] M. Backer, M. G. Hammes, M. Valet, M. Deppe, B. Conrad, T. R. Tolle, and G. Dobos, "Different modes of manual acupuncture stimulation differentially modulate cerebral blood flow velocity, arterial blood pressure and heart rate in human subjects," *Neuroscience letters*, vol. 333, no. 3, pp. 203–206, 2002.

[206] M. Bulla-Hellwig, J. Vollmer, A. Gatzen, W. Skreczek, and W. Hartje, "Hemispheric asymmetry of arterial blood flow velocity changes during verbal and visuospatial tasks," *Neuropsychologia*, vol. 34, no. 10, pp. 987–991, 1996.

[207] L. M. Cupini, M. Matteis, E. Troisi, M. Sabbadini, G. Bernardi, C. Caltagirone, and M. Silvestrini, "Bilateral simultaneous transcranial Doppler monitoring of flow velocity changes during visuospatial and verbal working memory tasks," *Brain*, vol. 119, no. 4, pp. 1249–1253, 1996.

[208] R. C. Oldfield, "The assessment and analysis of handedness: The Edinburgh inventory," *Neuropsychologia*, vol. 9, no. 1, pp. 97–113, 1971.

[209] A. V. Oppenheim and R. W. Schafer, *Discrete-time signal processing*. Prentice-Hall, Inc. Upper Saddle River, NJ, USA, 1989.

[210] V. Naranjo and A. Albiol, "Flicker reduction in old films," in *Proc. of International Conference of Image Processing 2000* (IEEE, ed.), (Piscataway), pp. 657–659, 2000.

[211] V. Naranjo, *Técnicas de análisis de secuencias de vídeo - Aplicación a la restauración de películas antiguas*. PhD thesis, ETSI Telecomunicación. Universidad Politécnica de Valencia, Valencia, 2002.

[212] E. Ifeachor and B. Jervis, *Digital signal processing: A practical approach*. Pearson Education, 2002.

[213] J. Theiler, S. Eubank, A. Longtin, B. Galdrikian, and J. Farmer, "Testing for nonlinearity in time series: The method of surrogate data," *Physica D: Nonlinear Phenomena*, vol. 58, no. 1-4, pp. 77 – 94, 1992.

[214] R. Govindan, K. Narayanan, and M. Gopinathan, "On the evidence of deterministic chaos in ECG: Surrogate and predictability analysis," *Chaos: An Interdisciplinary Journal of Nonlinear Science*, vol. 8, pp. 495–502, 1998.

[215] J. Llabres, X. Bornàs, M. Noguera, A. M. Lopez, and F. Barcelo, "¿Caos en el electrocardiograma de estudiantes con miedo a volar? Un análisis de no linealidad," *International Journal of Clinical and Health Psychology*, vol. 5, no. 2, pp. 273–284, 2005.

[216] T. Schreiber and A. Schmitz, "Improved surrogate data for nonlinearity tests," *Physical Review Letters*, vol. 77, no. 4, pp. 635–638, 1996.

[217] R. Hegger, H. Kantz, and T. Schreiber, "Practical implementation of nonlinear time series methods: The TISEAN package," *Chaos: An Interdisciplinary Journal of Nonlinear Science*, vol. 9, pp. 413–435, 1999.

[218] T. Schreiber and A. Schmitz, "Surrogate time series," *Physica D: Nonlinear Phenomena*, vol. 142, no. 3-4, pp. 346–382, 2000.

[219] X. Bornàs, J. Llabres, M. Noguera, and A. Pez, "Sample entropy of ECG time series of fearful flyers: Preliminary results," *Nonlinear dynamics, psychology, and life sciences*, vol. 10, no. 3, pp. 301–318, 2006.

[220] S. Pincus, "Approximate entropy (ApEn) as a complexity measure," *Chaos: An Interdisciplinary Journal of Nonlinear Science*, vol. 5, pp. 110–117, 1995.

[221] J. S. Richman and J. R. Moorman, "Physiological time-series analysis using approximate entropy and sample entropy," *American Jour-*

nal of Physiology, Heart and Circulatory Physiology, vol. 278, no. 6, pp. H2039–H2049, 2000.

[222] M. Costa, A. Goldberger, and C. Peng, "Multiscale entropy analysis of biological signals," *Physical Review E*, vol. 71, no. 2 Pt 1, pp. 021906–1–021906–18, 2005.

[223] M. Costa, A. Goldberger, and C. Peng, "Multiscale entropy analysis of complex physiologic time series," *Physical Review Letters*, vol. 89, pp. 068102–1–068102–4, 2002.

[224] M. Costa, C. Peng, A. Goldberger, and J. Hausdorff, "Multiscale entropy analysis of human gait dynamics," *Physica A: Statistical Mechanics and its Applications*, vol. 330, no. 1-2, pp. 53–60, 2003.

[225] P. Grassberger, "Information and complexity measures in dynamical systems," in *Information Dynamics* (H. Atmanspacher and H. Schreingraber, eds.), pp. 15–34, New York: Plenum Press, 1991.

[226] A. Goldberger, L. Amaral, L. Glass, J. Hausdorff, P. Ivanov, R. Mark, J. Mietus, G. Moody, C. Peng, and H. Stanley, "PhysioBank, PhysioToolkit, and PhysioNet: components of a new research resource for complex physiologic signals," *Circulation*, vol. 101, no. 23, pp. e215–e220, 2000.

[227] W. Pritchard and D. Duke, "Measuring chaos in the brain: A tutorial review of nonlinear dynamical EEG analysis," *International Journal of Neuroscience*, vol. 67, no. 1-4, pp. 31–80, 1992.

[228] B. Mandelbrot, *The fractal geometry of nature*. Wh. Freeman, 1982.

[229] E. Lorenz, "Deterministic Nonperiodic Flow," *Journal of the Atmospheric sciences*, vol. 20, pp. 130–141, 1963.

[230] F. Takens, "Detecting strange attractors in turbulence," in *Dynamical Systems and Turbulence, Warwick 1980*, pp. 366–381, 1981.

[231] M. Shelhamer, *Nonlinear dynamics in physiology. A state-space approach*. Singapore: World Scientific, 2007.

[232] P. Grassberger and I. Procaccia, "Characterization of strange attractors," *Physical review letters*, vol. 50, no. 5, pp. 346–349, 1983.

[233] M. Rosenstein, J. Collins, and C. Luca, "Reconstruction expansion as a geometry-based framework for choosing proper delay times," *Physica-Section D*, vol. 73, no. 1, pp. 82–98, 1994.

[234] M. Katz, "Fractals and the analysis of waveforms," *Computers in Biology and Medicine*, vol. 18, no. 3, pp. 145–156, 1988.

[235] C. Sevcik, "A procedure to estimate the fractal dimension of waveforms," *Complexity International*, no. 5, 1998.

[236] T. Higuchi, "Approach to an irregular time series on the basis of the fractal theory," *Physica D*, vol. 31, no. 2, pp. 277–283, 1988.

[237] M. Rosenstein, J. Collins, and C. D. Luca, "A practical method for calculating largest lyapunov exponents from small data sets," *Physica D*, vol. 65, no. 1-2, pp. 117–134, 1993.

[238] H. Lohmann, E. Ringelstein, and S. Knecht, "Functional transcranial Doppler sonography," in *Handbook on Neurovascular Ultrasound. Frontiers in Neurology and Neuroscience* (R. Baumgartner, ed.), vol. 21, pp. 251–260, Basel: Karger, 2006.

[239] B. Wiederhold, K. Davis, and J. Wiederhold, "The effects of immersiveness on physiology," in *Virtual Environments in Clinical Psychology and Neuroscience: Methods and Techniques in Advanced Patient-therapist Interaction* (G. Riva, B. Wiederhold, and E. Molinari, eds.), pp. 52–60, Amsterdam, Netherlands: IOS Press, 1998.

[240] M. Holden and E. Todorov, "Use of virtual environments in motor learning and rehabilitation," in *Handbook of Virtual Environments: Design, Implementation, and Applications* (K. Stanney, ed.), pp. 999–1026, Lawrence Erlbaum Associates, 2002.

[241] H. Kantz and T. Schreiber, *Nonlinear time series analysis*. Cambridge University Press, 2004.

[242] R. Heath, *Nonlinear dynamics: Techniques and applications in psychology*. Lawrence Erlbaum, 2000.

[243] J. Sprott, *Chaos and time-series analysis*. Oxford University Press, 2003.

[244] X. Bornàs, J. Llabrés, M. Noguera, A. M. López, J. M. Gelabert, and I. Vila, "Fear induced complexity loss in the electrocardiogram of flight phobics: A multiscale entropy analysis," *Biological psychology*, vol. 73, no. 3, pp. 272–279, 2006.

[245] X. Bornàs, J. Llabrés, M. Tortella-Feliu, M. A. Fullana, P. Montoya, A. López, M. Noguera, and J. M. Gelabert, "Vagally mediated heart rate variability and heart rate entropy as predictors of treatment outcome in flight phobia," *Biological Psychology*, vol. 76, no. 3, pp. 188–195, 2007.

[246] J. Z. Liu, Q. Yang, B. Yao, R. W. Brown, and G. H. Yue, "Linear correlation between fractal dimension of EEG signal and handgrip force," *biological Cybernetics*, vol. 93, no. 2, pp. 131–140, 2005.

[247] R. Esteller, G. Vachtsevanos, J. Echauz, and B. Litt, "A comparison of waveform fractal dimension algorithms," *IEEE Transactions on Circuits and Systems I: Fundamental Theory and Applications*, vol. 48, no. 2, pp. 177–183, 2001.

[248] N. N. Soe and M. Nakagawa, "Chaos and fractal analysis of electroencephalogram signals during different imaginary motor movement tasks," *Journal of the Physical Society of Japan*, vol. 77, no. 4, pp. 044801–044808, 2008.

[249] P. Kirsch, C. Besthorn, S. Klein, J. Rindfleisch, and R. Olbrich, "The dimensional complexity of the EEG during cognitive tasks reflects the impaired information processing in schizophrenic patients," *International Journal of Psychophysiology*, vol. 36, no. 3, pp. 237–246, 2000.

[250] D. E. Vaillancourt and K. M. Newell, "Changing complexity in human behavior and physiology through aging and disease," *Neurobiology of aging*, vol. 23, no. 1, pp. 1–11, 2002.

[251] A. Beck, N. Epstein, G. Brown, R. Steer, *et al.*, "An inventory for measuring clinical anxiety: Psychometric properties," *Journal of Consulting and clinical Psychology*, vol. 56, no. 6, pp. 893–897, 1988.

[252] M. Alcañiz, C. Botella, R. Baños, C. Perpiñá, B. Rey, J. A. Lozano, V. Guillén, F. Barrera, and J. A. Gil, "Internet-based telehealth system for the treatment of agoraphobia," *CyberPsychology & Behavior*, vol. 6, no. 4, pp. 355–358, 2003.

[253] B. Wiederhold, R. Gevirtz, and M. Wiederhold, "Fear of flying: A case report using virtual reality therapy with physiological monitoring," *CyberPsychology & Behavior*, vol. 1, pp. 97–104, 1998.

[254] B. Wiederhold and M. Wiederhold, "Lessons learned from 600 virtual reality sessions," *CyberPsychology & Behavior*, vol. 3, no. 3, pp. 393–400, 2000.

[255] L. M. Reeves, D. D. Schmorrow, and K. M. Stanney, "Augmented cognition and cognitive state assessment Technology-Near-Term, Mid-Term, and Long-Term research objectives," *Foundations of Augmented Cognition*, pp. 220–228, 2007.

[256] M. Grootjen, M. Neerincx, and J. van Weert, "Task based interpretation of operator state information for adaptive support," in *Augmented Cognition International - Human Factors and Ergonomics Society*, (San Francisco), pp. 236–242, 2006.

[257] J. Veltman and A. Gaillard, "Physiological workload reactions to increasing levels of task difficulty," *Ergonomics*, vol. 41, no. 5, pp. 656–669, 1998.

[258] A. Haag, S. Goronzy, P. Schaich, and J. Williams, "Emotion recognition using bio-sensors: First steps towards an automatic system," *Lecture Notes in Computer Science*, vol. 3068, pp. 36–48, 2004.

[259] P. Ehlert, "Intelligent user interfaces," Tech. Rep. DKS03-01, Faculty of Information Technology and systems, Delft University of Technology, 2003.

[260] L. Rothkrantz, P. Wiggers, J. van Wees, and R. van Vark, "Voice stress analysis," *Lecture Notes in Computer Science*, vol. 3206, pp. 449–456, 2004.

[261] H. V. Kuilenburg, M. Wiering, and M. D. Uyl, "A model based method for automatic facial expression recognition," in *Machine Learning: ECML 2005*, pp. 194–205, Berlin-Heidelberg: Springer, 2005.

[262] F. Freeman, P. Mikulka, L. Prinzel, and M. Scerbo, "Evaluation of an adaptive automation system using three EEG indices with a visual tracking task," *Biological Psychology*, vol. 50, no. 1, pp. 61–76, 1999.

[263] K. Izzetoglu, S. Bunce, B. Onaral, K. Pourrezaei, and B. Chance, "Functional optical brain imaging using Near-Infrared during cognitive tasks," *International Journal of Human-Computer Interaction*, vol. 17, no. 2, pp. 211–231, 2004.